Vol. 50 • No. 2

February 2007

Microwave Journal

RF Components and Systems

EM Enables Classic Filter Technique

Microwaves Across the Pacific

RF MEMS: Ready for Prime Time

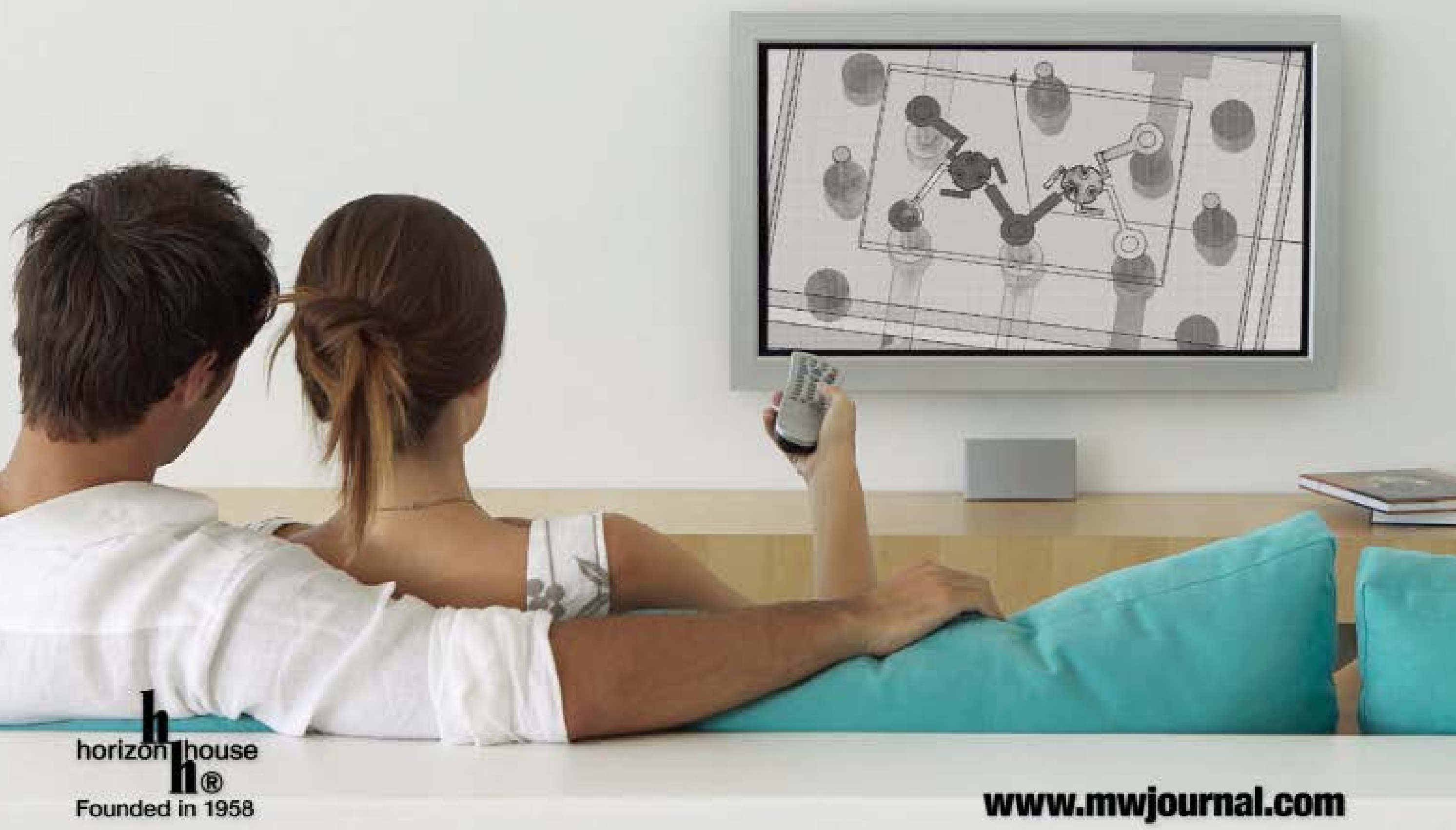

horizon house®
Founded in 1958

www.mwjournal.com

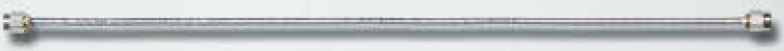

THE WORLD'S LARGEST SELECTION

POWER SPLITTERS/ COMBINERS

IN STOCK

2kHz to 12.6GHz *from* 79¢

COMPLIANT
RoHS models available, consult factory.

Need just the right surface mount, coaxial, thru mount, or flat pack power splitter or combiner for your project? Mini-Circuits is on the case offering you thousands of high performance, cost-effective models off-the-shelf and immediately available for your military and commercial applications. Choose from 2 and 3way to 48way; 0°, 90°, 180°; 50&75 ohms covering 2kHz to 12.6GHz and beyond, all characterized with detailed data and performance curves available to you in a flash 24/7 on "The Yoni Search Engine" at the Mini-Circuits web site. Surface mount products include highly reliable LTCC designs giving you extremely small size, ultra-low profile, excellent stability over temperature, and high performance repeatability. Tough built coaxial models are available with SMA, BNC, TNC, and Type-N connectors and include broadband ZX10 units standing less than $\frac{3}{4}$" in size. And when it comes to your custom needs…just let us know what you're looking for and our development team will go to work! Add our 1 year guarantee, knowledgeable applications support, and value pricing, and the decision is easy. Contact Mini-Circuits today!

Mini-Circuits…we're redefining what VALUE is all about!

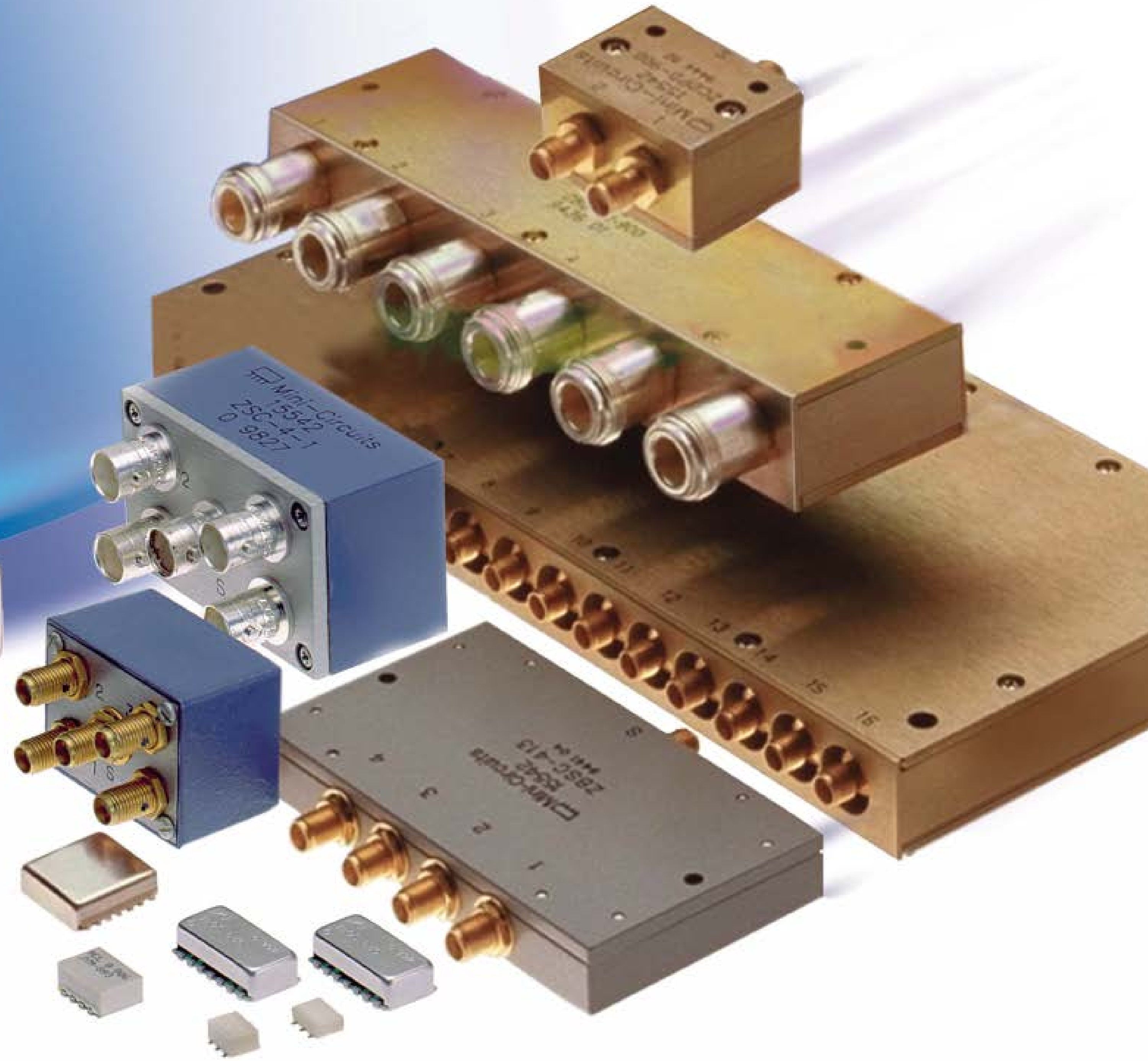
Mini-Circuits
15542
ZSC-4-1
0 9827

FEBRUARY 2007 VOL. 50 • NO. 2

FEATURES

SPECIAL REPORT

COVER FEATURE

TECHNICAL FEATURES

Microwave Journal (USPS 396-250) (ISSN 0192-6225) is published monthly by Horizon House Publications Inc., 685 Canton St., Norwood, MA 02062. Periodicals postage paid at Norwood, MA 02062 and additional mailing offices.

POSTMASTER: Send address corrections to *Microwave Journal*, PO Box 3256, Northbrook, IL 60065-3256 or e-mail mwj@omeda.com. Subscription information: (847) 291-5216. This journal is issued without charge upon written request to qualified persons working in that part of the electronics industry, including governmental and university installation, that deal with VHF through light frequencies. Other subscriptions are: domestic, $120.00 per year, two-year subscriptions, $185.00; foreign, $200.00 per year, two-year subscriptions, $370.00; back issues (if available) and single copies, $10.00 domestic and $20.00 foreign. Claims for missing issues must be filed within 90 days of date of issue for complimentary replacement.

Horizon House also publishes *Telecommunications*®

Posted under Canadian international publications mail agreement #0738654

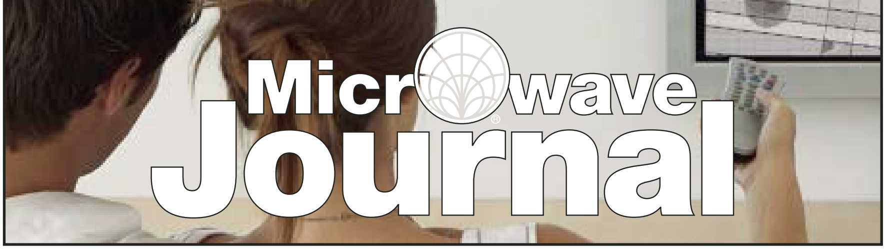

FEATURES

TECHNICAL FEATURES

PRODUCT FEATURES

DEPARTMENTS

THIS MONTH ON THE WEB

Visit www.mwjournal.com for the latest industry news and exclusive on-line articles

RFID: A Tale of Four Continents

RFID is being adopted worldwide but with very great differences of emphasis as revealed by the IDTechEx knowledge base of over 2450 case studies in 92 countries. This is a tale of four, very different continents.

IDTechEx

Passive Phase Shifters and Their Applications in RF Front-end Circuits

By Brian Kearns and Brendan McDonald
TDK Electronics Ireland Ltd.

Introduction to a two-port chip component designed to be matched to 50 Ω terminations at each of the two ports.

Defense Spending Increases Provide Robust Market for Compound Semiconductors

Radar, Communications, Smart Munitions and Electronic Warfare Contract Awards Exceed $16 B in 2006

Strategy Analytics projects that the market for GaAs devices will see continued growth at a CAAGR of 8% through to 2010.

STRATEGYANALYTICS
INSIGHTS FOR SUCCESS

IMS 2007: MICROWAVES ACROSS THE PACIFIC

Five months from now, Honolulu, HI will be the host city for what is widely regarded as the most prestigious microwave industry gathering in the world: the 2007 International Microwave Symposium (IMS 2007), to be held June 3–8, 2007.

IMS 2007 is the largest international conference devoted to the research, development and application of RF and microwave theory and techniques, and is expected to draw over 10,000 participants and 400 exhibiting companies from around the world. This conference is organized and sponsored by the Microwave Theory and Techniques Society (MTT-S) of the Institute of Electrical and Electronics Engineers (IEEE).

IMS 2007 marks the 50^{th} year that MTT-S has sponsored this symposium, and coincidentally it is being held in the 50^{th} state of the US. It is also the first time that this symposium is being held off of the North American continent. Hawaii has long been regarded as the Crossroads of the Pacific, and both the *Microwave Journal* and the IMS 2007 Steering Committee are using this opportunity to bridge East and West by encouraging attendees and exhibitors to interact in what is now a global microwave village.

From all indications we have had so far, IMS 2007 will be a well-attended event. We received 1039 technical paper submissions, higher than any other IMS year except for IMS 2003 (Philadelphia, PA), which received 1100. By comparison, the very well attended IMS 2005 (Long Beach, CA) and IMS 2006 (San Francisco, CA) received 984 and 982 submissions, respectively. Thirty-two percent of our paper submissions are from the US, and 30 percent are from Asian-Pacific Rim countries, again indicating the strong IMS 2007 participation from Asia. RFIC 2007, held in conjunction with IMS, received an all-time record of 350 papers, representing a 30 percent increase over last year.

Under the leadership of UCLA Professor Tatsuo Itoh, the Technical Program Committee is assembling a top-notch technical program that includes the usual array of technical papers, workshops, panel sessions and focused/special sessions. For the first time in recent IMS history, we will offer short courses from world-class experts that allow participants to receive IEEE continuing education units. We will also offer an expanded interactive forum in the morning and afternoon.

Our hotel rooms are selling at such a brisk pace that we are negotiating with hotels for larger room blocks to accommodate the demand. We are also planning an extensive guest program that the whole family can enjoy.

All in all, we anticipate IMS 2007 to be the microwave blockbuster event of the year. All of us on the IMS 2007 Steering Committee, the IEEE MTT-S and *Microwave Journal* look forward to seeing you in Hawaii this June. Aloha!

WAYNE A. SHIROMA
General Chair, IMS 2007

Ask Harlan

"Ask Harlan," a technical question and answer session with Harlan Howe, Jr., an industry veteran and long-time *Microwave Journal* editor, has been a regular part of our web site (www.mwjournal.com) for almost three years now. In an effort to better combine the editorial content of our magazine with our newly developed and retooled on-line presence, we have decided to develop Harlan's RF and microwave engineering advice into a monthly feature.

How it works: Harlan has selected one question from his "Ask Harlan" column to be featured in the magazine. Please visit www.mwjournal.com/askharlan to provide an answer to this month's featured question (see below). Harlan will be monitoring the responses and will ultimately choose the best answer to the question. Although all of the responses to the featured question will be posted on our web site, we plan to publish the winning answer in the April issue. All responses must be submitted by **March 6, 2007**, to be eligible for the participation of the February question.

The winning response will win a free book from Artech House, along with an "I Asked Harlan!" t-shirt. In addition, everyone who submits a legitimate response will be sent an "I Asked Harlan!" t-shirt.

December Question and Winning Response

The December question was submitted by Shanthi B. from Commercial Cellphone Makers:

Dear Harlan,

Why is the open/short/thru method the most preferred calibration method for RF measurements?

The winning response to the December question is from Roger Chandra of Aero Inc.:

There are mainly five reasons why it is preferred: 1.) This is the simplest method known for making RF measurements; 2.) The time needed for making a measurement is much less than any other known method; 3.) The results are very accurate and all benchmarking studies have proven that; 4.) The measurement setup and calibration methods of the instruments are relatively easy; 5.) Last but not the least, the cost involved is also less.

Harlan's response:

Dear Shanthi,

It is the most preferred because it is simple, fast, accurate and the calibration fixtures are relatively inexpensive to make and stable over time.

This Month's Question of the Month

(answer on-line at www.mwjournal.com/askharlan)

Peter Saul from Saul Research has submitted this month's question:

Dear Harlan,

What happened to the "Hula Hoop" antenna, AKA DDRR? It was reported in the 1960s, but not since. It appears from the references (*Microwave Journal*, Vol. 6, No. 11, November 1963, pp. 89–90; how can I get a copy?) to have had lots of promise.

If your response is selected as the winner,
you'll receive a free book of your choice from Artech House.
Visit the Artech House on-line bookstore at www.artechhouse.com
for details on hundreds of professional-level books in microwave engineering and related areas
(maximum prize retail value $150).

STAFF

Publisher: Carl Sheffres
Associate Publisher: Edward Johnson
Editor: Harlan Howe, Jr.
Managing Editor: Keith W. Moore
Technical Editor: Frank M. Bashore
Associate Technical Editor: Dan Massé
Staff Editor: Jennifer DiMarco
Editorial Assistant: Barbara Walsh
Consulting Editor: Howard I. Ellowitz
Consulting Editor: Peter Staecker
Consulting Editor: Dan Swanson
Web Editor: Stephen Heiser
Traffic Manager: Edward Kiessling
Traffic Administrator: Ken Hernandez
Director of Production & Distribution: Robert Bass
Multimedia Designer: Eli Conner
DTP Coordinator: Janet A. MacDonald

EUROPE

Deputy Publisher: Michel Zoghob
European Editor: Richard Mumford
Office Manager: Eugenie Hardy

CORPORATE STAFF

Chairman: William Bazzy
CEO: William M. Bazzy
President: Ivar Bazzy
Vice President: Jared Bazzy

Executive Editorial Office:
685 Canton Street, Norwood, MA 02062
Tel: (781) 769-9750
FAX: (781) 769-5037
e-mail: mwj@mwjournal.com

European Editorial Office:
46 Gillingham Street, London SW1V 1HH, England
Tel: Editorial: +44 207 596 8730 Sales: +44 207 596 8740
FAX: +44 207 596 8749

www.mwjournal.com

Printed in the USA

CALL FOR PAPERS

European Microwave Week (EuMW 2007)
by February 25, 2007
IEEE International Conference on Ultra-WideBand (ICUWB 2007)
by March 4, 2007

FEBRUARY

SATELLITE 2007
February 19–22, 2007 • Washington, DC
www.satellite2007.com

MARCH

MILITARY TECHNOLOGIES CONFERENCE
March 27–28, 2007 • Boston, MA
www.miltechconference.com

CTIA WIRELESS 2007
March 27–29, 2007 • Orlando, FL
www.ctiawireless.com

RF & HYPER EUROPE 2007
March 27–29, 2007 • Paris, France
www.rfhyper.com

INTERNATIONAL WIRELESS COMMUNICATIONS EXPO (IWCE 2007)
March 28–30, 2007 • Las Vegas, NV
www.iwceexpo.com

APRIL

IEEE RADAR CONFERENCE 2007
April 17–20, 2007 • Waltham, MA
www.radar2007.org

JUNE

IEEE MTT-S INTERNATIONAL MICROWAVE SYMPOSIUM AND EXHIBITION
June 3–8, 2007 • Honolulu, HI
www.ims2007.org

IEEE RADIO FREQUENCY INTEGRATED CIRCUITS SYMPOSIUM (RFIC 2007)
June 3–8, 2007 • Honolulu, HI
www.rfic2007.org

69TH ARFTG CONFERENCE
June 7–8, 2007 • Honolulu, HI
www.arftg.org

WCA 2007
June 11–14, 2007 • Washington, DC
www.wcai.com/events.htm

4TH INTERNATIONAL WORKSHOP ON ADVANCED GROUND PENETRATING RADAR (IWAGPR 2007)
June 27–29, 2007 • Naples, Italy
www.irea.cnr.it/IWAGPR2007

JULY

IEEE EMC SYMPOSIUM
July 8–13, 2007 • Honolulu, HI
www.emc2007.org

SEPTEMBER

IEEE INTERNATIONAL CONFERENCE ON ULTRA-WIDEBAND (ICUWB 2007)
September 24–26, 2007 • Singapore
www.icuwb2007.org

OCTOBER

EUROPEAN MICROWAVE WEEK (EUMW 2007)
October 8–12, 2007 • Munich, Germany
www.eumweek.com

ASSOCIATION OF OLD CROWS (AOC 2007)
October 28–31, 2007 • Orlando, FL
www.crows.org

MILITARY COMMUNICATIONS CONFERENCE (MILCOM 2007)
October 29–31, 2007 • Orlando, FL
www.milcom.org

NOVEMBER

ANTENNA MEASUREMENT TECHNIQUES ASSOCIATION (AMTA 2007)
November 4–9, 2007 • St. Louis, MO
www.amta.org

DECEMBER

ASIA-PACIFIC MICROWAVE CONFERENCE (APMC 2007)
December 11–14, 2007 • Bangkok, Thailand
www.apmc07.com

Workshops & Courses

Space-based Radar

■ **Topics:** The Space-based Radar (SBR) course will explore theory, applications and orbital considerations for both synthetic aperture radar (SAR) and moving target indication (MTI) modes. SBR technology issues covered include electronically scanned antennas, waveforms, tracking and on-board processing. While it emphasizes radar sensor issues, the course will include top-level satellite prime power, structure, thermal and altitude control. For more information, visit www.pe.gatech.edu.
■ **Site:** Atlanta, GA
■ **Dates:** March 5–9, 2007
■ **Contact:** Georgia Institute of Technology, Professional Education, PO Box 93686, Atlanta, GA 30377 (404) 385-3500.

Reverberation Chamber Theory and Experiment Short Course

■ **Topics:** This course is designed for engineers who will be involved in radiated emission or immunity testing of commercial or military systems using reverberation chambers. The theory portion will cover the statistical nature of reverberation chamber testing, characterization of the EM test conditions, and the tradeoff between uncertainty in test results and test time. The experiments include typical measurement techniques, chamber calibration, immunity, emission and pulse testing in reverberation chambers.
■ **Site:** Stillwater, OK
■ **Dates:** April 30–May 4, 2007
■ **Contact:** For more information, visit http://rc-course.okstate.edu.

Making Accurate Low Level Electrical Measurements

■ **Topics:** This course provides users with a detailed understanding of how to make accurate low level electrical measurements. Users will learn what constitutes a low level measurement, the limitations of these measurements, sources of measurement error and techniques to eliminate these errors.
■ **Site:** Cleveland, OH
■ **Dates:** June 19–20, 2007
■ **Contact:** For more information, visit www.keithley.com.

Practical Antenna Design

■ **Topics:** The course covers the important and timely issues involving modern antenna design and theory. Developed specifically for engineers and designers who work with radar and radio communications, this workshop will give participants the understanding of antenna theory and techniques, the skills to analyze, design and measure various antennas, and the knowledge of antenna measurements. For more information, visit www.conted.ox.ac.uk.
■ **Site:** Summertown, Oxford, UK
■ **Dates:** June 20–21, 2007
■ **Contact:** University of Oxford Continuing Education, +44 (0) 1865 286958 or e-mail: anthony.santiago@conted.ox.ac.uk.

The Entrepreneurial Engineer

■ **Topics:** This short course is an efficient and memorable introduction to the personal, interpersonal, business and organizational skills necessary to help engineers of applied science and mathematics perform at high levels in today's increasingly opportunistic organizations and enterprises. For more information, visit http://online.engr.uiuc.edu/shortcourses/tee/index.html.
■ **Site:** Archived on-line course.
■ **Dates:** Archived on-line for anytime viewing.
■ **Contact:** University of Illinois at Urbana-Champaign, 117 Transportation Bldg., 104 S. Mathews Avenue, Urbana, IL 61801 (217) 333-0897 or e-mail: deg@uiuc.edu.

PCB Design Techniques for EMC and Signal Integrity

■ **Topics:** This course will assist practicing engineers who are responsible for PCB designs and system-level products. Disciplines include PCB layout, logic design, regulatory compliance and EMC. For more information, visit http://epdwww.engr.wisc.edu.
■ **Site:** For location information, please visit url.
■ **Dates:** For date information, please visit url.
■ **Contact:** University of Wisconsin, Department of Engineering Professional Development, 432 North Lake Street, Madison, WI 53706 (800) 462-0876.

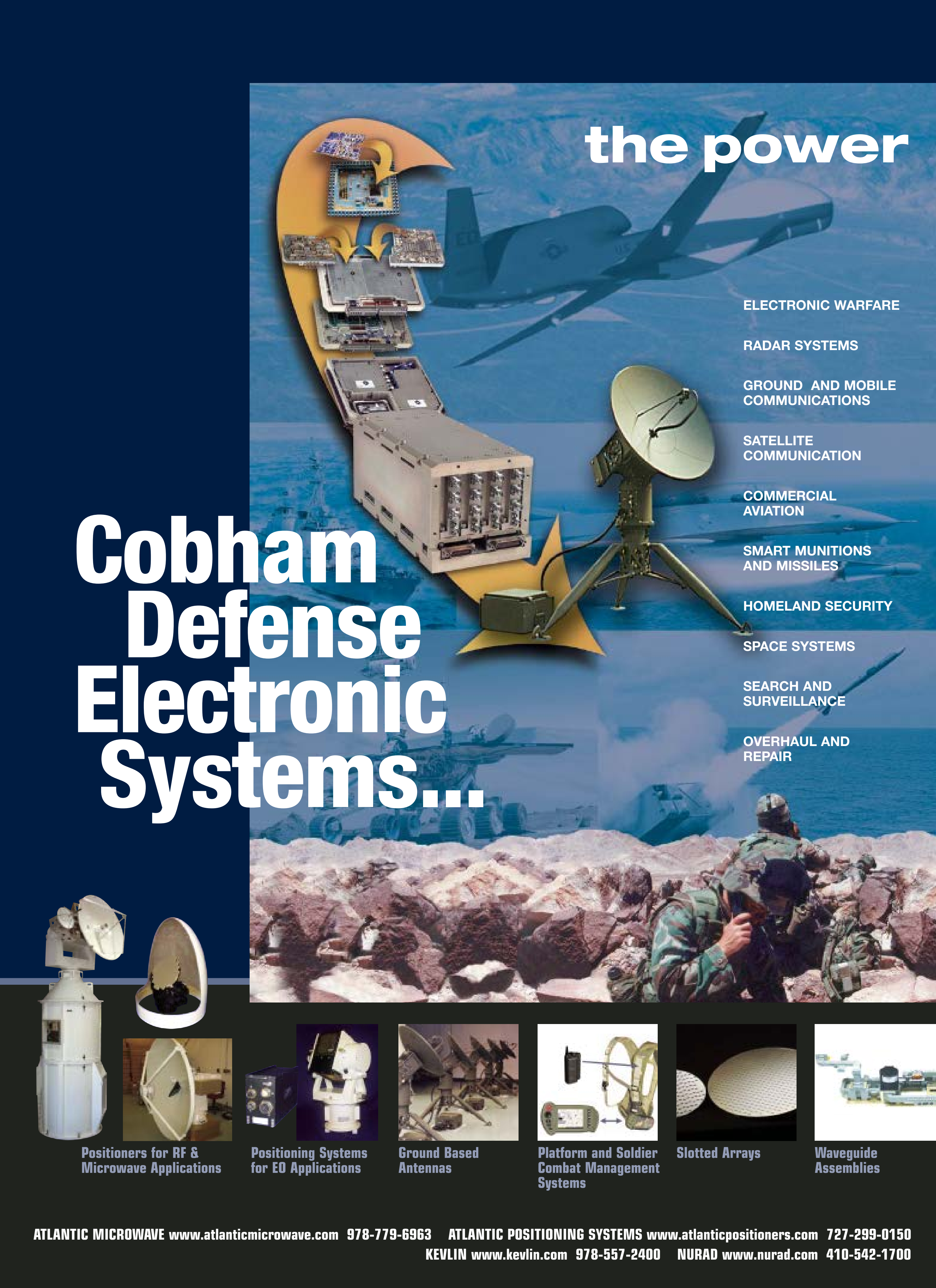
the power
ELECTRONIC WARFARE
RADAR SYSTEMS
GROUND AND MOBILE COMMUNICATIONS
SATELLITE COMMUNICATION
COMMERCIAL AVIATION
SMART MUNITIONS AND MISSILES
HOMELAND SECURITY
SPACE SYSTEMS
SEARCH AND SURVEILLANCE
OVERHAUL AND REPAIR
Cobham Defense Electronic Systems...
Positioners for RF & Microwave Applications
Positioning Systems for EO Applications
Ground Based Antennas
Platform and Soldier Combat Management Systems
Slotted Arrays
Waveguide Assemblies
ATLANTIC MICROWAVE www.atlanticmicrowave.com 978-779-6963
ATLANTIC POSITIONING SYSTEMS www.atlanticpositioners.com 727-299-0150
KEVLIN www.kevlin.com 978-557-2400
NURAD www.nurad.com 410-542-1700

COVER FEATURE
INVITED PAPER

RF MEMS: READY FOR PRIME TIME

The promises and shortcomings of microelectromechanical systems (MEMS) switch technology have become almost legendary. Perhaps no other electronic component in history has been the source of so much hype—and the cause of so much disillusionment. So much so, that Internet sites advise engineers to steer clear of MEMS switch technology. Fortunately for those who have patiently followed this technology, the troubling early days are finally over and MEMS switches are rapidly fulfilling all of their earlier promise. This article takes a fresh look at lessons learned and where things stand today, along with prospects for a bright future.

PAST

The first MEMS electrical switch was announced by IBM nearly 30 years ago.[1] Although the MEMS acronym was not coined for another decade,[2] this was one of the first practical microelectromechanical devices that used semiconductor fabrication techniques to build small mechanical structures in silicon that were moved or "actuated" electrically. It also showed that MEMS could create an entirely new class of switch technology that combined the advantages of semiconductor manufacturing with the best features of electromechanical relays. In particular, it was predicted that MEMS switches would be small, have low power consumption and low loss—and, if properly manufactured in high volume, would be low cost and highly reliable.

The first part of this promise was realized by MEMS switch prototypes developed at leading US industrial research centers during the early 1990s.[3] Work at Hughes Research Labs, Raytheon/Texas Instruments and the Rockwell Science Center clearly demonstrated that MEMS switches could be small and high performance, and that they could deliver bandwidth and linearity equal to or better than the best electromechanical relays. The only problem that (seemingly) remained to be solved was lifetime reliability, and the race was on.

When reliable commercial devices failed to quickly come out of Hughes, Raytheon and Rockwell, the door opened for other companies

JOHN MCKILLOP
TeraVicta Technologies Inc.
Austin, TX

to enter the race and the level of development activity exploded. By the end of the 1990s, more than 100 companies and research institutions throughout the world had started MEMS switch development programs. Visible commercial activity peaked between 2000 and 2001 with product "pre-announcements" from a number of major manufacturers and the launch of multiple startup companies.[4] Electrical performance was generally outstanding, but switch samples once again failed to meet customers' expectations for quality and reliability.

MEMS SWITCH CHALLENGES

Thinking that they were facing a "normal" set of technical challenges, MEMS switch developers consistently underestimated the difference between being able to sample a few prototype devices from a wafer and consistently manufacturing products that deliver high levels of quality and reliability. This created market expectations that are only now beginning to be met, and generated a considerable degree of skepticism concerning both MEMS companies and their products that still exists today. A number of technical issues contributed to this miscalculation, and to the difficulties in developing a reliable MEMS switch. Fortunately, hindsight allows us to highlight the most important of these issues and to identify the key solutions that were required to develop the first reliable RF MEMS switch products.

Unlike many other emerging technologies, MEMS switches must compete against established products based on very mature and stable technologies. Market entry products must have an initial defect rate of less than one percent and an operating life of at least 100 million cycles—10 times higher than a traditional electromechanical relay with otherwise comparable performance. This is a phenomenal expectation for an emerging technology product and a significant challenge in itself.

In parallel with this hurdle were two other serious technical issues that impacted nearly every MEMS switch development effort. The first was a subtle but important conflict between the market requirements for MEMS switches and stiction, the typical early failure mechanism of these devices (see ***Figure A1***).

RF MEMS switch users need low loss devices that are capable of reliably handling a few watts of RF power in a frequency band from DC to 5 GHz. This demand can only be met by ohmic contact switches with very low contact resistance (insertion loss). The requirement for low contact resistance, in turn, favors the use of relatively soft contact metals and/or high contact force, which makes the contacts stick together and fail (a phenomenon known in the MEMS community as stiction). Reliable low loss operation therefore requires stiff switch elements that provide enough return force to overcome stiction. High return force in turn requires a high enough operating voltage to generate enough closing force to overcome this stiffness and achieve an efficient contact. The correlation between design parameters and key failure mechanisms necessitates the use of high force actuator designs.

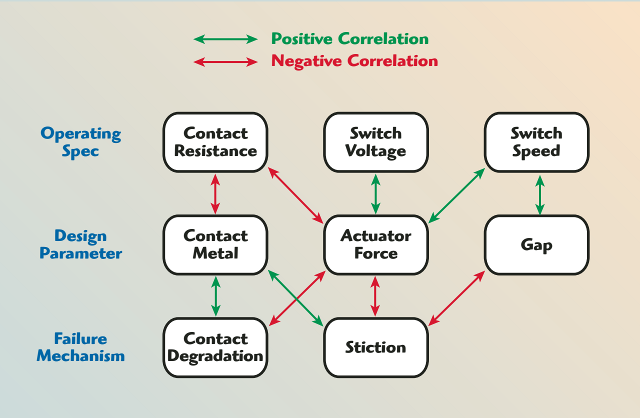

Fig. A1 Diagram illustrating the cross-correlation between operation specifications, design parameters and failure mechanisms of RF MEMS switches.

Low voltage actuator operation requires a compliant switch element (spring) that will necessarily have a limited return force. Thus, there is a fundamental conflict between the requirement for low switching voltage and the requirement for reliable, low loss operation. Although a variety of low voltage designs were investigated, all commercial solutions to date use "high force" actuator designs. This in turn requires high closing force, which can only be generated by high switch voltages.

Early MEMS switch designs were also plagued by the lack of hermetic packaging expertise within the MEMS industry. Contact degradation is one of two primary failure mechanisms for MEMS switches with ohmic contacts. This is primarily caused by contamination of the switch contacts and leads to steadily increasing values of switch resistance and insertion loss until the switch fails.

Long life MEMS switches thus require both high force actuation and manufacturing and packaging techniques that fabricate contaminant free switch contacts and keep them clean. This in turn requires cavity style packages that can protect the moving parts of the MEMS device from damage and contamination. A viable solution to this problem only emerged in the last several years as MEMS switch manufacturers adapted wafer bonding techniques to the fabrication of hermetic cavity packages. This advancement in packaging technology has shown the incredible sensitivity of MEMS switches to contamination. The crucial importance of hermetic packaging is highlighted by the fact that early MEMS switches attempted to get by with non-hermetic packaging technology. All failed to meet the 100 M cycle lifetime required for an entry-level product to compete with incumbent technologies. The MEMS switches manufactured by TeraVicta and Radant MEMS use in-line chip scale hermetic packages that are sealed in a clean room. This approach helps eliminate contamination of the MEMS switch contact and is a key factor in achieving operating lifetimes in excess of 100 M cycles.

Looking back with perfect hindsight, it is now possible to see that two key achievements were required to develop a commercial MEMS switch. The first was the realization that high force actuation was essential. The second was that in-line chip scale hermetic packaging was equally important in delivering highly reliable MEMS switches. TeraVicta and Radant MEMS have both solved the puzzle. ■

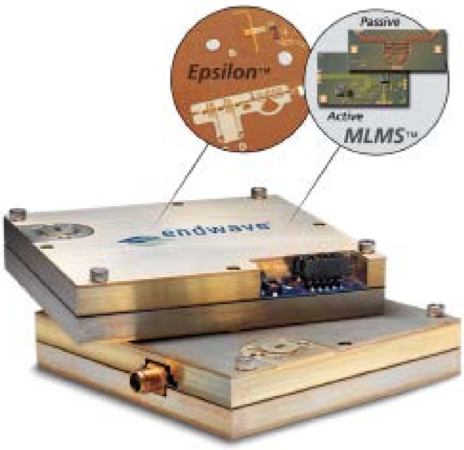

If you're ready to reach, we're ready to deliver.

When your applications have you reaching for higher frequencies, turn to Endwave. Our millimeter-wave products enable the "seeing and talking" behind broadband communications, high-resolution radars and advanced imaging systems.

You name it—E-Band T/R modules for gigabit radio links, a front-end to your Ka-Band seeker, or sensors for concealed weapons detection. If it's millimeter-waves, we have the team, experience and facilities you can lean on. With Endwave, nothing is out of reach.

Visit our Web site and learn more about our unique millimeter-wave experience on both commercial and defense related platforms.

Millimeter-wave Expertise

Active MLMS™ Flip-Chip Circuits
Passive MLMS™ Filters, Couplers
MMIC-based Assemblies
Discrete Hybrid Modules
Lightweight Epsilon™ Module Packaging
Automated Assembly/Test for Build-to-Print

Endwave. Plug us in.

endwave®

www.endwave.com

The extensive wait of nearly 10 years for a viable MEMS switch product made customers wary of the difficulties involved in commercializing this technology. Although there were a number of good reasons for these failures (see ***Inset***), the string of premature product announcements in 2000 and 2001 was the last straw. Customers became disillusioned by the hype surrounding MEMS switches and a cynical attitude toward the technology quietly settled into the marketplace. Driven by this serious case of market overexposure and a realization that hard proof of reliable product performance was the only way to successfully win customers, MEMS switch development moved into "stealth" mode after 2001. While much of this activity remains out of the public eye to this day, MEMS switch development efforts continue at some of the most prestigious companies throughout the world.

A basic search of MEMS switch and related patents issued after 2000 illustrates the breadth and depth of MEMS development. As shown in ***Figure 1***, nearly 200 US patents were issued for MEMS switch-related technology in the last seven years alone. In addition to the early pioneers in MEMS switching, patent assignees include major MEMS component manufacturers (Agilent, Analog Devices and Freescale) and other leaders in the semiconductor industry (Intel, IBM, Samsung and Toshiba).

Despite the massive deployment of resources and expertise by industry leaders, the first commercial MEMS switch was introduced by a relatively small company. Initial demonstration of what would become the first commercial MEMS switch was reported in the late 1990s by a team from Northeastern University working in collaboration with Analog Devices. This technology was ultimately licensed by Radant MEMS, a Stow, MA, company that is focused on the production of high reliability switches for government and military applications. Radant MEMS announced the first DC to 10 GHz single-pole single-throw (SPST) MEMS switch able to meet 100 M cycles (see ***Figure 2***) in 2004. The company has since in-

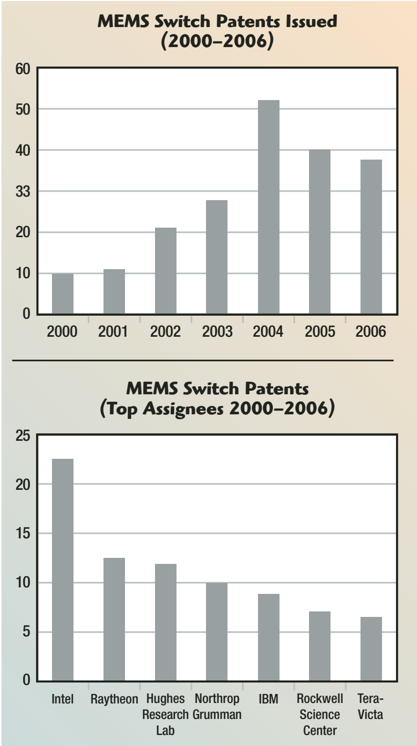

▲ *Fig. 1 Results of a US patent search on MEMS switch technology.*

troduced a single-pole double-throw (SPDT) switch that operates from DC to 20 GHz, and multi-contact series shunt switches that operate to 40 GHz.

The first commercially qualified MEMS switch was announced by TeraVicta Technologies in 2005 and began shipping in early 2006. Based on the company's patented high force disk actuator (HFDA) technology (see ***Figure 3***), the SPDT switch operates from DC to 7 GHz. TeraVicta led the industry by extending semiconductor qualification techniques to MEMS devices, and shipped the first-ever qualified commercial MEMS switch in early 2006. The company's RF MEMS switches have found their way into high volume commercial applications including automatic test equipment, instrumentation and wireless communications.

PRESENT

While a number of companies have disclosed either development efforts or limited sampling of advanced prototypes, at present only Radant MEMS and TeraVicta have MEMS switch products available in production quantities.[5] Radant MEMS markets its products almost exclusively to government and military customers in the United States, while TeraVicta actively sells its products to commercial customers worldwide.

A discussion of the features of the TeraVicta MEMS switch provides a useful illustration of current MEMS switch technology. This switch uses a "device on package" construction with the switch built directly on a ceramic (alumina) wafer with conductive metal vias (see ***Figure 4***). Individual switch features are patterned using conventional high volume semiconductor fabrication techniques, including sputter deposition and etching processes, with bulk metal layers fabricated via electroplating.

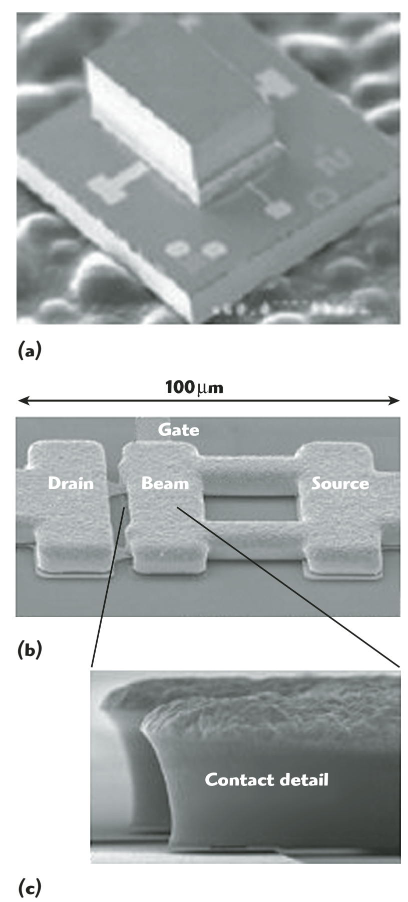

▲ *Fig. 2 SEM photographs of the Radant MEMS switch package (a) the actuator (b) with detail of the contact area (c).*

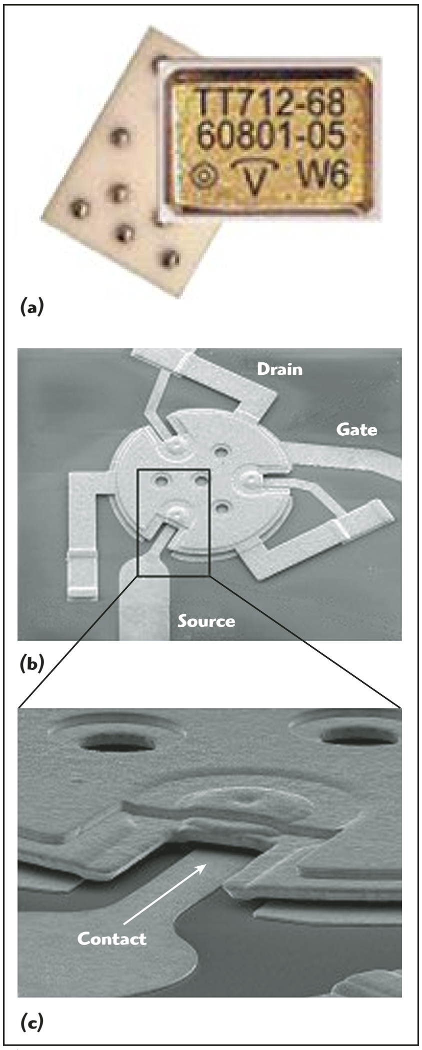

Fig. 3 Photographs of the TeraVicta TT712 MEMS package (a) and SEM photograph of the HFDA (b) with details of the switch contact area (c).

Device failures are minimized through the use of a proprietary high force disk actuator (HFDA), which provides substantial restoring force when the switch is in the closed position. This results in a very reliable operation, albeit at a relatively high switch voltage (68 V). Low voltage operation (3 to 5 V) is made possible through the use of a separate charge pump integrated circuit (IC). The package is completed by the attachment of a metal (Kovar) lid which provides a hermetic seal that eliminates the possibility of downstream contamination from backend manufacturing processes, and drastically reduces device failures due to contact contamination. The end result is a small (3.25 × 4.5 mm) surface-mountable micro-BGA ceramic package that provides a high efficiency, manu-

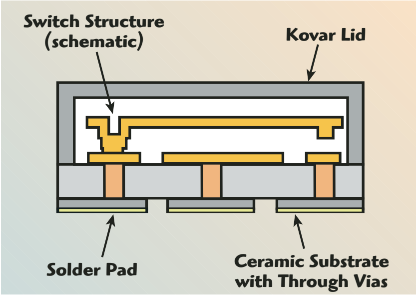

Fig. 4 Cross-section representation of the basic TeraVicta MEMS switch and chip-scale package.

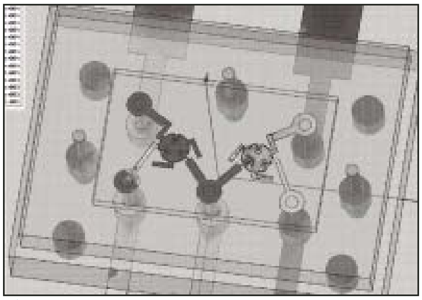

Fig. 5 Electromagnetic/solid model of an SPDT MEMS switch.

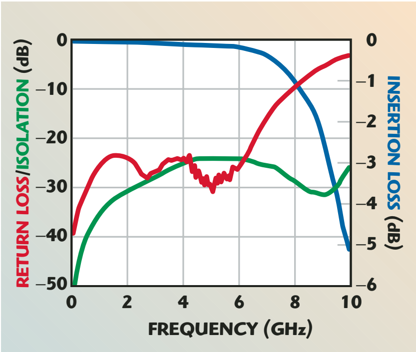

Fig. 6 RF performance characteristics of the TeraVicta DC to 7 GHz SPDT MEMS switch.

facturable electrical connection to the printed circuit board.

Switches with multiple contact configurations (SPDT, DPDT, etc.) can be constructed by connecting multiple HFDAs in a single package. This is illustrated by an RF electromagnetic/solid model of the basic DC to 7 GHz SPDT switch shown in ***Figure 5***. The RF signal is conducted into the switch through a central terminal (RF common), which connects to two HFDAs on the device. Closing either HFDA results in an electrical connection to its respective output pin. Note that since the HFDAs can be independently actuated, it is possible to open (or close) both switch contacts at the same time or to arbitrarily control the opening and closing sequence of the switch contacts. Typical HFDA switches currently have a 70 µs switching speed.

The HFDA technology used by TeraVicta also provides resistance repeatability that is typically much better than 10 mΩ, which enables insertion loss reproducibility of better than 0.4 dB across the entire 7 GHz band. These switches are also rated for continuous operation at up to 15 W, with a peak power handling capability of at least 30 W.

By comparison, Radant MEMS uses a conventional silicon micromachining approach to produce a very high force cantilever switch structure, along with a wafer bonded hermetic package to insure hermeticity. Although the stiffness of this cantilever structure results in even higher operating voltages (90 V), switching times are reduced to 10 µs. Electrical connection is provided by wire bonding from the top surface of the chip to either a chip carrier or directly to the printed circuit board.

The characteristic RF performance of the TeraVicta DC to 7 GHz SPDT switch is shown in ***Figure 6***. This MEMS switch delivers superior performance with insertion loss less than 0.1 dB at frequencies less than 1 GHz (0.4 dB at 7 GHz), with more than 20 dB of return loss and at least 25 dB of isolation. The simple construction of these switches also provides very low distortion for high power signals. Measured values of IP3 are typically in excess of 70 dBm, greater than the sensitivity of most measurement systems.

Although a number of MEMS switch developers have disclosed anecdotal results that show lifetimes of several billion cycles for individual switch samples, the perception of poor reliability still lingers in the marketplace. In response to this, TeraVicta has published lifetime data based on statistically significant samples of production devices.[6] This data, reproduced in ***Figure 7***, shows a Weibull plot of the failure distribution of current production devices. Included in the plot for comparison are representative failure distributions for competing electromechanical relays and reed relays. Additional data (green triangles) is included for devices that do not fail before 100 M cycles.

Device reliability in semiconductors and other electrical products is

typically described in terms of mean time before failure or MTBF. The useful life of an RF MEMS switch is usually limited by the number of switch cycles, not by elapsed time, however, and their reliability is better described in terms of cycles before failure. Current MEMS switch products, manufactured by TeraVicta, have a typical switch life or mean cycles before failure (MCBF) of approximately 200 million cycles, 20 times higher than the best electromechanical relays.

Like other small electromechanical switches, MEMS switch lifetimes are significantly de-rated in hot switching applications (opening or closing the switch with voltage present) at power levels above 0 dBm. Hot switching at 1 V/1 mA, for example, currently degrades the expected operating life by approximately a factor of 10.

MEMS switch prices are currently competitive with alternative switch technologies, and average sale prices will continue to decrease as volume manufacturing increases, making MEMS switches a viable option for some of the most price-sensitive consumer applications. Today, most commercial applications take advantage of one or more of the unique features of these devices: small size, low (repeatable) loss, high linearity and broad bandwidth. Leading applications include high speed digital channel switching in automated test equipment, antenna switching in wireless communications and filter bank switching in instrumentation, military and aerospace applications.

Finally, it should be noted that a number of MEMS switch development activities are still underway at leading companies and research institutions worldwide. Switch prototypes have recently been announced by Omron, Panasonic, WiSpry and XCom Wireless. Sampling to select customers is reportedly underway. As of this writing, only Radant MEMS and TeraVicta have demonstrated the ability to deliver MEMS switches in production volume.[5]

FUTURE

Three key trends will drive new applications for MEMS switches over the next three to five years: proliferation of a wide variety of new product configurations, substantial improvements in reliability, and significant reductions in switch size and cost.

The biggest change within the next year will be the emergence of a wide variety of new switch products. As an

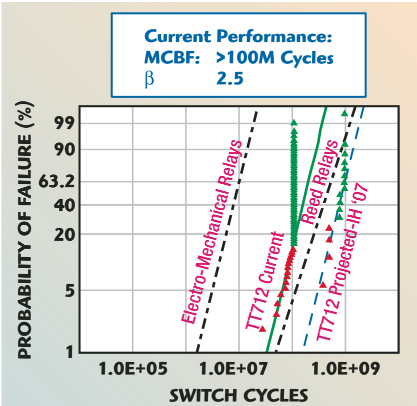

▲ *Fig. 7 Weibull plot of life test data for the TT712 SPDT switches operated to 100M cycles over the 0° to 70°C operating range of the device.*

example, during 2007 TeraVicta will deploy its proven HFDA technology in a variety of new high performance high reliability MEMS switches. This includes the introduction of a new high frequency switch line with products operating across the DC to 36 GHz band, and a range of new multi-pole multi-throw switch configurations within the existing 7 GHz product family.

In coming years, new MEMS switch companies and/or new product features should also begin to emerge. Anticipated new product features include high isolation (> 45 dB) switches, isolated gate (four-terminal) operation for relay replacement applications, as well as significant improvements in hot switching performance. Although current charge pump ICs can be used to drive independent banks of MEMS switches, in the future direct integration of high voltage drivers with MEMS switches will enable the introduction of high reliability low voltage switches that eliminate the need for high voltage on the printed circuit board, a key feature for high volume consumer applications.

Substantial improvements in switch reliability will also occur over the next few years. The vast majority of field failures for MEMS switches today are caused by increases in contact resistance due to contamination of the switch contacts. Improvements in process cleanliness and package integrity, along with the elimination of contamination from other materials, will dramatically improve product lifetimes. Although a quantitative forecast of lifetime improvement is difficult, comparison with other emerging technologies can provide a qualitative guide. Similar requirements for process and materials improvement were faced by early developers of semiconductor diode lasers, for example. These researchers were able to consistently improve diode laser lifetime by a factor of 10 every 18 months (see ***Figure 8***). A similar trend is likely for MEMS switches, with lifetimes of at least 10 B cycles and initial defect levels approaching 100 parts per million achieved over the next three to five years.

The most commercially significant trend over the next three to five years, however, will be reductions in switch size and cost. The substitution of lower cost materials, reductions in product size (proportional to cost) and higher fabrication utilization from increasing product sales will reduce product costs by a factor of 10 or more. Significant product size reductions will also occur, with packaged SPDT switches in form factors below 1.5 mm² (a 90 percent size reduction).

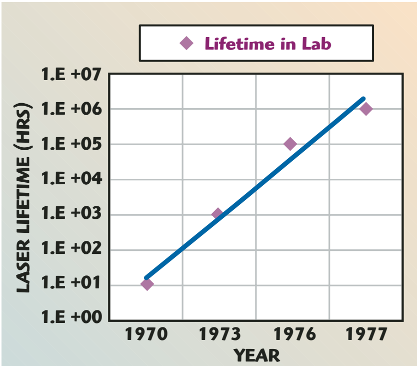

Fig. 8 Laboratory lifetime of early semiconductor lasers.

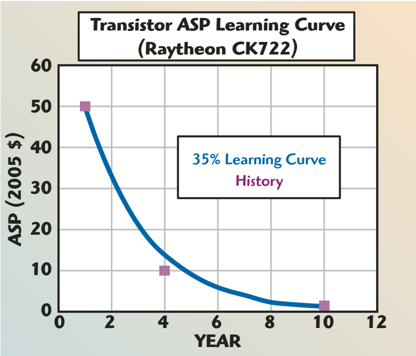

Fig. 9 Selling price "learning curve" for early transistors in constant 2005 dollars.

Although quantitative price forecasts are equally difficult, a review of historical price data from comparable technologies shows that most electronic devices experience a very uniform "learning curve," with a 35 percent reduction per year in the average selling price (ASP) of a given function (transistor, gate, or instructions executed per second). The learning curve for the first high volume transistors, for example, is shown in ***Figure 9*** (with prices adjusted to constant 2005 dollars). Although prices declined uniformly at the same rate of 35 percent per year, this analysis shows that the first transistors actually entered the market with a comparative unit price of $50. While there are reasons to suspect that limitations in size reduction will ultimately limit MEMS switch costs, price reductions of at least 35 percent per year are likely for the forseeable future. Already, MEMS switches are price competitive with existing switching solutions.

This fresh look at MEMS switch technology shows that despite lingering concerns about the reliability of this technology, a handful of MEMS switch manufacturers are finally delivering the first of a new family of high performance, high reliability switch products. These products are already finding high volume applications in automatic test equipment, instrumentation and communications. The list of applications is expected to explode as customers take advantage of all the benefits that MEMS switches have to offer. ■

References

1. K.E. Petersen, "Micromechanical Membrane Switches on Silicon," *IBM Journal of Research and Development*, Vol. 23, 1979, pp. 376–85.
2. N. Maluf, *An Introduction to Microelectromechanical Systems Engineering*, Second Edition, Artech House, Norwood, MA, 2004.
3. G.M. Rebeiz, *RF MEMS: Theory, Design and Technology*, John Wiley & Sons Inc., Hoboken, NJ, 2003.
4. P. Chalmers, "Relay Races," *Mechanical Engineering-CIME*, 1/1/2001.
5. M. Potin, *MEMS4Mobile 2006*, Yole Developpement, 2006.
6. J. McKillop, T. Fowler, D. Goins and R. Nelson, "Design, Performance and Qualification of a Commercially Available MEMS Switch," *Proceedings of the 2006 European Microwave Conference*.

John McKillop *received his BA degree in chemistry from Rice University and his PhD degree in chemistry from Stanford University. He held senior engineering and business development positions in a number of public companies and was a member of the research staff at IBM's T.J. Watson Research Center. He has more than 20 years experience managing engineering, operations, business and technology development for companies focused on emerging technologies, particularly in the fields of MEMS, lasers and electro-optics. He has authored numerous publications, been invited to present on the applications for MEMS technology and taught multiple MEMS short courses. He is now vice president of product development and CTO at TeraVicta Technologies Inc.*

Delivery From Stock!

MIXERS

Model Number	RF/LO Frequency (GHz)	IF Frequency (GHz)	LO Power (dBm)	Conversion Loss (dB) Typ./Max.	LO-to-RF Isolation (dB) (Min.)
DOUBLE-BALANCED VERSIONS					
DM0052LA2	0.5 – 2	DC – 0.5	7 – 13	6.5/8.5	30
DM0104LA1	1 – 4	DC – 1	7 – 13	5.5/7.0	30
DM0208LW2	2 – 8	DC – 2	7 – 13	7.0/8.0	30
DM0416LW2	4 – 16	DC – 4	7 – 13	7.0/8.0	30
DB0218LW2	2 – 18	DC – 0.75	7 – 13	6.5/8.5	22
DB1826LW1	18 – 26	DC – 2	7 – 13	7.5/9.5	20
DB0226LA1	2 – 26	DC – 0.5	7 – 13	9.0/10	20
DB0440LW1	4 – 40	DC – 2	10 – 15	9.0/10	20
M1826W1	18 – 26	DC – 8	10 – 15	9.0/12	25
M2640W1	26 – 40	DC – 12	10 – 15	10/12	28
TRIPLE-BALANCED VERSIONS					
TB0218LW2	2 – 18	0.5 – 8	10 – 15	7.5/9.5	20
TB0426LW1	4 – 26	0.5 – 8	10 – 15	10/12	20
TB0440LW1	4 – 40	0.5 – 20	10 – 15	10/12	18

PASSIVE DOUBLERS

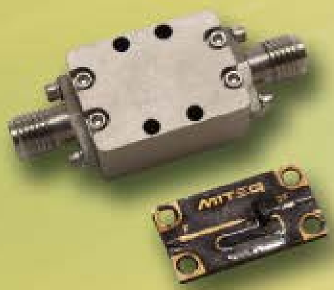

Model Number	Input Frequency (GHz)	Input Power (dBm)	Output Frequency (GHz)	Conversion Loss (dB) Typ./Max.	Rejection (dBc, Typ.) Fund.	Rejection (dBc, Typ.) Odd Harm.
DROP-IN VERSIONS						
SXS01M	0.5 – 3	8 – 12	1 – 6	13/16	-20	-25
SXS04M	2 – 9	8 – 12	4 – 18	13/15	-20	-25
SXS07M	3 – 13	8 – 12	6 – 26	13/17	-18	-25
CONNECTORIZED VERSIONS						
SXS2M010060	0.5 – 3	8 – 12	1 – 6	13/16	-20	-25
SXS2M040180	2 – 9	8 – 12	4 – 18	13/15	-20	-25
SXS2M060260	3 – 13	8 – 12	6 – 26	13/17	-18	-25

Additional models available with 60 day lead time, please contact MITEQ.
Above models also available with optional LO power ranges, please contact MITEQ.

Fastest Delivery Available! + 3 YEAR WARRANTY = MITEQ

NetFires Successfully Completes Joint Critical Design Review

NetFires LLC, a company composed of Raytheon Co. Missile Systems business and Lockheed Martin Missiles and Fire Control, successfully passed a joint critical design review (CDR) for the Non Line-of-Sight-Launch System Precision Attack Missile and Container Launch Unit. The Non Line-of-Sight-Launch System, which is one of the 18 Future Combat System's core systems, will operate as part of the Future Combat System Systems of Systems to meet the requirements of the Army's Future Brigade Combat Teams. It will provide increased capability for the Current Force's Modular Brigade Combat Teams.

Compared to systems with equivalent firepower (kill per combat load), the Non Line-of-Sight-Launch System provides a tailorable, modular, highly deployable and flexible precision fires capability to the US Army, US Navy and joint maneuver forces for a very low life-cycle system cost.

"This successful CDR was made possible by our dedicated government and industry personnel and I am pleased with the independent review team's assessment and approval of our success," said col. Doug Dever, Non Line-of-Site-Launch System project manager. "There are not enough words to express my sincere thanks to the hundreds of people throughout the United States who made this major milestone a success. The team has demonstrated a design that meets all design and performance requirements for the Non Line-of-Sight-Launch System."

The successful completion of the Non Line-of-Sight-Launch System Critical Design Review represents a significant milestone in meeting the design and performance parameters of the Non Line-of-Sight-Launch System supporting Future Combat System Spin Out 1 and weaponization of the Navy Littoral Combat Ships.

"Joint procurement of this system by the Army and Navy will result in significant economy, better interoperability and the potential for mutual support between land and sea forces in the littorals. It is a win for both services," said Capt. Mikem Good, Navy program manager for Littoral Combat Ship Mission Modules, Program Executive Office Littoral and Mine Warfare. "The Non Line-of-Sight-Launch System is one of the key Littoral Combat Ship mission modules in a spiral development process to meet future requirements and improve our warfighting capability."

The Non Line-of-Sight-Launch System consists of Raytheon's Precision Attack Missile and a joint Lockheed Martin and Raytheon Container Launch Unit. In 2004, the Army decided to accelerate the Raytheon's Precision Attack Missile and the joint Lockheed Martin and Raytheon Container Launch Unit for incorporation into the Army's Evaluation Brigade combat Team, Spin Out 1.

US Air Force Awards Northrop Grumman Contracts for Joint STARS Fleet Support

The US Air Force has awarded Northrop Grumman Co. two contracts worth a total of $254 M for the E-8C Joint Surveillance Target Attack Radar System (Joint STARS). The contracts cover work on the Joint STARS Total System Support Responsibility (TSSR) sustainment and Joint STARS Extended Test Support (JETS) programs.

The $140 M TSSR award is for a seventh year, through 2007, following an initial six-year $810 M contract awarded in 2000, bringing the total cumulative value of the TSSR contract to $950 M. The initial contract included options that could extend Northrop Grumman's participation on this program for more than two decades. Through this TRSS contract, the Air Force has reduced the cost of supporting the E-8C fleet by having the prime contractor, Northrop Grumman, partner with the Warner Robins Air Logistics Center. This cooperative business initiative has been a model for complete life cycle support.

The Air Logistics Center and Northrop Grumman use each other's best practices to provide economical Joint STARS support that fully meets the needs of the operational aircraft fleet. Northrop Grumman provides integrated management of all facets of depot maintenance, including some technology refreshment. The Air Force Logistics Center provided a dedicated management team in concert with software maintenance support, critical parts manufacture and repair of specific mission system items. Under this contract, most of the normal aircraft heavy depot maintenance repair and overhaul, including system upgrade modifications, will continue at the Lake Charles, LA Modification Center operated by Northrop Grumman. The contract also includes subcontract competition and small business participation.

The JETS II contract, worth $114 M over four years, provides test support capability for the Joint STARS Improvement Program. JETS II is a continuation of the current $64.8 M JETS program with similar objectives and provisions. The contract provides the critical skill infrastructure and the test assets necessary for the continued evolution and development of the Joint STARS system. The key mission objectives under the JETS II contract include: conducting government testing; providing training and proficiency flights for mission crew and primary aircrew; office facilities for the government Joint Test Force, engineering services; participation in system demonstrations and exercises; and installation, evaluation, demonstration and testing of potential system modifications and improvements. Both contracts are managed by the Air Force Material Command. The TSSR contract is managed through the Warner Robins Air Logistics Center at Robins Air Force Base, GA, and the JETS II contract is managed through the Electronic Systems Center at Hanscom Air Force Base, MA.

Harris Receives SCA-Certification for Falcon III AN/PRC-152(C)

Harris Corp., an international communications and information technology company, has announced that the Software Communications Architecture (SCA) of its Falcon® III AN/PRC-152(C) has been reviewed and tested by the Joint Program Executive Office of the Joint Tactical Radio System Test and Evaluation Laboratory (JPEO JTEL) and certified with waivers by Dennis Bauman, the Joint Program Executive Officer of the Joint Technical Radio System (JPEO JTRS). All JTRS radios must use the SCA software operating environment as the basis to run the radio's waveforms. With over 3000 AN/PRC-152(C) multiband handheld radios in service today and over 17,000 expected to be in service by summer 2007, the AN/PRC-152(C) is the first widely fielded tactical radio to receive SCA certification. "We are very happy to see Falcon III radio now SCA- and NSA-certified," said Bauman. "I am committed to removing JTRS market entry barriers and creating a competitive environment within the JTRS family. Products like the reprogrammable, SCA-compliant Falcon III will permit faster and cheaper means to upgrade the radio capabilities and implement crypto modernization. Our goal is to provide our Joint Warfighters with a family of interoperable, secure, affordable software-defined radios. I welcome Harris into the JTRS family."

"Fielding JTRS technology this early is a great win for the JTRS program and the government, and shows the true power of JTRS standards," said Dana Mehnert, president, Harris RF Communications Division. "The AN/PRC-152(C) was internally developed by Harris and implements key JTRS requirements: the SCA operating environment, and type 1, software-programmable encryption. By leaving the doors open to competition, the government can significantly benefit from commercial technology and accelerate getting new capabilities to the warfighter faster." The AN/PRC-152(C) and its associated vehicular adapter amplifier, the AN/VRC-110, are examples of commercial technology providing new capabilities to the warfighter. In service today, the AN/VRC-110 fits into a standard SINGARS vehicular communications mount, but unlike the dedicated-use SINGARS radio, the multimode AN/VRC-110 supports multiple waveforms: SINGARS, Havequick I/II, VHF/UHF AM&FM and MIL-STD-188-181B. ■


speed
execution
commitment
innovation
technology
a pearl is nature's gift
knowledge and experience are ours
For more than 30 years Lorch Microwave has been a leading supplier of RF and Microwave components, delivering innovative solutions for even the most demanding applications. From high performance micro miniature filters to ceramics, cavity and integrated assemblies, the Lorch Microwave name is found on military and commercial products worldwide. Let us put our knowledge and experience to work for you.
LORCH MICROWAVE
Salisbury, MD 21802
410.860.5100
800.780.2169
www.lorch.com
smiths


Your Dream
Our Design
SURFACE MOUNT TECHNOLOGY

New Horizons for Surrey NanoSystems

Set to have a major impact on the semiconductor industry is Surrey NanoSystems, a new company resulting from leading UK technology venture company IP Group teaming up with scientists from the University of Surrey's Advanced Technology Institute (ATI) and CEVP Ltd., a leader in plasma tool manufacture. The new company's remit is to provide commercial tools for producing nanomaterials.

IP Group has financed the joint venture company in which ATI scientists are developing a 'NanoGrowth'™ machine in conjunction with specialists from CEVP. Using patented technologies and recipes developed by the university, the NanoGrowth machine represents the world's first commercial tool for low temperature growth of carbon nanotubes, which can provide high quality, high speed connections to the next generation of silicon chips. The low temperatures used permit the use of existing silicon semiconductor materials which are not able to withstand the high growth temperatures previously required for the formation of nanotubes.

The low temperature carbon nanotube growth process is expected to be of considerable use in both academic and commercial laboratories for the development of practical nanomaterial production techniques for high technology applications. Likely applications include low resistance nanowires in integrated circuits, semiconducting nanotubes for fabricating high performance transistors, micro-miniature heat sinks, ultra-tough polymer composites, gas sensors and light sources for flat panel displays.

Outlining the potential significance of the initiative, Ben Jensen, technical director for CEVP, said, "I am incredibly excited by the partnership mix between IP Group, the University of Surrey and Surrey NanoSystems. This will enable the company to break new ground in the manufacturing and use of carbon nanotubes and nanostructures within the CMOS process window."

Thales Leads Development of First GMES Service

The European Commission has selected a consortium led by Thales to develop OSIRIS—Open architecture for Smart and Interoperable networks in Risk management based on In-situ Sensors, the first integrated service of the Global Monitoring for Environment and Security (GMES) programme. GMES will create an EU-wide capability to acquire, analyse, process and distribute information in support of European environment and security directives.

From 2008, GMES will provide services based on data from satellites and a range of in-situ sensors including seismographs, water analysers and air analysers to improve Europe's environment and, in turn, the quality of life for its citizens. With a total budget of €11 M, the OSIRIS project calls for the definition, development and testing of an integrated real-time surveillance and crisis management system. The system will significantly enhance Europe's ability to monitor environmental crises and manage and coordinate related operations and emergency responses.

The proposed architecture is open and scalable to allow for easy integration of new data from satellites and other sources to further improve the quality of service.

The OSIRIS programme is a prime illustration of the integrated services concept underpinning the European GMES system, which will provide the secure information and communication system architecture needed to deliver functions ranging from earth observation to end user services.

Diamond Set to be Semiconductors' Best Friend

Diamond Microwave Devices (DMD) is a new subsidiary set up by Element Six (E6), a world leader in the development of Chemical Vapour Deposition (CVD) diamond technology. The new company aims to develop novel diamond semiconductor materials and processing technology that will help create the next generation of high power, high temperature semiconductor devices for use in microwave power amplifiers and transmitters.

Element Six has also signed a collaboration agreement with Filtronic plc to work with DMD to develop this new technology. Filtronic and E6 will use their complementary high technology strengths in materials, semiconductor device processing and circuits to expedite the development of this new microwave technology that has the potential of revolutionising microwave power electronics.

E6 has been involved with major research and industrial programmes such as the UK's Department of Trade and Industry sponsored Carbon Power Electronics (CAPE) programme aimed at overcoming the technical challenges of developing diamond-based electronics components. For high power electronics, CVD diamond offers unique properties such as high breakdown voltage and high temperature operation. If a practical semiconductor device can be demonstrated, it could have the potential to provide superior microwave power and higher operating temperatures than existing semiconductor devices and technologies.

Dr. Richard Lang, general manager of DMD, said, "Whilst the technical challenges are high, a diamond MESFET could revolutionise the design of future microwave power modules. There is much work to be done in order to realise a practical device, and we are excited by the opportunity to explore the boundaries of this emerging technology."

Enterprising Tactics for EADS in Ireland

EADS and Enterprise Ireland have signed a strategic partnership agreement for aerospace research, technology development and procurement. The Memorandum of Understanding between the two parties forms the basis for co-operation until 2012 by which time the aim is to increase annual sales by Irish companies to EADS to a value of €35 M.

The primary aim of the agreement is to increase the level of procurement by EADS from Enterprise Ireland's client companies. Furthermore, the agreement aims to optimise opportunities for co-operation in technology research and development between EADS, Enterprise Ireland client companies and Science Foundation Ireland. It will also help maximise the benefits of the involvement of EADS, Enterprise Ireland and Science Foundations Ireland in the European Framework Program 7, a European Union programme for funding scientific research.

A significant part of the agreement is research and technology collaboration between EADS and The Centre for Telecommunications Value-Chain Research at Trinity College Dublin (TCD) and NUI Maynooth. The company will also fund a number of PhD programmes in key research areas of aerospace and security, with the first programme commencing at TCD.

Ericsson Strengthens Swedish-Chinese Relations

Ericsson and the Stockholm School of Economics have agreed to create a programme aimed at generating in-depth knowledge of Chinese business and economics and China's impact on global trade patterns. The programme began on 1 January 2007 and comprises several components designed to support the capacity of Sweden to follow developments in China, strengthen Swedish-Chinese relations in economics, business and research and its impact on the world economy.

The programme will be based at the Stockholm School of Economics in close cooperation with the China Centre for Economical Research at Peking University.

Carl-Henric Svanberg, president and CEO of Ericsson, commented, "This new initiative creates the base for a competence centre in Sweden with the aim of strengthening Ericsson's and Sweden's relations with China." ■

VERY HIGH IP3...to +36dBm

MIXERS

2 to 2500MHz

From $13.95 ea. Qty. (100) IN STOCK

- *Very Wide Band, 2-2500MHz*
- *Very High Isolation, up to 52dB*
- *Very High 1dB Compression, up to +23dBm*
- *Very Low Conversion Loss, from 6.3dB*

It's an industry first...only from Mini-Circuits!

Mini-Circuits shielded RoHS LAVI frequency mixers deliver the breakthrough combination of very high IP3 up to +36dBm, ultra-wideband operation, and outstanding electrical performance.

By combining our advanced ceramic, core & wire, and semi-conductor technologies, we've created these evolutionary broadband mixers that are specially designed to help improve overall dynamic range so you can realize lower distortion and combat interference in today's crowded spectrum. They're the very best, very low in cost, and immediately available off-the-shelf from the world leader in mixer technology, ***Mini-Circuits!***

TYPICAL SPECIFICATIONS

Model No.	Frequency (MHz) RF	LO	IF	LO Pwr. (dBm)	IP3 (dBm)	1dB Comp. (dBm)	Conv.Loss (dB)	Isolation (dB) L-R	L-I	Price $ ea. Qty.(1-9)
LAVI-9VH+	820-870	990-1040	120-220	+19	+36	+23	7.2	46	46	15.95
LAVI-10VH+	300-1000	525-1175	60-875	+21	+33	+20	6.3	50	45	22.95
LAVI-17VH+	470-1730	600-1800	70-1000	+21	+32	+20	6.8	52	50	22.95
LAVI-22VH+	425-2200	525-2400	100-700	+21	+31	+20	7.7	50	45	24.95
LAVI-2VH+	2-1100	2-1100	2-1000	+23	+34	+23	7.5	48	47	24.95
LAVI-25VH+	400-2500	650-2800	70-1500	+23	+32	+20	7.5	50	45	24.95

U.S. Patent Number 6,807,407

Pb RoHS COMPLIANT

Mini-Circuits®

ISO 9001 ISO 14001 CERTIFIED

ALL NEW minicircuits.com

P.O. Box 350166, Brooklyn, New York 11235-0003 (718) 934-4500 Fax (718) 332-4661 For detailed performance specs & shopping online see Mini-Circuits web site

YONI2™ ***The Design Engineers Search Engine*** *Provides ACTUAL Data Instantly From MINI-CIRCUITS At:* ***www.minicircuits.com***

RF/IF MICROWAVE COMPONENTS

412 RevB

Visit http://mwj.hotims.com/11713-81 or use RS# 81 at www.mwjournal.com/info

Global In-building Wireless Systems to Show 20 Percent Annual Growth Rate

Customer's dependence on wireless communications and their adoption of high bandwidth 3G cellular services are the primary drivers of the global growth for in-building wireless systems that extend and create wireless coverage indoors. According to a new study from ABI Research, deployments of these systems are expected to result in revenues in excess of $3.6 B by 2011.

Says ABI Research analyst Dan Shey, "People spend a significant amount of time indoors and, not surprisingly, they also expect indoor access from their outdoor wireless service. But indoor coverage does not just satisfy a need for service convenience; it is also used to improve business productivity." As a result, commercial buildings will be a major focus of the in-building wireless systems industry, affecting carriers, businesses, building owners, equipment manufacturers and solution providers.

Deployments and revenues of in-building wireless systems will be dominated by distributed antenna systems, commanding over 60 percent of the deployments and over 75 percent of the equipment revenues. These systems are most economical for buildings larger than 100,000 square feet, a size where coverage and signal level capacity from outdoor networks into buildings begin to fall significantly.

For buildings smaller than 100,000 square feet, repeaters are the primary solution; however, repeater shipment growth will slow, due to replacement by picocells and femtocells. According to Shey, "Repeaters are a cost-effective way to provide coverage inside buildings but they do not add capacity, which will be needed as 3G services usage increases. New picocells and femtocells, which can be backhauled via an IP connection are a cost-effective way to add capacity and coverage."

ABI Research's study, "In-Building Wireless Systems: Worldwide Deployment Scenarios for Active, Passive and Distributed Antenna Systems, Repeaters, Picocells and Femtocells," provides a comprehensive view of the global in-building wireless systems industry. It examines in-building wireless systems based on the value chain, building size and type; and system type, component, cost and functional capabilities. The analysis is complemented by worldwide forecasts for in-building wireless deployments, revenues, penetration and unit shipments for five global regions: North America, Europe, Asia-Pacific, Latin America and Rest of World. The study forms part of the firm's Wireless Infrastructure Research Service, which includes Research Reports, Research Briefs, Market Data, On-line Data Bases, ABI Insights, the ABI Vendor Matrix and analyst inquiry support.

Founded in 1990 and headquartered in New York, ABI Research maintains global operations supporting annual research programs, intelligence services and market reports in broadband and multimedia, RFID and contactless, M2M, wireless connectivity, mobile wireless, transportation and emerging technologies.

A New Industry Study on Active Electronically Scanned Arrays

The AESAs report details an extensive new study of Active Electronically-Scanned Arrays (AESA), which has just been released by Engalco.

AESAs have been already well proven in many new and upcoming radar systems and are increasingly being adopted for various platforms—with airborne installations (including UAVs) always forming the major segment.

According to Engalco's research, the overall "free world" market value for AESAs will grow from approximately $2.8 B in 2006 to more than $10 B in 2013. Engalco also estimates that the total value of the required transceiver modules will increase from $1.3 B in 2006 to $6 B in 2013 and therefore the requirements for the embedded semiconductors (being mainly X-band MMICs) will exhibit similar strong growth. Power amplifiers, required for every transceiver module, will always lead the market for these specialized semiconductors and GaN-based devices will take over in this application after 2010.

AESAs have a very large growth potential, notably for military end-users. With just one AESA, very high speed, multi-target radar tracking is possible, simultaneously with microwave communications and EW—all available using the same system. In addition, these systems intrinsically exhibit graceful degradation, which results in substantially reduced down times and maintenance costs, compared to traditional radars.

The systems identified and the quantitative data provided in the report are segmented operationally by airborne, land-based and ship-borne installations and geographically by Europe, North America and the "Rest of the World." Space-based AESAs are also considered. In every respect, North America always strongly leads in all markets and for sources of development and production. Markets for all segments are shown in detail within the report, with forecasts extending to 2014. A substantial number of mainly market-data charts are provided as well as more data tables. Transceiver unit prices (ASP) and shipment forecasts are also provided in most instances.

Forthcoming platforms having built-in AESAs are included, as well as AESA-upgrades for existing platforms.

In the report, 14 AESA OEM companies are profiled, with more extensive profiles provided for the major companies that own some of these OEMs.

Engalco is a tech-sector consultancy, industry analysis, market forecasting and publishing concern. With strong experience in all relevant commercial and defense segments, the firm specializes mainly in the RF/microwave, wireless, fiber-optics, photonics and related electronics sectors. The firm has been responsible for several published market reports and the completion of a number of private client projects in these sectors. Engalco's mission is to continue providing a range of vital types of analysis, research and publishing services, in addition to customized consultancy based upon the firm's specialist capabilities.

For further information, contact Engalco at +44 (0) 1262 424 249 (GMT) or e-mail: enquiries@engalco-research.com.

India Expected to Become a Semiconductor Manufacturing Player

India, with growing semiconductor consumption and acceleration in electronics manufacturing activities and with the setting-up of EMS shops, is destined to emerge as an important semiconductor manufacturing location, reports In-Stat. India is one of the fastest growing semiconductor-consuming markets in the world, the high-tech market research firm says. The rise of the middle class is driving the consumer market in India at an astounding pace.

"The semiconductor ecosystem, which is currently dominated by design services and embedded software, will be in place by 2010 with the setting-up of planned semiconductor manufacturing facilities," says Mayank Jain, In-Stat analyst. "Thus, by 2010, India will have the entire semiconductor industry in place, and will be in the reckoning among other Asia semiconductor manufacturing countries."

Recent research by In-Stat found the following:

- The market for semiconductors in India was valued at $1.18 B in 2005 and is forecast to reach $3.09 B by 2010.
- Television sets lead semiconductor consumption in the consumer segment.
- By 2010, communications is anticipated to be the major contributor to semiconductor consumption.

The research, "Indian Semiconductor Market Update: Consumption, Manufacturing and Future Development," gives a five-year forecast for semiconductor consumption in India and points out consumption trends across different segments.

It highlights the drivers in each segment and gives the breakdown of semiconductor products like microprocessors, microcontrollers, memory and DSP across each segment. The major players in various semiconductor segments are discussed to provide an overview of the market's direction. The report also analyzes the semiconductor manufacturing scenario in India.

This report is part of In-Stat's Asia Semiconductor and Manufacturing Service, which tracks semiconductor consumption by applications and by country.

This service forecasts application segments in crucial Asian markets, including China, India, Japan, Korea and Taiwan. Semiconductor manufacturing is also addressed by country and an additional step in identifying the largest markets for semiconductor consumption is presented with a look at CEM and assembly capacity by country. This research is an invaluable tool in identifying business opportunities in the increasingly important Asian marketplace. ■


DID YOU KNOW?

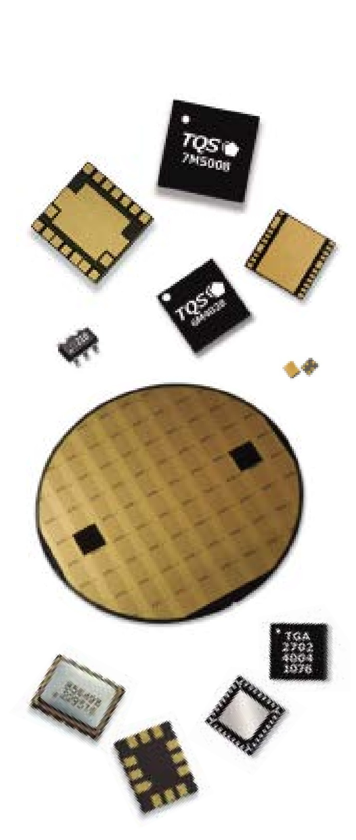

TriQuint Semiconductor is a global telecommunications supplier focused on media interface applications for both RF and optical systems. TriQuint continually strives to lower customers' costs by speeding manufacturing and improving system performance through advanced engineering expertise, dedicated service and forward-looking design. Our unique RF front-end module solutions free-up PC board space for new multimedia applications in wireless handsets.

TriQuint researches, designs and manufactures its products in advanced facilities staffed by some of the world's most creative engineering and service professionals. Design and manufacturing takes place in Oregon, Texas and Florida, with additional design facilities in New England, North Carolina and Germany. Our international locations include production and assembly operations in Costa Rica with sales and applications support in China, Korea and Taiwan. We connect the digital world to the global network as a premier supplier of advanced products based on gallium arsenide (GaAs), SAW and BAW technologies.

WIRELESS HANDSET: TriQuint is the supplier of choice for state-of-the-art RF front-end solutions including every critical module and component for GSM / EDGE, CDMA and WCDMA / HSDPA phones. We offer highly integrated module solutions for the handset RF front-end as well as discrete products including PA modules, pHEMT switches, LNAs, duplexers, triplexers and SAW filters.

BLUETOOTH & BROADBAND: TriQuint is a leading supplier of high-power and low-noise GaAs amplifiers for WLAN manufacturers as well as a wide variety of SAW filters for WLAN, WiFi, CATV / STB and Bluetooth systems, plus GPS and emerging WiMAX chipsets.

and Did You Know TriQuint is a Leader in Value and Innovation?

BASE STATION: TriQuint is a long-established supplier of base station products and leads the world in mobile network SAW filters. Our GaAs devices for communications networks, back-haul (digital) radios as well as custom Foundry designs are also leaders. TriQuint offers customers a full portfolio of general purpose ICs, GaAs MesFET, pHEMT and HFET power transistors (packaged or bare die).

MILITARY & AEROSPACE: TriQuint Semiconductor is proud of its military and aerospace heritage. Today we serve the needs of Defense Department offices and major contractors by providing basic research, modules, components and MMICs for a number of on-going programs. TriQuint parts are built into the newest generations of phased-array radar as well as numerous other communications and counter-measure systems that leverage our BAW, SAW and oscillator expertise. Our specialized GaAs 100mm Foundry services play a vital role in TriQuint military programs, with components appearing in applications as close as terrestrial battlefields, up to the 'middle ground' of orbiting payloads and all the way to far-flung worlds, including the latest generation of Mars rovers: 'Spirit' and 'Opportunity' where TriQuint amplifiers are still at work.

FOUNDRY SERVICES: TriQuint created many of the GaAs processes used to build today's most popular 'standard' microwave products – you can depend on the company that created the process for all your custom circuit needs. TriQuint has expanded its capacity for low-noise, power and logic applications (DC-80 GHz), offering the industry's widest GaAs process selection: HBT, pHEMT, E/D pHEMT, MesFET, PIN, HFET and mHEMT. For value, innovation, security and guaranteed supply, look to TriQuint Semiconductor.

TriQuint Semiconductor...

Connecting the Digital World to the Global Network.™

TriQuint® SEMICONDUCTOR

Phone: +1-503-615-9000 | Fax: +1-503-615-8900 | E-mail: info-sales@tqs.com | Website: www.triquint.com

INDUSTRY NEWS

■ **RF Micro Devices Inc.** (RFMD) announced it has signed an agreement to sell the majority of its Bluetooth® assets to **QUALCOMM** for $39 M. The pending transaction is expected to provide QUALCOMM access to next-generation Bluetooth technology. RFMD anticipates the transaction will enable it to increase its focus on its highest growth wireless business opportunities. Under the agreement, QUALCOMM will acquire the majority of RFMD's Bluetooth assets, including intellectual property, related to RFMD's next-generation SiW1722 and RF4000 series.

■ **Laird Technologies**, a designer and manufacturer of antenna solutions, electromagnetic interference (EMI) shielding products, telematics and thermal management solutions, announced the acquisition of **Steward Inc.** and its subsidiaries for $52.5 M. Steward is a provider of ferrite-based products that are used to remove unwanted EMI "noise" and other signals at unwanted frequencies from conductors. Steward revenues in its fiscal year ending September 30, 2006, were $50 M.

■ **CoorsTek Inc.**, a large technical ceramics supplier and manufacturer of critical components for high technology markets, announced the acquisition of **Gaiser Tool Co.**, a ceramic precision tooling manufacturer based in Ventura, CA with operations in Tokyo, Japan. CoorsTek plans to retain the Gaiser brand while infusing technical and material innovations to further enhance the company's high quality market position. With precision ceramic tools capable of part dimensions as small as 2 µm, CoorsTek also expects to expand its micro-component capabilities for a variety of markets.

■ **Comarco Wireless Test Solutions**, a supplier of wireless test systems for field applications, and **Ascom**, a specialist in wireless onsite communication solutions, announced that the two companies have formed a cooperative alliance to develop and market 3G and 4G wireless network Quality of Service, optimization and test measurement systems. This alliance will create a global leader by positioning the two companies to capitalize on the increasing interest of wireless carriers in improved Quality of Service, as well as the expected deployment of more advanced, high capacity next-generation broadband wireless networks.

■ **Response Microwave Inc.**, a global specialist in providing RF/microwave customer solutions, announced that it has moved into a new, larger facility in Devens, MA. The new facility includes office and meeting space for administrative tasks, as well as a complete microwave test and engineering lab for electrical measurements and simulations. The complete offering of passive control components and Compel connectivity solutions are also stocked within this space, which provides enhancements to existing Framingham and Leominster office areas. The facility is located at 94 Jackson Road, Suite 110, Devens, MA 01434, and all existing contact numbers for the company remain valid.

■ **2Wire**, a provider of broadband service delivery platforms, is expanding operations into the state of Texas, beginning with a new facility in San Antonio. Headquartered in Silicon Valley, 2Wire is rapidly growing to meet the needs of major telecom broadband providers, and plans to hire hundreds of employees to staff the new facility. The San Antonio facility includes a 38,000 square foot call center staffed by more than 500 technical support agents.

■ The **ZigBee™ Alliance**, a global ecosystem of companies creating wireless solutions for use in residential, commercial and industrial applications, announced the first group of ZigBee Certified Products, marking a major milestone in the Alliance's ultimate vision of creating an open, global, wireless sensor and control networking solution. Member companies earning ZigBee Certified Product status include MaxStream, NEC Engineering, S3C and Software Technologies Group.

■ **Provigent**, a provider of system-on-a-chip (SoC) solutions for the broadband wireless transmission market, announced that the company has been shipping lead free components for the past two years. Provigent SoC components are in compliance with the European Union's Restriction of Hazardous Substances (RoHS) legislation.

CONTRACTS

■ **Merrimac Industries Inc.** announced that it has received a contract that could reach a maximum value of $4.3 M over its five-year term from **ITT Corp.** to continue to provide a sophisticated Multi-Mix® multilayer filter assembly for use in an Airborne Electronic Countermeasures (ECM) application. The initial order placed on this contract is valued at $708,000 and is scheduled to be recognized during 2007. Under the terms of this contract, ITT will be able to order varying numbers of filter assemblies to support its Department of Defense contract managed by ITT's Electronic Systems Division.

■ **Triton Services Inc.**, Electron Technology Division, Easton, PA, has been awarded a contract for the development of a new Traveling Wave Tube Amplifier (TWTA) for a shipboard tracking radar. The value of the contract awarded by a European defense contractor exceeds $1 M for the development and the first pre-production lot.

■ **Goodrich Corp.** has been awarded a contract from the US Air Force Unmanned Aerial Vehicle Battlelab (UAVB) at Nellis Air Force Base (Nevada) to develop and fabricate a short-wave infrared (IR) sensor for the Spectre-Finder initiative. The purpose of the initiative is to rapidly demonstrate the potential of a small, air launched and recoverable Unmanned Aircraft System (UAS) to provide off-board sensing in support of future Air Force Special Operations Command concepts of operation. Under the terms of the contract, Goodrich's SUI team, headquartered in Princeton, NJ, will develop a SWIR camera payload assembly.

■ **M2 Global Technology Ltd.**, a San Antonio, TX-based engineering and contract manufacturer of satellite,

microwave, TV broadcast and radio subsystems, has been awarded a US Air Force (USAF) contract to develop an advanced Personal Locator Beacon (PLB). The new PLB will replace the aging AN/URT-33, which is a part of the survival equipment issued to USAF aircrew. The beacon will provide search and rescue satellite-aided tracking capabilities as well as multiple homing signals to assist in the location and rescue of downed aircrew.

■ **Mtel** (formally known as Mobiltel EAD), a wireless operator in Bulgaria, has selected and implemented **Andrew Corp.**'s Odyssey™ cellular radio planning software system to replace a market-leading radio planning tool. Odyssey, used by operators worldwide and backed by Andrew's global customer support services, provides radio frequency design for the complete network lifecycle and is an accurate radio prediction solution. It significantly enhances a wireless operator's ability to save network planning time and infrastructure costs.

■ **Agilent Technologies Inc.** has won a European-wide bid to supply the German Federal Armed Forces with more than 1500 digital storage oscilloscopes (DSO). The 6000 series oscilloscopes will be used by engineers and technicians to test electrical equipment at the maintenance and repair facilities of the German Air Force, Navy and Army.

■ **XCOM Wireless Inc.**, a developer of radio frequency (RF) products, has selected **Innovative Micro Technology** (IMT), a microelectromechanical systems (MEMS) contract manufacturer, to manufacture die for the company's RF MEMS relay product. XCOM and IMT have implemented an effective wafer manufacturing process to produce RF relay die with exceptional performance, reliability and environmental ruggedness.

FINANCIAL NEWS

■ **Plexus Corp.** reports sales of $396.9 M for the fourth quarter of fiscal 2006 ended September 30, 2006, compared to $322.2 M for the same period in 2005. Net income for the quarter was $42.6 M ($0.91/per diluted share), compared to a net income of $10.5 M ($0.24/per diluted share) for the fourth quarter of last year.

■ **Credence Systems Corp.**, a provider of test solutions from design-to-production for the worldwide semiconductor industry, announced that it has entered into separate privately negotiated agreements with certain holders of its outstanding 1.50 percent Convertible Subordinated Notes due 2008 (the "Outstanding Notes") under which such holders have agreed to exchange $72.5 M aggregate principal amount of Outstanding Notes for an equivalent principal amount of a new series of 3.50 percent Convertible Senior Subordinated Notes due 2010 and to purchase an additional $50 M aggregate principal amount of the new series of 3.50 percent Convertible Senior Subordinated Notes due 2010 (together, the "New Notes").

■ **Tower Semiconductor Ltd.** reports sales of $51.5 M for the third quarter ended September 30, 2006, compared to

Truly high-end

R&S®ZVA network analyzer – the culmination of our expertise

When Rohde & Schwarz introduces a new line of high-end products, you can expect the utmost in performance and innovation. The R&S®ZVA is a good example. This family of instruments incorporates the culmination of everything that's possible in network analysis today. Each instrument offers superior RF performance paired with maximum speed, yet it's easy and intuitive to operate. The R&S®ZVA makes amplifier and mixer measurements quick and easy – including with pulsed signals, of course. Intelligent measurement wizards turn the task of making complex settings into a quick and clear-cut process, saving you time and reducing operator errors to a minimum. Let the R&S®ZVA show you just how convenient state-of-the-art network analysis can be!

- Choose from our two-port and four-port models up to 8 GHz, 24 GHz, or 40 GHz (overrange up to 43.5 GHz)
- Complex measurements such as required on high-blocking filters are straightforward owing to exceptional dynamic range and output power
- Two internal signal sources (four-port model) mean fast intermodulation measurements and mixer characterization without an additional signal generator
- High measurement speed, optimized data transfer times, and truly parallel measurements maximize throughput in production
- And, for the first time, a new method enables you to perform pulse profile measurements of very short pulses at high dynamic range and resolution easily and cost-efficiently

ROHDE&SCHWARZ

www.rohde-schwarz.com/ad/zva

$20.6 M for the same period in 2005. Net income for the quarter was $39.5 M ($0.46/per share), compared to a net loss of $55.4 M ($0.83/per share) for the third quarter of last year.

■ **Alereon Inc.**, an ultra-wideband (UWB) technology leader for mobile WiMedia and Wireless USB solutions, announced it has received a $4 M investment from **Samsung Ventures'** strategic technologies investment fund.

PERSONNEL

■ **Lord Bach of Lutterworth** has been named chairman of Selex Sensors and Airborne Systems. Lord Bach, who was UK Minister for Defence Procurement from 2001 to 2005, will bring his deep understanding and experience of the defence environment in the UK and internationally, to support the Group's growth strategy. The company has two main operating subsidiaries, Galileo Avionica S.p.A. (Italy) and Selex Sensors and Airborne Systems Ltd. (UK), with over 4000 employees in the UK. The company also announced the appointment of **Giancarlo Grasso** as chief executive officer, with operational responsibility for the business.

■ Xceive® Corp., a developer of fully integrated multi-standard RF-to-baseband transceiver ICs for TVs, announced that **Rich Beyer**, CEO and director of Intersil Corp., has joined Xceive's board of directors. Following Intersil's acquisition of Elantec Semiconductor Inc. in 2002, Beyer held the position of president in addition to his two current titles. In early 2006, Beyer shifted rolls at Intersil and took his current position as CEO and director. Beyer also serves as director of Credence Systems Corp. and is currently on the board of directors of the Semiconductor Industry Association.

■ Amphenol Corp. announced that it has promoted **R. Adam Norwitt** to the newly created position of president and chief operating officer. Norwitt will focus on enhancing the company's growth in new technologies and new markets. Norwitt will also be assuming an active role in the further strengthening and expansion of the company's existing business, particularly in international markets. Norwitt has held a variety of management, business development and operating positions in Amphenol operations in Asia and the United States since joining Amphenol in 1998. Most recently, he served as senior vice president of the company and group general manager of Amphenol's worldwide RF and microwave products operations.

▲ Mike Edwards

■ Antenova has strengthened its management team with the appointment of **Mike Edwards** as vice president of worldwide sales and marketing and the promotion of **CL Lim** to vice president and general manager of Asia. Edwards' role is to drive the company's global sales activities. He has extensive applica-

▲ CL Lim

tions-oriented product marketing experience in the wireless device, telecoms, computer and telematics market sectors, from start-up firms to large multi-national corporations. Lim is to lead manufacturing and operations in Asia. He has more than 26 years experience in international sales, business development and technical operations and management in the wireless and telecommunication industry, which includes senior roles at Motorola and Sanmina.

▲ *David Smith*

■ Roke Manor Research Ltd. has appointed **David Smith** as managing director. Smith takes responsibility for a company employing more than 450 employees, a turnover of £40 M and a reputation for world-class research and development in both the defense and commercial sectors. He joined Roke in 2000 and became the head of the company's wireless business in 2001, building up the division on the strength of its expertise in cellular technology and defense communications.

■ Kulicke & Soffa Industries Inc. announced the appointment of **Richard Boulanger** as general manager of its die bonder operations located in Berg, Switzerland. Boulanger will be responsible for overall manufacturing, R&D, product development and business operations for the facility, including the development of a next-generation die bonder platform and expansion into new markets throughout the world. Boulanger has extensive experience in semiconductor assembly. Most recently, he served as vice president of the Advanced Semiconductor Assembly Division of Universal Instruments Corp., a business unit that provided full solutions for the precision placement of flip chips and bare die.

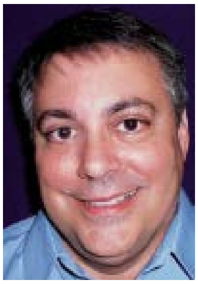

▲ *Paul J. Leo*

■ CobhamDES Corp. announced the addition of **Paul J. Leo** as director, business development for the Cobham Microwave Group. Leo will oversee the domestic and international sales channels and the development of CobhamDES's strategic product integration. Leo brings more than 25 years of experience in domestic and international business development to the industry.

■ RFMW Ltd. announced **Carolyn Evans** as the company's regional sales engineer covering Pennsylvania and southern New Jersey. Evans previous experience includes eight years as a field sales engineer at California Eastern Labs, as well as stints with M/A-COM, Amplifonix and Merrimac.

REP APPOINTMENTS

■ **Digi-Key Corp.** and **Nihon Dempa Kogyo Co. Ltd.** (NDK) announced the signing of a global distribution agreement. One of the fastest growing distributors of electronic components, Digi-Key Corp. ships products to

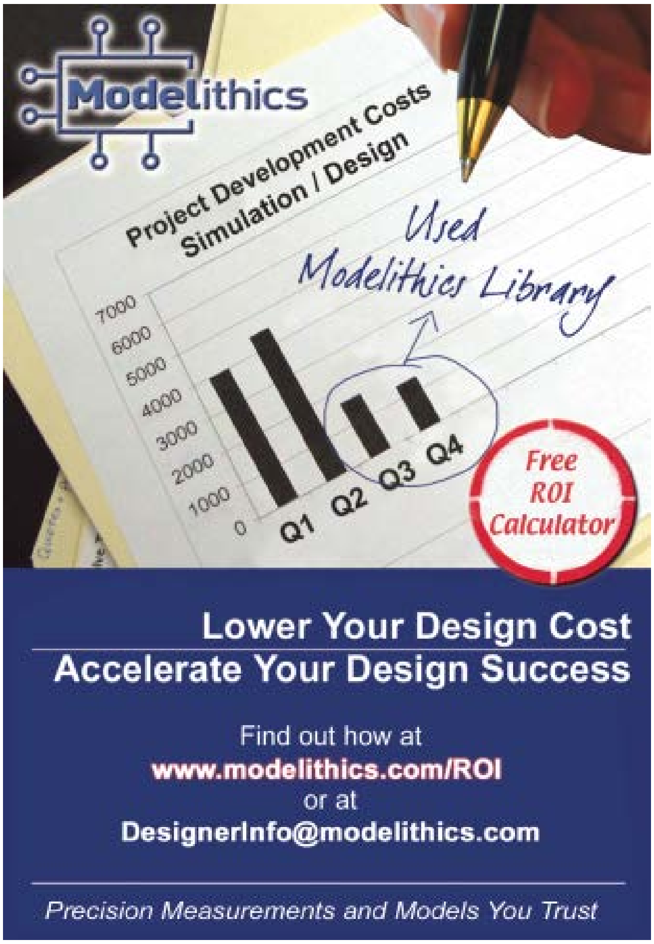

more than 140 countries from its single facility in Minnesota (US). The NDK surface-mount crystals and oscillators stocked by Digi-Key will be featured in both Digi-Key's print and on-line catalogs with this new distribution agreement enabling Digi-Key to fulfill both the design and production needs of its diverse customer base.

■ **Unity Wireless Corp.** announced that it has successfully signed a distribution agreement with Russia's largest wireless equipment distribution company. This agreement now gives Unity much needed relationships and access to Russia's tier-1 wireless network operators for the outdoor and new indoor repeater line of products.

■ **Auriga Measurement Systems LLC** announced the signing of four new representatives for its custom test, characterization, and modeling systems and services. **ProTEQ Solutions Inc.** will be the company's exclusive representative in five New England states while **Jay Stone Associates** (JSA), San Jose, CA, will cover northern California and northern Nevada. Existing representative **CWI Technical Sales** has expanded its territory to the entire east coast beyond New England. **Sematron UK Ltd.** has signed on as exclusive distributor for the UK and Ireland while **Testforce Systems Inc.** will exclusively cover Canada.

■ **MITEQ Inc.** announced the appointment of **SpanTech Microwave Technology S.A.** as the company's exclusive sales representative in Spain and Portugal. SpanTech Microwave will represent MITEQ's Component division of products, which includes amplifiers, mixers, frequency multipliers, passive power components, switches, attenuators, limiters, phase shifters, IF signal processing components, oscillators, synthesizers, integrated multifunction assemblies and fiber optic products. SpanTech Microwave can be contacted at +34-95-241-7024 or e-mail: sales@spantech.es.

■ **Temex** has concluded a representative agreement with **Nearzenith Technologies** to promote and sell the company's range of components, which includes SAW filters, VCOs, PLL synthesizers, crystal resonators and crystal oscillators, in China. Nearzenith Technologies is based in Shenzhen, Guangdong Province, China, and has branches in Hong Kong, Shanghai and Nanjing. The company has 21 employees, annual revenue of $6 M and clients in South, East, Central, Southwest and Northwest China.

■ **W.L. Gore & Associates**, a provider of aerospace wire and high data rate cable, announced **A.E. Petsche Co.** as the exclusive North America distributor of GORE™ Bulk Wire and Cable. This agreement enables Gore to continue to provide its key customers with excellent service and sales support.

■ **Zilker Labs Inc.** announced that it has signed **TLG Electronics Ltd.** as a distribution partner in China. TLG will complement the efforts of Zilker Labs' Asian subsidiary, Hong Kong-based Zilker Labs Asia Ltd., to expand Zilker Labs' Chinese business. Specifically, TLG will focus on forging new customer relationships and providing applications support to developing programs.

Broadband Amplifiers by AML Communications

To Order Call: (805)388-1345 ext. 203

Model	Frequency (GHz)	Gain (dB)	Flatness (dB) max	NF (dB) max	P1dB (dBm) min	VSWR (In/Out)	DC Current @ +12/+15VDC
Broadband Low Noise Amplifiers							
AML016L2802	0.1 – 6.0	28	±1.25	1.3*	+7	2.0:1	190
AML48L3001	4.0 – 8.0	30	±1.0	1.2	+10	1.8:1	150
AML412L3002	4.0 – 12.0	30	±1.5	1.5	+10	1.8:1	150
AML218L0901	2.0 – 18.0	9	±1.0	2.2	+5	2.5:1	60
AML0518L1601-LN	0.5 – 18.0	16	±1.0	2.7	+8	2.2:1	100
AML0126L2202	0.1 – 26.5	22	±2.25	3.5*	+8	2.2:1	170
AML1226L3301	12.0 – 26.5	33	±2.0	2.8	+8	2.5:1	200
Broadband Medium Power Amplifiers							
AML0016P2001	0.01 – 6.0	21	±1.25	3.2*	+23*	2.0:1	480
AML26P3001-2W	2.0 – 6.0	28	±2.5	6	+33	1.8:1	1500
AML28P3002-2W	2.0 – 8.0	30	±2.0	5.5	+33	2.0:1	2000
AML218P3203	2.0 – 18.0	32	±2.5	4	+25	2.0:1	450
AML618P3502-2W	6.0 – 18.0	35	±2.5	4	+33	2.0:1	1850
Narrow Band Low Noise Amplifiers							
AML23L2801	2.8 – 3.1	28	±0.75	0.7	+10	1.8:1	150
AML1414L2401	14.0 – 14.5	24	±0.75	1.5	+10	1.5:1	130
AML1718L2401	17.0 – 18.0	24	±0.75	1.6	+10	1.8:1	150

Low Phase Noise Amplifiers

Part Number	Frequency (GHz)	Gain (dB)	Output Power (dBm)	Phase noise (dBc/Hz) at offset 100Hz	1KHz	10KHz	100KHz
AML811PN0908	8.5 – 11.0	9	17	-154	-159	-167	-170
AML811PN1808	8.5 – 11.0	18	18	-152.5	-157.5	-165.5	-168
AML811PN1508	8.5 – 11.0	15	28	-145.5	-153.5	-158.5	-164.5
AML26PN0904	2.0 – 6.0	9	20	-150	-165	-165	-178
AML26PN1201	2.0 – 6.0	11	15	-155	-160	-160	-175

High Dynamic Range Amplifiers

Part Number	Frequency (MHz)	Gain (dB)	P1dB (dBm)	OIP3 (dBm)	DC
AR01003251X	2 – 32	21	32	52	+28V @ 470mA
AFL30040125	50 – 500	23	28	53	+28V @ 700mA
BP60070024X	20 – 2000	32	30	43	+15V @ 1100mA

*Above 500MHz.

Power Amplifiers by Microwave Power

To Order Call: (408)727-6666 ext. 42

Model	Frequency (GHz)	Psat (dBm)	Psat (W)	P1dB (dBm)	Gain (dB)	DC Current(A) @ +12V or +15V
Broadband Microwave Power Amplifiers						
L0104-43	1 - 4	42.5	17.8	41.5	45	14
L0204-44	2 - 4	44	25	42.5	45	14
L0206-40	2 - 6	40	10	38.5	40	8.5
L0208-41	2 - 8	41	12	40	40	17
L0218-32	2 - 18	32	1.4	31	35	5
L0408-43	4 - 8	43	20	41.5	45	17
L0618-43	6 - 18	43	20	41.5	45	22
L0812-46	8 - 12	46	40	45	45	28
Millimeter-Wave Power Amplifiers						
L1826-34	18 - 26	34	2.5	33	35	4
L1840-27	18 - 40	27	0.5	26	30	2
L2240-28	22 - 40	28.5	0.7	27	30	3
L2630-39	26 - 30	39	8.0	38	40	15
L2632-37	26 - 32	37	5.0	36	38	10
L2640-31	26 - 40	31	1.2	30	30	5
L3040-33	30 - 40	33	2.0	32	33	9
L3337-36	33 - 37	36	4.0	35	40	12
L3640-36	36 - 40	36	4.0	35	40	10

High-Power Rack Mount Amplifiers

Model	Frequency (GHz)	Psat (dBm)	Psat (W)	P1dB (dBm)	Pac (kW)	Height (in)
C071077-52	7.1 - 7.7	52.5	170	51.5	1.8	10.25
C090105-50	9 - 10.5	50	100	49	1	8.75
C140145-50	14 - 14.5	50.5	110	49.5	2	10.25
C1416-46	14 - 16	46	40	45	0.35	5.25
C1820-43	18 - 20	43	20	41.5	0.25	5.25
C2326-40	23 - 26	40	10	39	0.25	5.25
C2630-45	26 - 30	45	30	44	0.45	5.25
C3236-40	32 - 36	40	10	39	0.25	5.25
C3640-39	36 - 40	39	8	38	0.24	5.25

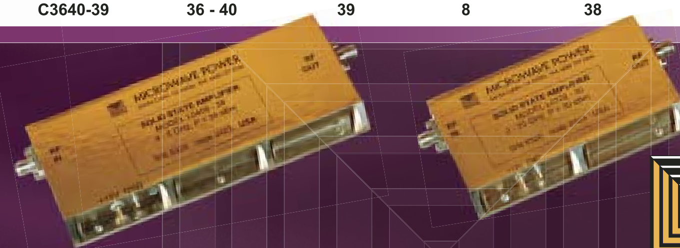

AML Communications

Camarillo, CA (805)388-1345 ext. 203

Over 1000+ amplifiers at

www.amlj.com

Visit http://mwj.hotims.com/11713-18 or use RS# 18 at www.mwjournal.com/info

Look for some serious power at

www.microwavepower.com

Microwave Power

An AML Communications Company

Santa Clara, CA (408)727-6666 ext. 42

Check us out at www.planarelec.com/02

PLANAR electronics technology

RF Distribution Unit

Planar Electronics Technology's new configurable system platform, the PET-VI is user configurable and is easily adaptable to meet many military and commercial requirements. The PET-VI features a 6" color LCD touch screen display which allows easy system control and configuration. This platform consists of three plug and play, field replaceable modules, namely the power supply module, computer module, and the RF module.

Possible Applications:

- Airborne RF Distribution Units
- Broadband Switch Matrices
- RF Attenuation featuring internal computer controlled linearization and touch screen attenuation selection.
- State-of-the-Art Up/Down Converters with integrated options such as linearized attenuation features and many others.
- High Speed Frequency Synthesizers
- Log Amplifiers featuring touch screen log slope selection.
- Multiple RF functions. The PET-VI RF Module can be populated to meet your desired system functions.

Features:

- Airborne Ruggedized 19" Rack Mount Chassis, 6U Height, 18" Deep
- 6" Color LCD Touch Screen Display
- Arcom SBC-GX533 400MHz Single Board Computer featuring AMD Geode GX Processor
- Linux or Windows CE Operating System
- Compact Flash contains all boot up and operation software. Can be removed for security purposes.
- Compatible with RS-232-C, RS-422, RS-485, PECL, TTL, and Ethernet protocols.
- Current monitoring of every internal RF component. Failures are displayed on the front panel display.
- Cooling Fan speed monitoring. Fan failures are displayed on the front panel display.
- RF module internal temp. monitoring. Over temp. conditions are displayed on the front panel display.
- Plug & Play, Modular design allowing in-the-field repairs & flexibility for custom configs. (3 Modules)
  - Power Supply Module can contain any required power supply.
  - Computer Module can be switched out in minutes.
  - RF Module can contain any set of RF components required. Up to 320 individual control lines can be accommodated.

Planar Electronics Technology & Planar Filter Company - (A division of Planar Electronics Technology, Inc.)

Phone: 1.877.PLANAR1 • 301.662.5019 • FAX: 301.662.1731

5715 Industry Lane, Unit 11, Frederick, MD 21704 USA

Email: PET-SALES@planarelec.com • Web: www.planarelec.com/02

FREE on-line order tracking system updated daily.

Track your order on-line at http://www.planarelec.com/OrderStatus/

A CMOS Frequency Synthesizer with Self-biasing Current Source for a 5 GHz Wireless LAN Receiver

This article describes a fully integrated 3.2 GHz synthesizer with a self-biasing current source for a 5 GHz wireless LAN receiver in the lower UNII band from 5.15 to 5.35 GHz. The circuit has been designed using a 0.18 µm one-poly six-metal CMOS technology of UMC. OFDM is considered one of the most attractive transmission techniques for future wireless multimedia communications in frequency selective channels. However, it also has the disadvantage of an increased sensitivity to phase noise generated by the local oscillators inside a communication transceiver. In order to achieve a high performance device, therefore, the simulation tool Simusyn has been implemented to predict the phase noise, spurious emissions and lock time of the synthesizer before its fabrication. The synthesizer consumes 53 mW with a power supply of 3.3 V. Furthermore, it has a bandwidth of 20 kHz and a phase noise of –118 dBc/Hz at 1 MHz offset frequency resulting in a total integrated phase noise over the channel bandwidth less than –32 dBc. Finally, the spurious sidebands at the center of adjacent channels do not exceed –64 dBc. These results made the circuit suitable inside a UNII band 5 GHz wireless LAN receiver.

In the past several years, the wireless local area network (WLAN) market has grown significantly due to the great demand for high speed wireless connectivity. Furthermore, there is a constant desire to keep power consumption, cost and size of the communication devices to a minimum. This has been possible thanks to continuing advances in integrated circuit (IC) technology allowing the development of devices capable of operating at multiple gigahertz carrier frequencies with data rates competitive with established wired alternatives.[1,2] In 1999, the IEEE ratified two wireless networking communications standards named 802.11a and b. The 802.11b standard operates in the 2.4 GHz industrial-

C. Quemada, H. Solar and G. Bistué
Centro de Estudios e Investigaciones Técnicas de Gipuzkoa (CEIT)
San Sebastián, Spain
J. de No and I. Sancho
Escuela Superior de Ingenieros Industriales de San Sebastián (Universidad de Navarra)
Spain

scientific-medical (ISM) band, using direct-sequence spread-spectrum (DSSS) modulation, while the 802.11a standard operates in the 5 GHz unlicensed national information infrastructure (UNII) band. On the other hand, 802.11a employs orthogonal frequency division multiplexing (OFDM) in order to compete more effectively with the peculiarities of indoor propagation.[1] The UNII frequency band provides 300 MHz of spectrum at 5 GHz (see ***Figure 1***). Those 300 MHz are divided into two frequency segments: a contiguous 200 MHz portion from 5.15 to 5.35 GHz and a separate 100 MHz segment from 5.725 to 5.825 GHz. Furthermore, depending on the allowed maximum level of transmitted powers, these frequency assignments are split into three equal domains. The bottom 100 MHz domain is limited to a maximum transmitted power of 50 mW, the next 100 MHz to 250 mW and the top 100 MHz to a maximum of 1 W (outdoor communications).[3] OFDM modulation subdivides a carrier into several individually modulated orthogonal subcarriers, all of which are subsequently transmitted in parallel. This technique mitigates the effect of multi-path. In the 802.11a standard, each OFDM channel consists of 52 subcarriers in a 16.6 MHz bandwidth (channel spacing of 20 MHz); 48 subcarriers are for data, the rest are for error correction (pilot signals).[2,3] Thanks to this subdivision, a variety of data rates with different modulations are possible, permitting different levels of service. Therefore, the data can be modulated with BPSK, QPSK, 16QAM, or 64QAM with data rates of 6 Mb/s, 12 Mb/s, 24 Mb/s and 54 Mb/s, respectively. The medium access control (MAC) protocol used to give multiple users access to a shared environment is the carrier sense multiple access with collision avoidance (CSMA/CA).[3]

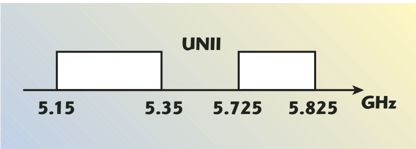

Fig. 1 The UNII frequency band.

The aim of this article is to implement a frequency synthesizer design flow. This design flow achieves two important improvements: prediction of the synthesizer specifications before its fabrication and reduction in the number of fabrication runs, minimizing the overall manufacturing cost and development time. The new generation systems that utilize OFDM modulation are extremely sensitive to phase noise, which is present in the up- and down-conversion synthesizers. Therefore, a proper prediction is essential to design a high performance device. A design flow has been implemented thanks to the development of a Matlab simulation tool that predicts the phase noise, spurious emissions and lock time of a frequency synthesizer with great accuracy before its fabrication. This procedure has been applied to the design of a frequency synthesizer for the IEEE 802.11a standard UNII band from 5.15 to 5.35 GHz. This synthesizer is part of a greater development, focused on the implementation of a heterodyne receiver built in a standard 0.18 µm CMOS technology. This choice is based on the continuing advances made in CMOS technology, which make high volume, low cost and high frequency solutions possible. Finally, since the 802.11a and HIPERLAN2 standards share many performance requirements for the RF signal processing blocks, this synthesizer will also be suitable for HIPERLAN2.[1]

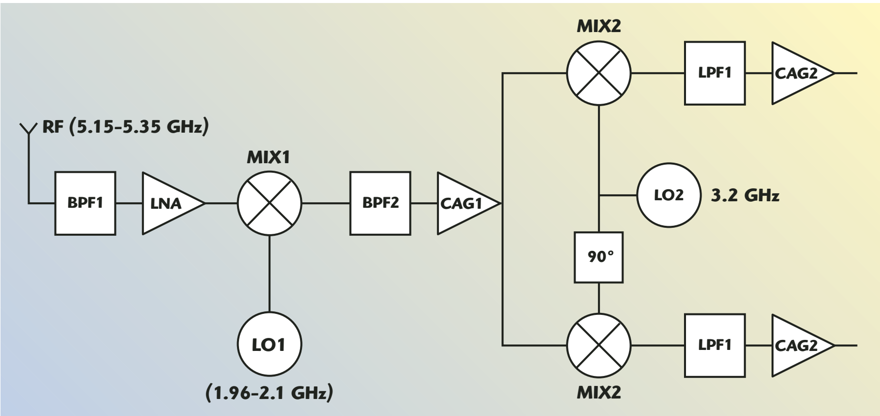

Fig. 2 Receiver architecture.

PERFORMANCE REQUIREMENTS

A rigorous choice of the performance requirements for the synthesizer is fundamental in order to achieve a competitive device within the WLAN market. The most important performance requirements are the operating frequency, frequency stability, crystal reference frequency, phase noise, spurious emissions and lock time. The requirements have been obtained from the IEEE 802.11a and HIPERLAN2 standards, and considering the fact that in a system with OFDM multiplexing, the synthesizer phase noise introduces intercarrier interference (ICI) and leads to a degradation in the signal-to-noise ratio (SNR). The operating frequency of the synthesizer depends on the receiver architecture chosen, which is a heterodyne receiver with the second downconversion in quadrature, as shown in ***Figure 2***. The main focus of this article is the implementation of the second local oscillator (LO2), which works at 3.2 GHz. An external 20 MHz crystal oscillator is used, matching up with the channel spacing for the IEEE 802.11a standard. Furthermore, this standard requires a maximum crystal frequency tolerance of ±20 ppm. Therefore, a crystal frequency tolerance less than that value is acceptable.[3] OFDM systems exhibit a sensitivity to phase noise higher than single carrier modulations. Because of this, the phase-noise specification is a key point in the synthesizer design. For that reason, two phase-noise specifications have been considered: VCO phase noise at 1 MHz offset and synthesizer total integrated phase noise over the channel bandwidth (20 MHz). The phase-noise requirements at 1 MHz offset come from two considerations: interferer strength and sensitivity of the OFDM scheme to phase impairments. With respect of the first consideration, for the highest data rate of 54 Mb/s, the receiver sensitivity is –65 dBm, and allowing for an adjacent interferer 40 dB stronger than

the desired channel, the VCO phase noise needs to be lower than –132 dBc/Hz at 17.3 MHz offset. This result has been obtained by integrating the phase noise over the adjacent channel (20 MHz) and assuming a pre-detection SNR of 19 dB for a BER of 10^{-6} in a 64-QAM system. Since the VCO phase-noise spectrum decreases 20 dB per decade, its value will be –107 dBc/Hz at 1 MHz offset. Furthermore, the degradation added by the second consideration must be included. The phase noise in the OFDM system introduces intercarrier interference (ICI) and leads to a degradation in SNR. For an SNR degradation less than 0.1 dB, the phase-noise specification at 1 MHz offset should be at least –110 dBc/Hz, assuming a 64QAM modulation with subcarrier spacing of 312.5 kHz and pre-detection SNR of 19 dB.[4] Therefore, in order to meet the requirements for the IEEE 802.11a standard, the VCO should have a phase-noise performance of at least –110 dBc/Hz at 1 MHz offset.

What is left to be determined is the total integrated phase noise, which is related to the synthesizer bandwidth. The influence of this requirement in OFDM-WLAN systems is well explained by Côme, et al.[5] According to this reference, a total integrated phase noise of –32 dBc results in low BER degradation for 64QAM modulation. Therefore, with the aim of fulfilling the requirements for the IEEE 802.11a standard, the total integrated phase noise must be at least –32 dBc. The spurious emissions also play an important role in the new generation of OFDM-WLAN systems. In an integer frequency synthesizer, the dominant spurious emissions appear at multiples of the reference frequency, matching up in this case with the crystal oscillator frequency. Using the first consideration made previously for the phase noise, the spurious emissions level should be at least –59 dBc.[4] Finally, the maximum setting time to switch from one channel to another is 1 ms.[3]

ACCURATE PREDICTION IN PHASE-LOCKED LOOPS

Some aspects of the synthesizers, such as phase noise, spurious emissions and lock time (T_L), can be key issues in a communications system design.[6] As previously presented, the present-day systems that utilize OFDM modulation are extremely sensitive to phase noise. Additionally, the reference spurs have a notable influence on the adjacent channel interferer. A high performance design requires an accurate prediction of the phase noise, spurs and lock time. Therefore, a simulation tool has been developed using Matlab to solve this problem. This simulation tool analyses the influence of different synthesizer parameters, such as the output frequency (f_{out}), reference frequency (f_{ref}), VCO gain (K_{vco}), charge pump current (K_ϕ), loop bandwidth (ω_p), spurs attenuation (ATTEN) and the division ratio (N), in the phase noise, spurs and lock time.[7]

Phase-locked Loop (PLL)

A phase-locked loop (PLL) is a feedback system that operates on the

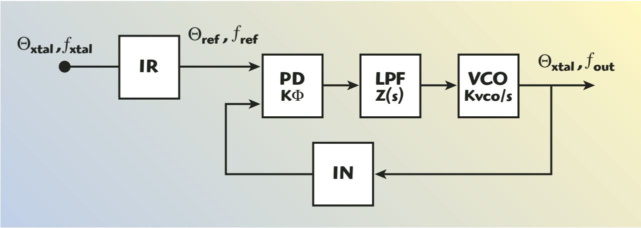

▲ *Fig. 3 Phase-locked loop.*

excess phase of nominally periodic signals. A PLL consists of a phase detector (PD), a low pass filter (LPF), a voltage-controlled oscillator (VCO) and two frequency divisors whose division ratios are N and R (see ***Figure 3***). The filter impedance Z(s) is calculated as the ratio of the output voltage to the input current. The units of K_{vco} and K_ϕ are Hz/V and A, respectively.

Spurs Level

The reference spurs, which appear at multiples of the reference frequency, can be classified into two kinds of spurious emissions: spurs based on leakage currents (leakage spurs) (Equation 1) and spurs based on charge pump mismatches (pulse spurs) (Equation 2)[7]

$$\text{leakage\_spurs} = \text{base\_leakage\_spur} + 20\log\left|\frac{\text{leakage}}{K_\phi}\right| + \text{spur\_gain} \quad (1)$$

$$\text{pulse\_spurs} = \text{base\_pulse\_spur} + 40\log\left|\frac{f_{ref}}{1\text{Hz}}\right| + \text{spur\_gain} \quad (2)$$

where base_leakage_spur is equal to 16 dBc and base_pulse_spur depends on charge pump mismatches, unequal transistor turn-on times and dead-zone elimination circuitry. Leakage is the parasitic leakage current through the charge pump, VCO and loop filter capacitors when the charge pump is in the tri-state state that is ideally high impedance. Finally, spur_gain can be calculated with Equation 3 and the total spur level is obtained by means of the sum of leakage_spurs and pulse_spurs

$$\text{spur\_gain} = 20\log\left|\frac{K_{vco}K_\phi Z(s)}{s}\right|_{s=j2\pi f_{ref}} \quad (3)$$

For older PLLs, where the leakage currents were in the microamp range, it is customary to model the reference spurs based entirely on leakage currents. However, modern PLLs typically have leakage currents of 1 nA or less, and therefore the pulse_spurs tend to be dominant, except at very low reference frequencies.

Phase Noise

The main PLL noise sources usually considered include: phase detector, VCO, crystal reference, frequency divider and loop filter. Equations 4 to 8 allow calculating the contribution to the total phase noise of each noise sources, respectively[7]

$$L_{PD}(f) = L_{1Hz} f_{ref} \left| \frac{G(s)N}{1+G(s)} \right|^2_{s=j2\pi f} \quad (4)$$

$$L_{VCO}(f) = \ell_{vco} \left| \frac{1}{1+G(s)} \right|^2_{s=j2\pi f} \quad (5)$$

$$L_{XTAL}(f) = \ell_{tcxo} f_{ref} \left| \frac{G(s)N}{R\left(1+G(s)\right)} \right|^2_{s=j2\pi f} \quad (6)$$

$$L_{DIV}(f) = \ell_{div} \left| \frac{G(s)N}{1+G(s)} \right|^2_{s=j2\pi f} \quad (7)$$

$$L_{term}(f) = \frac{2kTRK_{vco}{}^2 TR}{f^2} \quad (8)$$

L_{1Hz} = 1 Hz normalized phase detector noise floor
ℓ_{vco} = VCO phase noises
ℓ_{tcxo} = crystal reference phase noises
ℓ_{div} = frequency divider phase noises
TR = transfer function to calculate the noise voltage at the filter output
f = frequency offset
G(s) = Equation 9

$$G(s) = \frac{K_{vco} K_{\phi} Z(s)}{Ns} \quad (9)$$

The normalized phase detector noise floor, L_{1Hz}, is the phase detector noise floor when the reference frequency is 1 Hz and the filter noise, L_{term}, is the thermal noise of any loop filter resistor. The transfer functions that multiply each noise source are obtained through the block diagram. The PLL total output phase noise can be calculated adding the contributions of each noise source given by Equations 4 to 8. At frequency offsets much lower than the loop bandwidth, the phase detector noise is dominant, although the crystal and divider noises can also be considerable. On the other hand, at frequency offsets greater than the loop bandwidth, the VCO phase noise is dominant. Depending on the VCO gain and the resistor values of the loop filter, the thermal noise will be comparable with the VCO noise.

Transient Response

The lock time that a PLL takes to switch from one channel to another is strongly dependent on the loop filter used. For example, the lock time to switch from frequency f_1 to frequency f_2, for a passive third-order loop filter, is given by Equation 10[7]

$$T_L = \frac{-\ln\left(\frac{tol}{f_2 - f_1} \frac{\sqrt{1-\xi^2}}{1 - 2R2C2\xi\omega_n + \left(R2C2\omega_n\right)^2}\right)}{\xi\omega_n} \quad (10)$$

where

ω_n = PLL natural frequency
ξ = PLL damping factor
tol = PLL frequency tolerance

Simulation Tool

The phase noise, spurs and lock time prediction play a decisive role in the frequency synthesizers design. Furthermore, OFDM systems are highly sensitive to phase noise, which is present in the up- and down-con-

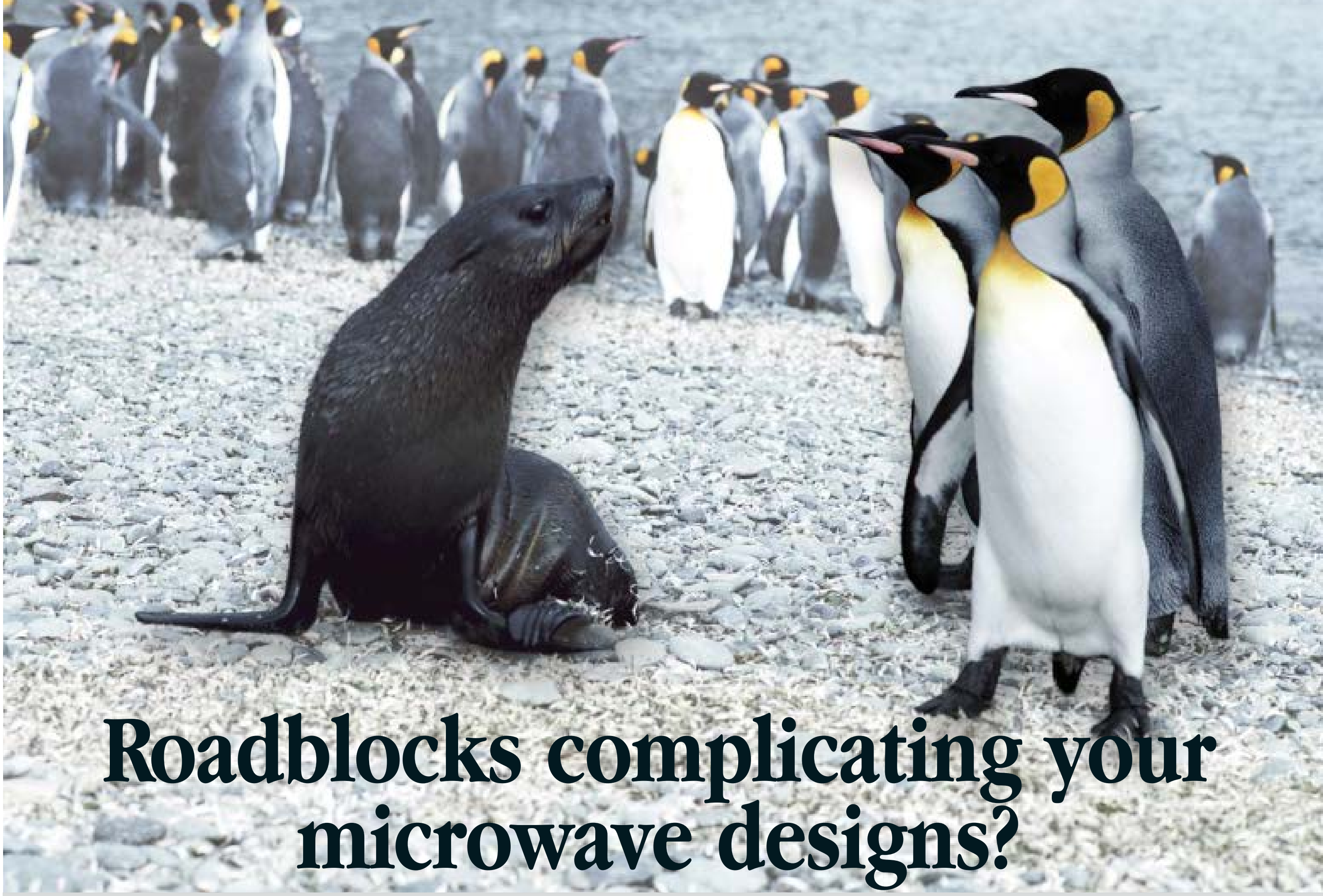

Teledyne Microwave can remove the roadblocks to your microwave designs. We have over 40 years experience as a worldwide leader in the design, development and manufacture of microwave components and integrated assemblies for the **communications**, **aerospace**, **defense**, **aviation** and **instrumentation** markets.

- ❏ **Synthesizer Subsystems**
- ❏ **Integrated Microwave Assemblies**
- ❏ **Transceiver Subsystems**
- ❏ **Power and Low-Noise Amplifiers**
- ❏ **BAW Delay Lines**
- ❏ **Isolators and Circulators**
- ❏ **Filters: Lumped Element, Combline, High Power**
- ❏ **Switched Filters**
- ❏ **YIG Oscillators and Filters**
- ❏ **Frequency Synthesizers**

Let our team help solve your microwave questions. Whether you need component-level or a complete subassembly Teledyne Microwave has the experience and know-how to find the right solution to meet your needs and budget.

Go on-line to order your copy of the new Teledyne Microwave 140-page catalog or CD

A Teledyne Technologies Company

1274 Terra Bella Avenue, Mountain View, CA 94043, Phone: +1-650-962-6944, Fax: +1-650-962-6845
www.teledynemicrowave.com e-mail: microwave@teledyne.com

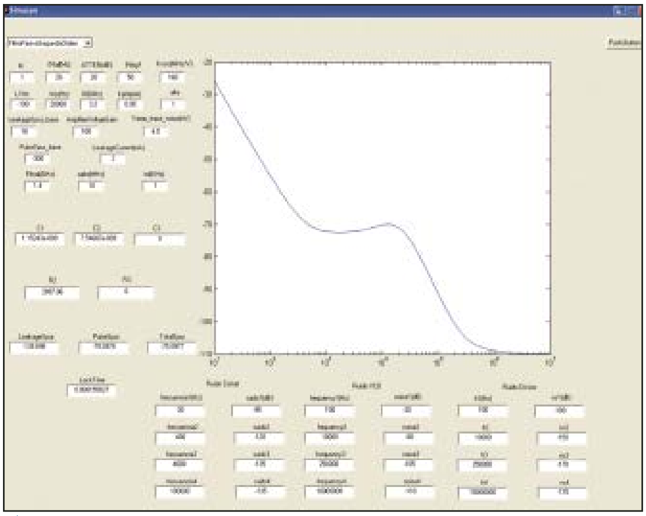

▲ *Fig. 4 Simusyn display.*

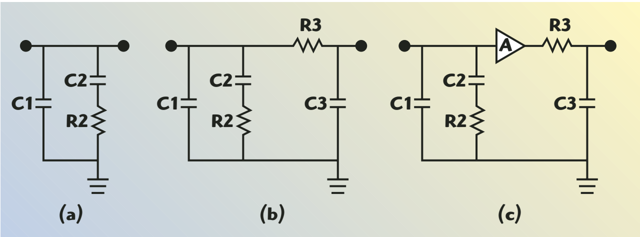

▲ *Fig. 5 Loop filters: (a) second-order passive; (b) third-order passive; and (c) third-order active.*

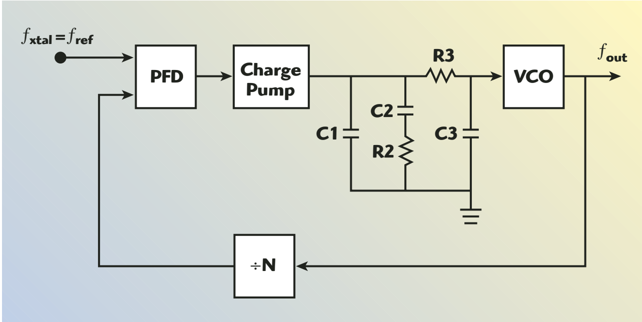

▲ *Fig. 7 Synthesizer architecture.*

version synthesizers. Consequently, a rigorous design requires an effective prediction to estimate accurately the phase noise, spurs and lock time. A simulation tool named Simusyn has been implemented using Matlab (see ***Figure 4***). This software predicts the phase noise, spurs and lock time, and calculates the loop filter components for the following inputs: reference divider, crystal frequency, spurs attenuation, VCO gain, phase margin, L_{1Hz}, loop bandwidth, output frequency, charge pump current, base_leakage_spur, base_pulse_spur, leakage current, frequency step and tolerance for lock time and divider, VCO and crystal reference phase noise. In addition, Simusyn allows using three kinds of loop filters: passive second-order, passive third-order and active third-order loop filters (see ***Figure 5***). If the active loop filter is used, it is necessary to know the amplifier voltage gain (A) and its input noise voltage. The last step before starting the synthesizer design involves verifying the Simusyn results with the measured National Semiconductor's LMX2330L commercial synthesizer. Phase noise, spurs and lock time have been verified for different synthesizer parameters. For example, in ***Figure 6***, the phase noise for charge pump currents of 1 and 4 mA are presented. The rest of the basic parameters include: output frequency of 1.408 GHz, reference frequency of 1 MHz, spurs attenuation of 20 dB, loop bandwidth of 10 kHz and VCO gain of 60 MHz/V. The Simusyn software bases its results on the theoretical expressions shown in this section.[7] Finally, the LMX2330L synthesizers have been controlled using Visual Basic software through the PC parallel port.

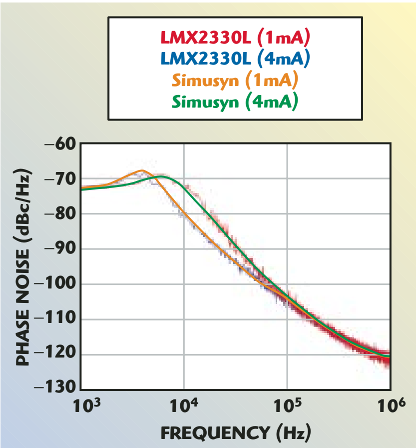

▲ *Fig. 6 LMX2330L phase noise for charge pump currents of 1 and 4 mA.*

DETERMINATION AND PREDICTION OF THE SYNTHESIZER SPECIFICATIONS

It is essential to determine with great precision all the Simusyn inputs to achieve a high performance prediction. For that reason, the synthesizer architecture is chosen and the specifications of each block now must be deduced. Furthermore, this determination tries to be a rigorous design guide that can be used for other devices.

The proposed architecture is an integer-N frequency synthesizer with self-biasing current source and without a reference divider (see ***Figure 7***). Furthermore, a passive third-order filter is employed to achieve additional filtering of the reference spurs. The frequency synthesizer consists of a phase-frequency detector (PFD), a high performance charge pump, an integer frequency divider and a VCO with self-biasing current source. The output signal of the VCO is divided by 160 and then is compared with a reference frequency of 20 MHz. Once the synthesizer architecture has been chosen, it is necessary to determine the general specifications of each block.

Voltage-controlled Oscillator

The voltage-controlled oscillator (VCO) is the core of the frequency synthesizer. A proper synthesizer design depends strongly on the VCO performance. The basic VCO specifications include: output frequency, frequency range, gain, output power and phase noise at 1 MHz offset. The output frequency has been established previously as 3.2 GHz.

The frequency range has been calculated considering the capacitive (four percent) and inductive (one percent) tank tolerances of the CMOS fabrication process with a safety margin of three percent. If the output frequencies were variable, the variation range would have to be included. The tank tolerances are obtained from the research team experience in the design of integrated inductors and varactors.

The frequency range limits are f_{HIGH} (3383 MHz) and f_{LOW} (3031 MHz) and are given by Equations 11 and 12, where L, C and f_{osc} are the inductor value, the varactor value and the VCO oscillation frequency, respectively

$$f_{HIGH} = \frac{1}{2\pi\sqrt{L0.99\ C0.96}}\frac{1}{0.97} = 1.057 f_{osc} \qquad (11)$$

$$f_{LOW} = \frac{1}{2\pi\sqrt{L1.01\ C1.04}}\frac{1}{1.03} = 0.947 f_{osc} \qquad (12)$$

The VCO gain is deduced from the frequency range and tuning voltage. If the tuning voltage is varied from 0.5 to 2.8 V, since the mismatch of the sink and source currents of the charge pump is very high at the power supply rails, the VCO gain is 153 MHz/V.

The phase noise requirement was determined as –110 dBc/Hz at 1 MHz offset. Before designing the VCO, it is essential to verify that this requirement can be fulfilled. For this reason, the quality factor (Q) of the tank required to achieve the required phase noise has been estimated by means of Equation 13, which calculates the necessary quality factor to obtain a certain value of phase noise ($\mathscr{L}$)[8,9]

$$Q = \frac{2kT(1+A)\omega_0}{LV_A^2 C\Delta\omega^2} \qquad (13)$$

where

V_A = differential output amplitude
C = varactor capacitor
A = excess noise factor of the amplifier
ω_0 = oscillation frequency
T = temperature
k = Boltzmann constant
$\Delta\omega$ = frequency offset from the carrier

Since the minimum differential input amplitude of the mixer employed in the frequency down-conversion is 0.5 V, a quality factor of 6.3 is necessary to obtain a phase noise of –110 dBc/Hz at 1 MHz offset, for a varactor capacitance of 0.8 pF and an excess noise factor of 2.[13] This quality factor can be achieved using the inductors and varactors provided by the foundry libraries. For example, in these libraries, there are inductors with a quality factor of 10 at 3.2 GHz and varactors whose quality factor is greater than 40 at 3.2 GHz.[10] Lastly, the output power depends on the mixer employed in the downconversion. In this case, the mixer is passive and needs a minimum input power of –3 dBm.

Charge Pump

The principal specification of this block is the charge pump current. Its value has been established to minimize the power consumption and taking into account that the capacitor in the loop filter next to the VCO is at least three times the VCO input capacitance.[7] Thus, the charge pump current is set to 50 µA.

Loop Filter and Phase-frequency Detector

There are several specifications related to the filter design. First, it is

necessary to choose the order of the loop filter and its gain (passive or active). It will be shown later that the VCO frequency range can be obtained with a passive filter, avoiding the amplifier noise. In addition, a third-order filter is selected to obtain an additional filtering of the reference spurs. There are two specifications related to the loop filter that are quite difficult to predict: $\mathcal{L}_{1Hz}$ and base_pulse_spur.

The 1 Hz normalized phase detector noise floor has a considerable importance in the total integrated phase noise over the channel bandwidth. A priori, it is not possible to predict $\mathcal{L}_{1Hz}$, but two methods have been used to estimate its value. The first is based on Equation 14, which calculates $\mathcal{L}_{1Hz}$ according to the charge pump current, $V_{GS}–V_T$ of the charge pump current source transistors, Boltzmann constant (K), temperature (T) and the time period during which the charge pump is active (t_{qp})[8]

$$L_{1Hz} = \frac{32\pi^2 t_{qp} KT}{K_\phi \left(V_{GS} - V_T\right)} \qquad (14)$$

This method is too optimistic, since using typical values of t_{qp} (5 ns) and $V_{GS}–V_T$ (0.5 V), $\mathcal{L}_{1Hz}$ achieves the value of –216 dBc/Hz. Therefore, the second method will have to be applied. It involves utilizing the worst $\mathcal{L}_{1Hz}$ of the bibliographic revision done by Banerjee[7] about the 1 Hz normalized phase detector noise floor of different commercial synthesizers. Consequently, a 1 Hz normalized noise floor of –200 dBc/Hz is chosen. In addition, this value determines the loop bandwidth. By means of Simusyn and considering the VCO phase noise and the synthesizer total integrated phase-noise specifications, a loop bandwidth of 20 kHz is obtained. Finally, the base_pulse_spur is the last one to complete all Simusyn inputs. This specification is the most difficult to estimate because it depends principally on the charge pump mismatches, unequal transistor turn on times and dead-zone elimination circuitry. There are some expressions given,[7] but they are not very useful in practice. The only solution entails selecting the worst base_pulse_spur (–292 dBc) of Banerjee's bibliographic revision about the spur levels of different commercial synthesizers. In the following section, with the use of CADENCE, base_pulse_spur and $\mathcal{L}_{1Hz}$ will be estimated with greater accuracy.

The values of the filter components are calculated using Simusyn by means of the well-known Application Note AN1001,[15] with the following warnings: the phase margin must be chosen between 40° and 70°; the added spurs attenuation is chosen to fulfill the total spur requirements; and the capacitor in the loop filter next to the VCO is at least three times the VCO input capacitance. Therefore, using Simusyn, the values of the filter components are C1 = 701.88 pF, C2 = 3.06 nF, C3 = 70.18 pF, R2 = 4.39 kΩ and R3 = 340.13Ω for the following input parameters: crystal reference frequency of 20 MHz, ATTEN of 20 dB, a phase margin of 55°, a loop bandwidth of 20 kHz, an output frequency of 3.2

GHz, a charge pump current of 50 µA and a VCO gain of 153 MHz/V.

Furthermore, with the filter components previously calculated, the total reference spurs are at –73 dBc and the total phase noise of the synthesizer is shown in ***Figure 8***, both results being obtained with Simusyn.

SYNTHESIZER BUILDING BLOCKS

Once the specifications of each block have been established, the design of each one is presented. Furthermore, the input specifications of the synthesizer will be determined with higher precision thanks to the use of CADENCE, allowing a more accurate prediction of its phase noise, reference spurs and lock time.

Figure 9 shows the schematic circuit of the VCO. The proposed architecture is a fully integrated differential NMOS VCO with a self-biasing current source. This architecture has been selected to maximize its tuning range. Two cross-coupled transistors with minimum dimensions M1 and M2 generate the negative impedance required to cancel the losses in the LC-tank. An oscillation safety factor of two and on-chip planar inductors have been used in this design. The key to the design of a low phase-noise oscillator is a high quality inductor. Therefore, a thick metal (2 mm) has been used to reduce the series resistance of the inductor. Its geometry has been selected to maximize the

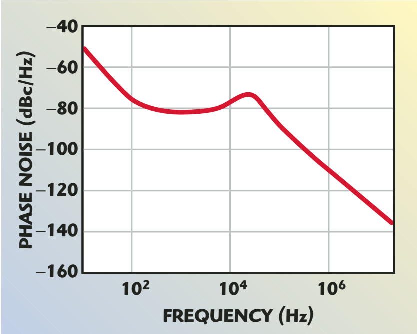

▲ *Fig. 8 Phase noise of the synthesizer.*

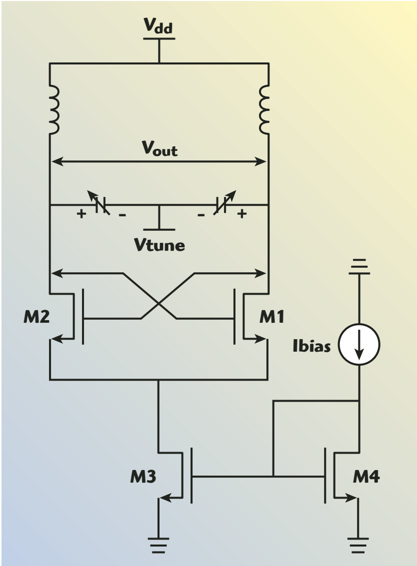

▲ *Fig. 9 Schematic circuit of the VCO.*

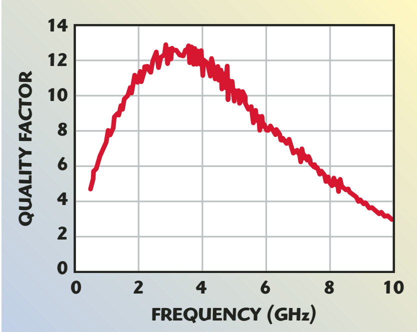

▲ *Fig. 10 Inductor quality factor.*

quality factor. As a result, two spiral inductors of 2.2 nH with a quality factor of 12 at 3.2 GHz have been

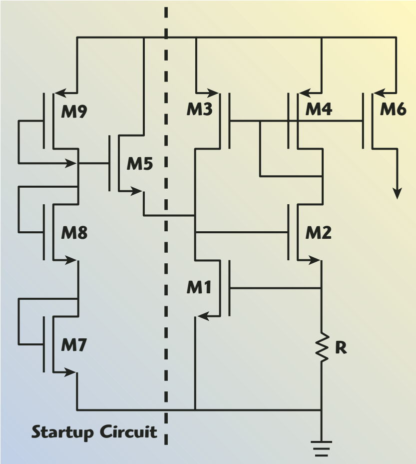

▲ *Fig. 11 Schematic circuit of the self-biasing current source.*

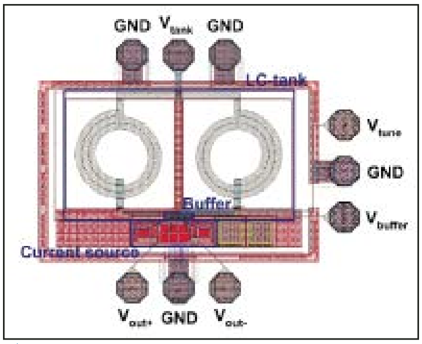

▲ *Fig. 12 Layout of the VCO.*

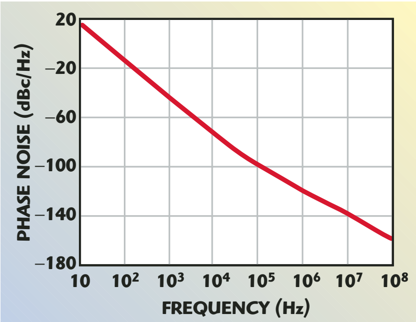

▲ *Fig. 13 VCO phase noise obtained from post-layout simulation.*

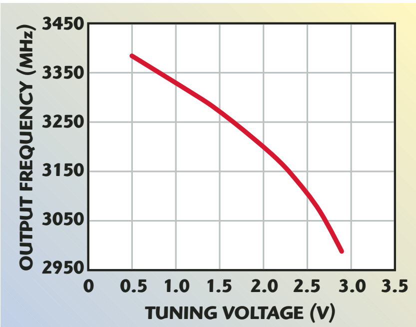

▲ *Fig. 14 VCO tuning range obtained from post-layout simulation.*

employed. The electromagnetic simulation tool Momentum of ADS has been used to achieve high accuracy in its design. Before designing the VCO, the inductors have been measured and modeled. ***Figure 10*** shows the measured quality factor of the inductor. As can be seen, this quality factor is optimized at the output frequency of the synthesizer (3.2 GHz).

The varactors are P-N junction capacitors with a maximum capacitance of 0.88 pF. Each varactor is laid out with 65 fingers, which are 10 µm wide and 161 µm long. The quality factor of these varactors at 3.2 GHz is estimated to exceed 40. The varactors have also been previously measured. The current of the tank is supplied by the self-biasing source shown in ***Figure 11***. A startup circuit has been employed to avoid I_{bias} being zero. The I_{bias} variation is lower than one percent for voltage supply variations of 10 percent.[11] The layout of the VCO is shown in ***Figure 12***, which measures $850 \times 1000\ \mu m^2$, including pads. The two inductors of the oscillator are situated at the top and the varactors are just below. The output buffer and negative resistance transistors are located in the middle of the die, whereas the current source is placed on the bottom.

Post-layout simulations allow determining the specifications of the VCO with high accuracy. In this way, the differential output amplitude of the VCO is 1.73 V, for a total tank current of 6 mA. This amplitude allows obtaining a phase noise of –120 dBc/Hz at 1 MHz offset. The phase noise and tuning range obtained from post-layout simulations are shown in ***Figures 13*** and ***14***, respectively. In order to predict with Simusyn the phase noise, spurs

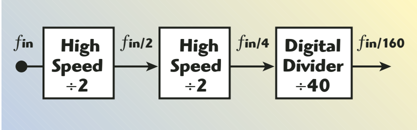

▲ *Fig. 15 Divider block diagram.*

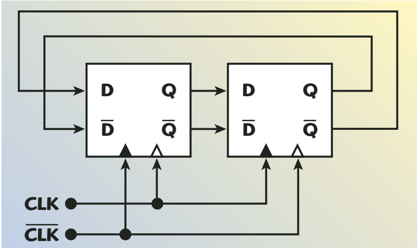

▲ *Fig. 16 High speed divide-by-two.*

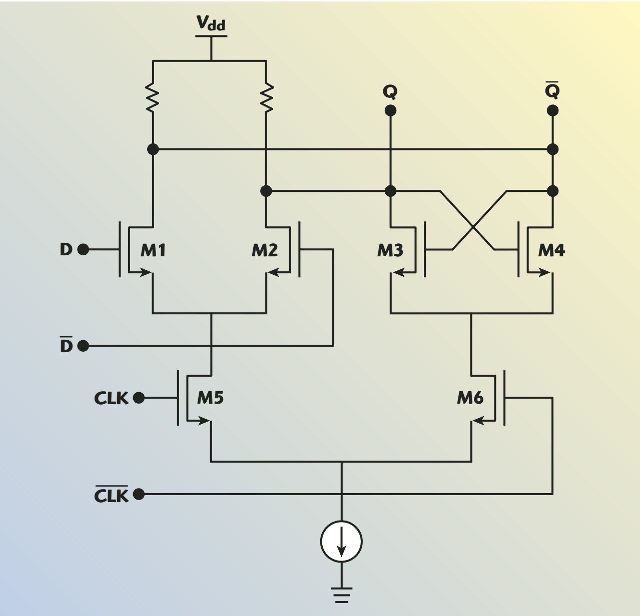

▲ *Fig. 17 Schematic circuit of each high frequency flip-flop.*

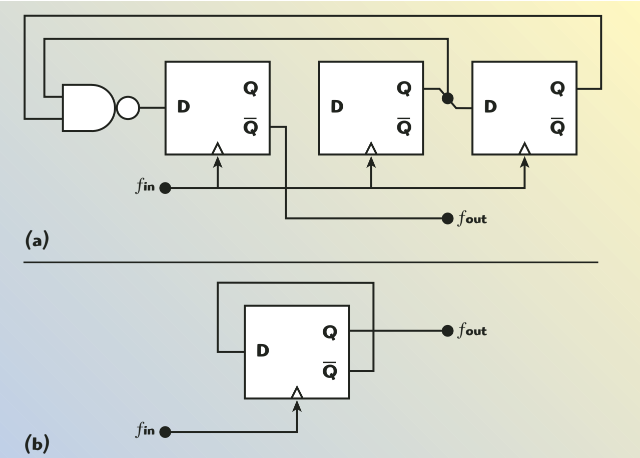

▲ *Fig. 18 The (a) digital divide-by-five and (b) digital divide-by-two.*

COME SEE WHAT'S NEW AT BOOTH 1407.

(WE'RE JUST TWO AISLES FROM THE CONVENTION CENTER RESTAURANT)

New products—and the same rapid response dependability, build-to-order flexibility, and personal attention you'll get only from Tampa Microwave.

We're your supplier of choice for up/down converters, loop test translators, and custom RF assemblies for military and commercial SATCOM. And we've added two exciting new product lines to our family of solutions:

- VIGILCOM™ line of measurement products for surveillance and remote monitoring of terrestrial and satellite communications
- SIGINT products for defense-related signal monitoring in the HF-UHF spectrum

We'll see you at Booth #1407!

TAMPA MICROWAVE™

UP/DOWN BLOCK CONVERTERS • LOOP TEST TRANSLATORS REMOTE SIGNAL MONITORING • SIGINT • CUSTOM RF ASSEMBLIES

813-855-2251 • www.tampamicrowave.com

THE RAPID RESPONSE SUPPLIER OF CHOICE

and lock time with greater safety, the maximum VCO gain will be utilized (~250 MHz/V). This gain is reached when the tuning voltage is 2.8 V. Finally, in order to improve the VCO performance, the following layout issues must be considered: to ensure layout symmetry to minimize the even-order distortion in the differential output signal, the metal track in the tank must be as short as possible to reduce the parasitic capacitance and as wide as possible to reduce the parasitic resistance, choosing a compromise between both of them, differential pairs have a common center to minimize the effect of the process gradient, and to take into account the inductance introduced by the metal track that interconnects the two inductors.

Frequency Divider

Figure 15 shows the divider block diagram. It consists of two high speed divide-by-2 and a digital divide-by-40. The block diagram employed to implement each high speed frequency divider is shown in ***Figure 16***, which consists of two D flip-flops connected in a master/slave configuration. Each D flip-flop is triggered by two complimentary inputs clock signals, CLK and CLKBAR. ***Figure 17*** shows the schematic circuit of a D flip-flop, which has been implemented using source-coupled logic (SCL).[6] The main advantages of this architecture include: as it does not utilize PMOS transistors and the signal goes through only two gates per cycle, this topology is very fast; and it allows very small swings for the input clock. The digital divide-by-40 is made up of three divide-by-2 and one divide-by-5. These digital dividers are implemented with digital D flip-flops and ***Figure 18*** shows their diagram.[8] The design of the first two divide-by-2 has been done especially carefully due to the high specification frequency. Proper sizing of the transistors results in a reasonable speed-power trade-off at gigahertz rates. Since it is a differential device, the layout symmetry plays an essential role in its performance characteristics. The phase noise of the divider obtained from post-layout simulations is –143 dBc/Hz at 10 kHz offset. The layout of the divider is shown in ***Figure 19***. It measures 663 × 734 μm^2, including pads. The high frequency divide-by-4 is placed at the top and the digital divider is located just below. It has been necessary to include a buffer at the output of the divider in order to allow its measurement out of the synthesizer. This buffer is situated at the bottom of the layout. Lastly, the main layout issues, in order to improve the VCO performance, lie in the high frequency divider. As this divider is a differential circuit, the same differential recommendations proposed for the

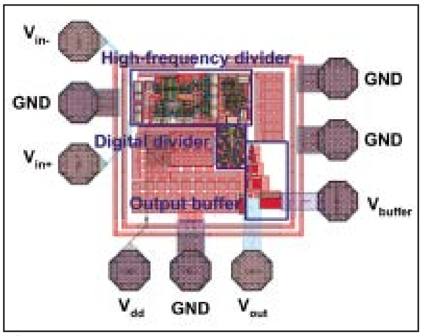

▲ *Fig. 19 Layout of the divider.*

VCO can be also applied. Furthermore, the parasitic capacitances of this divider play an important role at high frequencies. With the aim of reduce them, the following issues must be taken into account: the most external metal layer must be used to make the interconnections, the parallel metal tracks must be very widely spaced, the length of all metal tracks must be minimized and crosses must be avoided between metal tracks.

Phase-frequency Detector and Charge Pump

As shown in ***Figure 20***, the phase detector employed is a phase-frequency detector (PFD), which consists of two digital D flip-flops, a logic gate NAND and a delay that is composed of a certain number of inverter gates. This delay in the PFD reset path is used to avoid the dead zone of the synthesizer, which is the region where the charge pump currents cannot flow proportionally to the phase error. In order to avoid the dead zone, the minimum reset delay of the PFD must be equal to the charge pump switching time. This time can be approximated by the average of the rise time and the fall time of the UU signal.[13] The reset delay is also related to the reference spurs and $\mathcal{L}_{1Hz}$. For this design, four inverter gates have been employed. ***Figure 21*** shows the schematic circuit of the charge pump.[14] This architecture has been implemented to mitigate charge injection errors induced by the parasitic capacitors of the switches and current source transistors. A meticulous sizing of the charge pump transistors and a proper layout are essential for high performance since the reference spurs depend on the charge pump mismatches and unequal transistor turn-on times. The transistors M1 and M2 turn on at every phase comparison instant, therefore any mismatch between their magnitudes, duration, or absolute timing results in a net current that is drawn from the loop filter. Finally, the base_pulse_spur and $\mathcal{L}_{1Hz}$ specifications must be predicted with high precision before building the device. They both have been specified by means of the CADENCE simulation tool. The normalized phase detector noise floor has been considered as a cyclostationary noise. A noise is cyclostationary if its autocorrelation is periodic in time. In this case, the origin is a periodic bias current generating shot noise. Therefore, ***Figure 22*** shows the contribution of noise sources at 20 MHz to the total phase detector noise as a function of time. Calculating the average in a period, a phase detector noise of 2.7267 pA/Hz$^{1/2}$ is obtained. From this result and by means of Equation 14, it is possible to calculate a 1 Hz normalised noise floor of –202.3 dBc/Hz. Consequently, a PLL noise floor of –85.2 dBc/Hz is achieved. Last of all, CADENCE must also be used to specify the base_pulse_spur constant with greater accuracy. Therefore, by processing the discrete Fourier transform (DFT) of the synthesizer output signal for different loop filters when the PLL is locked, a base_pulse_spur value of –289 dBc is obtained. ***Figure 23*** shows the layout of the phase-frequency detector and the charge pump, which measures 850 × 1000 μm^2, including pads. The PFD is situated in the middle and on the left, whereas the charge


Now you can use that
hot plate for what it was
really made for.

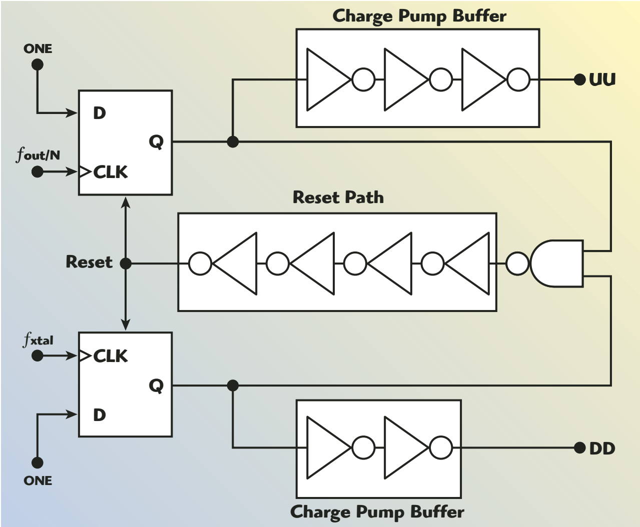

▲ *Fig. 20 Phase-frequency detector.*

pump is located just on the right. A lot of effort has been put into the reduction of charge injections at the switching times. Coupling of the digital signals in the phase-frequency detector and the charge pump to the VCO through the power supply, and noncomplete cancelling of the charge injection in the charge pump switches will modulate the output with a frequency equal to the reference frequency. The charge pump design has been optimised with respect to this aspect, and care has been taken to provide sufficient symmetry in the layout. The layout also contains some power supply decoupling capacitors.

Loop Filter

In the synthesizer architecture shown previously, an off-chip passive third-order filter has been employed to filter the charge pump pulses. As the VCO frequency range can be obtained with a tuning voltage variation from 0.5 to 2.8 V, a passive filter has been chosen. Furthermore, it is of a third-order to give an added attenuation to the reference spurs. Last of all, it is off-chip since the values of its components are too high to integrate them into the chip. Using Simusyn again and the application note AN1001,[15] the values of the filter components are C1 = 1.14 nF, C2 = 5.01 nF, C3 = 114.7 pF, R2 = 2.68 kΩ and R3 = 208.16Ω. These values have been calculated utilizing the maximum VCO gain (~250 MHz/V) in order to predict with Simusyn the phase noise, spurs and lock time with greater safety. This gain has been obtained by means of CADENCE and is reached when the tuning voltage is 2.8 V. The other Simusyn inputs to calculate these values coincide with those given in the determination and prediction of the synthesizer specifications section. Once all Simusyn inputs have been determined with high accuracy using CADENCE, it is possible to predict with Simusyn the phase noise and the spurs of the synthesizer minimizing the estimation error. ***Figure 24*** shows the total phase noise of the synthesizer before its fabrication. In the same way, the reference spurs level obtained with Simusyn does not exceed –70 dBc. Both results fulfill the performance requirements.

RESULTS

The WLAN synthesizer has been implemented using a 0.18 μm one-poly six-metal CMOS technology. ***Figure 25*** shows a micrograph of the synthesizer die with an area of 1 × 1.2 mm, including pads. The circuit has been tested with a 3.3 V supply. The loop filter is

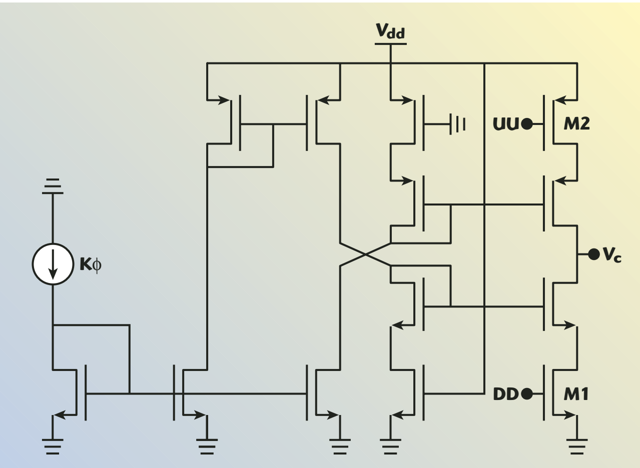

▲ *Fig. 21 Schematic circuit of the charge pump.*

not included on the chip because of the large values of its components.

More than 300 MHz (11 percent of the center frequency) of VCO tuning range is achieved for a tuning voltage variation from 0.5 to 2.8 V. ***Figure 26*** shows a comparison between the measured and simulated VCO tuning range. As can be seen, the operating frequency is reached when the tuning voltage is exactly half that of the power supply (1.65 V). The measured phase noise of the synthesizer is shown in ***Figure 27***. This phase noise is compared with two phase-noise simulations. The blue simulation trace has been obtained with Simusyn for the inputs given, whereas the yellow simulation trace refers to the phase noise simulated with Simusyn when its inputs are specified with CADENCE. The phase noises at 1 and 17.3 MHz offset frequencies are measured to be –118 and –143 dBc/Hz, respectively, which agree well with the values of the last simulation. Therefore, the phase-noise measurements fulfill the initial requirements. The total inte-

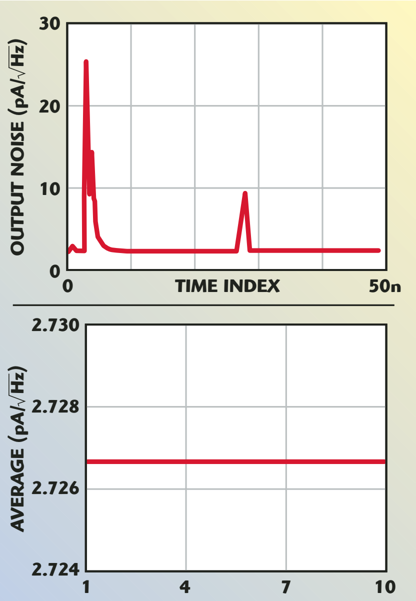

Fig. 22 Cyclostationary noise of the phase detector.

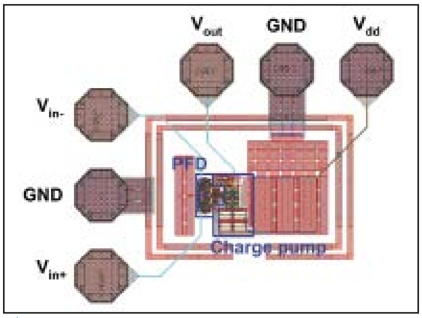

Fig. 23 Layout of the phase-frequency detector and charge pump.

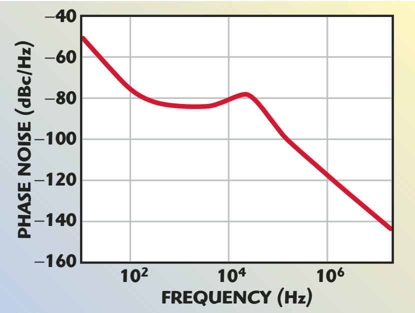

Fig. 24 Phase noise of the synthesizer using Simusyn and CADENCE.

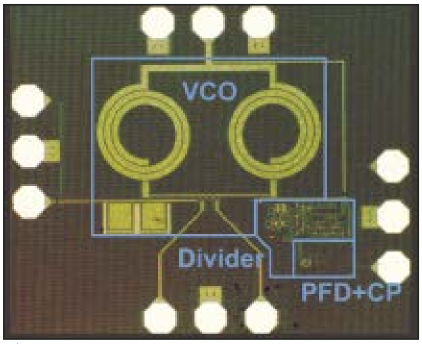

Fig. 25 Microphotograph of the synthesizer die.

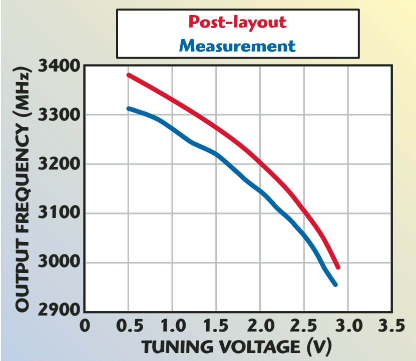

Fig. 26 Comparison between measured and simulated tuning range of the VCO.

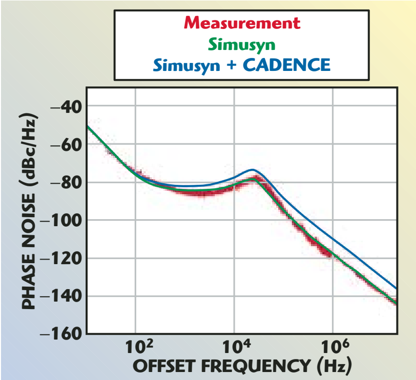

Fig. 27 Comparison between measured and simulated phase noise of the synthesizer.

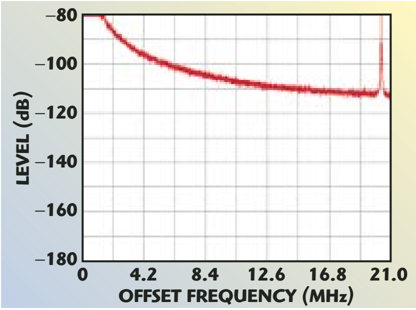

▲ *Fig. 28 Measured phase noise of the synthesizer as a function of offset frequency.*

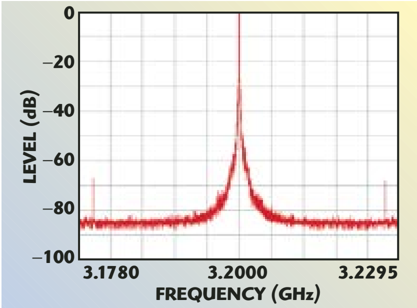

▲ *Fig. 29 Measured spectrum of the synthesizer output signal.*

grated phase noise over the channel bandwidth does not exceed –32 dBc. Furthermore, the measured phase noise of the synthesizer at 17.3 MHz offset is shown in ***Figure 28***. The phase noise of the synthesizer measured at offset frequencies beyond the PLL bandwidth is the inherent phase noise of the VCO. Thus, the phase noise of the VCO at 100 kHz offset is extrapolated to be –98 dBc/Hz, considering a slope of 20 dB per decade. As shown in ***Figure 29***, the reference spurious tones are more than 64 dB below the carrier. This result is also much lower than the original requirement (–59 dBc). The power of the synthesizer differential output signal is approximately 0 dBm, which is much higher than the required power by the down-conversion mixer. ***Table 1*** summarizes the performance of the synthesizer. Of the 53 mW total power consumption, less than 33.1 mW is consumed by the VCO. The self-biasing current source consumes 13.3 mW to supply a tank current of 6 mA. The frequency divider and phase detector consume 19.1 and 0.8 mW, respectively.

Finally, ***Table 2*** presents some of the latest works reported on synthesizers, operating for IEEE 802.11a standard for the UNII band from 5.15 to 5.35 GHz. Clearly, the work in this article compares well with state-of-the-art designs in terms of phase noise, reference spurs, operation frequency and technology.

TABLE I

MEASURED SYNTHESIZER PERFORMANCE

Synthesizer Performance	
Output frequency (GHz)	3.2
Reference frequency (MHz)	20
Channel spacing (MHz)	20
Frequency range (MHz)	> 300
Reference spurs (dBc)	–64
Phase noise@1 MHz (dBc)	–118
Loop bandwidth (kHz)	20
Total integrated phase noise (dBc)	< –32
Output power (dBm)	0
Frequency tolerance (ppm)	< 1
Power Consumption	
VCO (mW)	33.1
Divider (mW)	19.1
PFD + charge pump (mW)	0.8
Supply voltage (V)	3.3
Implementation	
Die area (mm^2)	1.2
Technology	0.18 µm CMOS

CONCLUSION

A low phase-noise fully integrated synthesizer, suitable for a 5 GHz wireless LAN receiver in the UNII band

TABLE II

COMPARISON BETWEEN SYNTHESIZERS FOR THE IEEE 802.11a WLAN STANDARD

	Operation Frequency (GHz)	CMOS Tech. (µm)	Phase Noise @ 1 MHz (dBc/Hz)	Reference Spurs (dBc)	Power Supply (V)	Power Consumption (mW)
This design	3.2	0.18	–118	–64.3	3.3	53
[16]	5.2	0.18	–115	–65	1.8	N/A
[17]	5.2	0.18	–110	N/A	1.8	N/A
[2]	3.5	0.18	–120	N/A	1.8	N/A
[18]	5.4	0.18	–110	–68	1.8	N/A
[19]	4.9	0.24	–101	–54	1.5/2	25
[20]	4.3	0.25	N/A	–58	2.5	117.5

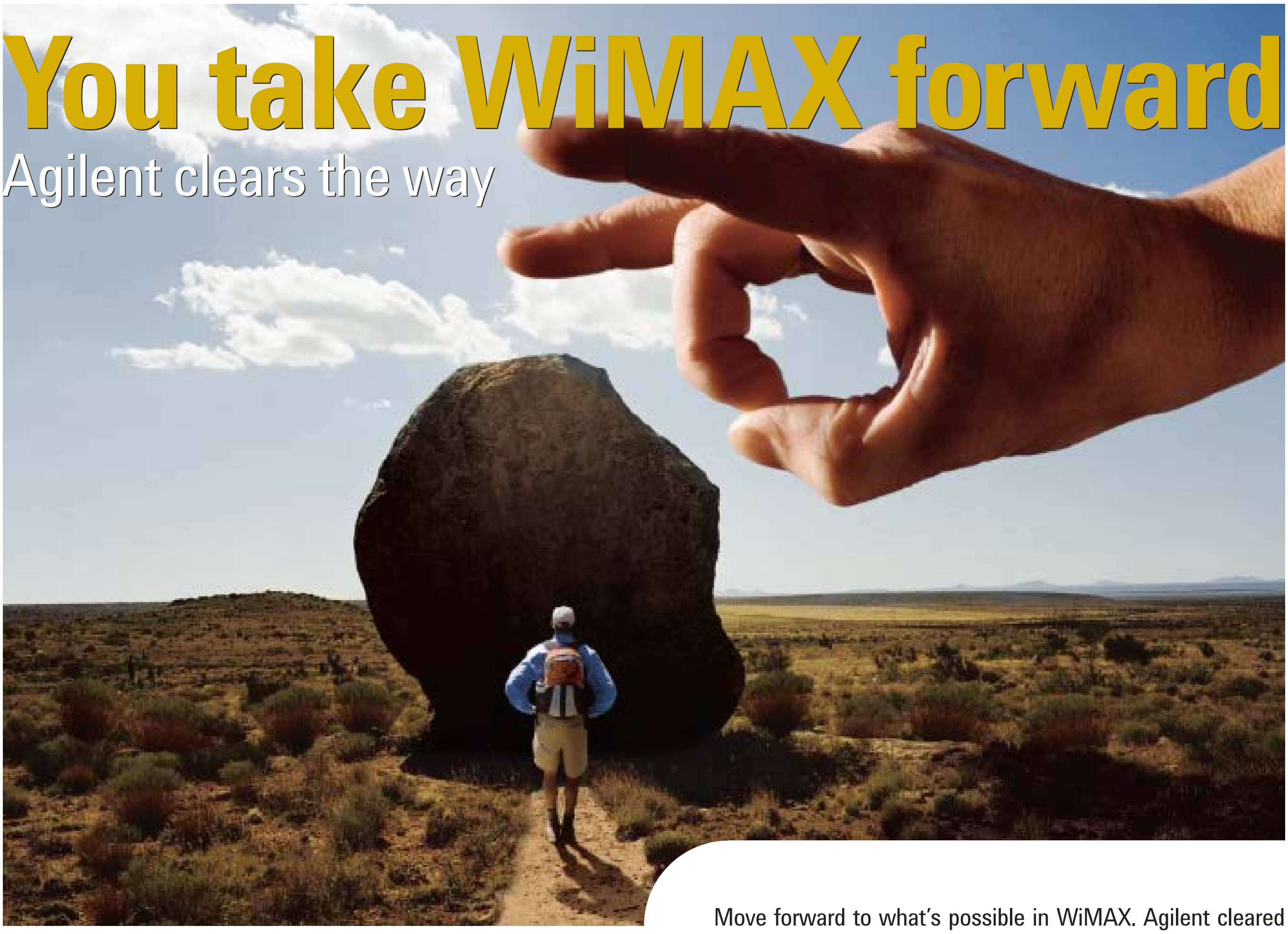

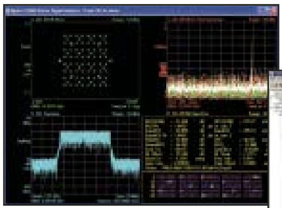

89601A 802.16 WiMAX
modulation analysis software

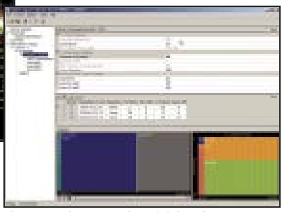

Signal Studio for 802.16 WiMAX

New Agilent MXA and MXG
for 802.16 WiMAX

u.s. 1-800-829-4444

canada 1-877-894-4414

www.agilent.com/find/wimaxad

Move forward to what's possible in WiMAX. Agilent cleared the way for fixed and mobile WiMAX and WiBro with the industry's first design tools. Tools like our Advanced Design System, the ESG signal generator with Signal Studio software, and VSA modulation analysis software have made WiMAX possible. Now, our latest products, like the Agilent MXG signal generators and MXA signal analyzers, can help you anticipate potential roadblocks and get you through them fast and efficiently. Stay ahead, find the edge, move it forward.

To see how Agilent's WiMAX test solutions let you bring your products to market faster, go to www.agilent.com/find/wimaxad. It's WiMAX testing at the edge of possibility.

Agilent Technologies

Visit http://mwj.hotims.com/11713-12 or use RS# 12 at www.mwjournal.com/info

from 5.15 to 5.35 GHz, has been designed. Through the development of Simusyn, the synthesizer's phase noise, reference spurs and lock time have been predicted with high accuracy before its fabrication. The use of high quality inductors, optimized at the operation frequency, allows obtaining a low phase-noise VCO. The use of a self-biasing current source in the tank provides a greater safety in the transconductance value and permits operation along more extreme operating points. The integrated synthesizer consists of a VCO with 0 dBm of output power and phase noise of –98 dBc/Hz at 100 kHz offset, a charge pump that mitigates the charge injection errors induced by the parasitic capacitors of the switches and current source transistors, and a fixed divide-by-160 circuit. The total phase noise of the synthesizer is –143 dBc/Hz at 17.3 MHz offset and the reference spurious does not exceed –64 dBc. With this phase noise and a loop bandwidth of 20 kHz, the total integrated phase noise of the synthesizer over the channel bandwidth is less than –32 dBc. Finally, the designed synthesizer consumes 53 mW with a power supply of 3.3 V. ■

References

1. T.H. Lee, H. Samavati and H.R. Rategh, "5 GHz CMOS Wireless LANs," *IEEE Transactions on Microwave Theory and Techniques*, Vol. 50, No. 1, January 2002, pp. 268–280.
2. P. Zhang, T. Nguyen, C. Lam, D. Gambetta, T. Soorapanth, B. Cheng, S. Hart, I. Sever, T. Bourdi, A. Tham and B. Razavi, "A 5 GHz Direct-conversion CMOS Transceiver," *IEEE Journal of Solid-State Circuits*, Vol. 38, No. 12, December 2003, pp. 2232–2237.
3. "Wireless LAN Medium Access Control (MAC) and Physical Layer (PHY) Specifications: High Speed Physical Layer in the 5 GHz Band," *IEEE Standard 802.11a*-1999, 2000.
4. J. Bhattacharjee, D. Mukherjee, E. Gebara, S. Nuttinck and J. Laskar, "A 5.8 GHz Fully Integrated Low Power Low Phase Noise CMOS LC VCO for WLAN Applications," *2002 IEEE MTT-S International Microwave Symposium Digest*, Vol. 1, pp. 585–588.
5. B. Côme, R. Ness, S. Donnay, L. Van der Perre, W. Eberle, P. Wambacq, M. Engels and I. Bolsens, "Impact of Front-end Non-idealities on Bit Error Rate Performances of WLAN-OFDM Transceivers," *Proceedings of the 2000 RAWCON*, pp. 91–94.
6. B. Razavi, *RF Microelectronics*, Prentice Hall, Los Angeles, CA, 1997.
7. D. Banerjee, *Performance, Simulation and Design*, Second Edition, National Semiconductor, 2001.
8. J. Craninckx and M. Steyaert, *Wireless CMOS Frequency Synthesizer Design*, Kluver Academic Publishers, Boston, MA, 1998.
9. J. Craninckx and M.S.J. Steyaert, "A 1.8 GHz Low Phase-noise CMOS VCO Using Optimized Hollow Spiral Inductors," *IEEE Journal of Solid State Circuits*, Vol. 32, No. 5, May 1997, pp. 736–744.
10. http://www.umc.com.
11. R.J. Baker, H.W. Li and D.E. Boyce, *Circuit Design, Layout, and Simulation*, IEEE Press, New York, NY, 1998.
12. F.W. Grover, *Inductance Calculations*, Van Nostrand, New York, NY, 1962.
13. H. Lee, T. Ahn, D. Jung and B. Park, "Scheme for No Dead Zone, Fast PFD Design," *Journal of the Korean Physical Society*, Vol. 40, No. 4, April 2002, pp. 543–545.
14. C. Lam and B. Razavi, "A 2.6 GHz/5.2 GHz Frequency Synthesizer in 0.4 μm CMOS Technology," *1999 VLSI Circuits Symposium Digest of Technical Papers*, pp. 117–120.
15. W.O. Keese, "An Analysis and Performance Evaluation of a Passive Filter Design Technique for Charge Pump Phase-locked Loops," *National Semiconductor, Application Note 1001*, May 1996.
16. I. Vassiliou, K. Vavelidis, T. Georgantas, S. Plevridis, N. Haralabidis, G. Kamoulakos, C. Kapnistis, S. Kavadias, Y. Kokolakis, P. Merakos, J.C. Rudell, A. Yamanaka, S. Bouras and I. Bouras, "A Single-chip Digitally Calibrated 5.15 to 5.825 GHz, 0.18 μm CMOS Transceiver for 802.11a Wireless LAN," *IEEE Journal of Solid-State Circuits*, Vol. 38, No. 12, December 2003, pp. 2221–2229.
17. A.R. Behzad, Z.M. Shi, S.B. Anand, L. Lin, K.A. Carter, M.S. Kappes, T. Lin, T. Nguyen, D. Yuan, S. Wu, V. Fong, A. Rofougaran and Y.C. Wong, "A 5 GHz Direct-conversion CMOS Transceiver Utilizing Automatic Frequency Control for the IEEE 802.11a Wireless LAN Standard," *IEEE Journal of Solid-State Circuits*, Vol. 38, No. 12, December 2003, pp. 2209–2220.
18. P. Zhang, L. Der, D. Guo, I. Server, T. Bourdi, C. Lam, A. Zolfaghari, J. Chen, D. Gambetta, B. Cheng, S. Gower, S. Hart, L. Huynh, T. Nguyen and B. Razavi, "A CMOS Direct-conversion Transceiver for IEEE 802.11a/b/g WLANs," *Proceedings of the 2004 IEEE Custom Integrated Circuits Conference*, pp. 409–412.
19. H. Rategh, H. Samavati and T. Lee, "A CMOS Frequency Synthesizer with an Injection-locked Frequency Divider for a 5 GHz Wireless LAN Receiver," *IEEE Journal of Solid-State Circuits*, Vol. 35, No. 5, May 2000, pp. 780–787.
20. F. Herzel, G. Fischer and H. Gustat, "An Integrated CMOS RF Synthesizer for 802.11a Wireless LAN," *IEEE Journal of Solid-State Circuits*, Vol. 38, No. 10, October 2003, pp. 1767–1770.

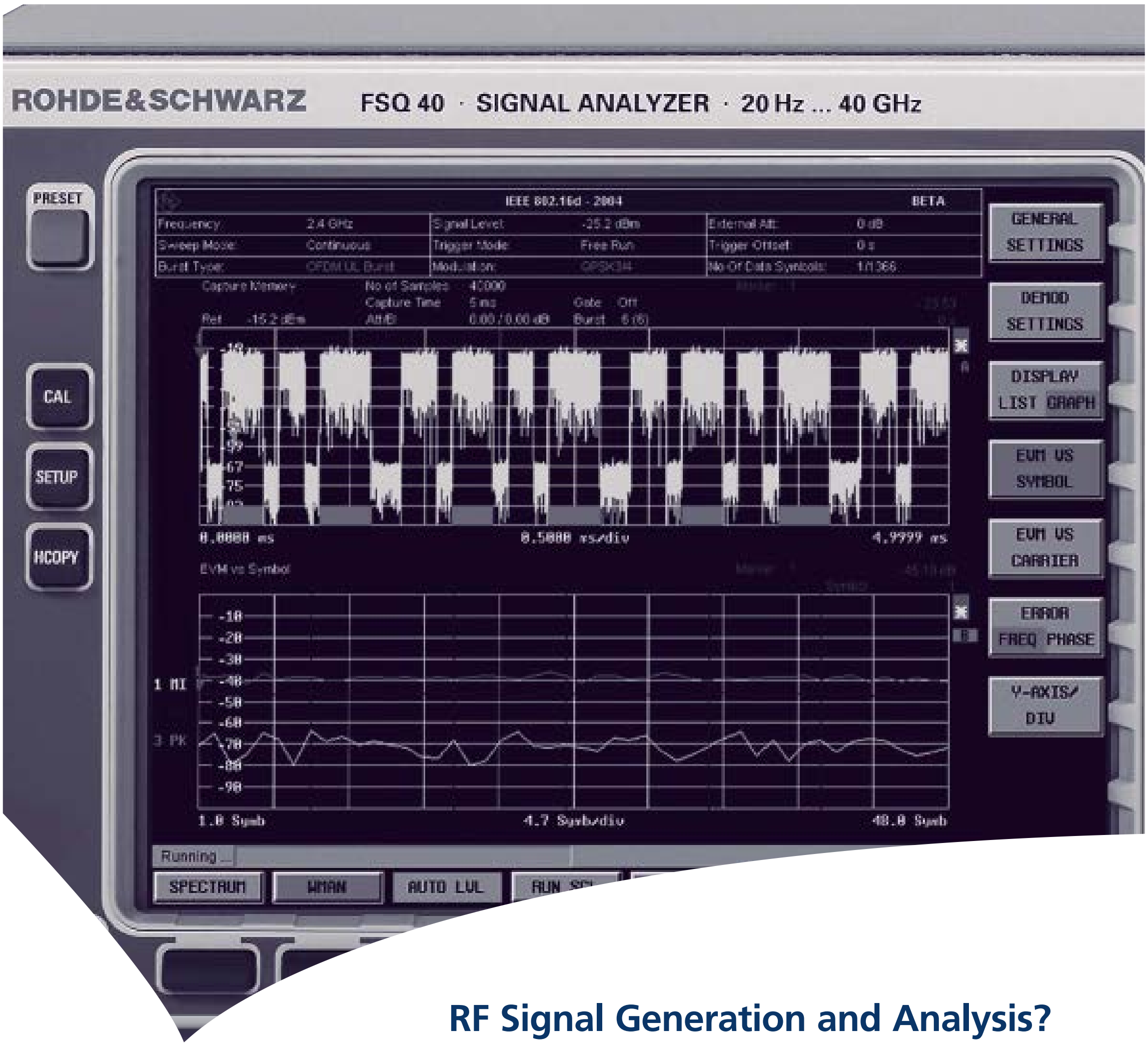

RF Signal Generation and Analysis?

Look inside for a selection of test equipment available for R&D, Production and Field applications

Livingston

The Right Technology - when you want it!

Vector Network Analysis

High-end Instruments for complex Vector Analysis Measurements

Agilent E5071C Network Analyser

Agilent E5071C Network Analyser
The Agilent E5071C Network Analyser offers the highest RF performance and fastest speed in its class, with a wide frequency range and versatile functions. The Agilent E5071C is the ideal solution for manufacturing and R&D engineers evaluating RF components and circuits from 9kHz to 8.5GHz.

Rohde & Schwarz ZVB Vector Network Analyser
The Rohde & Schwarz ZVB Vector Network Analyser covering the frequency range from 300kHz to 8GHz and 10MHz to 20GHz has been designed for universal measurements on passive and active components.

Anritsu MS462xA Transmission/Reflection Analyser
The MS462xA is the economical choice for transmission/reflection analysis (one path - two port network analyser). The "A" model has a 2-port configuration and is available in the frequency ranges of 10MHz to 6GHz (or 3GHz).

Anritsu MS2024 Vector Network Analyser
VNA Master MS2024A is a handheld Vector Network Analyser designed to make accurate vector corrected 1-port magnitude, phase, and Distance-To-Fault measurements and 1-path 2-port magnitude and phase measurements from 2MHz to 4GHz.

Spectrum Analysis

Spectrum Analysers to cope with the demands of modern RF Design

Rohde & Schwarz FSQ Signal Analyser

Rohde & Schwarz FSQ Signal Analyser
The Rohde & Schwarz FSQ Signal Analyser combines two instruments in one. It offers signal analysis at a demodulation bandwidth of up to 120MHz with the dynamic range of a high-end spectrum analyser.

Agilent E4407B Spectrum Analyser
The Agilent ESA-E Series mid-performance spectrum analyser sets the performance standard in measurement speed, dynamic range, accuracy, and resolving power for similarly priced products. Its flexible platform design appeals to R&D, manufacturing, and field service engineers.

Tektronix RSA3408A Real Time Spectrum Analyser
The Tektronix RSA3408A offers the ability of Real-Time Analysis, capturing up to 36MHz into memory, providing a unique understanding of time varying RF signals.

Anritsu MS2721A Spectrum Analyser
The MS2721A is the first fully-functional handheld spectrum analyser designed to conduct highly accurate analysis on the new wave of wireless LAN and cellular signals, including 802.11a, 3G, ultra-wideband and WiMAX.

If you can't see what you're looking for, please give us a call.

Tel 0845 4583274

Signal Generation

Signal Sources with the added flexibility of scalable Modulation Encoders

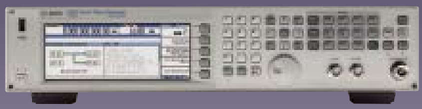

Agilent N5182A Signal Generator

Agilent N5182A Signal Generator

Featuring fast frequency, amplitude, and waveform switching, industry-best ACPR performance, high reliability, and simplified self-maintenance – all in two rack units (2RU) – Agilent MXG vector is optimised for manufacturing cellular communications and wireless connectivity components.

Rohde & Schwarz SMU200A Vector Signal Generator

The Rohde & Schwarz SMU200A Vector Signal Generator has been designed to meet all requirements encountered in research and development of modern communication systems as well as in their production.

Anritsu MG3681A Digital Modulation Signal Generator

The MG3681A is a high performance digital modulation signal generator that incorporates a broadband vector modulator. It has a frequency range of 250kHz to 3000MHz, covering the frequency bands of all major mobile communications systems.

Rohde & Schwarz SMJ100A Vector Signal Generator

The SMJ100A covers all the important frequency bands essential in digital RF transmission. The internal baseband generator option handles a multitude of digital standards, e.g. GSM/EDGE, W-CDMA, Wi-Max. Its characteristics make the R&S SMJ100A the ideal all-purpose vector signal generator.

RF Miscellaneous

Essential tools for all Radio Frequency Engineers/Designers

Agilent N8975A Noise Figure Analyser

Agilent N8975A Noise Figure Analyser

The Agilent N8975A is a high performance noise figure analyser designed to make fast, accurate and repeatable noise figure measurement.
With the N8975A ease of use features, you can set up complex measurements simply and easily giving you repeatable and reliable results you can trust.

Rohde & Schwarz NRT Power Meter

Compared to low-cost instruments, power meters like NRT provide a number of benefits: most importantly high measurement accuracy through excellent directivity and a measurement method that determines the average power like a thermal power meter.

Anritsu ML2480A Power Meter

The ML2480A series power meter and MA2491A Wideband Sensor have been designed for modern high-speed communication and aerospace applications. The ML2480A series has a 20MHz Signal Bandwidth and a 64 MS/s sample rate.

Agilent E4419B Power Meter

The E4419B power meter is designed for bench and automatic test equipment (ATE) use. It provides true dual-channel power meter capability, with two simultaneous power readings and fast measurement speed (up to 100 readings per second) over the GPIB, with E-series sensors.

Or go on-line to view our product catalogue.

www.livingston.co.uk

RF Components and Circuits need to be characterised and specified as part of the design, production and often, commissioning process. With the right test equipment for the job, the process can be straightforward, reliable and repeatable. Here at Livingston we aim to have a solution for all your RF needs from Vector Network and Spectrum Analysis to Signal Generation and Power measurements. Depending on your specific needs, choose from our range of Short Term Rental, Project Rental or Leasing solutions.

To find out how we can support your RF generation and measurement requirements now and in the future, please call our Applications Engineers on 0845 4583274 or visit our website www.livingston.co.uk

Livingston UK Limited

United Kingdom
Livingston House
2 Queens Road
Teddington
Middlesex
TW11 0LB

t 020 8943 5151
f 020 8977 6431
e sales@livingston.co.uk

Scotland
Phoenix House
13b Oakbank Parkway
Livingston
West Lothian
EH53 OTH

t 01506 442288
f 01506 442289
e alba@livingston.co.uk

www.livingston.co.uk

Livingston

The Right Technology - when you want it!

VCOs

10 to 4400MHz from $11.95 ea. (qty. 5)

Want a miniature surface mount, shielded plug-in, or rugged connectorized voltage controlled oscillator with the right stuff for your project? Contact Mini-Circuits! From custom designs to standard catalog models ***always in stock***, we'll supply extra robust, 100% tested VCO solutions you need at a price you can afford. Choose from narrow, to broad, to octave bandwidths. Select from models with low phase noise, linear tuning, load insensitivity, dual output, wide modulation bandwidths, or 5V models optimized for PLL ICs and synthesizers. And pick from an innovative array of miniature surface mount packages as small as 0.25" square, all featuring our exclusive glue-down process on each circuit component to give you ultimate reliability during reflow soldering. You can quickly find the model you need using our online catalog or "The YONI2 Search Engine" at the Mini-Circuits web site.
With YONI2, you just enter your specs…click…and immediately start evaluating suggested VCO solutions using the actual measured performance data displayed. But perhaps you need a custom design.
Not a problem! Contact us for our fast response, low prices, and quick turnaround. For your commercial, industrial, and military applications, choose Mini-Circuits VCOs!

RoHS COMPLIANT

RoHS models available, consult factory.

Mini-Circuits ...we're redefining what VALUE is all about!

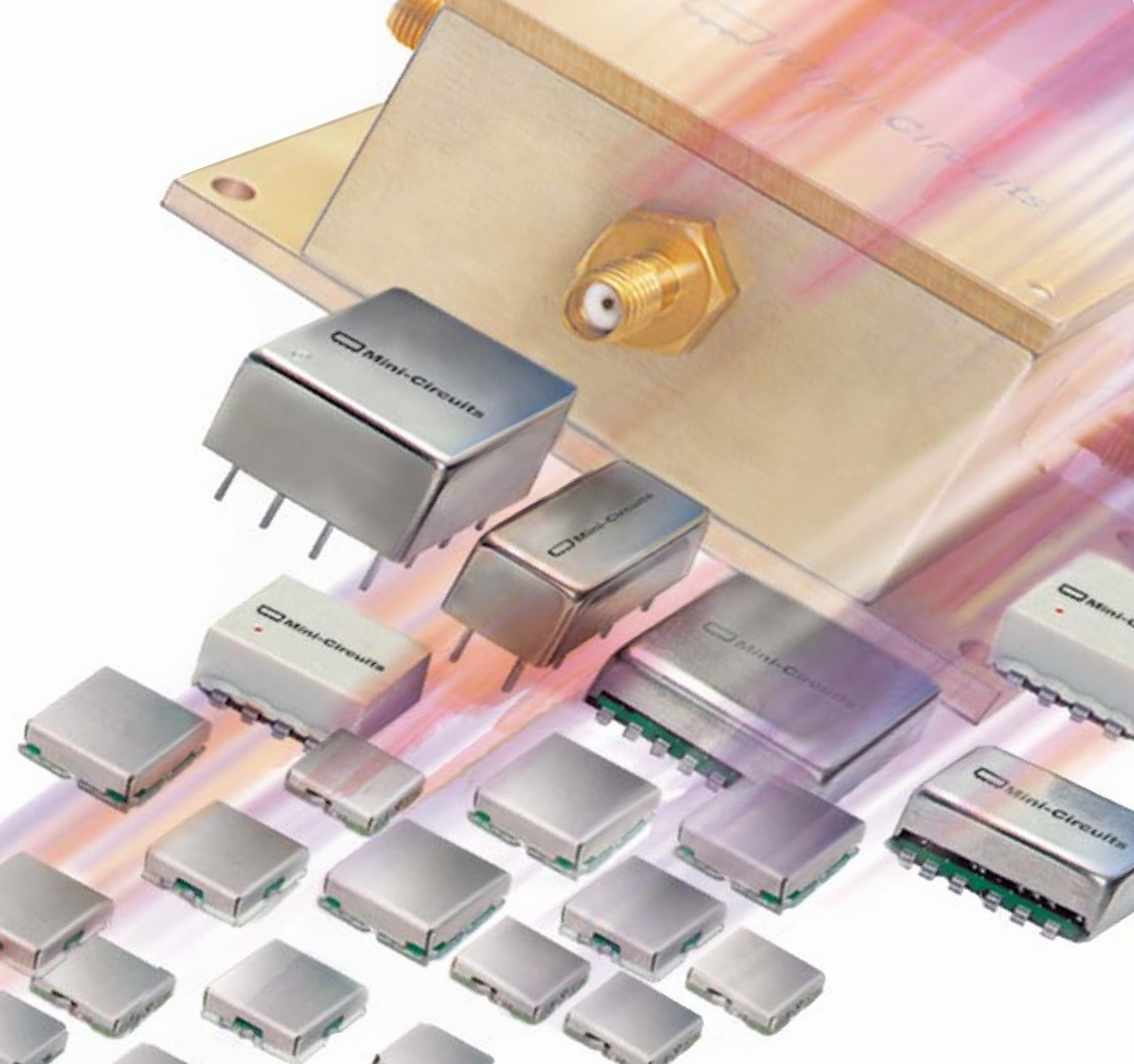

Agilent Technologies

For high reliability, all Mini-Circuits VCOs are tested with the Agilent E5052A Signal Source Analyzer.
www.agilent.com/find/ssa

Detailed Performance Data & Specs For Mini-Circuits VCOs
Available Online at: ***www.minicircuits.com/oscillat.html***

Mini-Circuits®
ISO 9001 ISO 14001 CERTIFIED

ALL NEW
minicircuits.com

P.O. Box 350166, Brooklyn, New York 11235-0003 (718) 934-4500 Fax (718) 332-4661 For detailed performance specs & shopping online see Mini-Circuits web site

YONI2™ ***The Design Engineers Search Engine*** *Provides ACTUAL Data Instantly From MINI-CIRCUITS At:* ***www.minicircuits.com***

RF/IF MICROWAVE COMPONENTS

402 Rev B

Visit http://mwj.hotims.com/11713-85 or use RS# 85 at www.mwjournal.com/info

DESIGN OF A NOVEL QUAD-BAND MICROSTRIP BPF USING QUARTER-WAVELENGTH STEPPED-IMPEDANCE RESONATORS

In this article, a new quad-band microstrip bandpass filter (BPF) is proposed. The BPF is composed of resonators whose first four resonant frequencies can be tuned to the desired passbands. Each resonator is formed by combining two unequal-size stepped-impedance resonators (SIR) with part of their structures shared. The designed quad-band BPF is implemented on an RT/Duroid 6010 substrate. The measured fractional bandwidths (minimum insertion losses) for the 1.57 GHz (GPS), 2.45 GHz (ISM), 3.55 GHz (WiMAX) and 5.25 GHz (WLAN) bands are 6.4 percent (1.85 dB), 8.2 percent (1.4 dB), 8.7 percent (2 dB) and 12.2 percent (1.06 dB), respectively, which agree well with the simulated results. For miniaturization purposes, the resonators are meandered to give an overall circuit size of only 12.3 × 9.1 mm.

Due to the increasing competition in the global wireless communication markets, many wireless terminals, such as mobile phones, personal dispatching assistants (PDA) and laptop computers, are being constructed to integrate more than one communication standard into the same apparatus. This allows the end-users to access different systems that provide various services. Since different communication standards may use different frequency bands, front-end components capable of supporting multiple frequency bands have received much attention.[1,2] These front-end components include couplers,[3–6] antennas[7,8] and bandpass filters (BPF).[9–13] In the literature, most multi-band couplers reported can support only two frequency bands[3–6] because of the high complexities involved in the design. However, antennas that can be operated in two or more frequency bands are very common.[7,8] In this work, the design of multi-band BPFs is the primary interest. Recently, dual-band BPFs have been intensively investigated,[9–11] where-

CHUNG-I G. HSU
Da-Yeh University
Changhua, Taiwan, ROC
CHING-HER LEE AND HE-KAI JHUANG
National Changhua University of Education
Changhua, Taiwan, ROC

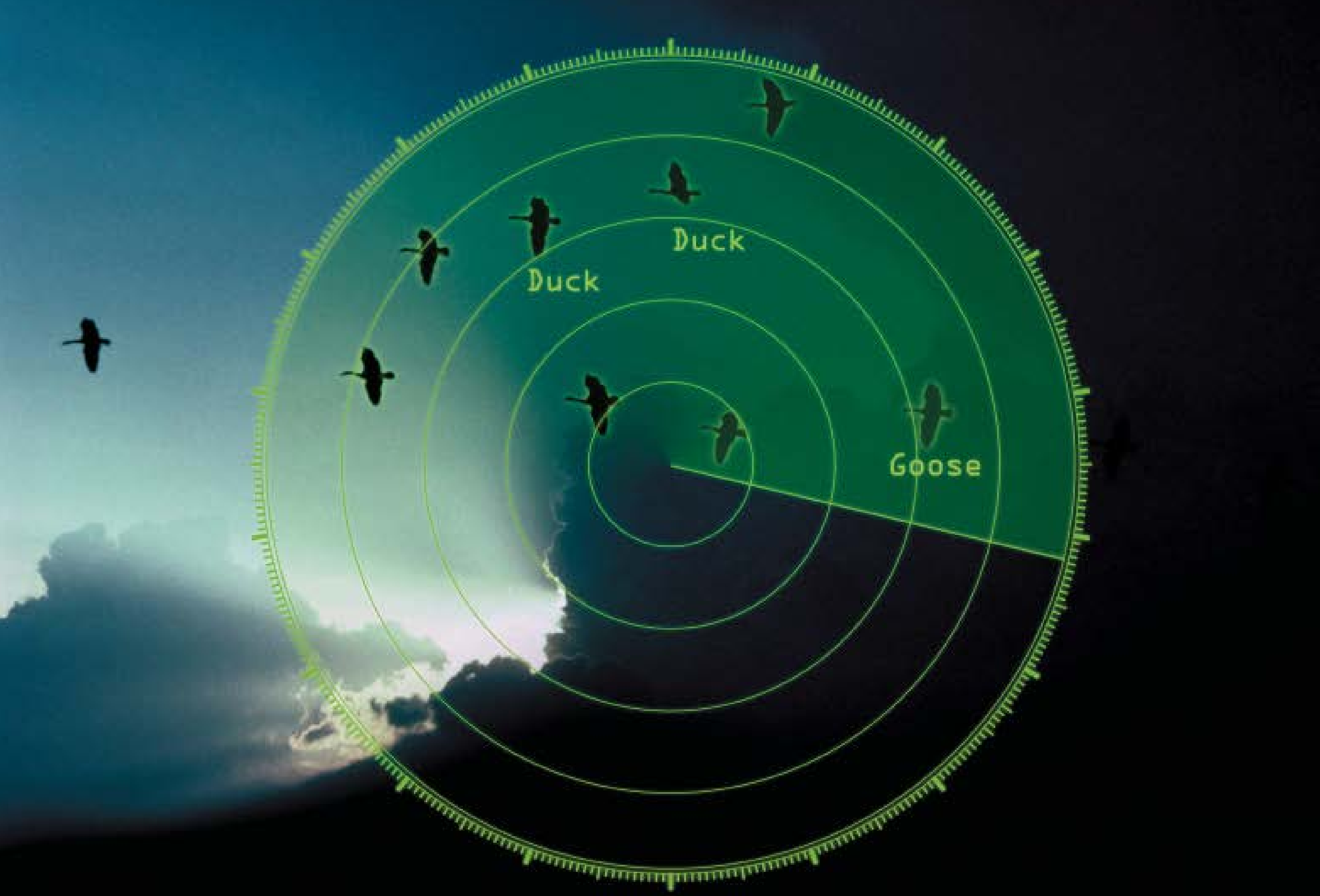
Duck
Duck
Goose

as the study of tri-band BPFs, which can support three practical commercial communication bands, is relatively scant.[12] Furthermore, a quad-band BPF that can simultaneously support four frequency bands is not yet available.

The most intuitive way of constructing a multi-band component is to build an individual circuit for each frequency band and then combine them in parallel, resulting in a large circuit size. Nevertheless, Miyake, et al.[9] have successfully extended the parallel-cascade structure[13] (originally proposed for a single-band BPF design) to implement a miniaturized, low temperature, co-fired ceramic dual-band BPF by stacking two stripline filters, one for the 900 MHz band and the other for the 1900 MHz band. Although highly compact, this filter needs extra impedance matching networks at its input/output ports. A more clever way of designing a dual-band BPF is to use resonators whose second resonant frequency can be tuned over a very wide frequency range. Stepped-impedance resonators (SIR), originally proposed by M. Makimoto, et al.,[14] possess such a property, and were successfully employed in a dual-band BPF design.[10] Alternatively, a dual-band BPF can be created by loading a transmission line with three unequal-length shunt open stubs,[11] which yield three transmission zeros. Similarly, a tri-band BPF can be constructed by placing four unequal-length open stubs in shunt to a transmission line,[12] resulting in four transmission zeros. Although this idea can be extended to implement a multi-band BPF supporting more than three frequency bands, so far, to the authors' knowledge, a quad-band BPF has not been reported in the literature. This is probably because too many open stubs will make the filter bulky and because mutual loading effects among the stubs have rendered the quad-band BPF topology impractical. Moreover, since the shunt stubs are open-ended, low frequency and DC signals will not be blocked by these filters,[11,12] a property that can be regarded as a drawback.

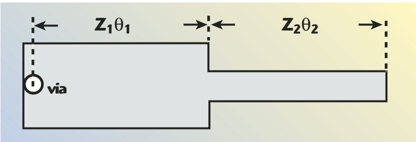

▲ *Fig. 1 Geometry of the λ/4 stepped-impedance resonator.*

The aim of this article is to design a quad-band BPF that can pass signals in the 1.57 GHz (GPS L1 channel), 2.45 GHz (ISM), 3.55 GHz (WiMAX) and 5.25 GHz (WLAN) bands. Two quarter-wavelength (λ/4) SIRs, when properly designed, can be combined to form a single resonator that resonates at the four desired frequencies. Because a λ/4 SIR offers a smaller circuit size and a higher third resonant frequency compared with a λ/2 SIR, it is used here as the building blocks of a BPF. In addition, the SIRs are meandered to reduce the size of the fabricated BPF, which measures only 12.3 × 9.1 mm. Since the quadruple-frequency resonators used in the BPF are mutually separated, low frequency and DC signals will be highly attenuated.

QUADRUPLE-FREQUENCY MICROSTRIP RESONATOR DESIGN

A BPF can be constructed by combining resonators with the same resonant frequencies in a proper manner. A resonator, with its four main resonances located at the desired frequencies, can be used as the building block of a quad-band BPF. Such a resonator can be composed of two primary resonators, each of which has its first two resonant frequencies identical to two of the four desired frequencies. The prime resonating structure adopted here is a λ/4 SIR, as shown in ***Figure 1***. The λ/4 SIR consists of two microstripline sections having characteristic impedances Z_1 and Z_2 and electric lengths θ_1 and θ_2. One end of the λ/4 SIR is grounded through a via of diameter D. For simplicity, the two resonator sections are assumed to have the same electrical length, that is, $\theta_1 = \theta_2 = \theta_0$. By neglecting the parasitic effects of the via and the step junction between the two line sections, the parallel resonance condition can be derived as $\tan^2\theta_0(f) = Z_2/Z_1 = R_z$, from which the resonant frequencies can be determined.[14] Here, R_z stands for the impedance ratio. Denote the nth resonant frequency of the SIR by f_n; then, for a given fundamental resonant frequency (f_1) of a λ/4 SIR, the associated second and third resonant frequencies, respectively, can be written as[14]

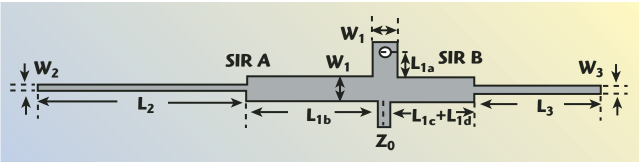

▲ *Fig. 2 Geometry of the quadruple frequency resonator with a 50 Ω microstrip tap.*

$$f_2 = f_1\left(\frac{\pi}{\tan^{-1}\sqrt{R_Z}} - 1\right) \quad (1)$$

and

$$f_3 = f_2 + 2f_1 \quad (2)$$

This implies that, for a given f_1, the second resonant frequency f_2 can be freely designed by choosing an appropriate R_z value for the λ/4 SIR. Furthermore, if both f_1 and f_2 are given, then f_3 is fixed and can be considered spurious.

As mentioned, two dual-frequency SIRs (designated as SIR A and SIR B) are needed in order to construct a quadruple-frequency resonator. Let f_{A1} = 1.57 GHz and f_{A2} = 3.55 GHz be the first two resonant frequencies of SIR A; thus, R_{ZA} = 2.07 and $\theta_{0A}(f_{A1})$ = 55.2°. Similarly, let f_{B1} = 2.45 GHz and f_{B2} = 5.25 GHz be associated with SIR B; R_{ZB} should then be 2.42 and $\theta_{0B}(f_{B1})$ = 57.3°. Note that the first spurious resonant frequencies f_{A3} (6.69 GHz) and f_{B3} (10.15 GHz) for SIRs A and B, respectively, are both greater than the highest of the four desired frequencies. In this article, the filter circuit is to be designed on a 0.635 mm-thick RT/Duroid 6010 substrate with a dielectric constant of 10.2 and a loss tangent of 0.0023. For SIR A, if Z_1 = 30.2 Ω (W_1 = 1.4 mm), then Z_2 = 62.5 Ω (W_2 = 0.3 mm). In order to combine SIR B with SIR A, the width and characteristic impedance of the first section of SIR B are set to be the same as those of SIR A. For differentiation purposes, the width and characteristic impedance of the second section of SIR B are denoted by W_3 and Z_3, respectively. The value of $R_{ZB} = Z_3/Z_1$ thus leads to Z_3 = 72.6 Ω (W_3 = 0.2 mm). These two SIRs can be combined into a single resonator, as

shown in ***Figure 2***, where SIRs A and B share part of the W_1-wide section. This common section has a length of L_{1a}, which is measured from the center of the via to the upper edge of the horizontal W_1-wide section. Also shown is the 50 Ω tapping microstrip that feeds the resonator at the junction of the two SIRs.

QUAD-BAND MICROSTRIP BPF IMPLEMENTATION

Note that the value of L_{1a} must be appropriately selected so as to meet the bandwidth requirements for the four passbands centered at f_{A1}, f_{B1}, f_{A2} and f_{B2} in the quad-band BPF design. The fractional bandwidths needed are approximately 3 percent (1557 to 1593 MHz), 4 percent (2400 to 2484 MHz), 8.5 percent (3.4 to 3.7 GHz) and 4 percent (5150 to 5350 MHz), respectively. Using a second-order Butterworth response as the target, the element values for the low pass filter prototype are $g_0 = g_3 = 1$ and $g_1 = g_2 = \sqrt{2}$. The required external quality factors (defined by $Q_{ei} = g_0g_1/\Delta$ with Δ being the 3 dB fractional bandwidth of the filter)[15] for these four bands are in general different. Let the external quality factor for the ith resonant frequency be denoted by Q_{ei} (i = A_1, B_1, A_2 and B_2), which can be computed by[10]

$$Q_{ei} = Z_0 \frac{f_i}{2}\frac{dB(f)}{df}\bigg|_{f=f_i} = \frac{Z_0}{2} \bullet \left\{ f\frac{d}{df}\left[B_0(f)+B_A(f)+B_B(f)\right]\right\}\bigg|_{f=f_i} \qquad (3)$$

where

Z_0 = characteristic impedance of the tapping microstrip

Moreover, the total input susceptance, looking from the tapping position toward the resonator, is B(f), which can be decomposed into $B_0(f)$, $B_A(f)$ and $B_B(f)$, that is the susceptances looking from the junction of SIRs A and B toward the upper side (toward the via), the left side and the right side of the quadruple-frequency resonator, respectively. The expressions for $B_0(f)$, $B_A(f)$ and $B_B(f)$ are easy to derive and are omitted here for brevity. Nevertheless, the expressions of $fdB_j(f)/df$, j = 0, A, B are listed in ***Appendix A*** for completeness. The Q_e versus L_{1a} curves, computed using Equation 3 for the four desired center frequencies, are shown in ***Figure 3***, which indicates that Q_e decreases with L_{1a}. Hence, the larger the value of L_{1a}, the larger the fractional

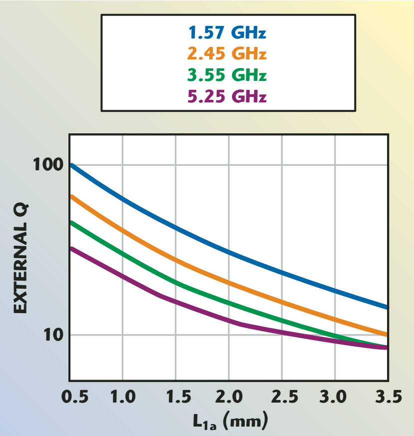

▲ *Fig. 3 External Q versus the resonator shared length.*

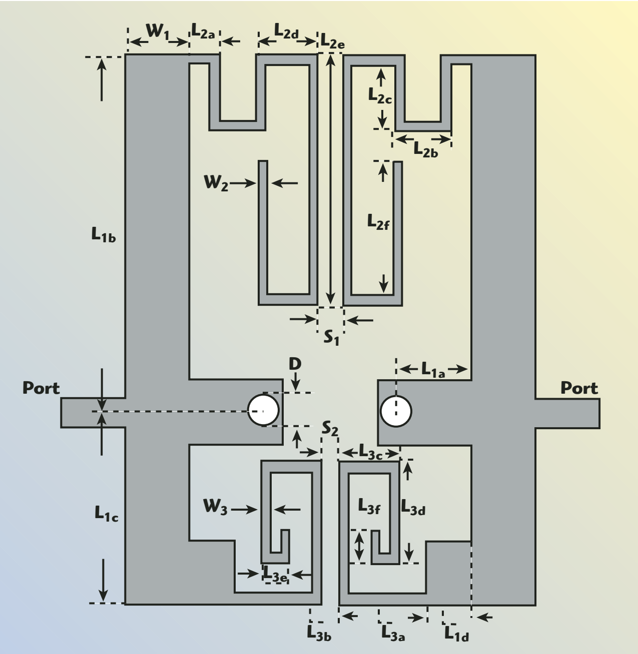

▲ *Fig. 4 Layout of the proposed quad-band microstrip BPF.*

bandwidth Δ (since $\Delta = g_0g_1/Q_e$). Obviously, the four required lengths of L_{1a} for the four desired passbands may be all different. Among them, the largest L_{1a} value must be selected to ensure that all the four passband bandwidths be greater than or equal to the actual required ones. If an L_{1a} value other than the largest one is chosen, some passband bandwidths will be smaller than needed, thus resulting in partial signal blocking in those particular passbands. Note that in Equation 3 and the associated expressions listed in Appendix A, many

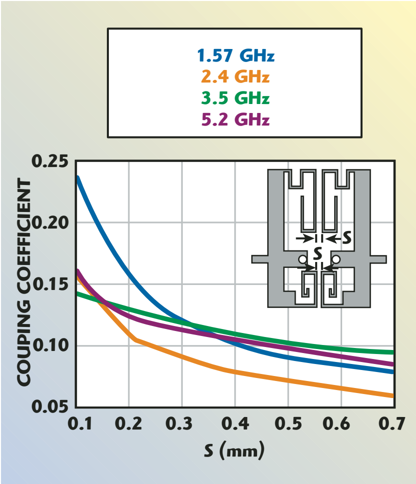

▲ *Fig. 5 Simulated coupling coefficients versus the gap width between resonators.*

TABLE I

OPTIMIZED DIMENSIONS OF THE QUAD-BAND BPF

Parameter	*Value (mm)*
W_1	1.40
W_2	0.15
W_3	0.20
S_1	0.60
S_2	0.30
D	0.60
L_{1a}	1.8
L_{1b}	8.0
L_{1c}	4.3
L_{1d}	1.0
L_{2a}	0.67
L_{2b}	1.19
L_{2c}	1.50
L_{2d}	1.29
L_{2e}	5.54
L_{2f}	3.03
L_{3a}	2.0
L_{3b}	3.2
L_{3c}	1.4
L_{3d}	2.3
L_{3e}	0.7
L_{3f}	0.8

factors have been neglected, including the dielectric loss, the conductor loss, the dispersion properties of the microstrip sections in the resonator and the effects of the structural discontinuities. Hence, the aforementioned largest L_{1a} value can only serve as a good start in the optimization process of designing the quad-band BPF and may still have to be fine-tuned in the design.

The geometry of the proposed quad-band BPF is shown in ***Figure 4***, where the two quadruple-frequency resonators are placed back to back with gaps S_1 and S_2 in the horizontal direction. The upper part of the BPF is the main path for signals around f_{A1} and f_{A2}, whereas the lower part is for signals around f_{B1} and f_{B2}. Since the resonators have been bent to reduce the circuit size, the structural parameters (W_1, W_2, W_3, $\theta_{0A}(f_{A1})$, $\theta_{0B}(f_{B1})$, L_{1a} and so on) may need to be further tuned during the full-wave optimization. For the f_i-referenced fractional bandwidths Δ_i (i = A1, B1, A2 and B2) determined for a selected L_{1a} value, the coupling coefficients between these two resonators can be computed using $M_i = \Delta_i\sqrt{g_1g_2}$. Once the values of M_I are known, the gaps between these two resonators can be determined through full-wave electromagnetic simulation.[15] ***Figure 5*** shows a set of simulated coupling coefficients as functions of the gap S. In the inset of the figure, the structure has been configured to have the same gap S for both the upper and the lower half of the juxtaposed resonators. This can be done by adjusting the individual lengths of L_{1c} and L_{1d} for a fixed L_{1c}+ L_{1d}. Once the required

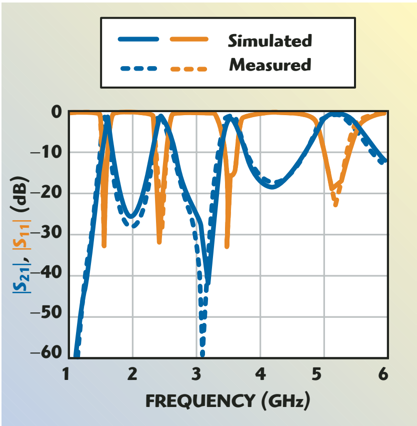

▲ *Fig. 6 Simulated and measured response of the quad-band BPF.*

McQ512 Trimmer Capacitor

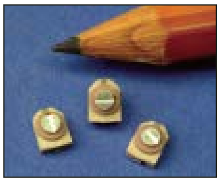

Tusonix's smallest Miniature All-Ceramic Surface Mount Trimmer Capacitor - the McQ 512 Series - is offered in an incredibly compact size for those applications that demand high Q and space-saving solutions. The state-of-the-art McQ 512 Trimmer is perfect for an endless variety of applications that require miniaturized capacitance trimming, including avionics apparatus, communications equipment, oscilloscopes, crystal oscillators and crystal filters.

Back Plane Mount Filtered Terminal Blocks

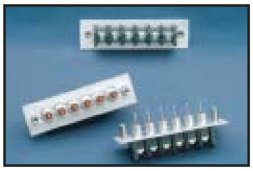

Tusonix now offers Back Plane Mount Filtered Terminal Blocks. These cost effective, premium filtered terminal blocks provide excellent EMI/RFI filtering of power and control lines. Available with 2-8 lines, our back plane mount terminal blocks (part no. 7602-551 through 7606-551) offer an effective insertion loss range from 10 MHz to 10 GHz. The capacitance range is 2000 pF to 5000 pF with a temperature range of -55°C to +105°C. And, each terminal block is tested for key parameters in efforts to ensure reliability.

Redesigned Shoulder Feed-Thru Capacitors

Tusonix offers a newly redesigned shoulder feed-thru capacitor. Our capacitors in the 2461 and 2463 series are an excellent solution to your EMI needs that involve a wide range of telecommunications applications. These capacitors, which are offered with a capacitance range of 5 to 2,500 pF and insertion losses up to 40dB, are a low cost alternative for existing applications using a similar product.

RoHS ✓ Compliant

TABLE II

PERFORMANCE OF THE DESIGNED QUAD-BAND BPF

		Simulation	Measurement
f_{A1} (1.57 GHz)	Minimum insertion loss (dB) 3 dB band (GHz) BW (%)	1.53 1.5 to 1.6 6.4	1.85 1.51 to 1.61 6.4
f_{B1} (2.45 GHz)	Minimum insertion loss (dB) 3 dB band (GHz) BW (%)	1.12 2.35 to 2.54 7.8	1.4 2.34 to 2.54 8.2
f_{A2} (3.55 GHz)	Minimum insertion loss (dB) 3 dB band (GHz) BW (%)	1.5 3.38 to 3.72 9.6	2.0 3.40 to 3.71 8.7
f_{B2} (5.25 GHz)	Minimum insertion loss (dB) 3 dB band (GHz) BW (%)	0.9 4.9 to 5.5 11.4	1.06 4.92 to 5.56 12.2

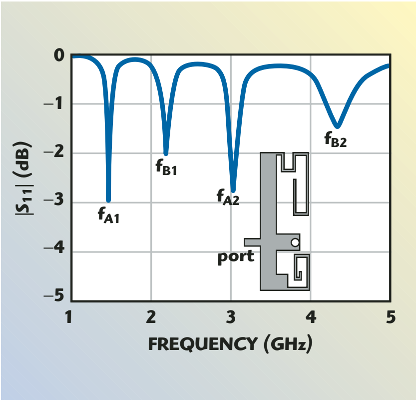

▲ *Fig. 7 Simulated reflection coefficient of one-half of the BPF.*

(M_{A1}, M_{A2}) and (M_{B1}, M_{B2}) are obtained for two possibly different values of S, S_1 will be equated to the value of S pertaining to (M_{A1}, M_{A2}) and S_2 to that pertaining to (M_{B1}, M_{B2}). If this task cannot be achieved, the values of L_{2e} and L_{3b} will have to be varied and another set of simulated coupling-coefficient curves generated. If still not successful, the value of L_{1a} may have to be changed to acquire a different set of Δ_i (thus, a different set of M_i) and search for an appropriate set of gaps (S_1 and S_2).

EXPERIMENTAL RESULTS

For the fabricated quad-band BPF with the optimized dimensions shown in ***Table 1***, the corresponding coupling coefficients $(M_{A1}, M_{B1}, M_{A2}, M_{B2})$ are approximately (0.0453, 0.052, 0.062, 0.0794) and the fractional bandwidths $(\Delta_{A1}, \Delta_{B1}, \Delta_{A2}, \Delta_{B2})$, computed from $M_i = \Delta_i/\sqrt{g_1 g_2}$, are 6.39, 7.4, 8.8 and 11.23 percent. ***Figure 6*** shows the simulated and measured frequency responses of the

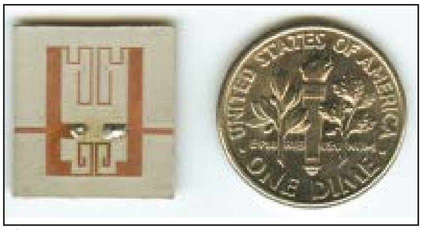

▲ *Fig. 8 The fabricated quad-band microstrip BPF.*

BPF, which are also summarized in ***Table 2*** for comparison. The measured results agree quite well with those obtained from the simulation done using Ansoft HFSS, a full-wave electromagnetic simulator. The measured 3 dB fractional bandwidths for the four passbands centered at f_{A1}, f_{B1}, f_{A2} and f_{B2} are found to be 1510 to 1610 MHz (6.4 percent), 2340 to 2540 MHz (8.2 percent), 3400 to 3710 MHz (8.7 percent) and 4920 to 5560 MHz (12.2 percent), respectively. The minimum insertion losses measured for these four passbands in the same sequence are 1.85, 1.4, 2.0 and 1.06 dB, respectively. The simulated return loss for a single microstrip line-fed quadruple-frequency resonator (half of the BPF structure) is shown in ***Figure 7*** to verify that the designed resonator indeed resonates at the four desired frequencies. A photograph of the fabricated BPF is shown in ***Figure 8***, which illustrates its very small area of only 12.3 × 9.1 mm.

CONCLUSION

In this article, a new quad-band microstrip bandpass filter (BPF) has been proposed and implemented. The novel resonators composed of

two SIRs have been designed to resonate at four desired frequencies, and have been subsequently employed in the BPF design. The circuit size has been greatly reduced by meandering the resonators. The measured frequency responses of the designed BPF have been found to agree with the simulated ones. To the authors' knowledge, this BPF is the first one reported in the literature that can support four practical frequency bands. ■

ACKNOWLEDGMENT

This work was supported by the National Science Council, Taiwan, ROC, under grant no. NSC 94-2213-E-018-006.

References

1. S.F.R. Chang, W.L. Chen, S.C. Chang, C.K. Tu, C.L. Wei, C.H. Chien, C.H. Tsai, J. Chen and A. Chen, "A Dual-band RF Transceiver for Multi-standard WLAN Applications," *IEEE Transactions on Microwave Theory and Techniques*, Vol. 53, No. 3, March 2005, pp. 1048–1055.
2. Y.S. Lin, C.C. Liu, K.M. Li and C.H. Chen, "Design of an LTCC Tri-band Transceiver Module for GPRS Mobile Applications," *IEEE Transactions on Microwave Theory and Techniques*, Vol. 52, No. 12, December 2004, pp. 2718–2724.
3. K.K.M. Cheng and F.L. Wong, "A Novel Approach to the Design and Implementation of Dual-band Compact Planar 90° Branch-line Coupler," *IEEE Transactions on Microwave Theory and Techniques*, Vol. 52, No. 11, November 2004, pp. 2458–2463.
4. M.J. Park and B. Lee, "Dual-band, Cross-coupled Branch-line Coupler," *IEEE Microwave and Wireless Components Letters*, Vol. 15, No. 10, October 2005, pp. 655–657.
5. I.H. Lin, M. DeVincents, C. Caloz and T. Itoh, "Arbitrary Dual-band Components Using Composite Right/Left-handed Transmission Lines," *IEEE Transactions on Microwave Theory and Techniques*, Vol. 52, No. 4, April 2004, pp. 1142–1149.
6. H.K. Jhuang, P.M. Hu, C.I.G. Hsu and C.H. Lee, "A Dual-band Branch-line Coupler Using Quasi-composite Right/Left-handed Transmission Lines," *Microwave Journal*, Vol. 49, No. 8, August 2006, pp. 176–184.
7. J.Y. Sze, C.I.G. Hsu and J.J. Jiau, "CPW-fed Circular Slot Antenna with Slit Back-patch for 2.4/5 GHz Dual-band Operation," *Electronics Letters*, Vol. 42, No. 10, May 2006, pp. 563–564.
8. N.C. Karmakar and M.E. Bialkowski, "Circularly Polarized Aperture-coupled Circular Microstrip Patch Antennas for L-band Applications," *IEEE Transactions on Antennas and Propagation*, Vol. 47, No. 5, May 1999, pp. 933–940.
9. H. Miyake, S. Kitazawa, T. Ishizaki, T. Yamada and Y. Nagatomi, "A Miniaturized Monolithic Dual-band Filter Using Ceramic Lamination Technique for Dual-mode Portable Telephones," *1997 IEEE MTT-S International Microwave Symposium Digest*, Vol. 2, pp. 789–792.
10. J.T. Kuo, T.H. Yeh and C.C. Yeh, "Design of Microstrip Bandpass Filters with a Dual-passband Response," *IEEE Transactions on Microwave Theory and Techniques*, Vol. 53, No. 4, April 2005, pp. 1331–1337.
11. C. Quendo, E. Rius and C. Person, "An Original Topology of Dual-band Filter with Transmission-zeros," *2003 IEEE MTT-S International Microwave Symposium Digest*, Vol. 2, pp. 1093–1096.
12. C. Quendo, E. Rius, A. Manchec, Y. Clavet, B. Potelon, J.F. Favennec and C. Person, "Planar Tri-band Filter on Dual Behavior Resonator (DBR)," *2005 European Microwave Conference Digest*, Vol. 1, pp. 269–272.
13. V. Osipenkov and S.G. Vesnin, "Microwave Filters of Parallel-cascade Structure," *IEEE Transactions on Microwave Theory and Techniques*, Vol. 42, No. 7, July 1994, pp. 1360–1367.
14. M. Makimoto and S. Yamashita, "Bandpass Filters Using Parallel Coupled Stripline Stepped-impedance Resonators," *IEEE Transactions on Microwave Theory and Techniques*, Vol. 28, No. 12, December 1980, pp. 1413–1417.
15. J.S. Hong and M.J. Lancaster, *Microstrip Filters for RF/Microwave Application*, John Wiley & Sons Inc., Hoboken, NJ, 2001.

Chung-I G. Hsu *graduated from the National Taipei Institute of Technology, Taiwan, in 1980. He received his MSc degree from the University of Mississippi and his PhD degree from Syracuse University, both in electrical engineering, in 1986 and 1991, respectively. He spent the 1992 spring semester at the microwave and electromagnetics laboratory, Texas A&M University, doing research on the modeling of microstrip antennas. He has been on the faculty of Da-Yeh University since August 1992, where he is presently an associate professor in the department of electrical engineering.*

Ching-Her Lee *received his BS degree in electronic engineering and his MS degree in automatic control engineering from Feng-Chia University, Taichung, Taiwan, in 1977 and 1981, respectively, and his PhD degree in electrical engineering from the University of Texas at Arlington, TX, in 1989. From 1981 to 1985, he was on the faculty of the Chin-Yih Institute of Technology, Taichung, Taiwan. In 1990, he joined the National Changhua University of Education, where he is presently dean of the college of engineering. His research interests include planar microwave circuits and microstrip antennas.*

He-Kai Jhuang *received his BS degree in industrial education from the National Changhua University of Education, Changhua, Taiwan, in 2004, and is currently working toward his MS degree in electronic engineering from the same school. His current interests include microstrip filter design and passive components for wireless communications.*

APPENDIX A

The detailed expressions pertaining to Equation 3 are given as follows:

$$f\frac{d}{df}B_0(f)=\frac{\phi}{Z_1}\csc^2\phi \qquad \text{(A1)}$$

$$\begin{aligned} f\frac{d}{df}B_A(f) &= \frac{1}{Z_1\left[R_{ZA}-\tan\theta_{0A}\tan(\theta_{0A}-\phi)\right]^2} \\ &\bullet\Big\{\big[\theta_{0A}\sec^2\theta_{0A} + R_{ZA}(\theta_{0A}-\phi)\sec^2(\theta_{0A}-\phi)\big] \\ &\bullet\big[R_{ZA}-\tan\theta_{0A}\tan(\theta_{0A}-\phi)\big] \\ &+\big[\theta_{0A}\sec^2\theta_{0A}\tan(\theta_{0A}-\phi) \\ &+(\theta_{0A}-\phi)\tan\theta_{0A}\sec^2(\theta_{0A}-\phi)\big] \\ &\bullet\big[\tan\theta_{0A}+R_{ZA}\tan\theta_{0A}\tan(\theta_{0A}-\phi)\big]\Big\} \end{aligned} \qquad \text{(A2)}$$

The term $fdB_B(f)/df$ can be obtained from Equation A2 by replacing the subscript A with B. Referring to Figure 2, one obtains

$$\phi(f)=\left(2\pi f\sqrt{\varepsilon_{r,eff,1}}/c\right)\left(L_{1a}+W_1/2\right)+\theta_{via}(f) \qquad \text{(A3)}$$

$$\theta_{0A}(f)=\left(2\pi f\sqrt{\varepsilon_{r,eff,1}}/c\right)\left(L_{1a}+L_{1b}+W_1/2\right)+\theta_{via}(f) \qquad \text{(A4)}$$

$$\theta_{0B}(f)=\left(2\pi f\sqrt{\varepsilon_{r,eff,1}}/c\right)\left(L_{1a}+L_{1c}+L_{1d}+W_1/2\right)+\theta_{via}(f) \qquad \text{(A5)}$$

where $\varepsilon_{r,eff,1}$ is the effective dielectric constant of the microstripline having a width of W_1 and c is the speed of light in free space. Furthermore, $\theta_{via}(f) = 2\pi f\sqrt{\varepsilon_r}h/c$ is an approximate phase correction term representing the phase delay from the via, where h and ε_r are the height and dielectric constant of the substrate, respectively.


Microwave
Honolulu, Hawai'i
Reserve a room at conference rates now at www.IMS2007.org
International Microwave Symposium
RFIC Symposium · ARFTG Symposium
IMS2007
IEEE
MTT-S
www.IMS2007.org
www.gohawaii.com
Photo by Laszlo Ilyes

Week 2007

3–8 June 2007

The premier microwave and wireless conference featuring technical sessions and workshops for commercial and military applications

- Field Analysis and Guided Waves
- Frequency Domain Techniques
- Time Domain Techniques
- CAD Algorithms and Techniques
- Linear Device Modeling
- Nonlinear Device Modeling
- Nonlinear Circuit Analysis and System Simulation
- Transmission Line Elements
- Passive Circuit Elements
- Planar Passive Filters and Multiplexers
- Non-Planar Passive Filters and Multiplexers
- Active and Integrated Filters
- Ferroelectric, Ferrite and Acoustic Wave Components
- MEMS Components and Technologies
- Semiconductor Devices and Monolithic IC Technologies
- Signal Generation
- Frequency Conversion and Control
- HF/VHF/UHF Technologies and Applications
- Power Amplifier Devices and Integrated Circuits
- High Power Amplifiers
- Low Noise Components and Receivers
- Millimeter-wave and Terahertz Components and Technologies
- Microwave Photonics
- Digital Circuits and Systems at GHz Speeds
- Packaging, Interconnects, MCMs and Hybrid Manufacturing
- Instrumentation and Measurement Techniques
- Biological Effects and Medical Applications
- Smart Antennas, Spatial Power Combining and Phased Arrays
- Radars and Broadband Communication Systems
- Wireless and Cellular Communication Systems
- Sensors and Sensor Systems

- Full guest program for the family

www.IMS2007.org

For further information, please contact Kristen Dednah at: kdednah@mwjournal.com or 781-769-9750

A COMPACT MICROSTRIP STEPPED-IMPEDANCE RESONATOR AND FILTER

The resonant performance of T-shaped microstrip resonators, a kind of stepped-impedance resonator (SIR), is computed and analyzed. Two novel SRI filters, a double-T-shaped bandstop filter and a double-H-shaped bandpass filter, are designed and their performances are calculated and optimized. The results show that the performance of the filters can be effectively improved by using defected ground structures (DGS), which suppress spurious responses by rejecting harmonics in the microwave circuits. The measured results are in good agreement with the simulated ones. The proposed filters have advantages such as a simple structure, wide bandwidth and high attenuation, and are quite useful in future applications in RF circuits.

Microstrip resonators have very important applications in microwave or millimeter-wave systems. They are important components of microstrip filters,[1–2] microstrip oscillators[3] and microstrip antennas,[4] and enable microwave equipment miniaturization with improved performance. A stepped-impedance resonator (SIR) is the fundamental resonant element that can operate from RF to millimeter-wave frequencies and can be used in many kinds of filters, oscillators and mixers. The performance of a microstrip resonator relies on electromagnetic field distribution, the resonant frequency and quality factor Q. Microstrip filters have advantages such as low cost, small volume, high selectivity and are widely used in a variety of microwave systems to transmit energy in one or more passbands and to attenuate energy in one or more stopbands.

A defected ground structure (DGS)[5,6] is a novel technique for improving the performance of filters or other microwave components and is formed by etching a pattern in the ground plane. This structure can change the current and its distribution in the ground plane, and thus increase the effective capacitance and inductance of the microstrip. Peri-

JIAN-KANG XIAO
South China University of Technology
Guangzhou, China
SHI-WEI MA
Shanghai Key Laboratory of Power Station Automation Technology
Shanghai, China
YING LI
College of Science, Shanghai University
Shanghai, China

odic and non-periodic DGSs have the property to reject certain microwaves in some frequencies, permitting elimination of spurious responses due to harmonics. In this article, a novel double-T-shaped microstrip bandstop filter with DGS and a novel double-H-shaped microstrip bandpass filter with DGS are proposed and their performances simulated and optimized. The calculated results show that the performance of the filters can be effectively improved by DGS and the experimental results verify the improvement.

ANALYSIS FOR CHARACTERISTICS OF A MICROSTRIP STEPPED-IMPEDANCE RESONATOR

A fundamental microstrip SIR is formed by joining together two microstrip transmission lines with different characteristic impedance Z_1 and Z_2, as shown in ***Figure 1***. Z_i is input impedance, Y_i is input admittance and β is phase constant. ℓ_1 and ℓ_2 are physical lengths corresponding to electric lengths θ_1 and θ_2, respectively. The equivalent circuit of the SIR is derived, as shown in Figure 1b, where L is inductance, C is capacitance and R_L is loaded-impedance. If the discontinuous of microstrip step and fringe capacitance of open-circuit port are omitted, Z_i can be expressed as

$$Z_i = jZ_2 \frac{Z_1 \tan\theta_1 + Z_2 \tan\theta_2}{Z_2 - Z_1 \tan\theta_1 \tan\theta_2} \tag{1}$$

The parallel resonant condition can be obtained on the base of $Y_i = 0$; it is

$$K = \tan\theta_1 \tan\theta_2 = \frac{Z_2}{Z_1} \tag{2}$$

Here, K is the impedance ratio. It can be seen from Equation 2 that the resonant conditions of SIR lie on θ_1, θ_2 and K. The total electric length of SIR can be expressed as

$$\theta_T = \theta_1 + \theta_2 = \theta_1 + \arctan\left(\frac{K}{\tan\theta_1}\right), K \neq 1 \tag{3}$$

$$\theta_T = \frac{\pi}{2}, K = 1 \tag{4}$$

It can be shown from Equation 3 that the resonator's length reaches a minimum value of $0 < K < 1$, and a maximum value for $K > 1$.[7] For $K = 1$, it is a conventional quarterwave uniform-impedance resonator (UIR), as shown in Equation 4.

On the resonant condition, SIR can also be equivalent by circuit,[8] as shown in Figure 1c. Here

$$L_0 = \frac{1}{\omega_0 b_s}, C_0 = \frac{b_s}{\omega_0}, R_0 = \frac{b_s}{Q_0} \tag{5}$$

where

ω_0 = resonant angular frequency
b_s = susceptibility slop
Q_0 = unloaded Q

b_s can be expressed as

$$b_s = \frac{\omega_0}{2} \frac{dB_s}{d\omega}\bigg|_{\omega=\omega_0} \tag{6}$$

where

$b_s(\omega)$ = susceptibility of resonator

If the susceptibility of quarter-wavelength SIR is defined as B_{SA} and the corresponding slop parameter is defined as b_{SA}, we have

$$B_{SA} = \mathrm{Im}\left[\frac{1}{Z_i}\right] = Y_2 \frac{\tan\theta_1 \tan\theta_2 - K}{\tan\theta_1 + K\tan\theta_2} \tag{7}$$

$$b_{SA} = \frac{\theta_{01} Y_2}{2}\left[\frac{K}{\left(1-K^2\right)\sin^2\theta_{01} + K^2} + \frac{\ell_1}{\ell_2}\right] \tag{8}$$

where

θ_{01} = resonant value of θ_1

An H-shaped resonator is a symmetrical structure that consists of two transmission lines with different characteristic impedance, as shown in ***Figure 2***. The electric length of outer step is θ_2, and that of inner step is $2\theta_1$. Its equivalent transmission line model[9] is shown in Figure 2b, where

$$Z_{in1} = jZ_1 \frac{2Z_1 \tan\theta_1 \tan\theta_2 - Z_2 \tan^2\theta_1}{Z_1 \tan\theta_2 - Z_1 \tan^2\theta_1 \tan\theta_2 + 2Z_2 \tan\theta_1} \tag{9}$$

$$Z_{in2} = -jZ_2 \cot\theta_2 \tag{10}$$

$$Z_{in} = jZ_2 \bullet \frac{2\left(1+K^2\right)\tan\theta_1 \tan\theta_2 - K\left(1-\tan^2\theta_2\right)\left(1-\tan^2\theta_1\right)}{2\left(K - \tan\theta_1 \tan\theta_2\right)\left(\tan\theta_2 + K\tan\theta_1\right)} \tag{11}$$

The input admittance seen from the open-circuit port can be expressed as

$$Y_i = jY_2 \frac{2\left(K\tan\theta_1 + \tan\theta_2\right)\left(K - \tan\theta_1 \tan\theta_2\right)}{K\left(1-\tan^2\theta_1\right)\left(1-\tan^2\theta_2\right) - 2\left(1-K^2\right)\tan\theta_1 \tan\theta_2} \tag{12}$$

Based on $Y_i = 0$, the resonant condition (impedance ratio) can be achieved as

$$K = \tan\theta_1 \tan\theta_2 \tag{13}$$

If $\theta_1 = \theta_2 = \theta$ the resonant condition and input admittance can be simplified.

The T-shaped microstrip SIR is shown in ***Figure 3***. The heights of the patches are W and W_1, and the widths are L_1 and L_2, respectively. The dimensions of all the dielectric substrates mentioned in this article are fixed to 50×50 mm^2 and their relative dielectric constant is $\varepsilon_r = 2.2$ or $\varepsilon_r = 2.6$. This kind of dielectric material has properties such as low dielectric loss ($\tan\delta \leq 5.10^{-4}$), low cost and easy manufacturability. The relationship between the resonant frequency f_0 and W is shown in ***Figure 4***. It can be seen that W variations have little influence on the reso-

It has great genes

The ENA carries on the family tradition

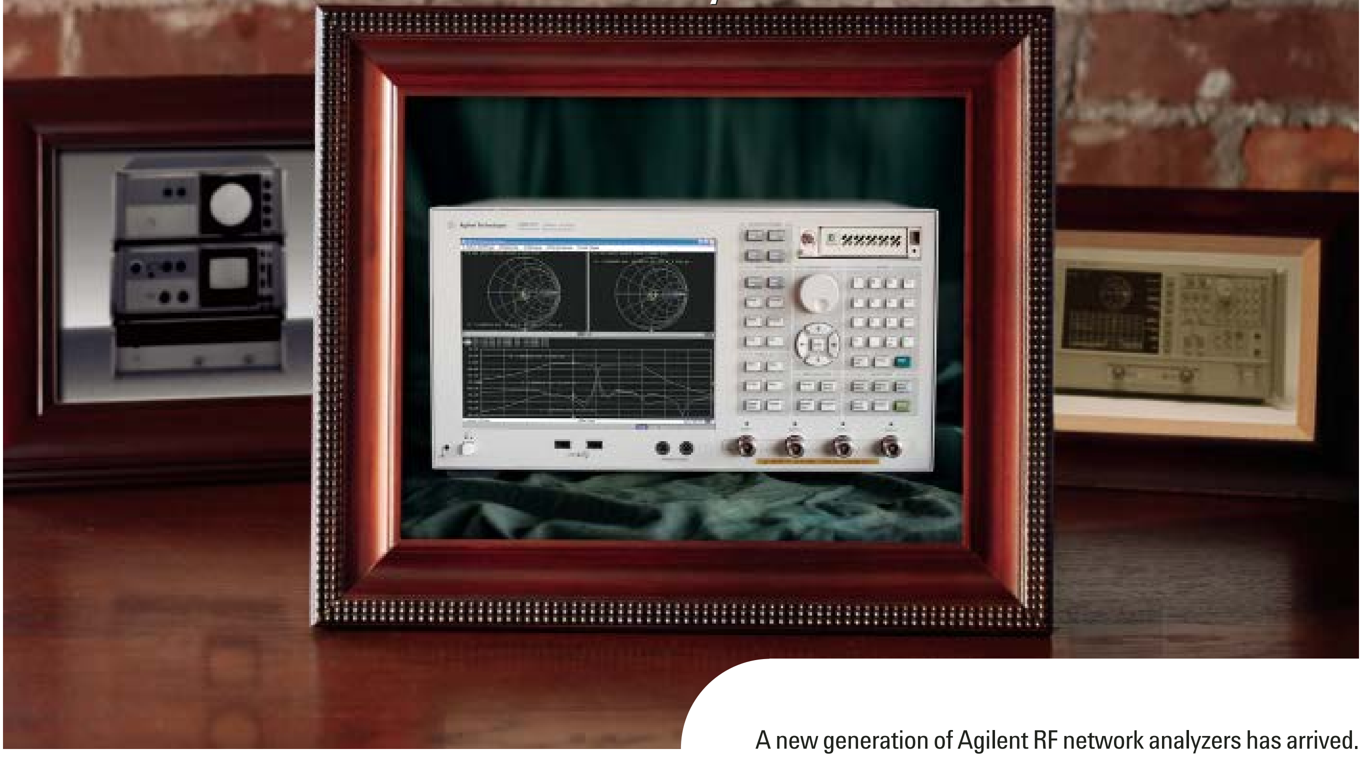

Agilent E5071C ENA
9 kHz to 8.5 GHz frequency range
> 123 dB dynamic range
Trace noise < 0.004 dB rms at 70 kHz IF bandwidth
39 ms measurement speed (1601 points, full 2-port calibration)
2- or 4-port measurements

A new generation of Agilent RF network analyzers has arrived. And its Agilent 8753 ancestors would be proud. The ENA Series builds on the family's 40-year legacy of excellence to deliver new standards in speed, accuracy, and versatility for RF network analysis.

With the ENA Series, you'll get excellent performance across its entire frequency range. No other network analyzer can match its dynamic range, trace noise, or measurement speed. And no one else has a frequency range that reaches from 8.5 GHz down to 9 kHz.

It's the kind of performance you'd expect from the 8753 family. Only now, it goes even further to help you do more—and do it better. It helps to have great genes on your side.

Put the ENA Series to work for you. For application notes and more information, visit www.agilent.com/find/genes.

u.s. 1-800-829-4444
canada 1-877-894-4414
www.agilent.com/find/genes

Agilent Technologies

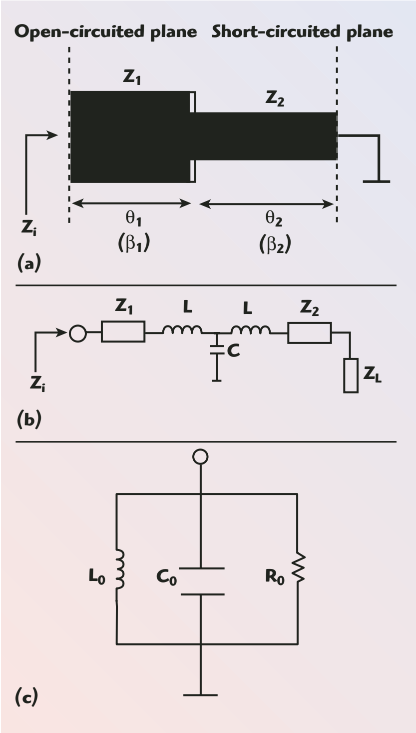

▲ *Fig. 1 Electric parameter of an SIR (a) its equivalent circuit (b) and the equivalent circuit at resonance (c).*

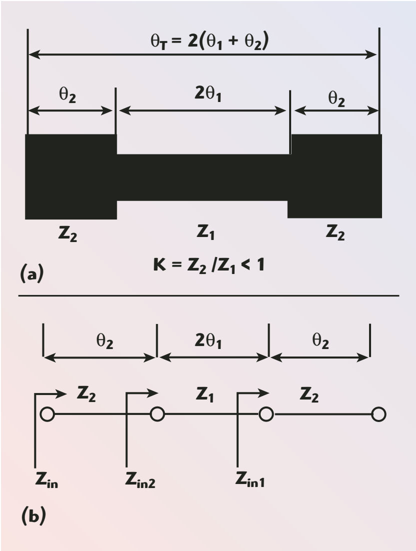

▲ *Fig. 2 Electric structure (a) of an H-shaped resonator and its equivalent transmission line model (b).*

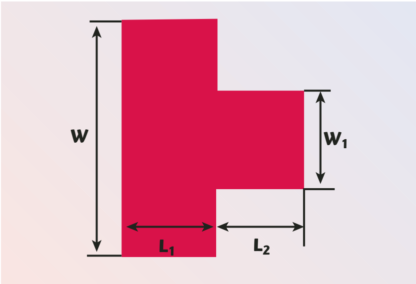

▲ *Fig. 3 T-shaped microstrip resonator.*

nant frequency. When W_1 = 10 mm, L_1 = 10 mm, L_2 = 10 mm and ε_r = 2.2, the resonant frequency of the dominant mode is nearly fixed at 2.85 GHz and that of the second-order mode is 4.52 GHz. When ε_r = 2.6, the resonant frequency of the dominant mode is 2.6 GHz and that of the second-order mode is 4.15 GHz. The relationship curves of the quality factor

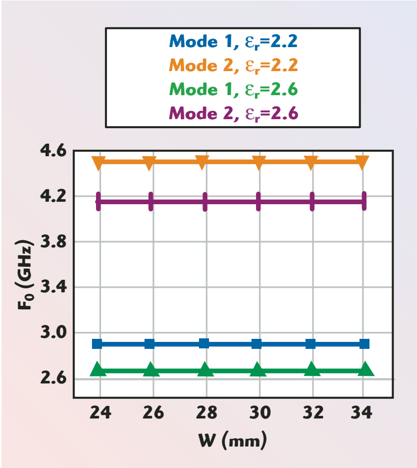

▲ *Fig. 4 Resonant frequency versus W.*

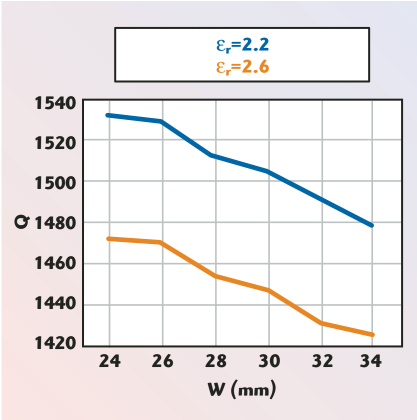

▲ *Fig. 5 Relationship of Q and W for the dominant mode.*

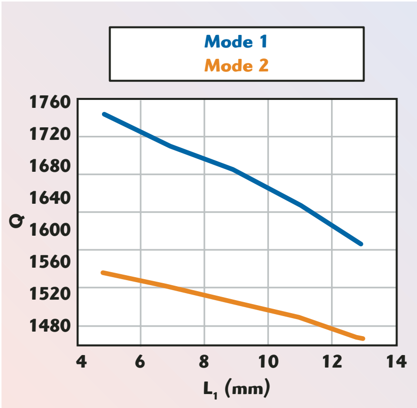

▲ *Fig. 6 Relationship of Q and L_1 (L_2 = 10 mm).*

From 21^{95} ea. Qty. (1-9) IN STOCK

DC-13 GHz Low & High Pass FILTERS

Mini-Circuits VLF Low Pass and VHF High Pass SMA Filters, featuring excellent stopband rejection and passband matching, flat passband response, and sharp roll-off, are unparalleled solutions for RF filtering over a wide range of bandwidths from DC to 13 GHz. Our unique patented Unibody package measures less than 1½" in length and is designed to minimize interconnect losses and improve reliability. Combine that with the temperature stability, performance repeatability, and low cost from our LTCC ceramic technology, and the result is a very rugged, high performance, competitively priced series. These filters are ideal for test set-ups as well as transmitter/receiver filtering in both tactical and commercial applications.

Mini-Circuits…we're redefining what VALUE is all about!

For RoHS compliant requirements, ADD + SUFFIX TO BASE MODEL No. Example: VLF-80+

Low Pass VLF Models $21.95 ea. (1-9)

Model	Passband (MHz)	fco, Nom. Loss 3 dB (MHz) Typ.	Stopband Loss >20 dB (MHz) Min.
VLF-80	DC-80	145	200
VLF-95	DC-95	165	220
VLF-105	DC-105	180	250
VLF-120	DC-120	195	280
VLF-160+	DC-160	230	330
VLF-180+	DC-180	270	370
VLF-190+	DC-190	280	400
VLF-225	DC-225	350	460
VLF-320	DC-320	460	560
VLF-400	DC-400	560	660
VLF-490	DC-490	650	800
VLF-530	DC-530	700	820
VLF-575	DC-575	770	900
VLF-630	DC-630	830	1000
VLF-800	DC-800	1075	1275
VLF-1000	DC-1000	1300	1550
VLF-1200	DC-1200	1530	1865
VLF-1400	DC-1400	1700	2015
VLF-1450	DC-1450	1825	2025
VLF-1500	DC-1500	1825	2100
VLF-1525	DC-1525	1750	2040
VLF-1575	DC-1575	1875	2175
VLF-1700	DC-1700	2050	2375
VLF-1800	DC-1800	2125	2425
VLF-2250	DC-2250	2575	2900
VLF-2500	DC-2500	3075	3675
VLF-2600	DC-2600	3125	3750
VLF-2750	DC-2750	3150	4000
VLF-2850	DC-2800	3300	4000
VLF-3000	DC-3000	3600	4550
VLF-3800+	DC-3900	4850	6000
VLF-4400+	DC-4400	5290	6700
VLF-5000	DC-5000	5580	6850
VLF-5500+	DC-5500	6200	7200
VLF-5850+	DC-5850	6540	7600
VLF-6000	DC-6000	6800	8500
VLF-6400+	DC-6400	7200	8300
VLF-6700	DC-6700	7600	9300
VLF-7200+	DC-7200	8150	9500

U.S. Patent Numbers 6,790,049 & 6,943,646

High Pass VHF Models $24.95 ea. (1-9)

Model	Passband (MHz)	fco, Nom. Loss 3 dB (MHz) Typ.	Stopband Loss >20 dB (MHz) Min.
VHF-650	710-2490	650	480
VHF-740	780-2800	740	550
VHF-880	950-3200	880	640
VHF-1200	1220-4600	1180	940
VHF-1300	1400-5000	1300	930
VHF-1320	1400-5000	1320	1060
VHF-1500	1600-5500	1550	1250
VHF-1600	1650-5000	1600	1290
VHF-1760	1900-5500	1760	1230
VHF-1810	1900-4750	1810	1480
VHF-1910	2000-5200	1910	1400
VHF-2000	2260-6250	2000	1530
VHF-2100	2200-6000	2100	1530
VHF-2275	2450-7000	2275	1770
VHF-2700	2650-6500	2500	1800
VHF-2700A+	2900-8700	2700	2150
VHF-3100+	3400-9900	3100	2450
VHF-3500+	3900-9800	3500	2800
VHF-3800	4250-10000	3800	3200
VHF-4400+	5000-10100	4400	3500
VHF-4600+	5000-11000	4600	3800
VHF-5050+	5500-10000	5050	4200
VHF-5500	6000-11500	5500	4500
VHF-7150+	7900-11000	7150	6150
VHF-8400	9000-13000	8400	6000

U.S. Patent Number 6,790,049

Mini-Circuits®

ISO 9001 ISO 14001 CERTIFIED

ALL NEW minicircuits.com

P.O. Box 350166, Brooklyn, New York 11235-0003 (718) 934-4500 Fax (718) 332-4661 For detailed performance specs & shopping online see Mini-Circuits web site

YONI2™ ***The Design Engineers Search Engine*** *Provides ACTUAL Data Instantly From MINI-CIRCUITS At:* ***www.minicircuits.com***

RF/IF & MICROWAVE COMPONENTS

394 Rev P

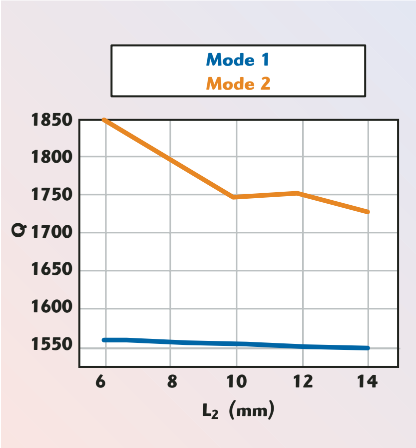

▲ *Fig. 7 Relationship of Q and L_2 (L_1 = 5 mm).*

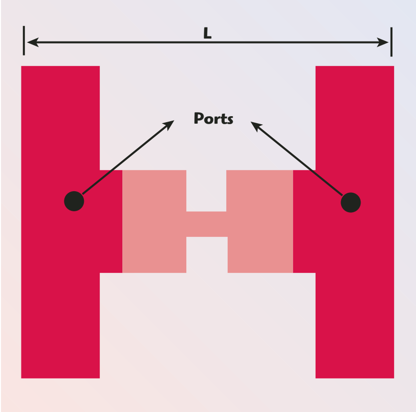

▲ *Fig. 8 Double-T-shaped bandstop filter with DGS.*

Q and W are shown in ***Figure 5***. It can be seen that the quality factor decreases when both W and ε_r increase. The relationship curves of Q and L_1, L_2 are shown in ***Figures 6*** and ***7***, respectively, with W = 30 mm and W_1 = 10 mm. They show that Q decreases when L_1 and L_2 increase and the Q of the second-order mode is larger than the one of the dominant mode.

DESIGN OF NOVEL SIR COUPLING MICROSTRIP FILTERS

A novel double-T-shaped bandstop filter with DGS is shown in ***Figure 8***. The dimensions of each T-shaped patch are W = 30 mm, W_1 = 10 mm, L_1 = 5 mm and L_2 = 4 mm. The overall width of the coupled patch is L = 26 mm. The double-T-shaped resonators form a bandstop filter when coupled to each other, but the filter performance is not acceptable because of its narrow passbands near the stopband; consequently, DGS was used. The performance of the bandstop filter was calculated with Ansoft

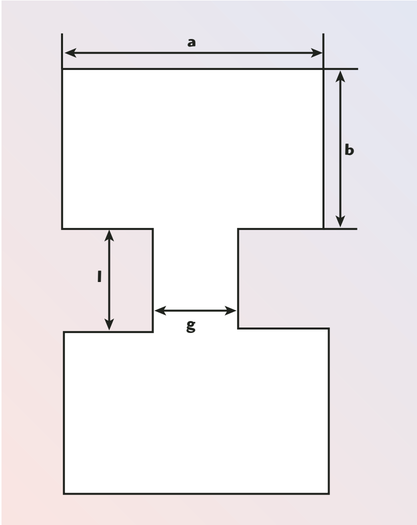

▲ *Fig. 9 DGS on the ground plane.*

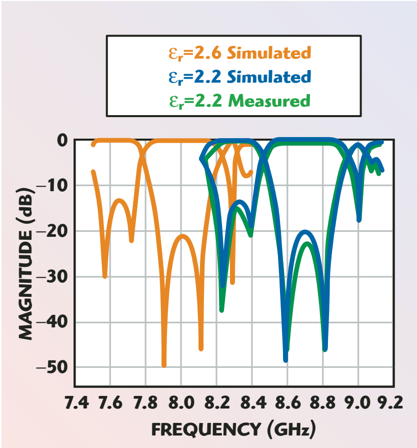

▲ *Fig. 10 S-parameters of the double-T-shaped filter.*

HFSS software. The dumbbell-shaped DGS on the ground plane is shown in ***Figure 9***, where a = 10 mm, b = 4 mm, g = 3 mm and l = 2 mm.

The simulated S-parameters of the filter are shown in ***Figure 10***. If the relative dielectric coefficient of dielectric substrate is ε_r = 2.2, it can be seen that there is a wide stopband at a center frequency of 8.71 GHz, with a 0.49 GHz bandwidth (5.62 percent). If ε_r = 2.6, there is a stopband at a center frequency of 8.004 GHz, with a 0.444 GHz bandwidth (5.55 percent). It can be seen that the attenuation within the stopband is greater than 20 dB, the stopband center frequency will shift with different dielectric substrates and the 3 dB bandwidth of the passband near the operational stopband is more than 200 MHz. The experimental results, measured with a HP8510 vector

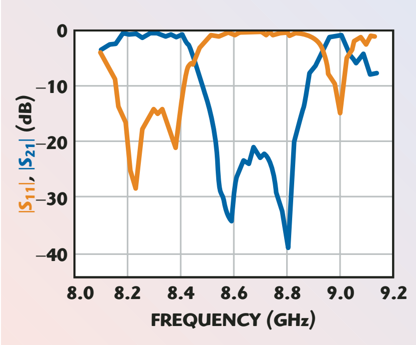

▲ *Fig. 11 Measured S-parameters of the double-T-shaped filter.*

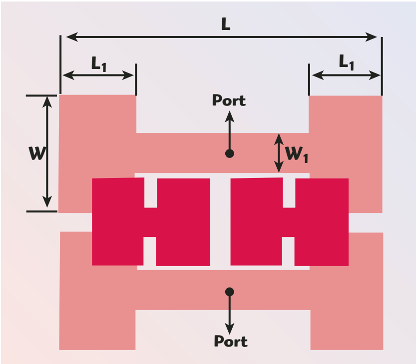

▲ *Fig. 12 Double-H-shaped bandpass filter with DGS.*

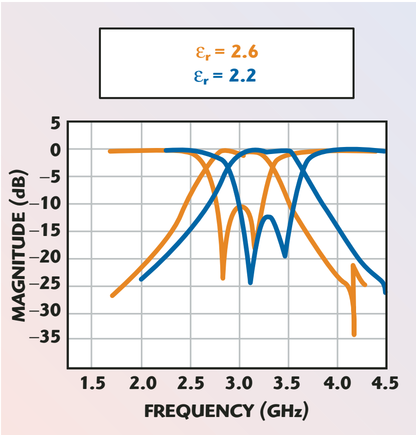

▲ *Fig. 13 Simulated S-parameters of the double-H-shaped filter.*

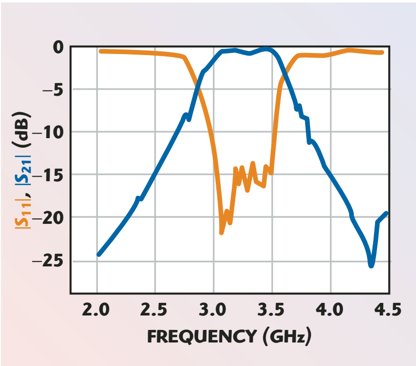

▲ *Fig. 14 Measured S-parameters of the double-H-shaped filter with $\varepsilon_r = 2.2$.*

network analyzer, are shown in ***Figure 11*** with $\varepsilon_r = 2.2$. They agree with the simulated ones.

The layout of a novel double-H-shaped microstrip bandpass filter is shown in ***Figure 12***. The dimension of every H-shaped patch is w = 15 mm, $w_1 = 5$ mm, L = 40 mm, $L_1 = 10$ mm. The coupling coefficient k is bandpass filter can be expressed as

$$k = \frac{B_r}{\sqrt{g_i g_{i+1}}} \qquad (14)$$

where

B_r = relative bandwidth

g_i (i = 1, 2, …, n–1) = low pass prototype value corresponding to the desired filter responses

n = order of filter

In order to improve the performance of the filter effectively, a pair of DGSs is applied, and for each DGS, a = 9 mm, b = 5 mm, l = 4.2 mm and g = 3 mm. The simulated S-parameters of the double-H-shaped microstrip bandpass filter are shown in ***Figure 13***, and the experimental results are shown in ***Figure 14***. For $\varepsilon_r = 2.2$, it can be seen that the center frequency is 3.275 GHz and there is an attenuation pole at 4.5 GHz. The 3 dB bandwidth is 0.75 GHz, the maximum insertion loss is 0.55 dB at the center frequency and the coupling coefficient is k = 0.229. For $\varepsilon_r = 2.6$, the center frequency is 3 GHz, the 3 dB bandwidth is 0.676 GHz, the maximum insertion loss is 0.37 dB at the center frequency and the coupling coefficient is k = 0.225. There is an attenuation pole at 4.18 GHz, and the maximum attenuation is greater than 32 dB. It can be seen from the figures that the simulated and measured frequency responses are in good agreement.

CONCLUSION

In this article, the performance of stepped-impedance resonators are computed and analyzed. A novel double-T-shaped microstrip bandstop filter with DGS and a double-H-shaped microstrip bandpass filter with DGS are designed and their performance is calculated, measured and analyzed.

The simulated and measured frequency responses show good agreement. The proposed filters have advantages such as compact and simple structures, they are easily integrated and manufactured, and they show wide bandwidths, high attenuations and also demonstrate that the filters' performance can be effectively improved by using DGS. ■

ACKNOWLEDGMENT

This work was supported by the Shanghai Leading Academic Discipline Project (No. T0103) and the National Natural Science Foundation of China (No. 60571054).

References

1. J.S. Hong, M.J. Lancaster, D. Jedamzik, R.B. Greed and J.C. Mage, "On the Performance of HTS Microstrip Quasi-elliptic Function Filters for Mobile Communications Application," *IEEE Transactions on Microwave Theory and Techniques*, Vol. 48, No. 7, July 2000, pp. 1240–1246.
2. J.S. Hong and M.J. Lancaster, "Aperture-coupled Microstrip Open-loop Resonators and Their Applications to the Design of Novel Microstrip Bandpass Filters," *IEEE Transactions on Microwave Theory and Techniques*, Vol. 47, No. 9, September 1999, pp. 1848–1855.
3. L.H. Hsieh and K. Chang, "High Efficiency Piezoelectric-transducer-tuned Feedback Microstrip Ring-resonator Oscillators Operating at High Resonant Frequencies," *IEEE Transactions on Microwave Theory and Techniques*, Part 1, Vol. 51, No. 4, April 2003, pp. 1141–1145.
4. S.K. Satpathy, G. Kumar and K.P. Ray, "Compact Shorted Variations of Triangular Microstrip Antennas," *Electronics Letters*, Vol. 34, No. 8, 1998, pp. 709–711.
5. J.S. Yun, G.Y. Kim, J.S. Park, D. Ahn, K.Y. Kang and J.B. Lim, "A Design of the Novel Coupled Line Bandpass Filter Using Defected Ground Structure," *2000 IEEE MTT-S International Microwave Symposium Digest*, Vol. 1, pp. 327–330.
6. D. Ahn, J.S. Park, C.S. Kim, J. Kim, Y.X. Qian and T. Itoh, "A Design of the Low Pass Filter Using the Novel Microstrip Defected Ground Structure," *IEEE Transactions on Microwave Theory and Techniques*, Vol. 49, No. 1, January 2001, pp. 86–93.
7. J.R. Crute and L. Davis, "A Compact Microstrip Interdigital Stepped-impedance Bandpass Filter With Enhanced Stopband," *Microwave and Optical Technology Letters*, Vol. 34, No. 5, 2002, pp. 336–340.
8. M. Makimoto and S. Yamashita, *Microwave Resonators and Filters for Wireless Communication*, Springer-Verlag, Berlin Heidelberg, 2001.
9. D.C. Chung and B.S. Han, "HTS Microstrip Filters Using H-Type Resonators," *IEEE Transactions on Applied Superconductivity*, Vol. 11, No. 1, January 2001, pp. 388–391.

Jian-kang Xiao *received his BS degree in electronics from Lanzhou University, China, in 1996, and his MS degree in radio physics from Lanzhou University in 2004. He is currently working toward his PhD degree. Since 1996 he has been an electrical engineer at the Institute of Modern Physics, Chinese Academy of Sciences. His research interests include microwave and millimeter-wave theory and their applications.*

Shi-wei Ma *received his BS, MS and PhD degrees in radio physics, electronics, control theory and control engineering from Lanzhou University, Shanghai University, China, in 1986, 1991 and 2000, respectively. After two years as an STA research fellow at the Japan National Institute of Industrial Safety, he is now an associate professor in the automation department of Shanghai University. His current research interests include signal processing, time-frequency analysis theory, and applications and microsystems integration.*

Ying Li *is currently a professor at Shanghai University. His research interests include electromagnetic theory, microwave and millimeter-wave techniques and their applications.*

A 40 TO 900 MHz CMOS BROADBAND DIFFERENTIAL LNA FOR A DTV RF TUNER

This article describes a 40 to 900 MHz CMOS broadband differential LNA with gain control for a DTV RF tuner application. The LNA is fabricated in a TSMC 0.18 µm CMOS process. The broadband differential LNA uses dual-feedback and shunt-shunt feedback topologies to achieve high gain and a flat broadband response. The LNA is designed with 75 Ω differential input and output impedances for a 75 Ω TV system application. The circuit measurement is performed using an FR-4 PCB test fixture. In the frequency range from 40 to 900 MHz, the LNA exhibits a gain of 20.26 ±0.41 dB, a noise figure less than 5 dB, and an input P1dB between –19.5 and –20.3 dBm. The gain tuning range is from 20 to –42.8 ±4.9 dB over the 40 to 900 MHz range. The power consumption is 43 mW at V_{DD} =1 8 V.

Digital TV offers a far wider choice of TV viewing and a reduction of the interference that may be experienced on analog TV. Recently, many RF circuits realized in the CMOS process have been reported and the 0.18 µm process is a good candidate for highly integrated systems-on-chip (SOC) applications. The requirements of low power and low cost push the trend toward a single radio chip. ***Figure 1*** shows the up-down architecture of a DTV RF tuner.[1,2] The RF signal is upconverted to 1.2 GHz by the first mixer and then downconverted by the second mixer to the IF. Rather than bulky tunable filters used traditionally in direct-down architec-

Fig. 1 Up-down architecture of a DTV RF tuner.

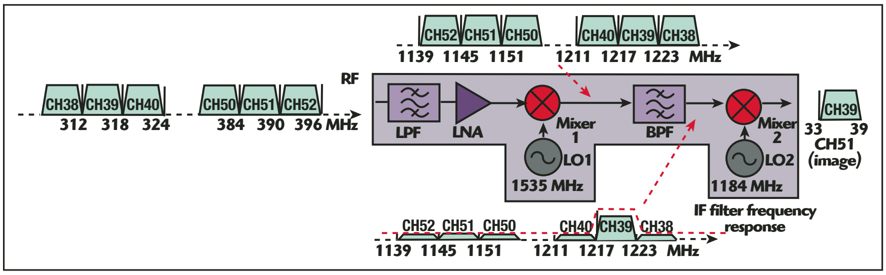

D.R. HUANG AND H.R. CHUANG
National Cheng Kung University
Tainan, Taiwan, ROC
Y.K. CHU
Himax Technologies
Tainan, Taiwan
C.L. LU
Kun Shan University
Tainan, Taiwan, ROC

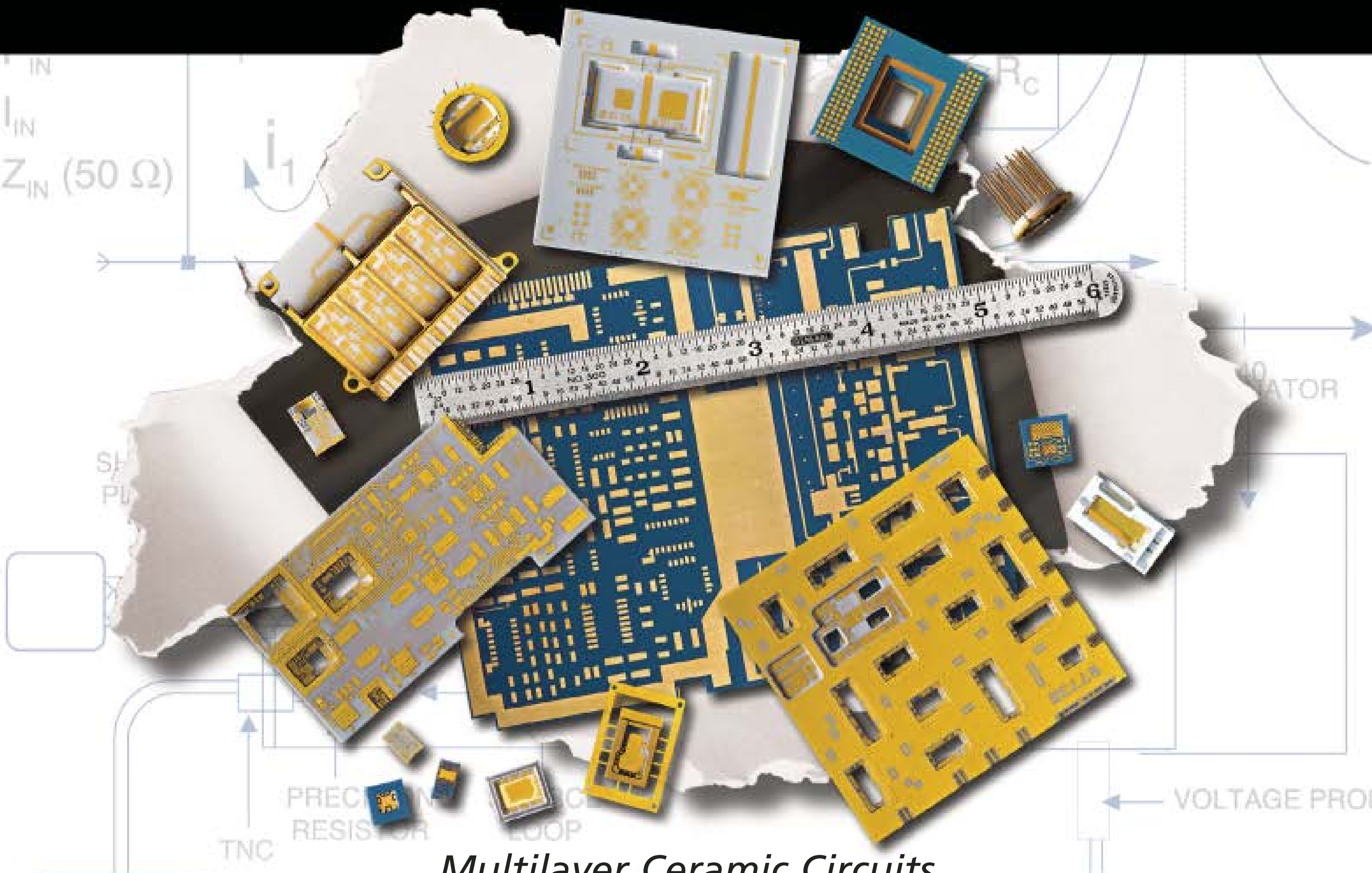

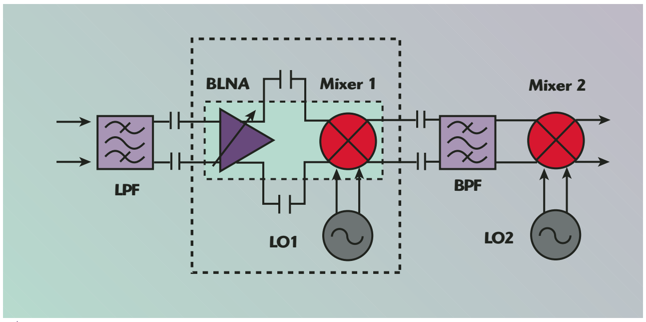

▲ *Fig. 2 Block diagram of a DTV tuner differential RF front-end.*

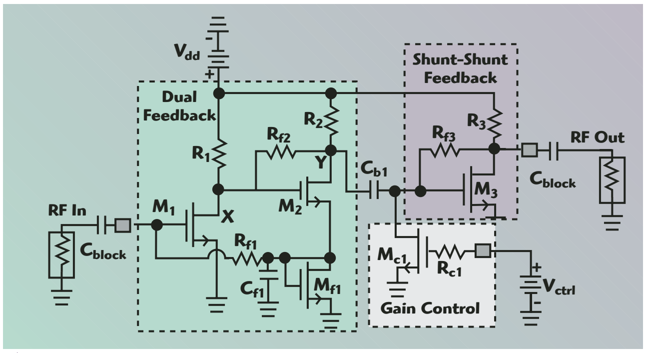

▲ *Fig. 3 Half circuit schematic of the designed broadband differential LNA with gain control.*

ture, the up-down architecture has the advantage of providing a good image rejection by using a 1.2 GHz bandpass filter.

For an RF TV tuner application, the LNA not only requires low noise and high gain but also high linearity and flat response over the 40 to 900 MHz frequency range. In this article, a broadband differential LNA with gain-control, using dual-feedback and shunt-shunt feedback topologies, is adopted to achieve high gain and a flat broadband response. The controllable gain can prevent saturation of the receiver when the input signal level is relatively high. The broadband LNA is implemented in a TSMC 0.18 μm CMOS process.

LNA TOPOLOGY AND CIRCUIT DESIGN

Figure 2 shows the block diagram of a DTV tuner differential RF front-end, in which the presented three-stage LNA includes two feedback amplification stages and one gain-control stage (see ***Figure 3***). It uses dual-feedback and shunt-shunt feedback stages to achieve a high and flat broadband response. The dual-feedback stage is the first stage and the shunt-shunt feedback stage is the second stage, to increase the gain. The gain-control stage is used to prevent saturation.

It is known that the differential circuit can mitigate the effects of common mode noise. As shown, this LNA, which did not use a high impedance at the source terminal, is a pseudo-differential circuit structure. The reason not to use a true differential amplifier circuit is that, for low voltage RFIC design (1.8 V, for example) a high impedance at the source terminal will compress the voltage headroom and output voltage swing, which will reduce the amplifier gain. Also, this pseudo-differential LNA circuit can still reject the common mode noise from V_{DD}.

Feedback Stages

The dual-feedback stage adopts the Kukeilka architecture.[3–5] This architecture is a refinement of the traditional shunt-series feedback. The output of the dual-feedback stage is capacitively coupled to the shunt-shunt feedback stage input through a DC block capacitor.

The M_1 and M_2 of the dual-feedback stage dissipates 2 and 4 mA of DC current, respectively. The aspect ratios (W/L) of M_1 and M_2 are chosen

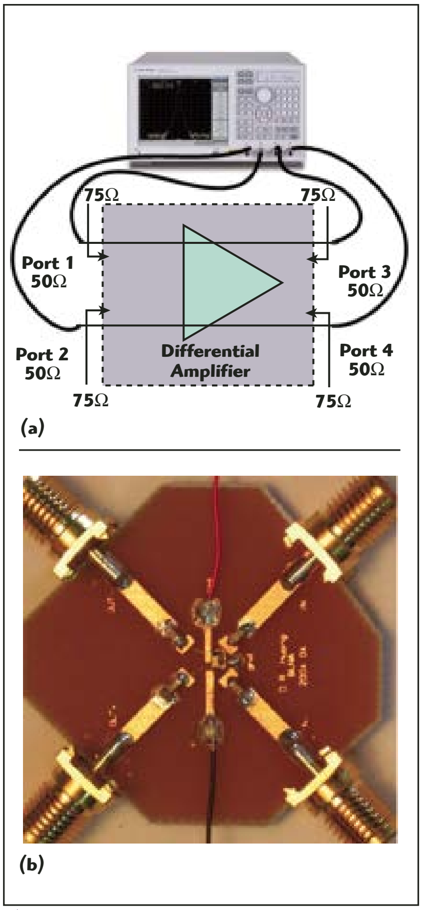

▲ *Fig. 5 Block diagram (a) and photograph (b) of the PCB test fixture to measure the differential S-parameters.*

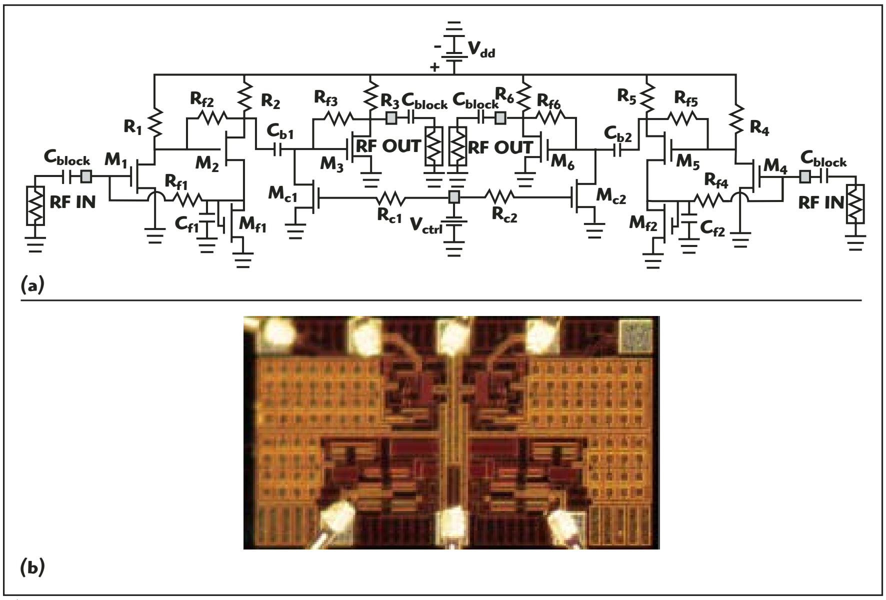

▲ *Fig. 4 Complete circuit schematic (a) and chip micrograph (b) of the designed differential LNA.*

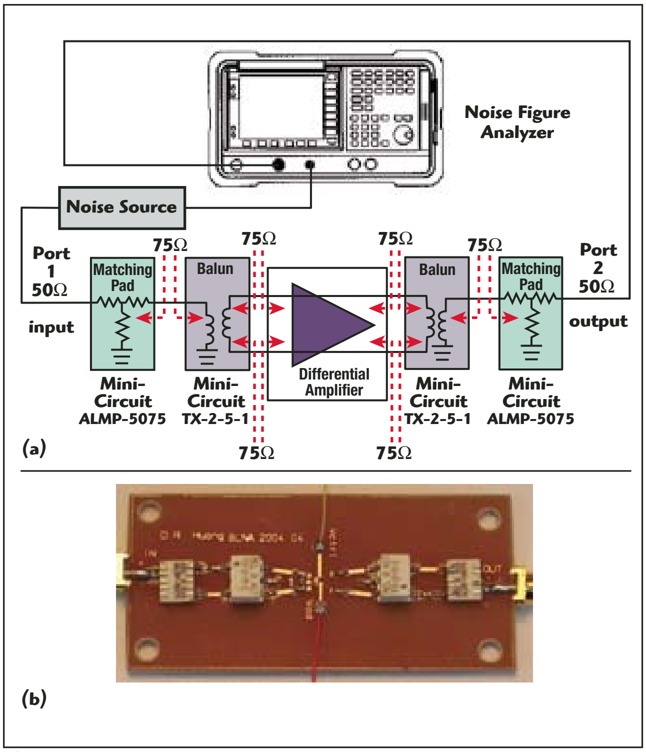

▲ *Fig. 6 Block diagram of the 50 to 75Ω and single-ended to differential input/output conversion scheme (a) and photograph (b) of the test fixture.*

to be the same. To ensure M_1 is operating in the saturation region, the size of the diode-connected transistor, M_{f1}, is chosen to be twice that of M_1. In addition, C_{f1} is added in parallel with M_{f1} to compensate the overdamped characteristic of this structure. However, the dual-feedback stage does not provide the desired gain for the LNA. In order to achieve a higher gain, a shunt-shunt feedback stage[6] is added. M_3 dissipates 6 mA of DC current and the shunt-shunt feedback stage dissipates 12 mA due to the differential topology.

Gain-control Stage

As shown, M_{c1} is used to implement a gain-control mechanism. The voltage, V_{ctrl}, applied to M_{c1}, controls the variable gain. This topology yields a negative slope gain-control curve. The LNA has its maximum gain when the control voltage is zero and vice versa.

SIMULATION AND MEASUREMENT RESULTS

Figure 4 shows the complete circuit schematic and chip micrograph of the designed differential LNA. The chip die size is 1.007 × 0.568 mm. The circuit measurement is performed using an FR-4 PCB test fixture. For differential S-parameter measurements, a four-port network analyzer was used. Since the four-port analyzer can support differential measurement, no baluns are needed. ***Figure 5*** shows the block diagram and photograph of the test fixture for differential measurement environment. It is noted that, although this circuit is designed for 75 Ω DTV systems, 50 Ω instruments are used for measurement. In order to match the two different characteristic impedances used in the system, matching pads (Mini-Circuit ALMP-5075) are used to convert the impedance from 50 to 75 Ω and vice versa. For single-ended instruments such as the signal generator, spectrum analyzer and noise figure analyzer, a balun (Mini-Circuit TX-2-5-1) is used to convert the differential input/output to single-ended input/output. ***Figure 6*** shows the block diagram of the conversion scheme and a photograph of FR-4 PCB test fixture.

The simulated and measured results are shown in ***Figures 7*** to ***11***, where the measurements of S_{21} and S_{12} are shown with the losses of the baluns and matching pads de-embedded. When the control voltage is zero (high gain mode), the LNA exhibits a gain of 20.26 ±0.41 dB, a noise figure less than 5 dB, an input P1dB between –19.5 and –20.3 dBm, and an IIP3 between –12.7 and –10.9 dBm from 40 to 900 MHz. When the control voltage is at 1.8 V (low gain mode), the LNA gain is –42.8 ±4.9 dB. The power consumption is 43 mW at V_{DD} = 1.8 V. It is noted that for the S-parameters, since the measurement with 50 Ω systems and the simulation using 50 Ω loads show good agreement, it is believed that

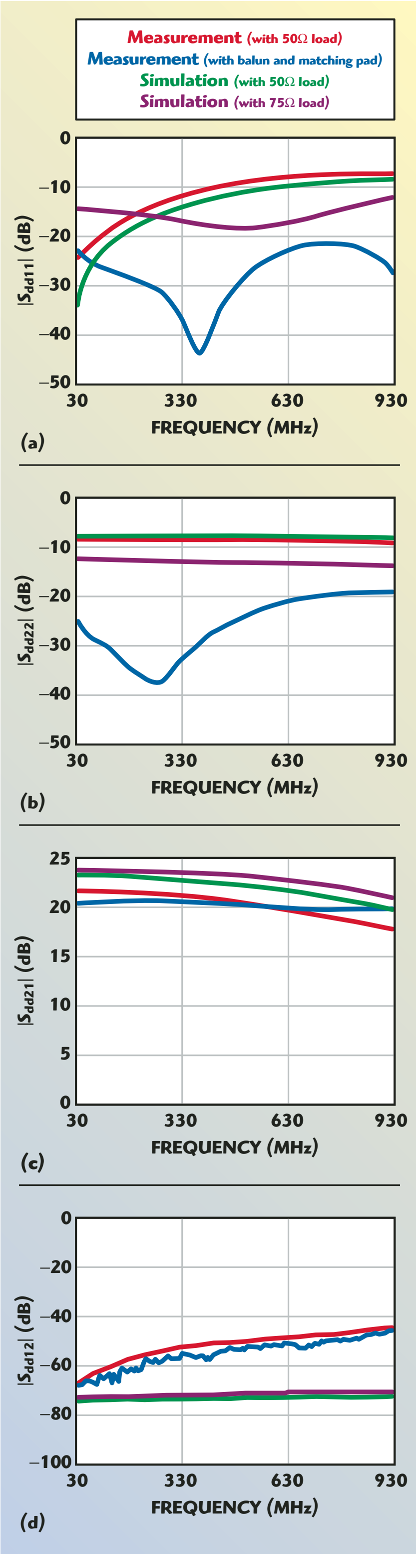

▲ *Fig. 7 High gain mode S-parameters.*

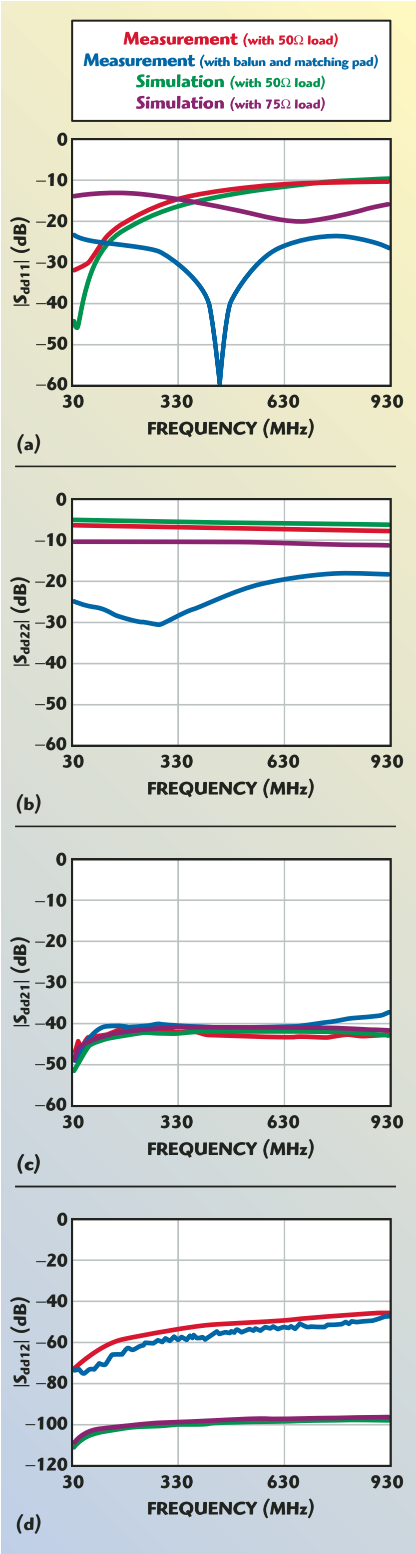

▲ *Fig. 8 Low gain mode S-parameters.*

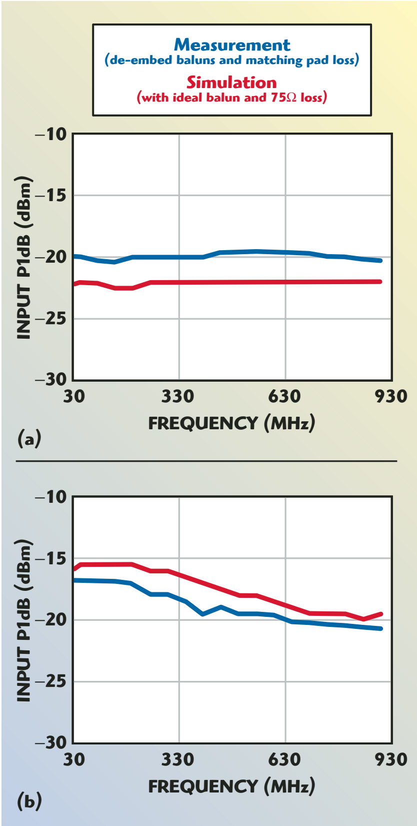

▲ *Fig. 9 Input P1dB versus frequency; (a) high gain mode and (b) low gain mode.*

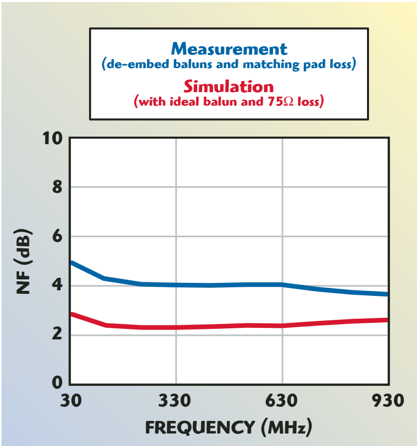

▲ *Fig. 10 Noise figure versus frequency in the high gain mode.*

the measurements with a 75 Ω system (not provided) and the simulations will also be in good agreement. ***Table 1*** gives a summary of the measured and simulated performance of the CMOS broadband differential LNA with gain control.

CONCLUSION

A 40 to 900 MHz CMOS broadband differential LNA with gain control, implemented in a 0.18 μm CMOS process, for a DTV RF tuner application is described. The LNA uses both a dual-feedback and shunt-feedback topology to achieve a high and flat broadband response. The LNA is designed with 75 Ω differential input and output impedances. The chip die size is 1.007 × 0.568 mm. The circuit measurement is performed using an FR-4 PCB test fixture. Since typical measurement instruments are 50 Ω systems, matching pads are used in the measurement to match the impedances between 50 and 75 Ω. For single-ended measurements such as with spectrum

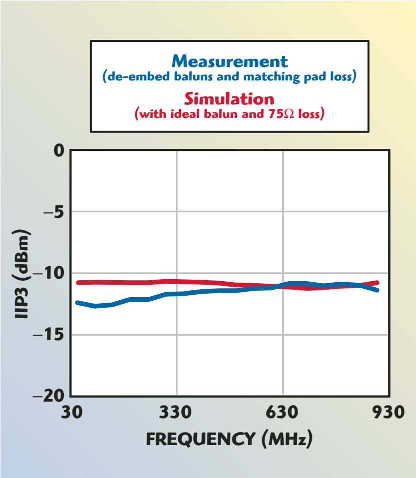

▲ *Fig. 11 IIP3 versus frequency in the high gain mode.*

and noise figure analyzers, a balun is used to convert the differential input/output to single-ended input/output. In the 40 to 900 MHz frequency range, the LNA exhibits a gain of 20.26 ±0.41 dB, a noise figure less than 5 dB, an input P1dB between –19.5 and –20.3 dBm, and an IIP3 between –12.7 and –10.9 dBm. The gain tuning range is from 20 to –42.8 ±4.9 dB over the 40 to 900 MHz range. The power consumption is 43 mW at V_{DD} = 1.8 V. ■

TABLE I

SIMULATED AND MEASURED PERFORMANCE OF A CMOS BROADBAND DIFFERENTIAL LNA WITH GAIN CONTROL

	Simulation	Measurement
Frequency range (MHz)	40~900	
Operating voltage (V)	1.8	
Current/power consumption	22.8 mA/41.04 mW	24 mA/43.2 mW
Input/output return loss (dB)	> 8.4/7.7 (50 Ω load) > 12.6/12.5 (75 Ω load)	> 7.4/8.5 (50 Ω load) –
Gain (dB)	21.6±1.6	20.3±0.4
Noise figure (dB)	< 2.8	< 5
Input P1dB (high gain/ low gain mode) (dBm)	–22~–22.5/ –15.5~–20	–19.5~–20.3/ –16.8~–20.7
IIP3 (high gain mode) (dBm)	–10.7~–11.1	–10.8~–12.7
Gain tuning range (dB)	21.6±1.6~–46.1±3.8	20.3±0.4~–42.8±4.9
Die size (mm)	1.007 × 0.568	

ACKNOWLEDGMENT

The authors would like to thank the Chip Implementation Center (CIC) of the National Science Council, Taiwan, ROC, for providing the TSMC CMOS process.

References

1. S. Birleson, et al., "Silicon Single-chip Television Tuner Technology," *2000 ICCE Conference Digest of Technical Papers*, pp. 38–39.
2. B. Taddiken, et al., "Broadband Tuner on a Chip for Cable Modem, HDTV and Legacy Analog Standards," *2000 IEEE RFIC Symposium Digest*, pp. 17–20.
3. C.D. Hull and G.B. Mayer, "Principle of Monolithic Wideband Feedback Amplifier Design," *International Journal of High Speed Electronics*, Vol. 3, February 1992, pp. 53–93.
4. F.T. Chien and Y.J. Chan, "Bandwidth Enhancement of Transimpedance Amplifier by Capacitive-peaking Design," *IEEE Journal of Solid-State Circuits*, Vol. 34, August 1999, pp. 1167–1170.
5. Y.C. Chen and S.S. Lu, "Analysis and Design of CMOS Broadband Amplifier with Dual-feedback Loops," *2002 ASIA-PACIFIC Conference on ASICs*.
6. B. Razavi, *Design of Analog CMOS Integrated Circuits*, McGraw-Hill, New York, NY, 2001.
7. B. Razavi, *RF Microelectronics*, Prentice Hall, Upper Saddle River, NJ, 1997.
8. D.A. Johns and K. Martin, *Analog Integrated Circuits Design*, John Wiley & Sons Inc., Hoboken, NJ, 1997.
9. D.E. Bockelman and W.R. Eisenstadt, "Combined Differential and Common-mode Scattering Parameters: Theory and Simulation," *IEEE Transactions on Microwave Theory and Techniques*, Vol. 43, No. 7, July 1995, pp. 1530–1539.

THE GLOBAL SOLUTION... AND BEYOND!

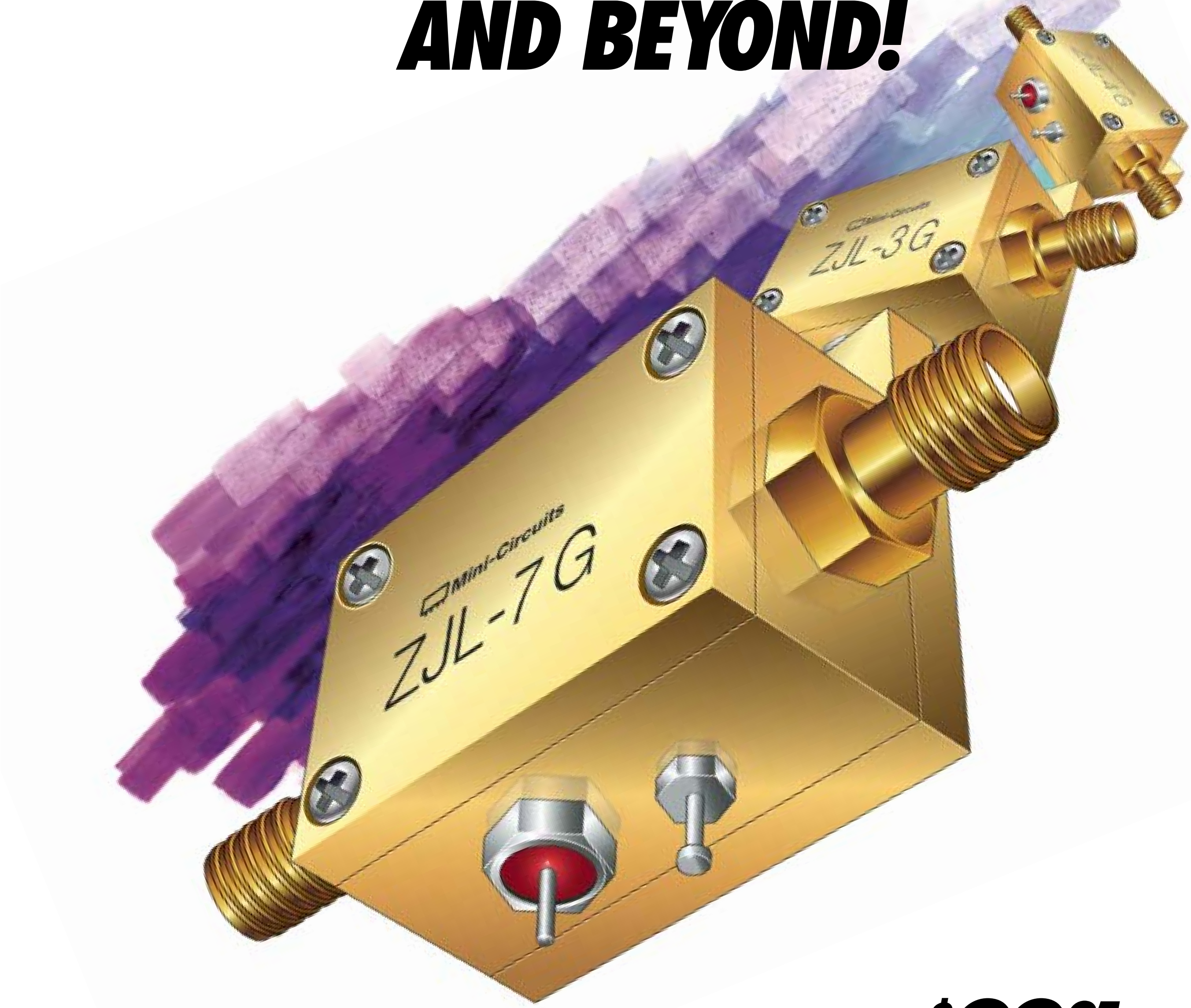

10 MHz to 7 GHz AMPLIFIERS from $99.95 (1-9 qty.)

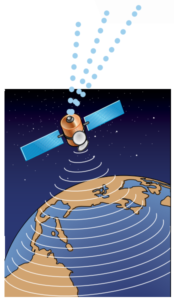

From amateur radio to cellular to satellite applications, with medium output power up to 17 dBm, Mini-Circuits versatile ZJL and ZKL connectorized amplifiers offer the broad range of choices designers demand for achieving high system performance goals. Ultra-wideband models deliver **gain ranging from 9 to 40 dB** and IP3 up to +32 dBm. But beyond the performance and reliability built into these miniature 12V amplifiers lies another important feature, the low price...from only $99.95! Call now for fast delivery.

Mini-Circuits...we're redefining what VALUE is all about!

SPECIFICATIONS

Model	Freq (MHz)	Gain (typ) Midband (dB)	Gain (typ) Flat (±dB)	Max. P_{out}[1] (dBm)	Dynamic Range (Typ @2 GHz[2]) NF(dB)	Dynamic Range (Typ @2 GHz[2]) IP3(dBm)	I(mA)[3]	Price $ea. (1-9)
ZJL-5G	20-5000	9.0	±0.55	15.0	8.5	32.0	80	129.95
ZJL-7G	20-7000	10.0	±1.0	8.0	5.0	24.0	50	99.95
ZJL-4G	20-4000	12.4	±0.25	13.5	5.5	30.5	75	129.95
ZJL-6G	20-6000	13.0	±1.6	9.0	4.5	24.0	50	114.95
ZJL-4HG	20-4000	17.0	±1.5	15.0	4.5	30.5	75	129.95
ZJL-3G	20-3000	19.0	±2.2	8.0	3.8	22.0	45	114.95
ZKL-2R7	10-2700	24.0	±0.7	13.0	5.0	30.0	120	149.95
ZKL-2R5	10-2500	30.0	±1.5	15.0	5.0	31.0	120	149.95
ZKL-2	10-2000	33.5	±1.0	15.0	4.0	31.0	120	149.95
ZKL-1R5	10-1500	40.0	±1.2	15.0	3.0	31.0	115	149.95

NOTES:
1. Typical at 1 dB compression.
2. ZKL dynamic range specified at 1 GHz.
3. All units at 12V DC.

Mini-Circuits®
ISO 9001 ISO 14001 CERTIFIED

ALL NEW minicircuits.com

P.O. Box 350166, Brooklyn, New York 11235-0003 (718) 934-4500 Fax (718) 332-4661 For detailed performance specs & shopping online see Mini-Circuits web site

YONI2™ ***The Design Engineers Search Engine*** *Provides ACTUAL Data Instantly From MINI-CIRCUITS At:* ***www.minicircuits.com***

RF/IF MICROWAVE COMPONENTS

232 Rev E

EM ENABLES CLASSIC FILTER TECHNIQUE

Electromagnetic (EM) tools are indispensable for simulating high frequency designs, but they are poorly suited for synthesizing filters that require the determination of multiple parameters. This article describes how to use EM simulation to aid a classic and under-utilized technique for filter design. The classic technique requires building prototypes of a few select resonators and plotting certain measured data. From these plots the filter dimensions are easily synthesized. Modern EM simulation breathes new life into this classic technique by eliminating the need to construct prototypes. This is particularly important when a process requires a long manufacturing cycle time. Unusual resonators such as compact planar, MEMS and multi-layer structures are increasingly used to solve challenging design requirements, but are poorly modeled by analytical formulas. The technique described here is particularly well suited for such structures.

THE CLASSIC TECHNIQUE

The classic technique is also referred to as the general procedure, because it enables the design of bandpass filters of almost any type. This article emphasizes the application of EM to the procedure. Puglia[1] gives a comprehensive description of the general procedure. For completeness, the procedure is briefly reviewed here.

Bandpass filters entail only three first principles:

1. the resonators must exist,
2. the resonators must couple to each other and
3. the structure must couple to the terminations.

The general procedure is based directly on these first principles. The designer selects a form of resonator. Essentially, the only restrictions are that the resonator realizability and some method of coupling must exist. Next, data is acquired that relates the degree of resonator coupling to a variable parameter. Finally, data is acquired that relates termination coupling to a variable parameter. From this data, the filter is synthesized using simple analytical expressions.

Filter tables are usually published in the form of prototype values for a low pass filter

RANDY RHEA
Susina LLC

TABLE I

LOW PASS PROTOTYPE VALUES FOR A 0.1 dB PASSBAND RIPPLE CHEBYCHEV FOR ORDER N = 2 TO 9

N	g (0)	g (1)	g (2)	g (3)	g (4)	g (5)	g (6)	g (7)	g (8)	g (9)	g (N+1)
2	1	0.843	0.622								1.335
3	1	1.032	1/147	1.032							1.000
4	1	1.109	1.306	1.770	0.818						1.335
5	1	1.147	1.371	1.975	1.371	1.147					1.000
6	1	1.168	1.404	2.056	1.517	1.903	0.862				1.335
7	1	1.181	1.423	2.097	1.573	2.097	1.423	1.181			1.000
8	1	1.190	1.435	2.120	1.601	2.170	1.564	1.944	0.878		1.335
9	1	1.196	1.443	2.135	1.617	2.205	1.617	2.135	1.443	1.196	1.000

with 1 radian cut-off frequency and a source impedance of 1 Ω. An example for 0.1 dB passband ripple Chebyshev filters of orders 2 through 9 is given in ***Table 1***. Many authors, including Puglia,[1] provide simple formula for finding Chebyshev prototype values for other passband ripple and order criteria. g_0 is the normalized source termination and g_{N+1} is the normalized load termination. Notice that for odd-order Chebyshev $g_0 = g_{N+1}$. For even-order, g_{N+1} increases for increasing passband ripple. There are N reactive values for an Nth order prototype.

The general procedure utilizes k and q values rather than low pass prototype values. k values relate to resonator couplings and q values relate to end-resonator loaded Qs. k and q values are easily derived from low pass prototype values.

$$k_{n,n+1} = \frac{1}{\sqrt{g_n \bullet g_{n+1}}} \text{ for } n = 1 \text{ to } (N-1) \quad (1)$$

$$q_1 = g_0 \bullet g_1 \quad (2)$$

$$q_N = g_N \bullet g_{N+1} \text{ for N odd} \quad (3)$$

$$q_N = \frac{g_N}{g_{N+1}} \text{ for N even} \quad (4)$$

As an example, the Chebyshev table with N = 5, $q_1 = q_5 = 1.147$, then $k_{12} = k_{45} = 0.797$ and $k_{23} = k_{34} = 0.608$.

These k and q values are normalized by the filter fractional bandwidth, bw.

$$bw = \frac{f_{upper} - f_{lower}}{f_0} \quad (5)$$

where

f_{upper} = passband upper cut-off frequency

f_{lower} = passband lower cut-off frequency

and

$$f_0 = \frac{f_{upper} + f_{lower}}{2} \quad (6)$$

Then the actual filter couplings and loaded Qs are

$$K_{n,n+1} = bw \bullet k_{n,n+1} \quad (7)$$

$$Q_1 = \frac{q_1}{bw} \quad (8)$$

$$Q_N = \frac{q_N}{bw} \quad (9)$$

Notice that the capitalized symbols refer to actual couplings and loadings while noncapitalized symbols refer to normalized values.

DETERMINING A STRUCTURE'S K VALUES

Consider the pair of resonators shown in ***Figure 1***. The red areas are the microstrip metal, the blue areas are the via pads on the ground plane layer and the gray lines are the EM simulation grid. Each grid square is 15 mils on a side. The microstrip resonators are 90 mils wide and 240 mils long on a 31-mil thick PTFE-fiberglass substrate. The resonators are grounded with via holes at the bottom and are loaded with capacitors C_1 and C_2 at the top, thus forming a conventional combline. This metal layout pattern is simulated using the EMPOWER electromagnetic simulator in the GENESYS software suite.[2] Test ports 1 and 2 are very loosely coupled to the resonators through input and output lines and very small capacitors C_3 and C_4. The edge-to-edge resonator spacing is 11 grid squares or 165 mils.

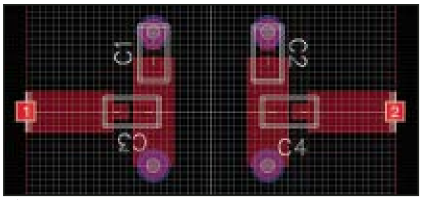

Fig. 1 Layout of combline microstrip resonators used for EM simulation.

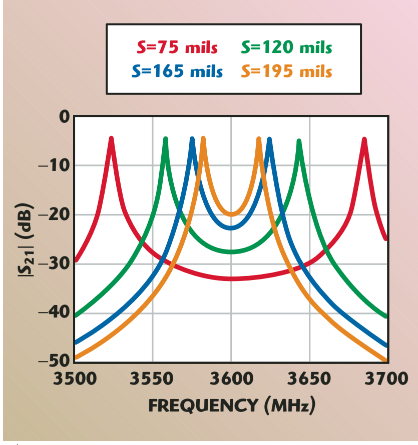

Fig. 2 S_{21} response of coupled combline resonators with variable edge-to-edge spacing S.

The frequency domain responses of this system are shown in ***Figure 2*** for edge-to-edge spacings of 195, 165, 120 and 75 mils. C_1 and C_2 are tuned to center the response at the desired filter center frequency, in this case 3600 MHz. Two response peaks are observed when the loading coupling is very loose. The coupling coefficient of this system is given by

$$K = \frac{f_{upper} - f_{lower}}{f_0} \quad (10)$$

For the spacing of 165 mils, f_{upper} = 3624.8 MHz and f_{lower} = 3575.2 MHz, so K = 0.0138.

The general procedure involves plotting this data, as illustrated in ***Figure 3***. The green curve is obtained by EM simulation, while the blue curve is the result of circuit theory simulation. The red curve is the difference, in percent, between these data. A feature of the general procedure is that K is typically a monotonic function of the variable parameter,

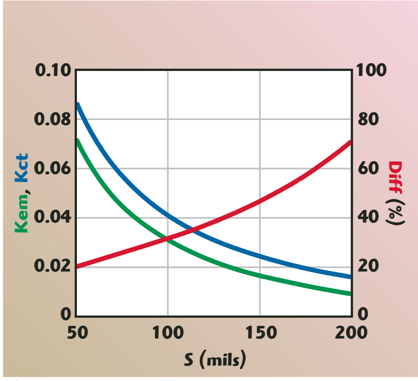

▲ *Fig. 3 Coupling coefficient K versus edge-to-edge spacing S.*

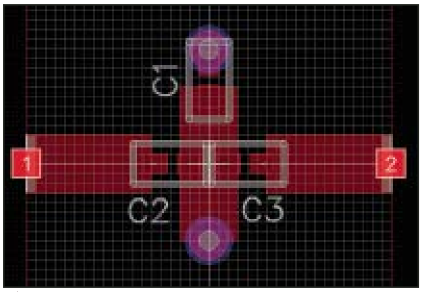

▲ *Fig. 4 Layout of a microstrip combline resonator used for EM simulation of the double-loaded Q vs. coupling capacitance.*

and a smooth curve is easily drawn through a small number of data points. Here the data has been extrapolated to 50 and 200 mils. A plot of the coupling coefficient K for any spacing between these limits is now created.

DETERMINING A STRUCTURE'S Q VALUES

Consider the resonator shown in ***Figure 4***. The resonator is grounded with a via at the bottom and is loaded with capacitors C_1 at the top. It is a single resonator identical to the coupled resonators. Test ports 1 and 2 are coupled to the resonators through input and output lines and capacitors C_2 and C_3 that control the loaded Q of each end resonator in the final filter. A frequency domain response of this system is shown in ***Figure 5***, where the values of C_2 and C_3 are 0.3 pF. C_1 is tuned to center the response at the desired filter center frequency each time a different value is tried for the coupling capacitors. The singly terminated loaded Q is given by

$$Q = \frac{2f_0}{f_{upper} - f_{lower}} \qquad (11)$$

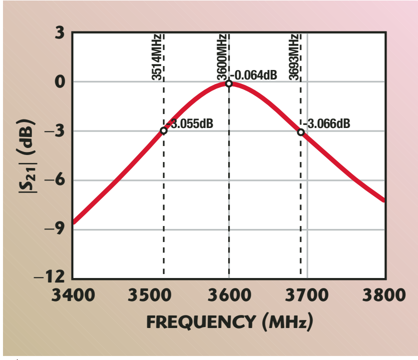

▲ *Fig. 5 Response of a doubly-loaded resonator with coupling capacitors of 0.3 pF.*

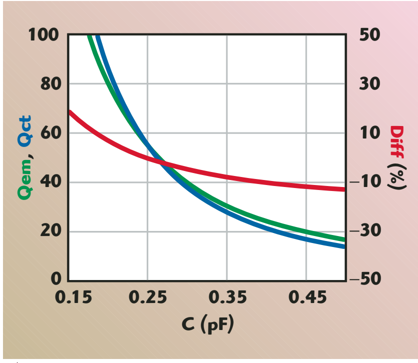

▲ *Fig. 6 Singly-loaded Q as a function of the coupling capacitor C.*

In this case f_{upper} = 3693 MHz and f_{lower} = 3514 MHz, so Q = 40.2.

The general procedure involves repeating this data for a few different values of coupling capacitance. The Q was computed by EM simulation for capacitance values of 0.2, 0.3 and 0.45 pF. As was the case with K, the Q is typically a monotonic function of the variable parameter and a smooth curve is easily drawn through a small number of data points. ***Figure 6*** shows the data extrapolated to capacitor values of 0.15 to 0.5 pF. The Q from EM simulation is shown in green, while the one obtained by circuit theory simulation is shown in blue. Their difference in percent is shown in red. A plot of the resonator loaded Q for any capacitance value between these limits is now available.

DESIGNING THE FILTER WITH K AND Q DATA

The plots of coupling coefficient and loaded Q contain sufficient data to design on this substrate a 3600 MHz combline filter with any bandwidth, any order and any transfer approximation shape, provided only that the required spacings and capacitor coupling values fall within the given


HIGH-PERFORMANCE
IC DESIGN & VERIFICATION
HIGH-PERFORMANCE
SIGNAL & POWER INTEGRITY
HIGH-PERFORMANCE
RF & MICROWAVE DESIGN
HIGH-PERFORMANCE
EM SYSTEMS DESIGN
ANSOFT.COM

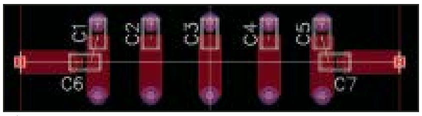

▲ *Fig. 7 Layout of the final 3600 MHz combline bandpass filter.*

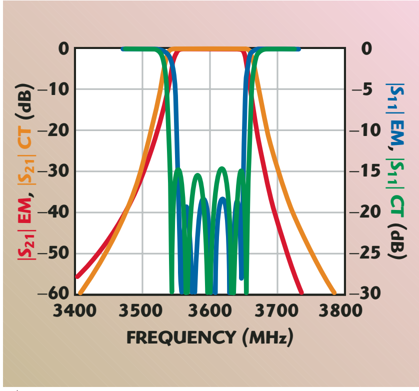

▲ *Fig. 8 Combline filter S-parameters computed by EM simulation and from circuit theory.*

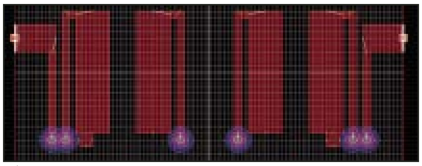

▲ *Fig. 9 Layout of a four-section, 1700 MHz stepped-impedance resonator (SIR) bandpass filter.*

ranges. Consider, for example, a filter with the following parameters:

$$f_0 = 3600 \text{ MHz}$$
$$BW = 100 \text{ MHz}$$
$$N = 5$$
$$\text{Shape} = \text{Chebyshev}$$
$$A_r = 0.1 \text{ dB}$$

From Equations 1 through 9, it is found that $Q_1 = Q_N = 1.147/0.0278 = 41.29$. From the green trace in the plot of Q vs. C, the required input and output coupling capacitors are shown to be approximately 0.28 pF. From the same equations, $K_{1,2} = K_{4,5} = 0.797 \times 0.0278 = 0.0222$ and $K_{2,3} = K_{3,4} = 0.608 \times 0.0278 = 0.0169$. From the green trace of the plot of coupling coefficient vs. spacing, the spacing between resonator 1 and 2, and 4 and 5, is approximately 120 mils, and the spacing between 2 and 3, and 3 and 4, is 150 mils.

RESULTS USING THE GENERAL PROCEDURE

The layout of the final 3600 MHz combline bandpass is shown in ***Figure 7***, with the dimensions given above. The EM and circuit theory computed responses are given in ***Figure 8***. After EM simulation of the metal pattern, the loading capacitors C1 through C5 were optimized for the best response. The input and output coupling capacitors were fixed at the computed value of 0.28 pF. From the EM simulation, the resulting bandwidth is approximately 92 MHz, 8 percent lower than the desired 100 MHz, and the return loss is approximately 18 dB, 2 dB worse than desired. For comparison purposes, the circuit theory results show a bandwidth of approximately 116 MHz, 16 percent wider than desired and a return loss of only 15 dB, 5 dB worse than desired. Considering again the plot of coupling coefficient vs. spacing, the red trace is the percentage error of the circuit theory coupling with respect to the EM coupling.

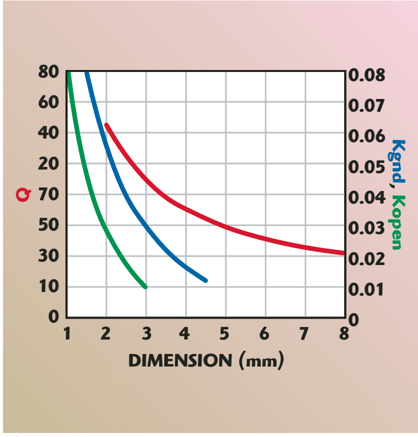

▲ *Fig. 10 Loaded Q versus line length and coupling coefficients for adjacent lines.*

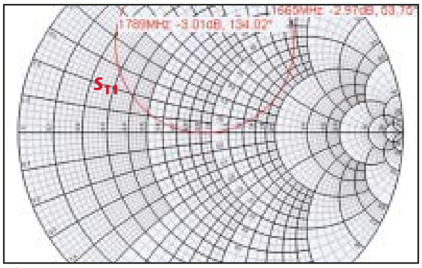

▲ *Fig. 11 Smith chart plot for measuring the end-resonator loaded Q vs. length of the coupling line.*

Notice that, with a spacing of 50 mils the error is 25 percent, while with a spacing of 195 mils the error is 68 percent. This confirms the known phenomena in edge-coupled filters that a bandwidth error increases with narrow bandwidth filters. With wideband filters the error is often unnoticed while with narrow filters the error can be extreme.

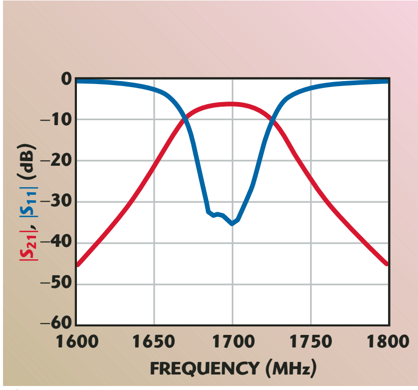

▲ *Fig. 12 Transmission and return loss for the 1700 MHz SIR bandpass filter.*

There is another important lesson here. The failure of the circuit theory accuracy is obvious, yet there are only two resonators. This means that the error is not attributable to coupling between non-adjacent resonators, as is often believed.

The source of the circuit theory bandwidth error is evanescent modes. The effects of these modes are naturally considered by EM simulation but they are difficult to simulate using circuit theory, because their effect depends on the orientation and loading of the lines, the filter bandwidth and the substrate properties. The error increases with thicker substrates. Interestingly, inter-digital filters are far less susceptible to evanescent modes.

The design of filters, using EM simulation to find K and Q values, is more accurate than the design using circuit theory synthesis and simulation techniques. The simplicity of the math used to design this combline filter results naturally because the general procedure relies directly on the three first principles.

SECOND EXAMPLE

The layout of a four-section, 1672 to 1728 MHz bandpass filter is given in ***Figure 9***, using a unique stepped-impedance resonator (SIR).[3,4] SIR technology shortens the required physical length of the resonators by increasing the inductance of high current sections of transmission lines and/or increasing the capacitance of high voltage sections. These quarter-wavelength 1700 MHz SIR resonators are 18.5 mm long on a 1.28 mm thick Rogers 3006 substrate with a relative dielectric constant of 6.15. The narrow sections of line are 0.5

TINY CERAMIC LOW & HIGH PASS FILTERS

80 to 13000 MHz…Immediate Delivery

from **99¢** ea. qty.1000

Measuring only 0.12"x0.06", these tiny hermetically sealed filters cover 80 to 13000 MHz. Utilizing our advanced *Low Temperature Co-fired Ceramic (LTCC) technology,* their superior thermal stability, high reliability and very low cost make them a must for your system requirements.

HIGH PASS FILTERS *(HFCN)*

Model	Passband MHz	Stopband MHz (Loss >20 dB) Min.	Price $ ea. Qty. 10	DESIGNER'S KITS (5 of each model) K1 79.95	K2 99.95
HFCN-650+	710-2490	480	1.99	•	
HFCN-740+	780-2800	550	1.99	•	
HFCN-880+	950-3200	640	1.99		•
HFCN-1200+	1220-4600	910	1.99	•	
HFCN-1300+	1400-5000	930	1.99		•
HFCN-1320+	1400-5000	1060	1.99		•
HFCN-1500+	1600-5500	1250	1.99	•	
HFCN-1600+	1650-5000	1290	1.99		•
HFCN-1760+	1900-5500	1230	1.99	•	
HFCN-1810+	1950-4750	1480	1.99		•
HFCN-1910+	2000-5200	1400	1.99		•
HFCN-2000+	2260-6250	1530	1.99	•	
HFCN-2100+	2200-6000	1530	1.99		•
HFCN-2275+	2450-7000	1770	1.99	•	
HFCN-2700+	2650-6500	1800	1.99	•	
▲HFCN-2700A+	2900-8700	2150	2.99		
▲HFCN-3100+	3400-9900	2450	2.99		
▲HFCN-3500+	3900-9800	2800	2.99		
▲HFCN-3800+	4250-10000	3200	2.49		•
▲HFCN-4400+	5000-10100	3500	2.99		
▲HFCN-4600+	5000-11000	3800	2.99		
▲HFCN-5050+	5500-10000	4200	2.99		•
▲HFCN-5500+	6000-11500	4500	2.99		
▲HFCN-7150+	7900-11000	6150	2.99		
▲HFCN-8400+	9000-13000	6000	2.99		•
			Total number of units in kit:	40	50

HFCN Models: -3800+, -5500+, -8400+ Patent Pending

LOW PASS FILTERS *(LFCN)*

Model	Passband MHz	Stopband MHz (Loss >20 dB) Min.	Price $ ea. Qty. 10	DESIGNER'S KITS (5 of each model) K1 99.95	K2 119.95	K3 109.95	K4 175.95	K5 129.95
LFCN-80+	DC-80	200	3.99			•		
LFCN-95+	DC-95	230	3.99			•		
LFCN-105+	DC-105	250	3.99			•		
LFCN-120+	DC-120	280	3.99			•		
LFCN-160+	DC-160	330	2.99					
LFCN-180+	DC-180	370	2.99					
LFCN-190+	DC-190	400	2.99					
LFCN-225+	DC-225	460	2.99	•		•		
LFCN-320+	DC-320	560	2.99	•		•		
LFCN-400+	DC-400	660	2.99	•		•		
LFCN-490+	DC-490	800	2.99	•		•		
LFCN-530+	DC-530	820	2.99	•		•		
LFCN-575+	DC-575	900	2.99	•		•		
LFCN-630+	DC-630	1000	2.99	•		•		
LFCN-800+	DC-800	1400	1.99		•		•	
LFCN-900+	DC-850	1275	1.99		•		•	
LFCN-1000+	DC-1000	1550	1.99		•		•	
LFCN-1200+	DC-1200	1865	1.99		•		•	
LFCN-1325+	DC-1325	2100	1.99		•		•	
LFCN-1400+	DC-1400	2015	2.99				•	
LFCN-1450+	DC-1450	2025	2.99				•	
LFCN-1500+	DC-1500	2100	2.99				•	
LFCN-1525+	DC-1525	2040	2.99				•	
LFCN-1575+	DC-1575	2175	2.99				•	
LFCN-1700+	DC-1700	2375	1.99		•		•	
LFCN-1800+	DC-1800	2425	2.99				•	
LFCN-2000+	DC-2000	3000	1.99		•		•	•
LFCN-2250+	DC-2200	2900	1.99		•		•	•
LFCN-2400+	DC-2400	3600	1.99		•		•	•
LFCN-2500+	DC-2500	3675	1.99					•
LFCN-2600+	DC-2600	3750	1.99					•
LFCN-2750+	DC-2750	4000	1.99					•
LFCN-2850+	DC-2800	4000	1.99					•
LFCN-3000+	DC-3000	4550	1.99					•
LFCN-3800+	DC-3900	6000	2.99					•
LFCN-4400+	DC-4400	6700	2.99					•
LFCN-5000+	DC-5000	6850	1.99		•		•	•
LFCN-5500+	DC-5500	7200	1.99					
LFCN-5850+	DC-5850	7600	1.99					
LFCN-6000+	DC-6000	8500	1.99		•		•	•
LFCN-6400+	DC-5400	8300	1.99					
LFCN-6700+	DC-6700	9300	1.99		•		•	•
LFCN-7200+	DC-7200	9500	1.99					
			Total number of units in kit:	35	60	55	90	65

LFCN Models: U.S. Patent 6,943,646 except LFCN-800+, -1325+, -2000+ & -2400+.

7 Designer's Kits Available *(see table):*
Order kits by prefix (K1, K2, etc.)
Followed by -LFCN+ or -HFCN+
Example: K1-LFCN+

HFCN+ & LFCN+ ▲HFCN+

mm wide and the wide sections are 2.5 mm. Conventional, 1.5 mm wide, unstepped quarter wave 1700 MHz resonators on this substrate are 20 mm long. Folding also conserves space. The grid cells are 0.25 × 0.5 mm. This structure is poorly modeled using circuit theory transmission line models. However, it is a classic candidate for design using the general procedure, with EM simulation to find resonator couplings and end-resonator loaded Qs. Plotted in ***Figure 10*** are the couplings and loaded Qs determined by EMPOWER. Notice that this SIR filter has two types of resonator couplings. Resonators one and two have lines that are open-ended adjacent to each other. The resonator coupling for this configuration is plotted in green, with the independent horizontal axis being edge-to-edge resonator spacing in millimeters. Resonators two and three have via grounded lines adjacent to each other. This coupling is plotted in blue. Plotted in red is the end resonator, singly loaded, Q vs. length of coupling line from the bottom edge of the input line to the centerline of the via. The left/right asymmetry of the SIR resonator precludes a doubly terminated measurement of the loaded Q, so an alternative method is used. For the EM simulation, a resonator is singly loaded and the resistivity of the metal is increased until the effective parallel loss resistance loads the resonator to a degree equal to the load termination. This occurs when the input return passes through the center of the Smith chart, as shown in ***Figure 11***. The frequencies of the 3.01 dB return loss are then used in Equation 11 to find the singly terminated end-resonator loaded Q. For simulated coupling line lengths varying from two to eight millimeters, the required resistivity varies from 4.5 to 120. For the figure, a coupling line length of 5 mm and a resistivity of 75 were used. The input and output termination coupled-line transformers have the effect of slightly increasing the frequency of the end resonators. This was compensated empirically by adding small areas of metal to the end resonators, while examining the EM simulated response. The final SIR filter transmission and input return loss responses, computed by EMPOWER, are given in ***Figure 12***. This filter occupies only about 40 percent of the space required by a conventional inter-digital structure. The general procedure and EM simulation are effective toolmates for quick and accurate design of filters with structures that are difficult to model analytically. ■

References

1. K.V. Puglia, "A General Design Procedure for Bandpass Filters Derived from Low Pass Prototype Elements," *Microwave Journal*, Part I, Vol. 43, No. 12, December 2000, pp. 22–38; Part II, Vol. 44, No. 1, January 2001, pp. 114–134.
2. EMPOWER Manual, Agilent Technologies Inc.
3. S. Yamashita and M. Makimoto, "Miniaturized Coaxial Resonator Partially Loaded with High Dielectric-constant Microwave Ceramics," *Transactions on Microwave Theory and Techniques*, Part I, Vol. 31, No. 9, September 1983, pp. 697–703.
4. R. Rhea, *HF Filter Design and Computer Simulation*, Noble Publishing, Raleigh, NC, pp. 116–121.

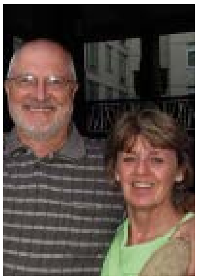

Randall Rhea *is a graduate of the University of Illinois (1969) and Arizona State University (1973). His thesis was construction of an earth station that monitored Apollo 16 & 17 Unified S-band signals from the moon. He worked briefly at the Boeing Co. and Goodyear Aerospace and for 14 years at Scientific-Atlanta, where he became principal engineer. He founded Eagleware Corp. in 1985, recently acquired by Agilent Technologies, and Noble Publishing in 1994, recently acquired by SciTech Publishing. He has authored numerous technical papers, tutorial CDs and the books* Oscillator Design and Computer Simulation *and* HF Filter Design and Computer Simulation. *He has taught oscillator and filter design techniques to over 1000 engineers through full-day seminars at trade shows, the Georgia Institute of Technology and corporations. His hobbies include antiques, historical properties, astronomy and amateur radio (N4HI). He and his wife Marilynn have two adult children and reside near Thomasville, GA.*

Visit www.mwjournal.com to read "Technology Enables New Components," Randy Rhea's Cover Feature that appeared in the November 2006 issue of *Microwave Journal*.

CONCEPT AND METHOD OF HIGH EFFICIENCY IN A PRECISION KA-BAND SUBMINIATURE COAXIAL CONNECTOR

This article presents the design approach and test results of a Ka-band narrow flange receptacle (NFR), subminiature version A (SMA) connector based on transmission line theory, involving multi-step impedances and air-layer characteristics to increase its maximum frequency of operation. In order to increase its frequency performance, the connector is designed with a dual outward form (a hook structure), a thick outer conductor wall and a very thin inner pin. The return loss increment due to the hook and multi air-layer structures is minimized to 2 and 1.5 dB, respectively. A VSWR of less than 1.2 is obtained from DC to 30 GHz and the connector performance is stable from room temperature to 120°C.

During the late 1950s and early 1960s, 7 mm coaxial transmission lines with standard SMA connectors were only used at frequencies between 10 and 12 GHz. In the mid-1960s, the US Department of Commerce established the Joint Industry Research Committee for the Standardization of Miniature Precision Coaxial Connectors (JIRF/SMPCC). The result of that effort yielded a voluntary product standard in 1972.[1,2] The air transmission line size was reduced to 3.5 mm to extend the mode-free operation of that line to 36 GHz. With increasing demand for high speed data transmission rates, the operating frequencies of commercial communication systems are currently increasing to achieve wider bandwidth.[3] Consequently, the development of microwave products was undertaken in the United States, Europe and Asia. Korea also developed microwave amplifiers, oscillators and mixers. In this article, a Ka-band connector is designed on the basis of transmission line theory and then fabricated. In order to meet the Ka-band operating frequency range, a multi-step impedance technique, utilizing air layers, is applied. Moreover, for commercial purposes, the connector must be able to operate at high temperature in order that the hook structure and step transition satisfy military (MIL) specifications.

JAE-HO YOON, WON-YONG CHO, AH-RAH KOH, SEUNG-JUN LEE, BHANU SHRESTHA, GARY P. KENNEDY AND NAM-YOUNG KIM
Kwangwoon University
Seoul, Korea

Full selection of laminates and prepreg for RF/Microwave and High Speed Digital applications.

Dk AND Df VALUES AT 10 GHz*

- **IS640-280 =** Dk 2.80, Df 0.0025
- **IS640-300 =** Dk 3.00, Df 0.0032
- **IS640-320 =** Dk 3.20, Df 0.0032
- **IS640-325 =** Dk 3.25, Df 0.0032
- **IS640-333 =** Dk 3.33, Df 0.0035
- **IS640-338 =** Dk 3.38, Df 0.0035
- **IS640-345 =** Dk 3.45, Df 0.0035

*All are available in 0.020", 0.030" and 0.060" thicknesses.

IS640 laminate and prepreg material is a unique formulation for the RF/Microwave and High Speed Digital markets. IS640 exhibits stable electrical properties over a broad frequency range of 2 to 20 GHz. Produced with stringent thickness and electrical tolerances, IS640 provides designers with consistent line impedance.

IS640 is available in multilayer core thicknesses (0.0025" - 0.018") and thicker core (0.020", 0.030" and 0.060") for RF and Microwave applications. Standard panel sizes are available, providing a complete materials package solution.

IS640 MULTILAYER AVAILABILITY

PREPREG GLASS STYLES		PREPREG GLASS STYLES	PRESSED THICKNESS NOMINAL
0.0025	0.0080	106	0.0030″
0.0030	0.0100	1080	0.0040″
0.0040	0.0120	2113	0.0043″
0.0050	0.0140	3070	0.0048″
0.0060	0.0160	2116	0.0054″
0.0066	0.0180	1652	0.0060″

IS640 PRODUCT STRENGTHS

- Superior Signal Integrity - stable Dk Df 2 - 20 GHz
- Customized Dk on 0.020", 0.030" and 0.060" thicknesses, Dk available = 2.80, 3.00, 3.20, 3.25, 3.33, 3.38 and 3.45
- Utilizes Standard E-glass
- Full compliment of multilayer cores from 0.0025" to 0.018"
- 6 glass styles available for prepreg
- No ceramic filler in the base resin
- Good drilling and routing performance
- Thermal coefficient of Dk, dielectric constant, = 55 ppm/°C from - 40°C to 125°C
- Thermal coefficient of Df, loss tangent, = 6 ppm/°C from - 40°C to 125°C
- Very good power handling results
- Compatible with Isola FR406, IS410, 370HR, IS415, FR408 and IS620 for hybrid applications

TCK DK

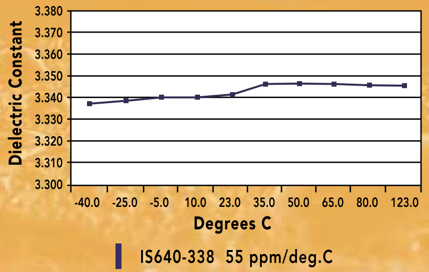

Epoxy based systems are at 300 to 400 ppm/deg C level

TCK LOSS TANGENT

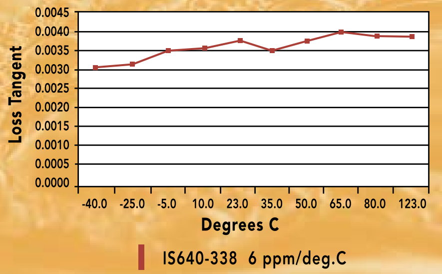

Low TCK - Df ppm level very good for Power Handling

The data, while believed to be accurate and based on analytical methods considered to be reliable, is for information purposes only. Any sales of these materials will be governed by the terms and conditions of the agreement under which they are sold.

* Isola utilizes the IPC-TM650-2.5.5.5 Stripline Resonator to test material with thickness of 0.030 and above as a means of determining a nominal value for dielectric constant and loss tangent test frequency is set at 10 GHz. Please note that for laminate dielectric thickness below .030 the test method that is utilized to determine the Dk and Df values is referred to as the Bereskin Stripline Resonator method. The Bereskin Stripline Resonator test method lends itself to the test and measurement of Dk and Df values of thinner dielectric laminate materials as those that would fall below .030. In the event we are requested to test the Dk and Df of a dielectric laminate that is below .030 per the IPC-TM650-2.5.5.5 test method we would employ a building block stack method to construct the test specimens in order to arrive at a laminate dielectric thickness that would be sufficient for the test to be conducted accurately. The effect of air gaps between the dielectric test specimens would then be back calculated out of the equation to provide for a more accurate result. Departures from these test methods and/or frequency may produce different values. Isola ensures the consistency and repeatability of the property sets in the product that we produce, however we encourage prospective users to conduct a thorough evaluation with appropriate modeling software during the design process to determine the value sets that are best suited for his/her application.

Isola Corp. 3100 West Ray Rd., Suite 301, Chandler, AZ 85226, (800) 845-2904, www.isola-group.com

isola

IMPEDANCE OF THE COAXIAL LINE

The common structure of a connector is similar to a coaxial line, as shown in ***Figure 1***. A coaxial line propagates in a TEM mode and is characterized by an inner (a) and outer (b) radius. The primary parameters may be rigorously derived for a coaxial line that is uniformly filled with a dielectric material. The dielectric material has a relative permittivity ε_r with respect to the free space value, $\varepsilon_0 = 8.854\ 10^{-12}\ \mathrm{Fm}^{-1}$. The coaxial line supports radial electric fields and circumferential magnetic fields, with a longitudinal current flow in the conductors.

For the purpose of understanding the impedance characteristics of the air line section of precision coaxial connectors, a lumped constant circuit representation of a low loss coaxial line is a convenient starting point. The general equation for the low loss coaxial line characteristic impedance is[3]

$$Z_0' = \sqrt{\frac{R + j\omega L}{G + j\omega C}} \qquad (1)$$

where

Z_0' = characteristic impedance
R = intrinsic resistance (of the conductor) per unit length
G = dielectric conductance per unit length
L = inductance per unit length
C = capacitance per unit length

Considering the special case where R and G are both equal to zero, Equation 1 reduces to

$$Z_0' = \sqrt{\frac{L}{C}} \qquad (2)$$

At microwave frequencies, the inductance per unit length is very nearly equal to the external inductance per unit length and the capacitance per unit length can be calculated using[2,3]

$$L = \frac{\mu}{2\pi}\ln\frac{b}{a} \qquad C = \frac{2\pi\varepsilon}{\ln\frac{b}{a}} \qquad (3)$$

These inductance and capacitance values depend on the ratio of the outer to inner conductor radii of the coaxial cable, b/a. μ is the permeability of the non-magnetic material and ε is the dielectric constant of the insulator.

Also, the effective resistance per unit length (R) of the coaxial line is given by[4–6]

$$R = \frac{R_s}{2\pi}\left(\frac{1}{a} + \frac{1}{b}\right) \qquad R_s = 1/\sigma\delta \qquad (4)$$

where

R_s = surface resistance of the coaxial line
σ = metal conductivity of the coaxial line
δ = skin depth

For impedance matching to the measurement equipment, the coaxial line should have a characteristic impedance[3–6]

$$Z_0 = 60\sqrt{\frac{\mu}{\varepsilon}}\ln\frac{a}{b}\ [\mathrm{ohms}] \qquad (5)$$

DESIGN OF A KA-BAND NARROW FLANGE SMA CONNECTOR

Subminiature coaxial connectors are commonly used in low power applications at higher microwave frequencies, particularly in the Ku-, K- and Ka-bands. In this article, the Ka-band SMA connector is designed using a Teflon-filled 50 Ω coaxial line. The structure of the Ka-band SMA connector is shown in ***Figure 2***. This SMA connector consists of a central conductor, a dielectric and the body.[4] The SMA connector is designed to operate in the Ka-band and is capable of providing a much higher operating frequency, free of higher orders, using arbitrary surface discontinuities inside the connector, as shown in ***Figure 3***. In addition, adding an air layer and a step transition to the connector enhances its high frequency performance.

The connector used in the measuring equipment uses an air-layer structure. Although the mechanical strength of the connector is weak, it is better than having a dielectric layer structure at high temperature, since the rigid plastic supporting the center pin is very thin. This problem was solved by using an air layer inside the PTFE dielectric and fixing the center pin. Thus, the narrow

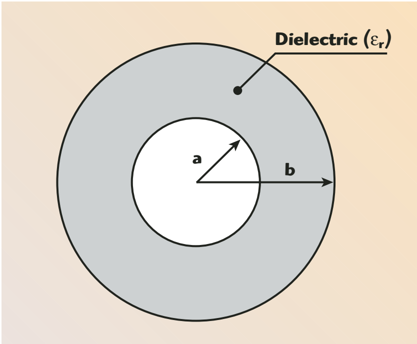

▲ *Fig. 1 Cross-section of a coaxial line.*

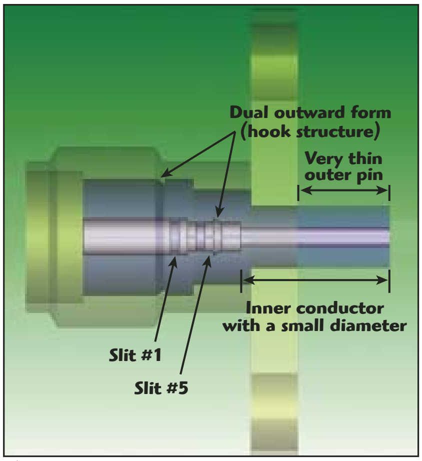

▲ *Fig. 2 Cross-sectional view of the Ka-band SMA connector.*

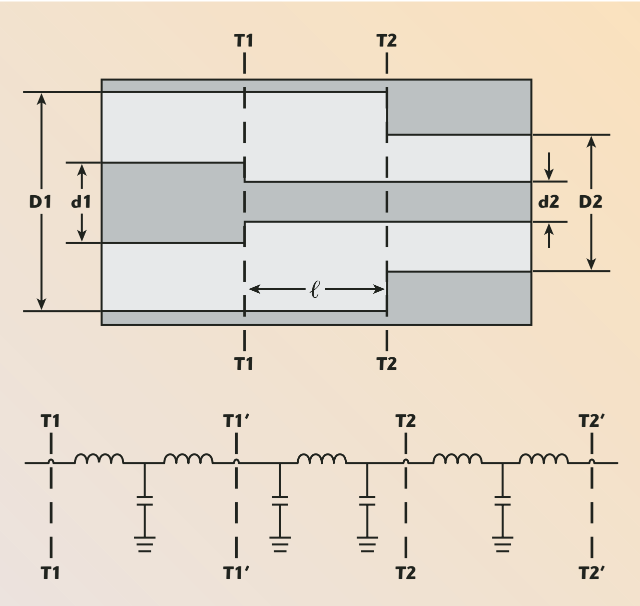

▲ *Fig. 3 Equivalent circuit of a coaxial line compensated with the length ℓ of the discontinuity.*

TRADE-IN your old MICROWAVE COUNTER

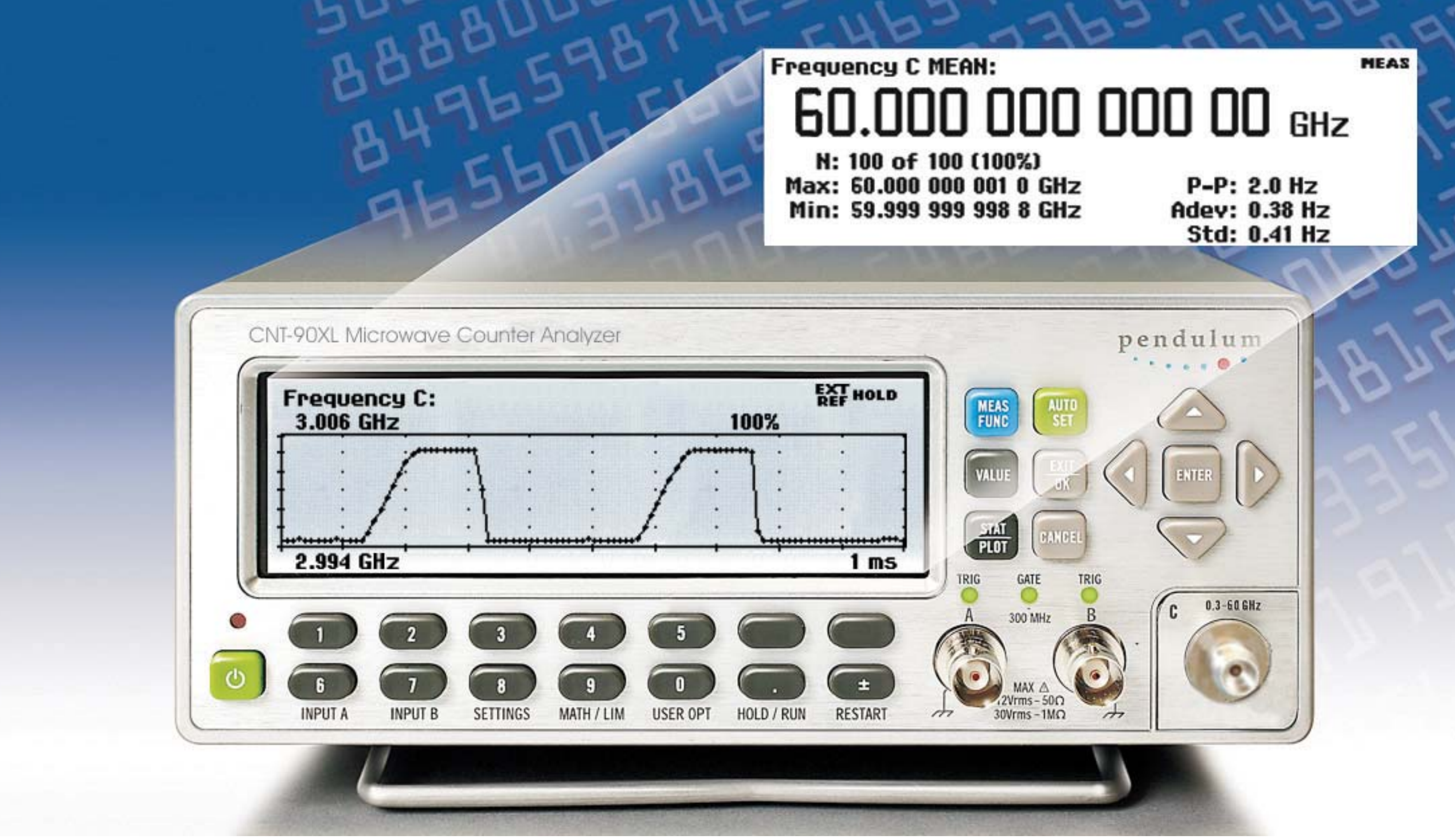

Get up to **$5000** off when buying a CNT-90XL Microwave Counter/Analyzer

Please visit **www.pendulum-instruments.com/tradein.php**

ULTRAHIGH RANGE, SPEED & RESOLUTION

- *27, 40, 46 or 60 GHz frequency range*
- *250k meas. / sec. of frequency or power*

VERSATILITY

- *Frequency or power, CW or burst to 60 GHz*
- *All Timer / Counter functions to 300 MHz*

FAST ANALYSIS

- *Modulation domain analysis to 60 GHz*
- *View FM or AM on graphical display*
- *Frequency or power stability, settling or drift*

AFFORDABLE

- *The world's best Timer / Counter included!*

pendulum

Incorporating XL Microwave

Pendulum Instruments

- Experts in Time & Frequency Calibration, Measurement and Analysis

Phone: +1 510-428-9488 (US), +46 8 598 510 55 (Int.)

www.pendulum-instruments.com

flange SMA connector has a good Ka-band frequency performance, due to the multi-air and multi-step layers. Furthermore, for commercial purposes, this connector is designed to have a guaranteed operating temperature up to 120°C. Four mechanical structures were applied in the design of the connector. First, a dual structure having a main body and a cover was used in order to avoid separation of the dielectric from the connector. Second, the hook structure in the center conductor is used to prevent separation between the dielectric and the inner conductor. Third, a thick outer conductor wall is used. This also provides great strength to ensure reliability in repeat matings. Finally, a very thin inner pin was used to obtain high frequency performance, which is a result of the high impedance line section.

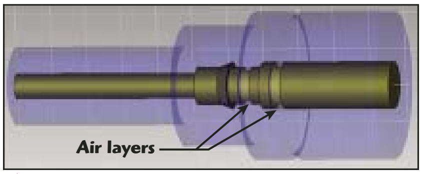

▲ *Fig. 4 Structure of the inner conductor of the Ka-band SMA connector.*

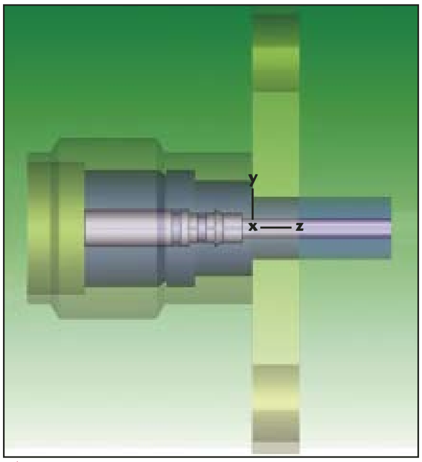

▲ *Fig. 5 Inner structure of the Ka-band SMA connector.*

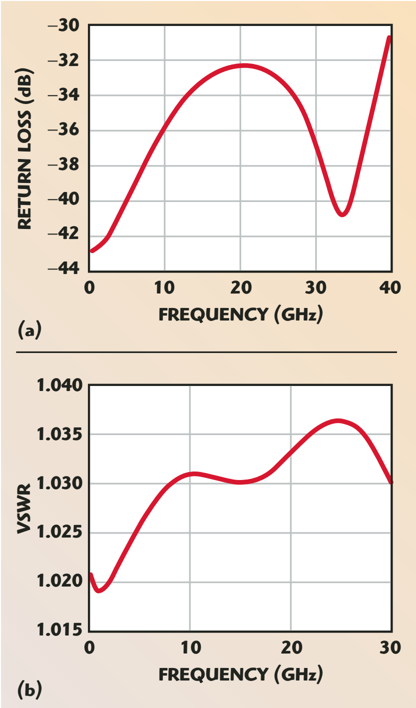

▲ *Fig. 6 Simulated return loss (a) and VSWR (b) of the Ka-band SMA connector.*

When the stepped-discontinuity structure is added, the inductance per unit length of the transmission line is decreased and the capacitance per unit length is increased. The higher order cut-off frequency was also increased as a result of the discontinuity. To avoid the problem of having an infinite VSWR, the arbitrary length between T1 and T2 should be as long as possible. The length l of the discontinuity in the transmission line is a very important parameter controlling the VSWR characteristics of the connector, as it is a factor in deciding the discontinuity size for 50 Ω matching.[4]

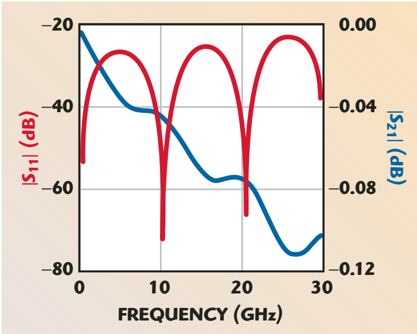

▲ *Fig. 7 Simulation results for the microstrip line used in the measurements.*

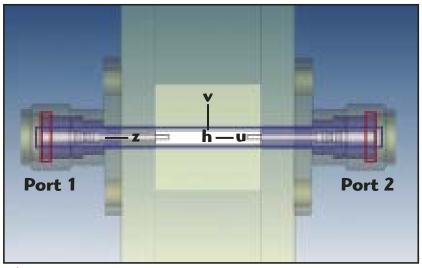

▲ *Fig. 8 Test fixture for the simulation and measurement of the Ka-band SMA connector.*

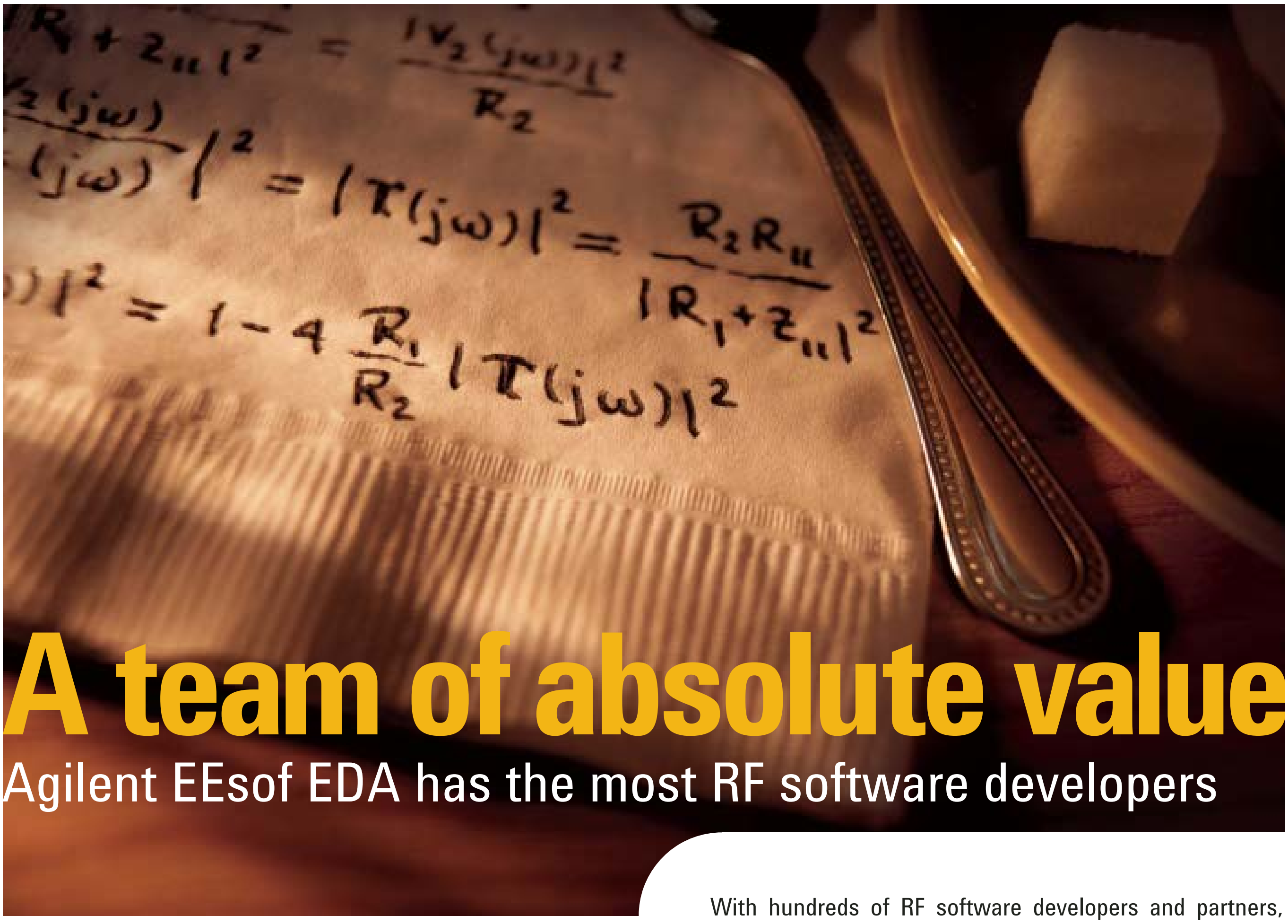

A team of absolute value

Agilent EEsof EDA has the most RF software developers

With hundreds of RF software developers and partners, Agilent works the high frequency EDA equation like no other company.

Our 25-year experience in high-frequency design began with Agilent RF engineers creating design software for their own use. The result has been the absolutely broadest selection of capabilities to meet both technical and budget needs of high-frequency designers. And as our team grows you can expect upgrades and new technologies proportional to our size – all focused on helping you tackle the latest design challenges and communication standards.

Now the Agilent EEsof EDA team has grown larger with the addition of Eagleware-Elanix and its own team of experts. Combine this with technical support that consistently ranks the best in the high-frequency EDA industry – and you can be confident that you're with the right team.

Let the world's largest team of RF EDA experts help you find the right solution for your needs and budget. Visit www.agilent.com/find/eesof-innovations for details

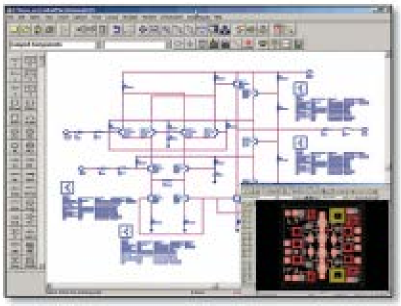

EAGLEWARE
ELANIX

Eagleware-Elanix is now part of Agilent EEsof EDA.

www.agilent.com/find/eesof-innovations

Agilent Technologies

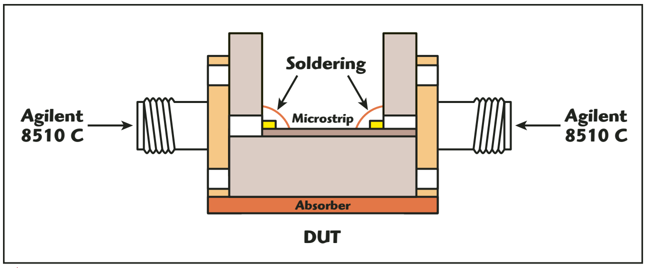

▲ *Fig. 9 Test fixture for the Ka-band SMA connector.*

SIMULATION RESULTS

In this article, the degradation in RF performance of the connector is minimized by simulating the multi-air and hooked structure using a 3D simulator from a Computer Simulation Technology (CST) tool based on the finite element method (FEM). The inner conductor, shown in ***Figure 4***, was fabricated with two air layers to enhance the high frequency performance of the connector. ***Figure 5*** shows the inner structure of the Ka-band NFR SMA connector. Generally, when the coaxial line uses an air dielectric, the mechanical strength of the connector is weak. To solve this problem, a PTFE dielectric was used. As shown in ***Figure 6***, the simulated return loss and VSWR increase as the frequency increases, but they are less than –32 and 1.04 dB, respectively, in the frequency range from DC to 30 GHz. ***Figure 7*** shows the simulation results for the microstrip line used in the measurements. The microstrip line was 10 mm long and 1.3 mm wide, made on a Teflon PCB for high frequency performance. ***Figure 8*** shows a cross-sectional view of the test fixture used for the simulation and measurement of the Ka-band SMA connector using a microstrip line. The interface between the inner conductor and the Teflon dielectric is in accordance with MIL-STD-348. Furthermore, its performance is better than for similar RF connectors, matching the military standards MIL-PRF-39012 and MIL-C-83517, thereby enabling it to be treated as a microwave component.

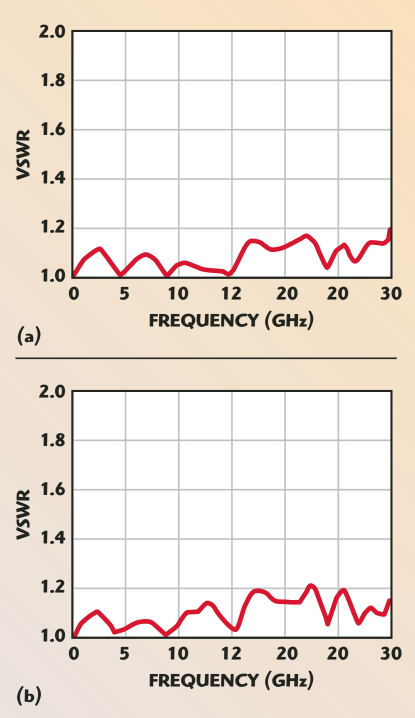

▲ *Fig. 10 Measured VSWR of the Ka-band SMA connector (a) at room temperature and (b) after one hour at 120°C.*

MEASUREMENT RESULTS

Figure 9 shows the test fixture used to measure the Ka-band SMA connector. It uses a microstrip line with a width of 1.3 mm and a length of 10 mm. The dimensions of the microstrip line were optimized after testing. The measurement was performed using a network analyzer (HP 8510C). ***Figure 10*** shows the measured VSWR as a function of frequency at room temperature and after being subjected to 120°C for an hour. The VSWR near 30 GHz is 1.19; therefore, the connector is expected to be useful up to 30 GHz. Furthermore, after subjecting the connector to a temperature of 120°C for one hour, the measurement was performed again to qualify it for use as a commercial product. Very little difference in VSWR was recorded between the two tests. Therefore, its RF performance has been shown to be stable with temperature. ***Figure 11*** shows photographs of the test fixture and of the fabricated connector.

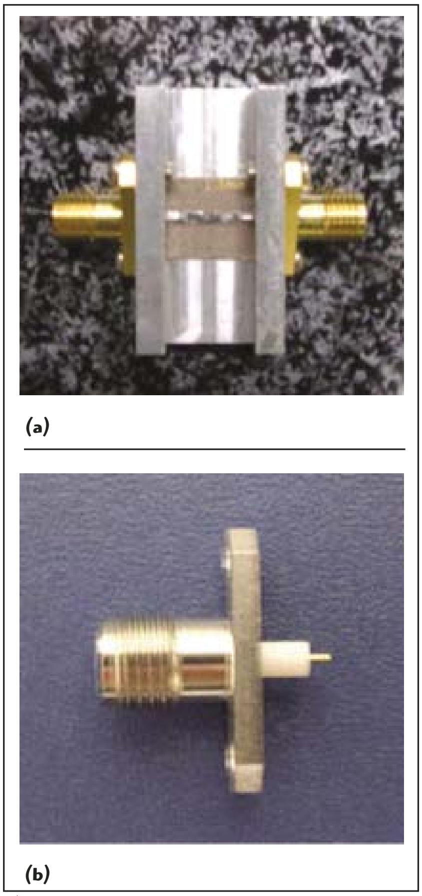

▲ *Fig. 11 The test fixture (a) and the fabricated Ka-band SMA connector (b).*

CONCLUSION

In this article, a reliable miniature SMA connector for use at Ka-band was designed and fabricated using the characteristic impedance of a coaxial line, a discontinuous transmission line, and the characteristics of dielectric bead-air line interfaces. The VSWR is less than 1.2 from DC to 30 GHz and was realized by adopting a slit construction and by optimizing the conductor pattern on a PCB. Its reliability is confirmed by electrical and environmental tests. The use of this SMA connector is possible in Ka-band RF module or system applications. ■

ACKNOWLEDGMENTS

This research was supported by the Ministry of Information and Communication (MIC), Korea, under the Information Technology Research Center (ITRC) support program supervised by the Institute of Information Technology Assessment (IITA) (IITA-2005-(C1090-0502-0034)), by a research grant from Kwangwoon University in 2006, by the Realistic 3D-IT Research Program of Kwangwoon University under the National Fund from the Ministry of Education and Human Resources Development (2005), and has been performed through the Support Project of Mission Telecom Co. (MTC), Dongjin-TI Co. and A&P Technology Co.

References

1. H.Y. Yoo and J.H. Yoon, "A High Durability Ka-band Spark-plug SMA Connector," *Digest of the 2004 Microwave and Propagation Fall Conference in KEES of the IEEE MTT/AP/EMC Korea Chapter*, Vol. 14, No. 1, November 2004, pp. 119–122.
2. A.E. Sanderson, "A New High Precision Method for the Measurement of the VSWR of Coaxial Connectors," *IEEE Transactions on Microwave Theory and Techniques*, Vol. 9, No. 6, November 1961, pp. 524–528.
3. P.A. Rizzi, *Microwave Engineering Passive Circuits*, Prentice Hall, Upper Saddle River, NJ, 1988.
4. N.J. Sladek, "Fundamental Considerations in the Design and Application of High Precision Coaxial Connectors," *IRE International Convention Record*, Vol. 13, Part 5, March 1965, pp. 182–189.
5. T.E. MacKenzie, "Recent Advances in the Design of Precision Coaxial Standards and Components," *IRE International Convention Record*, Vol. 13, Part 5, March 1965, pp. 190–198.
6. B.O. Weinschel, "Standardization of Precision Coaxial Connectors," *Proceedings of the IEEE*, Vol. 55, No. 6, June 1967, pp. 923–932.

Jae-Ho Yoon *received his BS degree in electronic materials of engineering from Kwangwoon University, Korea, in 2004. He was an exchange student in the 2nd IT Global Wireless Communication Course at the University of California San Diego (UCSD) from February to August 2004. He is currently pursuing his MS degree. His research interests include RFIC/MMIC harmonic noise frequency filtering VCOs, mixers, LNAs and CDMA wireless systems design.*

Won-Yong Cho *received his BS degree in electronics engineering from Kwangwoon University, Korea, in 2006. He is pursuing his MS degree and works at the RFIC Center at Kwangwoon University as a 3D RF tool education teaching assistant.*

Ah-Rah Koh *received her BS degree in electronics engineering from Kwangwoon University, Korea, in 2005. She is currently pursuing her MS degree and works at the RFIC Center at Kwangwoon University as an MMIC tool education teaching assistant. Her research interests include RFIC/MMIC VCOs, LNAs and CDMA wireless system design.*

Bhanu Shrestha *received his BS and MS degrees in electronic engineering from Kwangwoon University, Korea, in 1999 and 2004, respectively. His research interests include RFIC/MMIC/RFID circuits and system design.*

Gary P. Kennedy *received his BSc degree in applied physics from Liverpool John Moores University in 1988 and his PhD degree in solid-state physics/micro-electronics from the University of Liverpool in 1993. After completing his studies, he worked as a researcher and research fellow at the University of Liverpool and Southampton, respectively. In January 2000, he began working as a reliability engineer at the European Semiconductor Manufacturing Ltd., UK. He is currently a research professor in the ITRC RFIC Center of Kwangwoon University, Korea. His research interests include SiGe RFIC.*

Nam-Young Kim *received his BS degree in electronic engineering from Kwangwoon University, Korea, in 1987, and his MS and PhD degrees from the State University of New York at Buffalo in 1991 to 1994, respectively. He was a research scientist of CEEM at SUNY, Buffalo, in 1994. Since September 1994, he has been a professor in the department of electronic engineering at Kwangwoon University, Korea. He received M.Div and DCE degrees in 2001 and 2005, respectively. He has been director of the RFIC Education and Research Center since March 1998. His research interests include semiconductor device modeling, ASIC, RFIC and MMIC design.*

A LOW NOISE PHEMT DEVICE

Pseudomorphic high electron mobility transistor (PHEMT) low noise amplifiers (LNA) are capable of operating at higher frequencies than LNA devices manufactured using other technologies. They also offer higher gain at the lower frequencies. The other key performance parameter of a LNA is the noise figure. In order to optimise the noise figure the DC power consumption of the device must be minimized.

Therefore, having offered the FPD750 in a SOT343 package, Filtronic has added a smaller, low cost LNA with lower DC power consumption—the FPD6836SOT343—to the PHEMT family. This device is usable from frequencies of 900 MHz (cellular) to 3.5 GHz (for WiMAX applications) and even as high as 5.8 GHz. It can be biased as low as 3 V, 20 mA and thus produces low noise. The noise figure ranges from 0.3 dB at 900 MHz to 0.9 dB at 5.8 GHz.

Fig. 1 The tuned gain and minimum noise figure frequency response of the FPD6836SOT343.

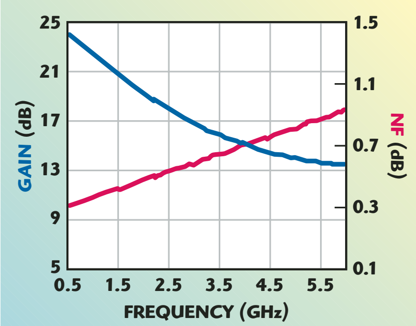

The FPD6836 family is offered in chip form and in two different package styles. The FPD6836P70 uses a P70 high frequency package with usable gain up to 18 GHz, while the FPD6836SOT343 is more cost effective and produces respectable gain beyond 6 GHz. It is this device that is the subject of this article. ***Figure 1*** illustrates its measured gain and noise figure performance. The measurements were taken on a noise figure measurement system using electronic tuners to present the device input with a reflection coefficient optimized for noise figure.

The gain plot is the associated gain of the device at the minimum noise figure. The curves show a noise figure of 0.5 dB at 1.85 GHz and 0.65 dB at 3.5 GHz with associated gain of above 19 and 16 dB, respectively. The part is biased at 3 V with a quiescent current of 50 mA. The gain is so stable at low bias that this can be reduced to 20 mA for even lower noise figure performance.

REFERENCE DESIGNS

Two reference designs using the FPD6836SOT343 are presented. The first is aimed at the 1.85 GHz cellular band and the second at the 3.5 GHz WiMAX band. Both designs are realised on low cost PC boards with minimal components.

Figure 2 is the schematic of the circuit design at 1.85 GHz. The FPD6836SOT343 is reactively matched on the input and the output with a series chip inductor and a shunt capaci-

FILTRONIC COMPOUND SEMICONDUCTORS LTD.
Newton Aycliffe, UK

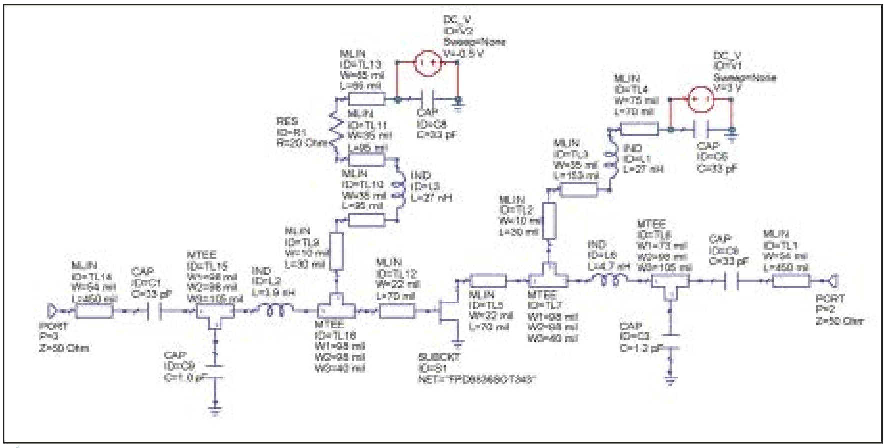

▲ *Fig. 2 FPD6836SOT343 1.85 GHz evaluation board schematic.*

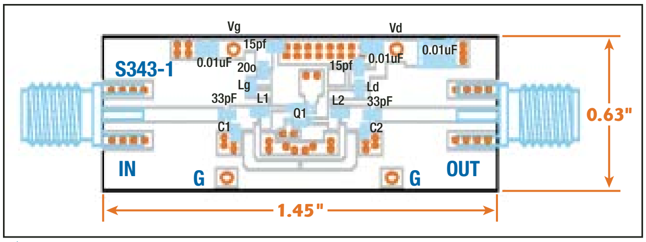

▲ *Fig. 4 1.85 GHz evaluation board layout.*

tor tuned for minimum noise figure and maximum gain. The device input and output reflection coefficients can be calculated as

$$\Gamma_{in} = \Gamma_{opt}^{*} \qquad (1)$$

$$\Gamma_{out} = S_{22} + \frac{S_{12}S_{21}\Gamma_{opt}}{1 - S_{11}\Gamma_{opt}} \qquad (2)$$

Γ_{opt} at 1.85 GHz is obtained from the device's data sheet table, which is posted on the company's web site. DC blocking capacitors, RF choke inductors and a 20 Ω gate resistor form the core of the circuit. Additional capacitors are used on the DC supply lines for power supply stability.

TABLE I

1.85 GHz CRITICAL COMPONENT VALUES AND VENDOR INFORMATION

Component	Value	Vendor
Lg	27nH	TOKO (LL1608)
Ld	27nH	TOKO (LL1608)
L1	3.9nH	TOKO (LL1005)
L2	4.7nH	TOKO (LL1005)
C1	1.0pF	ATC (600S)
C2	1.2pF	ATC (600S)
Eval board material	30 mil thick FR4 1/2 Ounce Cu	

The measured RF performance of the design is shown in ***Figure 3***. Gain, input and output return loss and noise figure are plotted on the graph. This circuit can be used for frequencies up to 2.1 GHz and has a gain of 19 dB and a noise figure of 0.7 dB at 1.85 GHz. Output third-order modulation measurements made using two CW tones spaced 5 MHz apart at an output power level of 4 dBm per tone show an output IP3 of 34 dBm. Higher output power levels are achievable with the same OIP3 performance, which show the good dynamic range of the device. The P1dB of the reference design is 14.5 dBm. ***Figure 4*** shows the layout of the PCB.

The size of the circuit (excluding the SMA connectors' ground pads and unused lines) is less than 0.5" × 0.5". The board material is low cost FR-4 with a dielectric thickness of 30 mm. The physical dimensions of the

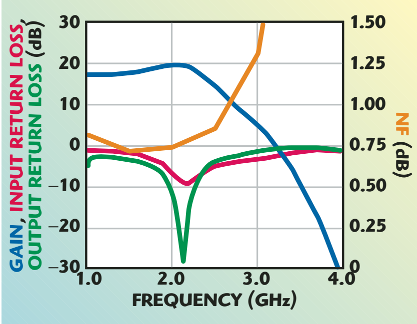

▲ *Fig. 3 1.85 GHz evaluation board gain, return loss and noise figure.*

microstrip lines can be obtained from the schematic in Figure 2. Critical component values are given along with vendor information in ***Table 1***.

Figure 5 shows the schematic of the design for 3.5 GHz. The FPD6836SOT343 is reactively matched on the input with a series chip inductor and a shunt capacitor tuned for minimum noise figure. The output is matched with a series capacitor and a shunt inductor for maximum gain. The device input and output reflection coefficients can be calculated using Equations 1 and 2.

Γ_{opt} at 3.5 GHz is extrapolated from the device's data sheet table. DC blocking capacitors, RF choke inductors and a 20 Ω gate resistor form the core of the circuit. Additional capacitors are used on the supply to ensure power supply stability.

The measured RF performance of the design is shown in ***Figure 6***, where the gain, input and output return loss and noise figure are plotted. This circuit covers the 3.4 to 3.6 GHz band and has a gain of 15 dB and noise figure of 0.85 dB at 3.5 GHz. OIP3 measurements (made with two CW tones at 4 dBm per tone 5 MHz apart) gives an output IP3 of 33 dBm.

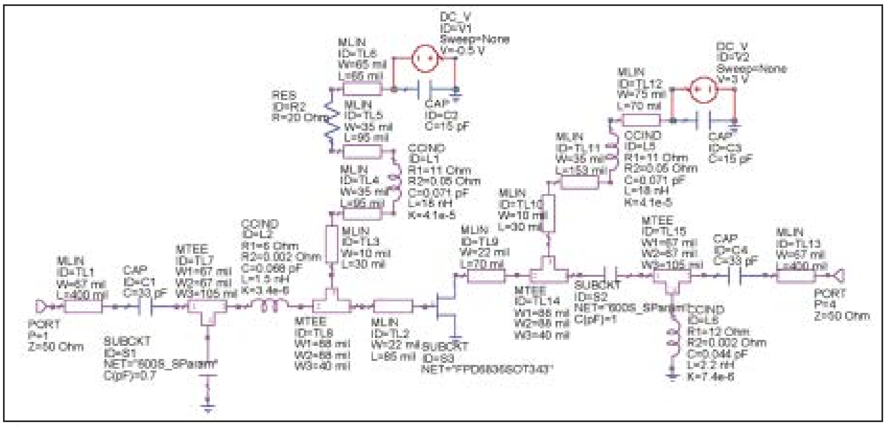

▲ *Fig. 5 FPD6836SOT343 3.5 GHz evaluation board schematic.*


So you've used the same design tools for years. Or has it been the other way around?
AWR
Why struggle to create great designs with vintage tools? A recent EDA survey indicated that you-know-who finished near the bottom of leading EDA vendors in customer satisfaction. Life is short. There's a better design path that's been empirically proven: Microwave Office.™ Thousands of users have already discovered that superior layout technology, great technical support and faster simulations lead to shorter design cycles and first pass success. Stop beating your head against the monitor. Download a 30-day trial today and break the habit.
Microwave
Office
appwave.com
© 2006 Applied Wave Research, Inc. All rights reserved.
Visit http://mwj.hotims.com/11713-21 or use RS# 21 at www.mwjournal.com/info

Again, the good dynamic range allows higher output power levels with the same OIP3 performance. P1dB for this design is 14 dBm. Note that both reference designs are not optimized for P1dB since it has been observed that a gain matched output tends to enhance the linearity of the part.

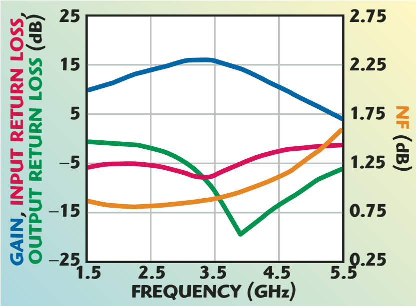

▲ *Fig. 6 3.5 GHz evaluation board gain, return loss and noise figure.*

Figure 7 shows the layout of the PCB. Again, the components occupy an area excluding the SMA connectors of less than 0.5" × 0.5". The board is composed of 30 mm thick Rogers 4003 material. This low loss dielectric avoids high line losses, which would degrade the noise figure at these frequencies had FR-4 material been used. The dimensions of the microstrip lines are given in Figure 5. Critical component values are given along with vendor information in ***Table 2***.

The FPD6836SOT343 can also be used as a 50 Ω gain block with no matching at the input and the output of the part at all. At 1.85 GHz the device has a typical noise figure of 0.9 dB, a small-signal gain (SSG) of 18 dB and P1dB of 18.5 dB when matched into 50 Ω with no matching components.

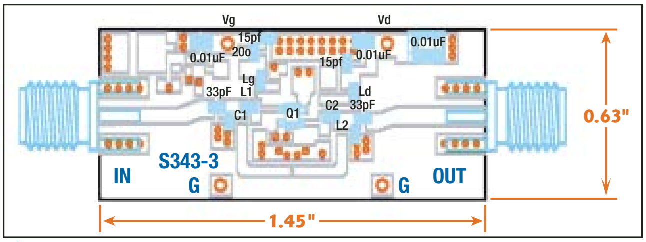

▲ *Fig. 7 3.5 GHz evaluation board layout.*

TABLE II 3.5 GHz CRITICAL COMPONENT VALUES AND VENDOR INFORMATION		
Component	***Value***	***Vendor***
Lg	18nH	Coil Craft (0603CS)
Ld	18nH	Coil Craft (0603CS)
L1	1.0nH	Coil Craft (0402CS)
L2	2.2nH	Coil Craft (0402CS)
C1	0.7pF	ATC (600S)
C2	1.0pF	ATC (600S)
Eval board material	Rogers 4003 30 mil Thick 1/2 Ounce Cu	

STABILITY AND RELIABILITY

The low noise PHEMT device also exhibits very good temperature stability. The maximum variations over temperature for P1dB, SSG and IM3 have been calculated from measured data for three critical parameters:

$$\Delta P1dB = 0.9\ dB$$
$$\Delta SSG = 0.6\ dB$$
$$\Delta IM3 = 2\ dB$$

The measurements were obtained with the device biased at 3.0 V and 50 mA on a 1.85 GHz evaluation board similar to the reference design previously explained. These were taken at temperature intervals from –40° to +85°C. The process used for fabrication allows a maximum operating channel temperature of 150°C, at which the MTTF is calculated as 7.0×10^6 hours.

CONCLUSION

The FPD6836SOT343 is a versatile device that can be used as a matched low noise amplifier with very low DC power consumption. It can also be used as a low cost gain block with no matching for applications where noise figure is non-critical. Applications for this part exist for a frequency range of up to 6 GHz. PCS/cellular base stations (800 MHz to 2.4 GHz), WLL and WLAN systems (2.6, 3.5 and 5.8 GHz) are some examples of the wide range of applications for which the device can be used.

Filtronic Compound Semiconductors Ltd., Newton Aycliffe, UK, +44 1325 301111, www.filtronic.com.

RS No. 301

Shown with optional equipment.

Bring Wireless Products to Market Quickly, Our AMS 8050 System Is the Solution!

Test As You Design

ETS-Lindgren presents the AMS 8050 Antenna Measurement System: a compact antenna lab for making fast, over-the-air (OTA) performance measurements of small wireless devices and mobile handsets. It's perfect for research and development, design qualification, production sampling, and pre-certification measurement. It's everything you need to beat the competition to market.

TRP, TIS and More

Small in size but big on performance, the AMS 8050 System lets you measure 3-D spherical pattern and 2-D pattern-cut measurements, and perform tests to determine quantities such as total radiated power (TRP), effective isotropic radiated power (EIRP), total isotropic sensitivity (TIS), effective isotropic sensitivity (EIS), near-horizon partial radiated power (NHPRP), and near-horizon partial isotropic sensitivity (NHPIS).

Know Before You Go

If you're using an outside test house for certification testing, our system can help you go fully prepared. OTA measurements made in the AMS 8050 have demonstrated good correlation to measurements made in larger, fully compliant chambers. Use the AMS 8050 System to make tests during product development, and you'll be able to identify and correct problems before leaving your lab.

Built by Experts

The AMS 8050 System is designed and built by people who know something about OTA wireless testing – ETS-Lindgren. We were the first lab authorized by the CTIA to perform certification testing per their OTA performance test plan. And our OTA test systems are used in 75% of CTIA Authorized Test Labs (CATL) worldwide. Click on our website for more information.

Enabling Your Success

ETS·LINDGREN™
An **ESCO Technologies** Company

www.ets-lindgren.com

Company offices: USA +512.531.6400, Finland +358.2.8383300, Japan +81.3.3813.7100, China +86(10)8273.0877
Additional locations in the US, UK, Finland, France, Singapore, Japan and China
Representatives and Distributors Worldwide

Visit http://mwj.hotims.com/11713-50 or use RS# 50 at www.mwjournal.com/info

AN LTCC MIXER FOR INSTRUMENTATION AND MILITARY APPLICATIONS

Test instrumentation may need to accommodate signals having a wide-percentage frequency bandwidth. For ease of processing such RF signals, the input can be upconverted in order to reduce the percentage bandwidth. To facilitate upconversion ahead of higher frequency receivers, Mini-Circuits has developed a high performance passive mixer that allows original-equipment manufacturers (OEM) to optimize receiver design. Such mixers are also useful in military applications.

The company's model SIM-U742MH+ mixer is based on a combination of low temperature-cofired-ceramic (LTCC) technology, semiconductor technology and a highly manufacturable circuit layout. The patented combination[1] results in small size, high insensitivity to electrostatic discharge (ESD), excellent stability with temperature and is part of a growing family of SIM mixers.

Fig. 1 The SIM-U742MH+ double-balanced mixer block diagram.

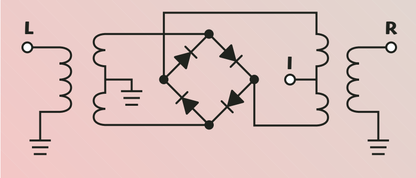

Instrumentation and military transmitters need components, such as mixers and oscillators that provide stable performance over time and under different environmental conditions, including temperature. The SIM-U742MH+ mixer is built on a LTCC substrate, ideally suited for designs with multilayer circuits. In contrast to conventional planar circuit designs, in which all circuit elements are placed on one side of a single-layer printed circuit board, LTCC circuits can be designed and fabricated in three dimensions, even with embedded components between layers, to save space. The approach results in a mixer that measures just 0.2" × 0.18" × 0.08" (5.1 × 4.6 × 2.1 mm), which is smaller than some commercial semiconductor-based mixers. While the SIM-U742MH+ mixer incorporates semiconductors to accomplish its frequency-translation function, it is a passive design that operates without DC bias (compared to a standard integrated-circuit mixer which requires the application of constant DC bias).

The SIM-U742MH+ is a double-balanced mixer (see **Figure 1**) built around a reliable

MINI-CIRCUITS
Brooklyn, NY

TABLE I

THE SIM-U742MH+ MIXER'S PERFORMANCE

Parameter	
RF range (input) (MHz)	0.1–3300
IF range (output) (MHz)	2300–7400
LO range (input) (MHz)	2300–7400
LO power (nominal) (dBm)	+13
Conversion loss (typical) (dB)	8.0
LO-IF isolation (typical) (dB)	23
LO-to-RF isolation (typical) (dB)	17
Compression point (P1dB) (dBm)	+9
Operating temperature range (°C)	–40 to 85
Storage temperature range (°C)	–55 to 100
Size (in)	0.2 × 0.18 × 0.08
Case style	HV1195

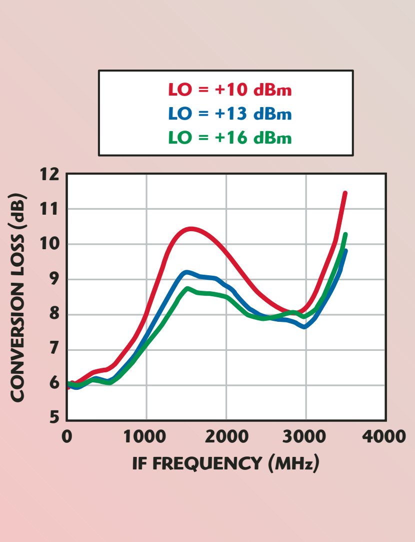

▲ *Fig. 2 The SIM-U742MH+ mixer's conversion loss at an RF output of 4075 MHz.*

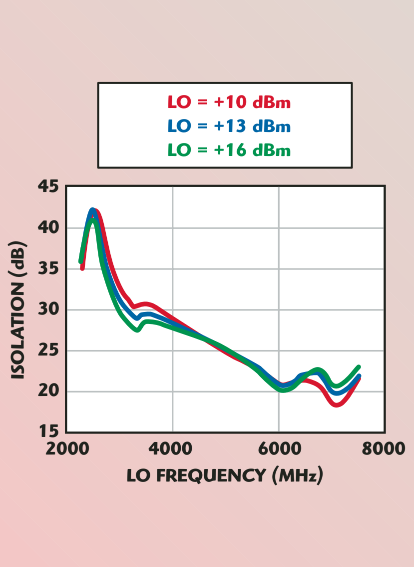

▲ *Fig. 3 The mixer's LO-to-IF isolation.*

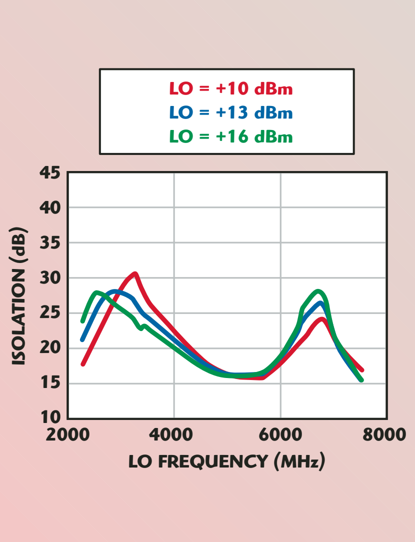

▲ *Fig. 4 The mixer's LO-to-RF isolation.*

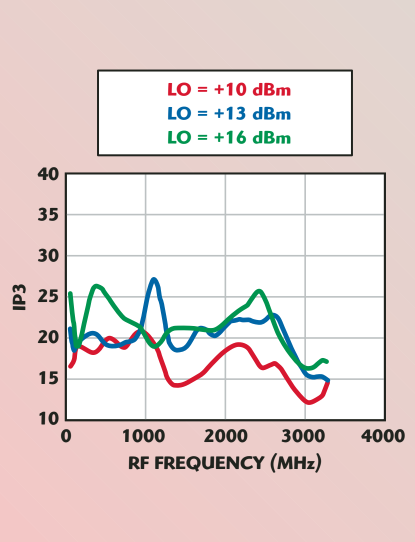

▲ *Fig. 5 The measured input third-order intercept performance at 4075 MHz RF output.*

diode quad. Except for the diodes, the entire structure is implemented in multiple layers of LTCC, which is inherently hermetic. By integrating components in LTCC, the mass of the mixer is minimized, making it extremely rugged in terms of withstanding mechanical shock and vibration. In fact, the entire mixer structure can withstand the environmental extremes usually associated with tough military components, regarding temperature, humidity, vibration and mechanical shock.

The mixer is RoHS-compliant, constructed without lead-based solder or other hazardous materials. It is also built to withstand severe ESD scenarios under conditions normally hazardous to monolithic semiconductor mixers. The SIM-U742MH+, like other members of the company's SIM mixer line, meets Class 1C ESD requirements: a level of 1000 V when tested per the Human Body Model (HBM), compared to standard semiconductor mixers which are typically rated as Class 1A, 250 V for HBM testing. The SIM-U742MH+ mixer also meets Class M2 ESD requirements (testing at 100 V) according to the ESD Machine Model. ***Table 1*** summarizes the performance characteristics of the SIM-U742MH+ mixer.

EVALUATING PERFORMANCE

The SIM-U742MH+ mixer accepts radio-frequency (RF) signals from near 0.1 to 3300 MHz and local-oscillator (LO) signals from 2300 to 7400 MHz and a nominal LO level of +13 dBm to produce IF output signals from 2300 to 7400 MHz. It performs the frequency upconversion with a typical conversion loss of 8.0 dB. The mixer's conversion loss increases with RF frequency. ***Figure 2***


EWT
Filters
Duplexers
Multiplexers
Commercial • Military • Wireless
Eastern Wireless TeleComm specializes in custom designed RF and Microwave filters and filter based products for Commercial, Wireless, Military, and Space applications.
With more than 35 years of design and manufacturing experience, we are able to incorporate the latest proven design techniques into our products, maximizing performance and repeatability.
EWT...the most cost effective solution for your filter requirements.
• Cavity
• Waveguide
• Surface Mount
• Lumped Element
• Custom Assemblies
• All Applications to 40 GHz
Eastern Wireless TeleComm, Inc.
www.ewtfilters.com
Tel: 410.749.3800 Fax: 410.749.4852
sales@ewtfilters.com

shows test results with LO drive levels of +10, +13 and +16 dBm. The variation of conversion loss with LO drive power is typically +1.0/–0.5 dB across the 3300 MHz measured bandwidth.

The LO-to-RF isolation of the SIM-U742MH+ mixer was evaluated at the three LO drive levels used in the conversion loss test, to understand the effect of variations in LO power on isolation. As ***Figure 3*** shows, the LO-to-IF isolation is high (typically 23 dB) and very well behaved at all three LO drive levels. Variation in isolation as a function of LO power is negligible.

Similarly, the LO-to-RF port isolation was also evaluated at the three LO drive levels. The SIM-U742MH+ mixer exhibited typically 17 dB isolation across an LO frequency range of 4100 to 7400 MHz (see ***Figure 4***).

Since wide dynamic range is important in instrumentation applications, the input third-order intercept point (IIP3) of the SIM-U742MH+ mixer was also evaluated at the three LO drive levels (+10, +13 and +16 dBm) and at an RF output range of 3900 to 4300 MHz. IP3 is consistently about +20 dBm up to 2.5 GHz and then derates to +15 dBm at 3.3 GHz (see ***Figure 5***).

The LTCC double-balanced mixer features typical LO port return loss of 3.5 to 8.5 dB. The return loss measured at the RF port is 5.5 dB typical, while the return loss at the IF port is typically 17 dB.

The mixer supports conventional surface-mount applications, and can be supplied in tape-and-reel formats for use with automated assembly equipment. The RoHS-compliant mixer is designed to withstand high levels of ESD mishandling compared to more sensitive, and often larger, semiconductor mixers.

Mini-Circuits' LTCC mixers have been tested extensively and qualified for environmental conditions such as humidity, thermal shock and vibration. To evaluate the durability and reliability of the solder joints, 20 of the LTCC mixers were soldered onto FR-4 PCB motherboards and thermally cycled (1000 cycles) over the operating temperature range of –40° to 85°C. The DC continuity was measured from the motherboard trace to the top of the LTCC board, with no failures found.

CONCLUSION

The model SIM-U742MH+ high performance mixer leverages LTCC, semiconductor technology and patented circuit techniques to achieve high frequency low loss upconversion for both instrumentation and military applications. Additional information on it and other SIM mixers may be obtained from the company's web site under the model series SIM.

Reference

1. United States Patent No. 7,027,795 (2006).

Mini-Circuits,
Brooklyn, NY (718) 934-4500,
www.minicircuits.com.

RS No. 300

High Power
Caseless 90° Couplers
Stock To 30 Day Delivery

Fastest Delivery Available!

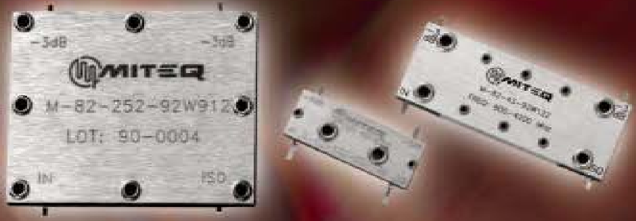

FREQUENCY (MHz)	MODEL NUMBER	AVERAGE POWER (CW Watts)	AMPLITUDE BALANCE (±dB, Max.)	PHASE BALANCE (±Deg., Max.)	ISOLATION (dB Min./Typ.)	INSERTION LOSS (dB, Max.)	VSWR (Max.)
50 – 110	M-51-111-96W802	600	0.3	2.0	20/23	0.30	1.2:1
100 – 500	M-12-52-92W502	200	0.85	2.5	14/18	0.85	1.35:1
100 – 500	M-12-52-98WF502	800	0.8	2.0	18/20	0.30	1.2:1
120 – 230*	M-121-231-92W012	300	0.5	2.0	20/27	0.30	1.2:1
150 – 250	M-151-251-94W012	400	0.3	2.0	20/25	0.30	1.2:1
200 – 400*	M-22-42-92W102	250	0.5	2.0	20/25	0.30	1.2:1
200 – 400	M-22-42-95WB302	500	0.4	2.0	19/23	0.25	1.2:1
200 – 1000*	M-22-13-92WD502	250	0.75	3.0	20/23	0.50	1.3:1
250 – 500	M-251-52-92W102	250	0.5	2.0	20/25	0.30	1.2:1
300 – 500	M-32-52-92W102	250	0.4	2.0	20/23	0.25	1.2:1
300 – 950	M-32-951-92W102	250	0.6	2.0	20/23	0.25	1.25:1
400 – 550	M-42-551-92W102	250	0.2	2.0	20/25	0.20	1.2:1
400 – 700	M-42-72-92W012	250	0.5	2.0	20/25	0.30	1.2:1
400 – 1000*	M-42-13-92W102	250	0.6	2.0	18/20	0.25	1.2:1
400 – 1000	M-42-13-95WB302	500	0.6	2.0	20/23	0.20	1.2:1
400 – 1000	M-42-13-91KW402	1000	0.6	2.0	20/25	0.20	1.2:1
440 – 880	M-441-881-92W102	250	0.5	2.0	20/25	0.20	1.2:1
700 – 1400*	M-72-142-92W102	250	0.5	2.0	18/25	0.30	1.25:1
800 – 1600	M-82-162-92W102	250	0.5	2.0	20/23	0.25	1.2:1
800 – 1600	M-82-162-95WB302	500	0.5	2.0	20/25	0.20	1.25:1
800 – 1600	M-82-162-91KWB912	1000	0.5	2.0	20/25	0.20	1.3:1
800 – 2500*	M-82-252-92W122	200	0.6	4.0	18/20	0.40	1.25:1
800 – 4200	M-82-43-92W122	200	0.5	4.0	16/20	0.20	1.2:1
960 – 1220	M-961-1221-92W102	200	0.3	2.0	18/25	0.30	1.25:1
960 – 1220	M-961-1221-95WB302	500	0.4	2.0	20/23	0.20	1.2:1
1000 – 2000	M-13-23-92W102	200	0.5	3.0	18/24	0.30	1.25:1
1000 – 2000	M-13-23-95WB302	500	0.5	3.0	18/22	0.20	1.2:1
1200 – 1400	M-122-142-92W102	250	0.4	3.0	20/23	0.25	1.2:1
1200 – 1400	M-122-142-95WB302	500	0.4	2.0	20/25	0.20	1.2:1
1300 – 3000	M-132-33-92W102	200	0.6	3.0	18/23	0.25	1.2:1
1400 – 2400	M-142-242-92W102	200	0.5	3.0	16/20	0.25	1.2:1
1400 – 2800	M-142-282-92W102	200	0.5	3.0	16/20	0.25	1.2:1
1500 – 3000	M-152-33-92W102	200	0.6	3.0	18/22	0.25	1.25:1
1700 – 2500	M-172-252-92W102	200	0.4	3.0	20/23	0.25	1.2:1

* Multiple packages are available on these models, please contact MITEQ.180 degree and coaxial versions are available upon request

For additional information or technical support,
please contact our Sales Department at (631) 439-9220
or e-mail components@miteq.com

3 YEAR WARRANTY

MITEQ

100 Davids Drive, Hauppauge, NY 11788
(631) 436-7400 FAX: (631) 436-7430
www.miteq.com

EMC TEST SOFTWARE

The model SW1006 is the latest version of the company's radiated susceptibility, conducted immunity and pre-compliance emissions software. Model SW1006 automatically performs both calibration and immunity testing in full compliance with IEC 61000-4-3, 4-6, MIL-STD 461/462 RS103, CS114, RTCA/DO160 Section 20 specifications. The software also supplies the user with selectable test parameters and a "thresholding" mode for pre-compliance investigation of equipment susceptibility, as well as closed loop leveling. Pre-compliance emission testing can be done with the use of a spectrum analyzer and either a pre-amp or LISN. The SW1006 software is designed for use with the supplied NI PCI-GPIB interface card for instrument communication.

AR Worldwide RF/Microwave Instrumentation,
Souderton, PA (215) 723-8181, www.ar-worldwide.com.
RS No. 310

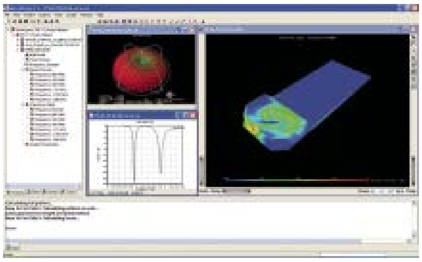

EM SIMULATION

The MicroStripes 3D EM simulation solution for RF/microwave and antenna design, which integrates with Applied Wave Research's Microwave Office® circuit design software, has reached version 7.5. It enables users to import any desired excitation waveform during the modeling process, run the simulation and evaluate the results without any additional post-processing. This makes it possible, for example, to simulate the effect of a lightning strike, electromagnetic pulse or electrostatic discharge on a system using a pre-computed, analytic or measured waveform. In version 7.5, ground planes can also be used for models without meshing all of the space between the system and ground plane. Version 7.5 also reduces the computational resources required to model ferrite tiles.

Flomerics Ltd.,
Hampton Court, Surrey, UK +44 (0) 20 8487 3000,
www.flomerics.com.
RS No. 311

PARAMETRIC PRODUCT SEARCH TOOL

The parametric product search tool is designed for the RF engineer to specify important product parameters and view the company's products that match a specific requirement in a specification-compliance format. Unlike conventional search engines that eliminate products that narrowly fall outside of specification, the parametric product search tool can show these products allowing the engineer to make intelligent design trade-off decisions to "fine tune" the requirement to specific needs. View this and other product software support tools including Product Cross Reference, PLL Phase Noise and Mixer Spur Chart Calculators on the company's site.

Hittite Microwave Corp.,
Chelmsford, MA (978) 250-3343, www.hittite.com.
RS No. 312

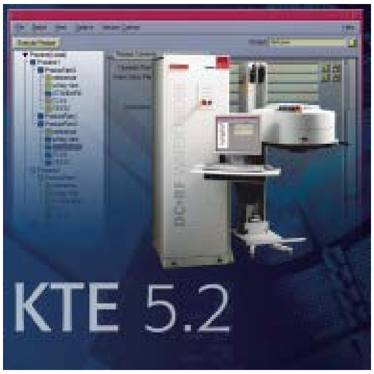

PARAMETRIC TEST SOFTWARE

The release of KTE V5.2 is the company's Interactive Test Environment software for the Series S600 Parametric Test System. KTE V5.2 provides a number of features that dramatically increase throughput for circuit materials testing, such as those requiring RF level frequencies, as well as incorporating improvements in parallel test routines used for lab and production applications. In addition, the KTE V5.2 software update offers significant improvements in ease of use that simplify testing. Keithley's KTE is a powerful wafer test development and execution environment that guides test engineers through the development of a test plan. Users can create individual electrical tests at the subsite level by drawing on pre-defined libraries of test, then defining parameters and connections.

Keithley Instruments Inc.,
Cleveland, OH (440) 248-0400, www.keithley.com.
RS No. 314

Phase Shifters for every Application to 40GHz

Specifications

Type: Varactor, PIN, MMIC, FET
Frequency
Power
Phase shift range
Switching speed
Insertion Loss
Phase Linearity
Phase flatness
Digital control
Bit size
Analog control
Bias/control voltages
Package size -,SM, Connector
Mechanical / electronic adjust
Loss vs phase change
Price
Unit-to- unit tracking
Insertion phase
Temperature and environment
Hermetic
Fixed phase offset module
Thermal compensation
Modular for integration

You prioritize the specifications; We'll design the Phase Shifter to fit the application:.

Our phase shifters cover the range from "MHz to 40 GHz" with PIN diode, varactor, or the latest MMIC or FET performance.

You can choose either analog, digital, or mechanical adjustment controls. You'll be able to select from our wide range of designs with any combination of specifications listed in surface mount or connector packages.

Or, you may want to integrate the phase shifter with an attenuator, Time Delay, or other microstrip circuit for a higher level assembly.

The latest high performance radar phased arrays require the ultimate in phase and amplitude accuracy that is achieved with the optimum combination of specifications that Aeroflex provides.

Performance is guaranteed for all conditions and backed with our ISO 9001 verification testing.

For more information contact us at **973-887-5700 x500** or e-mail **sales@aeroflex-kdi.com**

AEROFLEX
A passion for performance.

Rev:01-10-1

Visit http://mwj.hotims.com/11713-6 or use RS# 6 at www.mwjournal.com/info

FILTER SYNTHESIS AND SELECTION TOOL

Filter Wizard[SM] has been enhanced to incorporate additional all-pole and elliptic bandreject solutions, including high-Q ceramic puck options. Filter Wizard accelerates user progress from specs to RFQ for RF and microwave filters spanning an ever-increasing range of response types, bandwidths and unloaded Q values from 500 kHz to 50 GHz.

K&L Microwave Inc.,
Salisbury, MD (410) 749-2424, www.klfilterwizard.com.
RS No. 313

MICROWAVE/RF ASSEMBLY BUILDER

The GORE™ microwave/RF assembly builder is an on-line interactive design guide that provides simple step-by-step instructions for configuring GORE microwave/RF cable assemblies. Gore's new microwave/RF configurator—available at www.gore.com/rfcablebuilder—simplifies the assembly design and configuration process enabling the user to build an assembly and submit an RFQ using the simple step-by-step configuration tool, with no registration required to access the process.

W.L. Gore & Associates Inc.,
Elkton, MD (302) 292-5100, www.gore.com.
RS No. 315


In Pursuit of Excellence Through Engineering Since 1978
Military and Industrial Products From 10 MHz to 40 GHz
SOLID STATE SWITCHES
• DC to 40 GHz
• SPST Through SP64T
• Sub-Octave Band and Octave Band
• Broadband and Ultra-Broadband
• With and Without Integral Drivers
• TTL, ECL, CMOS and RS422 Contol Types
• Rectangular and Radial Mechanical Outlines
• Connectorized and Surface Mount
• High Speed, High Isolation and Low Loss Models
• Variable Rise Time and Other Specialty Switches
DIGITAL ATTENUATOR
SOLID STATE VARIABLE ATTENUATORS
• 10 MHz to 18 GHz
• Up to 120dB Dynamic Range
• Sub-Octave, Octave and Broadband
• Non-Linear Current Control
• Linearized Analog Voltage Control
• Linearized Digitally Programmable Voltage Control
• Up to 12 Bit Digitally Controlled Resolution
• High Speed and Low Speed Models
• Switched Bit Attenuators
DETECTOR LOGARITHMIC VIDEO AMPLIFIERS
• 10 MHz to 40 GHz
• 45dB and 70dB Dynamic Ranges
• All Models are Truly DC-Coupled
• CW and Noise Immunity Models
• Very High Sensitivity Models
• Linear Detector Models
• Miniature Models Available
• Sub-Octave, Octave, Broadband and Ultra-Broadband
• Integrated SuperComponents and Sub-Systems Available
AMERICAN MICROWAVE CORPORATION
DIGITAL ATTENUATOR
DETECTOR LOG VIDEO AMPLIFIER
American Microwave Corporation
7311-G Grove Road • Frederick, Maryland 21704, USA
(301)662-4700 • FAX: (301)662-4938
www.americanmicrowavecorp.com/amc
Email: sales@americanmicrowavecorp.com
ISO 9001 : 2000 Certified
Screening to MIL-STD-883 Available for all Products

Ultra Broadband Bias Tee

The model BT-50K18 Option PS is a miniature 50 kHz to 18 GHz bias tee, usable to 15 kHz.

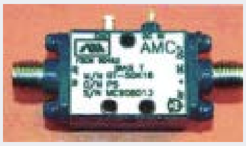

It has an insertion loss of 0.75 dB and a VSWR of 1.75 is typical. This model offers 60 dB RF/DC isolation between 10 MHz and 18 GHz. The phase of a transmitted signal is shifted less than ±7.5°. The bias port has a series resistance of 2.5 Ω and will handle DC voltage of 15 V and current of 200 mH maximum. Size: 0.8" × 0.62" × 0.4" with removable SMA connectors.

American Microwave Corp., Frederick, MD (301) 662-4700, www.americanmicrowavecorp.com.

RS No. 216

Directional Couplers

These high performance directional couplers have 'Air-line' structures that offer low thru-line loss while maintaining high directivity. The couplers are available to cover the 100 MHz to 70 GHz frequency range in a variety of different configurations. The coupler can be supplied as a stand-alone component or as a section of an integrated assembly.

Channel Microwave Corp., Camarillo, CA (805) 482-7280, www.channelmicrowave.com.

RS No. 217

Waterproof QMA Connector

This connector is claimed to be the first waterproof QMA connector optimized for applica-

tions up to 6 GHz and a minimum of 100 cycles. With an IP 68 waterproof rating it features the Quick-Lock locking mechanism, allows 360° rotation and small dimensions. It can be mated with QLF certified QMA connectors and is vibration resistant as SMA to MIL standard. It supports all radio frequency connections and has been designed for users who need fast and space-saving connections in outdoor applications such as wireless communications and transmission systems, portable radio systems, air traffic control and monitoring systems, and assemblies for mobile radio base stations.

Huber + Suhner AG, Herisau, Switzerland +41 (0) 71 353 4111, www.hubersuhner.com.

RS No. 220

High Power T/R Switch

The P/N M20-064 is a high power T/R switch that operates in a frequency range from 20 to

2500 MHz. These switches utilize the company's multi-octave technology that is compatible with the latest GaN and LDMOS solid-state amplifiers. The switches are designed for both prototyping and high volume low cost production. This T/R switch is capable of handling up to 100 W, with an ultra low insertion loss of only 1 dB maximum and an output VSWR of < 1.42.

Comtech PST, Hill Engineering Division, Topsfield, MA (978) 887-5754, www.comtechpst.com.

RS No. 218

Connectorized Double-balanced Mixer

The model HMC-C035 is a connectorized GaAs MMIC double-balanced mixer module

that is ideal for use as an upconverter or downconverter in military EW/ECM, radar, microwave radio, space and test equipment applications from 23 to 37 GHz. This model is a general purpose, double-balanced mixer housed in a miniature, hermetic module. This mixer provides an input IP3 of +19 dBm, 35 dB of LO/RF and LO/IF suppression, and typical conversion loss of 9 dB.

Hittite Microwave Corp., Chelmsford, MA (978) 250-3343, www.hittite.com.

RS No. 219

High Isolation OMTs

This range of ortho-mode transducers (OMT) provides isolation better than 40 dB between

the Tx and Rx ports, with 100 dB possible by integrating the OMT with an optional transmit rejection filter. The OMTs are designed to be attached to the conical feed horn in a mobile SATCOM system, and their function is to separate Tx and Rx polarizations and frequencies. Spearheading the range is a Ku-band OMT, which is made from aluminum and measures 55.5 mm in length (excluding filter). It has a typical Rx bandwidth of 11 to 12.75 GHz and a typical Tx bandwidth of 13.75 to 14.50 GHz, with a maximum transmit power of 56 dBm. The range also includes a C-band OMT for use in commercial SATCOM systems and an X-band version for military applications.

Link Microtek Ltd., Basingstoke, Hampshire, UK +44 (0)1256 355771, www.linkmicrotek.com.

RS No. 221

Nine-channel Switched Filter

The model 9IFA-20/600-SR is a nine-channel switched filter band used in airborne counter-

measure test set applications. Specifications include: nine channels with bandwidth ranging from 10 to 550 MHz; insertion loss of 5 dB; and VSWR of 2.0. This filter offers rejection of 60 dB to 10 GHz, TTL logic, switching speed of 250 ns and DC power of +5 V at 200 mA.

Lorch Microwave, Salisbury, MD (410) 860-5100, www.lorch.com.

RS No. 222

Wireless Band Loads

The *V-Line* RF loads are optimized for excellent performance across all wireless bands.

Their rugged construction makes them ideal for both base station and in-building wireless systems. These wireless band loads are available from stock, even in large quantities.

MECA Electronics, Denville, NJ (973) 625-0661, www.e-meca.com.

RS No. 223

High Pass Filters

Using a seven-section high pass filter design, the VHF series filters provide excellent passband

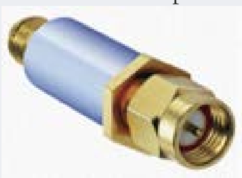

matching (typical VSWR is 1.5), flat passband response and a sharp transition band. The high pass filters deliver excellent sub-harmonic rejection of 850 to 13000 MHz. Built with solid stainless steel unibody construction and coated with a durable gold finish, these units feature SMA type connectors, can handle high power (up to 7 W at input) and are temperature stable from –55° to 100°C. These filters are ideal for eliminating sub-harmonics and for DC blocking. Typical applications include transmitter/receiver filtering, repeaters and lab test setups. Price: in stock, from $24.95 each (Qty. 1–9).

Mini-Circuits, Brooklyn, NY (718) 934-4500, www.minicircuits.com.

RS No. 224

PCS Receive Filter

The part number 8C9-1880-X60N11 is a PCS receive band filter. This unit is centered at

1880 MHz with a flat passband of 60 MHz. Passband insertion loss comes in at less than 0.8 dB, with a passband return loss of greater than 16 dB. The filter also has 60 dB of attenuation at 1930 to 1990 MHz. This unit sized at only 1.75" high × 2.75" wide × 5.5" long has Type N connectors, but can be fitted with most any RF connector.

Reactel Inc.,
Gaithersburg, MD (301) 519-3660,
www.reactel.com.

RS No. 225

WiFi Surface-mount Isolator

The model 2W6NB is a surface-mount microstrip isolator that is designed for WiFi IEEE 802.11a wireless-local-area-network (WLAN) applications from 5.15 to 5.35 GHz. This model provides an excellent match between the antenna and the WLAN receiver circuitry. Occupying a footprint of only 12 × 12 mm for use in PCMCIA cards, the compact isolator achieves port-to-port isolation of 17 dB with an insertion loss of 0.4 dB. Price and availability: less than $5.00 (1,000,000 qty.).

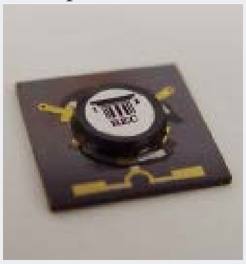

Renaissance Electronics Corp.,
Harvard, MA (978) 772-7774,
www.rec-usa.com.

RS No. 226

Waveguide Broadwall Coupler

This standard range of multi-hole broadwall directional couplers operates in the frequency range from 40 to 2.6 GHz in standard waveguide sizes. The electrical characteristics of high directivity and coupling flatness are achieved by using a precise machined coupling hole pattern and a precision load in the secondary arm. Non-standard configurations or selected parameters are available on request.

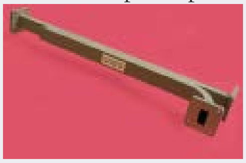

RLC Electronics Inc.,
Mount Kisco, NY (914) 241-1334,
www.rlcelectronics.com.

RS No. 227

EDGE Radio

The Helios™ II-Plus EDGE radio provides a high level of integration and robust performance. The Helios II-Plus is ideal for manufacturers developing next-generation quad-band handsets incorporating advanced multimedia features such as DVB-H, FM radios, MP3 players, digital cameras and Web browsing. Helios II-Plus reduces radio frequency (RF) board space by an additional 25 percent when compared to the company's previous Helios design. Skyworks' radio solution also interfaces with virtually any analog baseband and radically simplifies factory calibration, allowing OEMs to substantially increase production throughput. In addition, Helios II-Plus surpasses GSM and EDGE specifications under a variety of real-world conditions such as extreme temperature, low battery voltage and antenna mismatch. Most importantly, Helios II-Plus enables increased user talk times by exceeding transmitted radiated power (TRP) specifications for improved current consumption.

Skyworks Solutions Inc.,
Woburn, MA (781) 376-3000,
www.skyworksinc.com.

RS No. 228

RF SAW Filter

The W007 is a RF SAW filter for GPS receivers, which is designed for marine navigation as well as automotive and leisure-industry applications. For GPS applications RF filters must be capable of combining a low insertion loss and high rejection and the W007 offers excellent insertion loss/rejection trade-offs. The device has a minimum absolute attenuation of 40 dB at 1710 MHz. The filter center frequency is 1575.42 MHz with a bandwidth of 2.4 MHz, over a temperature range of –40° to +85°C. It is RoHS compliant and available in a lead-free SMD 2.5 × 2 × 0.9 mm package.

TEMEX SAS,
Sophia-Antipolis, France
+33 (0) 4 97 23 30 00, www.temex.com.

RS No. 229

Cavity Filter

The model CFB7-800 is a cavity filter designed to address the interference mitigation requirements for the Public Safety and SMR markets. This filter features a passband of 794 to 806 MHz with an insertion loss of 1 dB. Isolation is specified at 90 dB at F<776 MHz and F>827 MHz. Connectors are SMA female. The design provides high "Q" and stable temperature performance in a small package. Applications include tower top amplifiers and in-building bi-directional amplifier configurations where component size is critical. Size: 2.25" × 3.063" × 7".

Trilithic Inc.,
Indianapolis, IN (317) 895-3600,
www.trilithic.com.

RS No. 230

AMPLIFIERS

Pulsed Radar Amplifier

The model SSPA 3.1-3.5-1500-RM is a high power, pulsed RF amplifier that operates from 3.1 to 3.5 GHz in a rack-mounted configuration. It will also operate down to 3 GHz, if requested. This PA is ideal for S-band military radars. It is packaged in a 3u high, 19-inch rack-mounted enclosure. This amplifier has a typical peak output power of 2000 W at a 5 percent duty cycle with a 64 µs pulse width. This amplifier offers a typical saturated gain of 55 dB with a typical power flatness of ±1 dB.

Aethercomm Inc.,
San Marcos, CA (760) 598-4340, www.aethercomm.com.

RS No. 231

High Performance Amplifiers

The model AMP2G18-28 is a broadband high performance amplifier that operates in a frequency range from 2 to 18 GHz with a nominal gain of 28 dB. Gain flatness is better than ±2 dB with typical values of ±1.5 dB. Noise figure is better than 4 dB with mid-band values of below 3 dB typical. This amplifier features a P1dB of at least +10 dBm and VSWR is typically better than 2.0. The AMP2G18-28 utilizes the latest in microwave semiconductor technology resulting in an integrated and economical high performance solution.

Amplical Corp.,
Verona, NJ (201) 919-2088, www.amplical.com.

RS No. 232

Ultra-low Noise Amplifiers

This new line of ultra-low noise JCA amplifiers has just been released. With over twenty new models available to cover many of the popular microwave frequency bands, narrowband models can be optimized for sub 0.5 dB noise figures over 100 to 200 MHz sub-bands, with broadband multi-octave noise figure performance under 1 dB maximum for C-band frequencies and below. Higher frequency models are available upon request.

Endwave Defense Systems,
Sunnyvale, CA (408) 522-3180, www.endwave.com.

RS No. 233

Detection Log Video Amplifier

The model SDLVA-61F-80-582987-004 option TBRK, MS is a matched set of successive detection log video amplifiers in a compact stacked configuration. This unit operates over 61.25 MHz ±250 kHz and has been designed so that both modules share a common power terminal.

Planar Monolithics Industries,
Frederick, MD (301) 631-1579, www.planarmonolithics.com.

RS No. 234

ANTENNA

Telemetry Antenna System

This lightweight segmented reflector antenna system is designed for telemetry applications with integral LNA. Operation is over a 10 percent bandwidth. This antenna system features a lightweight rugged segmented composite construction that breaks down into seven separate pieces for ease of transportation. This reflector antenna operates from 1.71 to 1.85 GHz and provides nominal gain of 23.5 dBi. Also available is an associated low directivity antenna and switch that allows

TINY RF & MICROWAVE
TRANSFORMERS

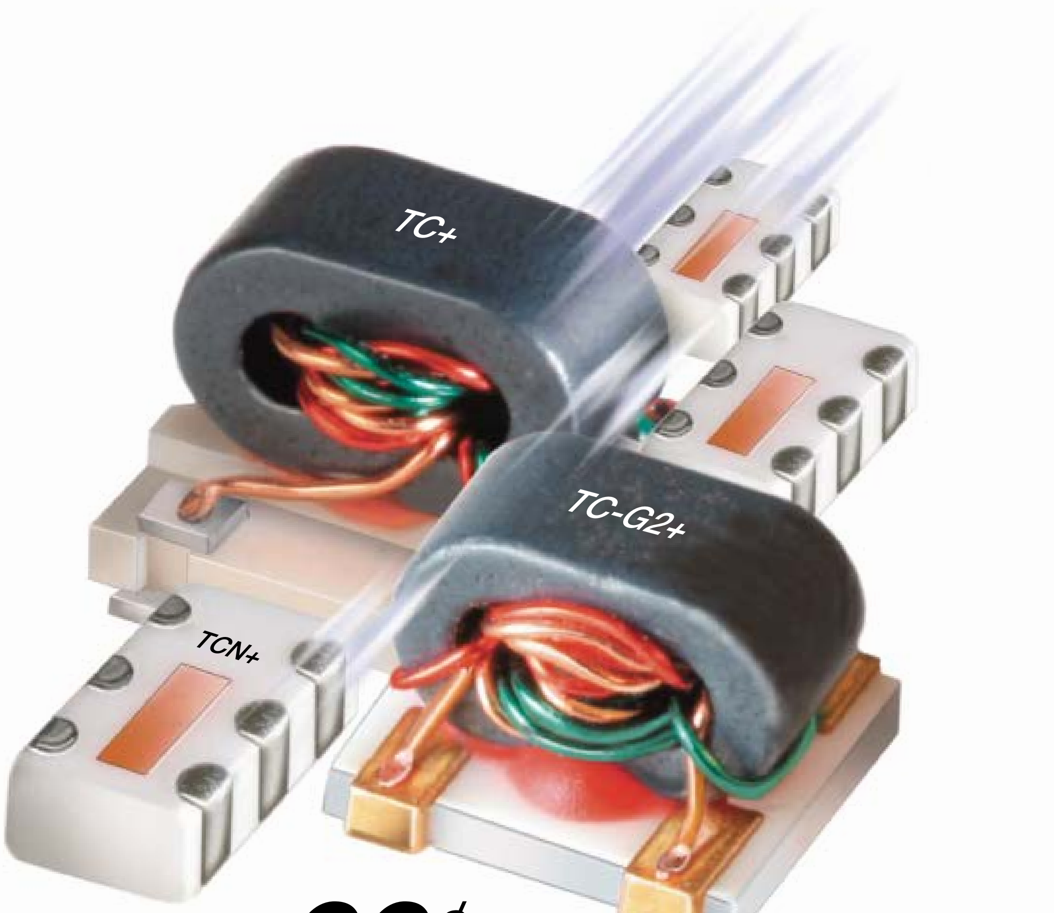

.3-3000MHz as low as **99¢** IN STOCK each (qty. 100)

Mini-Circuits wide selection of broadband transformers demonstrates excellent VSWR with impedance ratios from 1:1 up to 16:1, covering from 300KHz to 3GHz. To meet your demanding size, performance, and environmental requirements Mini-Circuits offers three package styles to accommodate your transformer Microwave & RF needs.

TCN+ *mini-packaged Low Temperature Co-fired Ceramic transformers deliver outstanding thermal stability high reliability, and permit fast high volume manufacturing.*

TC+ *models have compact open case design, all-welded construction, and offer high-strength plastic base for low cost commercial applications.*

TC-G2+ *ceramic base with gold plated terminations, for military and high reliability requirements*.

These low cost transformers are the best price/performance buy in the business! For detailed specifications, full data, and *Designer Kits* see our Website.

Mini-Circuits...we're redefining what VALUE is all about!

Available as RoHS compliant.

.12"x .06" .15"x .15"

Mini-Circuits®

ISO 9001 ISO 14001 CERTIFIED

ALL NEW **minicircuits.com**

P.O. Box 350166, Brooklyn, New York 11235-0003 (718) 934-4500 Fax (718) 332-4661 For detailed performance specs & shopping online see Mini-Circuits web site

YONI2™ ***The Design Engineers Search Engine*** *Provides ACTUAL Data Instantly From MINI-CIRCUITS At:* ***www.minicircuits.com***

RF/IF MICROWAVE COMPONENTS

377 RevK

selection between high and low directivity antennas for far/near communication links. Other models are also available for other frequency ranges and applications.
Cobham Defense Electronic Systems,
Nurad Division,
Baltimore, MD (410) 542-1700,
www.cobhamdes.com.

RS No. 235

INTEGRATED CIRCUIT

Receiver and Transmitter Chipset

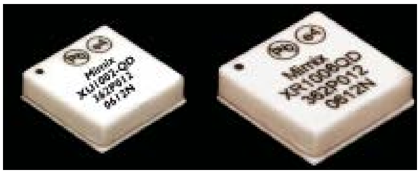

The GaAs MMIC, sub-harmonically pumped receiver and transmitter devices are identified as XR1006-QD and XU1002-QD, respectively. These chips integrate an image reject sub-harmonic anti-parallel diode mixer, an LO buffer amplifier and a low noise amplifier for the receiver, and an output amplifier for the transmitter. The image reject mixer eliminates the need for an image bandpass filter after the amplifier to remove thermal noise at the image frequency. Using 0.15 micron gate length GaAs PHEMT device model technology, these devices cover the 17 to 25 GHz frequency bands. The receiver offers a noise figure of 2.5 dB and 20 dB image rejection across the band.
Mimix Broadband Inc.,
Houston, TX (281) 988-4600,
www.mimixbroadband.com.

RS No. 236

SOFTWARE

EM Modeling Tool

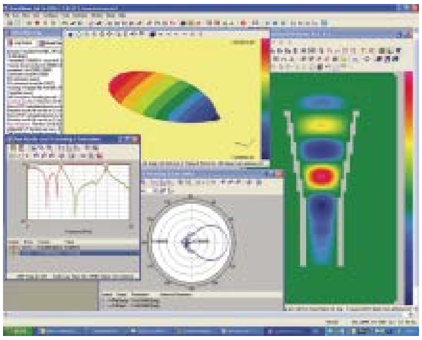

Additions to the Concerto series 6 high frequency electromagnetic modeling tool include new and enhanced solvers, sophisticated model parameterization and an enhanced scripting capability. Component or system models can be imported from CAD programs, or created using a powerful, built-in, 3D geometric modeler. Users have a choice of three simulation methods to characterize performance. As standard, Concerto offers a 3D Finite Difference Time Domain simulator. A 2D FDTD simulator for axisymmetric geometry is available as is adaptive meshing. Depending on the application, users have two further simulation options—a Method of Moments tool and a new Finite Element Method tool.
Vector Fields Ltd.,
Kidlington, Oxford, UK
+44 (0)1865 370151,
www.vectorfields.com.

RS No. 239

SOURCES

Customized Direct Synthesizers

The company now offers customized direct frequency synthesizers to meet the most exacting specifications. The company has added the capability to produce variations of standard models with auxiliary outputs and fixed frequency/single frequency, among other options. With its modular architecture, the company can produce many "specials" to fit within 19" cabinets. The standard product line includes high quality, fast-switching, low noise synthesizers in 14 different ranges, with frequency ranges from 0.1 to 40 MHz to 1 to 6400 MHz with optional resolution (μHz to kHz). Switching time runs from 1-20 μs, depending on the digit (decade) switched.

Programmed Test Sources Inc.,
Littleton, MA (978) 486-3400,
www.programmedtest.com.

RS No. 241

Multi-band Synthesizer

The MBS-500 multi-band frequency synthesizer is a wideband frequency source designed for use in RF test and measurement applications. This synthesizer operates in a frequency range from 100 to 500 MHz in a single unit. The MBS-500 features step size of 100 kHz, output power of +14 dBm and phase noise of less than –95 dBc/Hz at 10 kHz offset. Including its internal frequency reference, the MBS-500 is packaged in a 3.5" × 2.5" × 0.6" package with SMA output connector.
EM Research Inc.,
Reno, NV (775) 345-2411,
www.emresearch.com.

RS No. 240

Surface-mount Synthesizer

The model FSFS315555-500 is a frequency synthesizer that tunes in 5 MHz steps and can work with any external reference source from 10 to 250 MHz, specified for settling time of 50 microseconds or less to within 10 kHz of a new frequency. Fast switching speed and low phase noise are often conflicting goals for a frequency synthesizer, but the new FSFS315555-500 miniature surface-mount frequency synthesizer provides outstanding performance for both parameters across a 2400 MHz tuning range from 3150 to 5550 MHz. The frequency synthesizer is programmed by means of a simple three-wire serial interface.

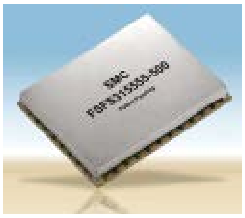

Synergy Microwave Corp.,
Paterson, NJ (973) 881-8800,
www.synergymwave.com.

RS No. 242

L-band Frequency Synthesizer

The model SFS1680A-LF is an ultra-small smart synthesizer series that eliminates external programming. This product is a new class of synthesizer for a high quality, fixed frequency stable signal source, and makes life simpler for the system designer. The smart design takes care of locking every time the circuit is switched on or even every time it looses lock due to external factors. The design includes features like lock detect. SFS1680-LF delivers clean stable signal with reference spurious suppression better than –80 dBc and phase noise of –106 dBc/Hz at 10 kHz offset. Size: 0.60" × 0.60". Price: $49.00/unit (5 pcs min). Delivery: three to five weeks.

Z-Communications Inc.,
San Diego, CA (858) 621-2700,
www.zcomm.com.

RS No. 243

RS 68

RS 125

RS 63

RS 37

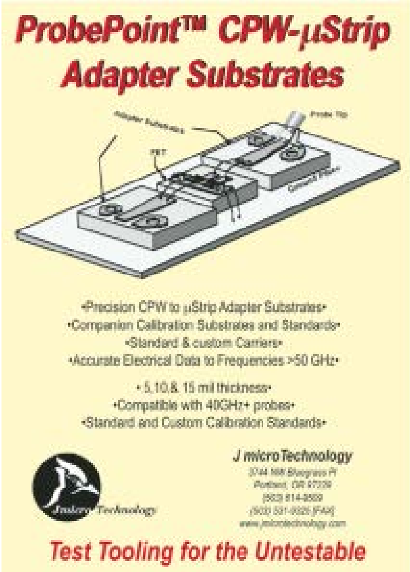

RS 64

RS 152

RS 48

RS 2

RS 65

Microwave Journal CALL FOR PAPERS

To see one's work in print is the rightful reward of every creative engineer and scientist. The editors of *Microwave Journal* invite you to submit your technical manuscripts for consideration to be published in one of our upcoming issues. Technical articles, application notes and tutorial articles based on the monthly editorial themes are encouraged. Editorial themes include wireless, radar and antennas; RF components and systems; test, measurement and CAD; amplifiers and oscillators; semiconductors, MMICs and RFICs; satellite and mm-wave applications; communications and wireless applications; passive components; and control devices and modulation.

Design features should contain new and innovative technical ideas of practical use and interest to our predominantly engineering readers. Papers should be 14 to 16 double-spaced pages and contain 8 to 12 visual aids in the form of sketches, graphs, photographs or tables.

Papers should be submitted to the attention of the Technical Editor and will be reviewed promptly by our Editorial Review Board prior to acceptance. Articles outside of the monthly themes also will be encouraged.

SEND ALL MATERIAL TO:

Microwave Journal
685 Canton Street
Norwood, MA 02062
(781) 769-9750
Fax (781) 769-5037
e-mail:
fbashore@mwjournal.com

NEW LITERATURE

APPLICATION NOTE

This application note, "Preamplifiers and System Noise Figure," is designed to assist engineers in learning how to improve the accuracy of their measurements by using a low noise amplifier in front of a spectrum analyzer to reduce the effective noise figure of RF and microwave test systems. This paper discusses applications and characteristics of Agilent's latest amplifier technology. Highlighted are Agilent's 87405C portable preamplifiers that provide exceptional gain of 25 dB and a probe-power bias connection.

Agilent Technologies Inc.,
Palo Alto, CA (800) 829-4444,
www.agilent.com.

RS No. 200

RELAY & SWITCH CATALOG

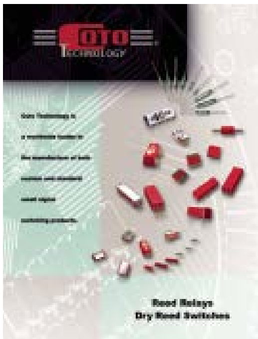

This product catalog features the company's reed relays and dry reed switches. The catalog includes detailed product information, electrical specifications and mechanical drawings for its full product line, including Coto's many new product series and configurations. The catalog also provides updated technical applications sections and color performance graphs.

Coto Technology,
Warwick, RI (401) 943-2686,
www.cotorelay.com.

RS No. 201

PRODUCT CATALOG

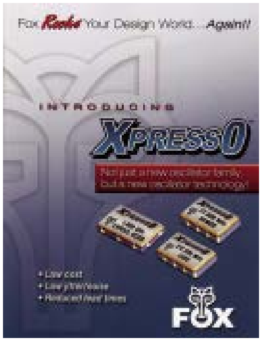

This catalog features the company's family of XpressO™ oscillators and outlines its new oscillator technology, which makes it possible for these XpressO configurable crystal oscillators to deliver more accurate performance over a wide range of parameters at a low cost. Advantages of these oscillators include frequencies that range from 1 MHz to 1.1 GHz, stabilities as tight as ±20 ppm, and low jitter and phase noise.

Fox Electronics,
Fort Myers, FL (888) 438-2369,
www.foxonline.com.

RS No. 202

PRODUCT CATALOG

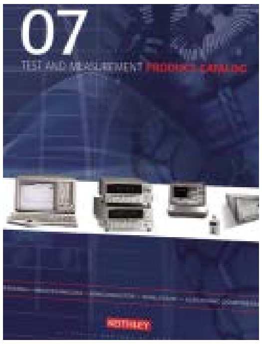

The 2007 test and measurement product catalog offers details and specifications on the company's general-purpose and sensitive sourcing and measurement products, DC switching, RF switching and measurement, data acquisition solutions, semiconductor test systems and optoelectronics test hardware. Arranged by major product type and application area, each section of the catalog contains a tutorial on test-system design and use with practical tips.

Keithley Instruments Inc.,
Cleveland, OH (800) 688-9951,
www.keithley.com.

RS No. 203

PRODUCT LITERATURE

This product literature features the company's new 18 GHz SCM Fiber Optic Link. The 18 GHz version is an addition to the company's successful SCM Fiber Optic Link product line. The SCM links are "Plug and Play," requiring no external circuits. These links exhibit high dynamic range and low noise contribution. Typical applications include antenna remoting, LO remoting, Inter-Facility RF links, EMC test setups and scientific applications.

MITEQ Inc.,
Hauppauge, NY (631) 436-7400,
www.miteq.com.

RS No. 204

SELECTION GUIDE

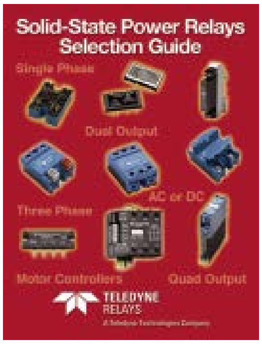

The solid-state power relays selection guide is designed for industrial applications and features 40 families of relays and motor controllers in a tabular format designed in an easy to use format to quickly assist engineers in choosing a product. The 24-page digest provides detailed information about the AC and DC relays and motor controllers, with output up to 125A, 690Vac.

Teledyne Relays,
Hawthorne, CA (800) 284-7007,
www.teledynerelays.com.

RS No. 205

The Design of CMOS Radio-frequency Integrated Circuits: Second Edition

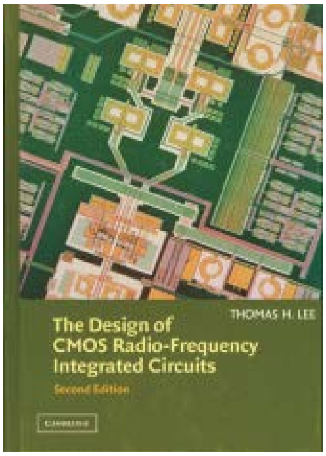

Thomas H. Lee
Cambridge University Press • 815 pages; $80
ISBN: 0-521-83539-9

Since publication of the first edition of this book in 1998, RF CMOS has made a rapid transition to commercialization. Back then, the only notable examples of RF CMOS circuits were academic and industrial prototypes. Today, the situation is quite different, with many companies now manufacturing RF circuits using CMOS technology and with universities around the world teaching at least something about CMOS as an RF technology. This second edition now includes a chapter on the fundamentals of wireless systems. A few illustrative systems—such as IEEE 802.11 wireless LAN, second- and third-generation cellular technology and emerging technologies such as ultra-wideband (UWB)—are briefly examined. The chapter on passive RLC components now directly precedes a much-expanded chapter on passive IC components, rather than following it. The chapter on CMOS device physics has likewise been updated to reflect recent scaling trends. The related chapter on LNA design includes a detailed discussion of our much-improved understanding of MOS noise mechanisms at radio frequencies. In another rearrangement, the chapter on feedback now precedes that on power amplifiers in order to establish principles necessary for understanding several linearization methods. The chapter on power amplifiers has been greatly expanded to include much more on the subject of techniques for linearization and efficiency enhancement. The chapter on transceiver architectures now includes much more detailed coverage of the direct conversion architecture. Persistent, dedicated work by a host of determined engineers has overcome many of the daunting challenges that underlie the pessimism expressed in the first edition. Significant refinements, clarifications and corrections have been applied to nearly all the chapters, thanks to a wealth of ongoing research.

To order this book, contact:
Cambridge University Press
100 Brook Hill Drive
West Nyack, NY 10994-2133
(845) 353-7500

Hybrid CMOS: Single-Electron-Transistor Device and Circuit Design

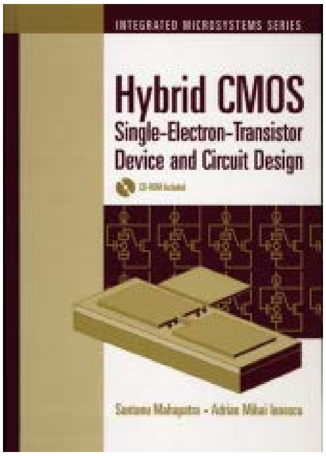

Santanu Mahapatra and Adrian Mihai Ionescu
Artech House • 229 pages; $129, £78
ISBN: 1-59693-069-1

This book addresses, from an engineering perspective, the basic physics and the new designs and functionality that can be supported by single-electron devices. Rather than suggesting this new technology as a replacement solution for silicon CMOS, the authors foresee, with some concrete examples and arguments, the hybridization of single-electron devices and MOS transistors to address some of the great challenges associated with nanoscale integrated circuits. Chapter 1 introduces the reader to the CMOS scaling principles and limits, and the appearance of the single electronic field. Single-electron transistor (SET) and MOSFET devices are compared from the perspective of device operation and some of their complementary characteristics are highlighted. In Chapter 2, the state-of-the-art in the simulation of a single-electron device is reviewed, along with the related physics. It is shown that advanced single-electron circuit design requires the development of compact models and one such successful model (MIB) is presented in detail and discussed. Chapter 3 discusses SET logic circuits and the MIB model is used to illustrate the circuit configurations with realistic simulations. Static currents in SET inverters and related power dissipation are estimated and analyzed. Chapter 4 deals with the concept of the hybridization of the SET and CMOS. It discusses co-simulation and co-design issues for hybrid circuits and proposes a CAD framework, including examples. Chapter 5 addresses the application of the SET for developing multiple valued logic and memory. It is demonstrated that single electronic implementation can outperform CMOS alternatives for such applications. Chapter 6 introduces the reader to the fabrication of SET devices with nanoscale features. Despite the fact that no industrial SET technology is available today, the reported progress in the field is very significant.

To order this book, contact:
Artech House
685 Canton St.
Norwood, MA 02062
(781) 769-9750 ext. 4030; or
46 Gillingham St.
London SW1V 1HH, UK
+44 (0) 207-8750

ADVERTISING INDEX

ADVERTISING INDEX

RS No.	Advertiser	Page No.	Phone	Fax	Web Address
61	ITT Corporation	103	978-441-0200		http://mwj.hotims.com/11713-61
62	IWCE 2007	94	800-927-5007		http://mwj.hotims.com/11713-62
63,64,65	J microTechnology	187	503-614-9509	503-531-9325	http://mwj.hotims.com/11713-63
66	JFW Industries, Inc.	133	317-887-1340	317-881-6790	http://mwj.hotims.com/11713-66
67	K&L Microwave, Inc.	7	410-749-2424	443-260-2268	http://mwj.hotims.com/11713-67
68	KR Electronics, Inc.	187	732-636-1900	732-636-1982	http://mwj.hotims.com/11713-68
69	Locus Microwave, Inc.	122	814-466-6275	814-466-1104	http://mwj.hotims.com/11713-69
70	Lorch Microwave	45	800-780-2169	410-860-1949	http://mwj.hotims.com/11713-70
71	M/A-COM, Inc.	11	800-366-2266	978-442-5350	http://mwj.hotims.com/11713-71
72	Marki Microwave, Inc.	46	408-778-4200	408-778-4300	http://mwj.hotims.com/11713-72
73	Maury Microwave Corporation	9	909-987-4715	909-987-1112	http://mwj.hotims.com/11713-73
74	MECA Electronics, Inc.	88	973-625-0661	973-625-9277	http://mwj.hotims.com/11713-74
75	Micro Lambda Wireless, Inc.	105	510-770-9221		http://mwj.hotims.com/11713-75
76	Microwave Development Laboratories	89	781-292-6680/6684	781-453-8629	http://mwj.hotims.com/11713-76
	Microwave Journal	98,190,197	800-225-9977	781-769-5037	www.mwjournal.com
77	Mimix Broadband, Inc.	COV 3	281-988-4600	281-988-4615	http://mwj.hotims.com/11713-77
78,79,80, 81,82,83, 84,85,86, 87,88,89, 90,91	Mini-Circuits	4–5,18,35, 49,50,61, 75,100–101,121, 137,145,157, 185,195	718-934-4500	718-332-4661	http://mwj.hotims.com/11713-78
92	Mini-Systems, Inc.	96	508-695-0203	508-695-6076	http://mwj.hotims.com/11713-92
93,94	MITEQ Inc.	40–41,175	631-436-7400	631-436-7430	http://mwj.hotims.com/11713-93
95	Modelithics, Inc.	64	888-359-6359	813-558-1102	http://mwj.hotims.com/11713-95
96	Narda Microwave-East, an L3 Communications Co.	8	631-231-1700	631-231-1711	http://mwj.hotims.com/11713-96
97	Networks International Corporation	34	913-685-3400	913-685-3732	http://mwj.hotims.com/11713-97
98	Noisecom	21	973-386-9696	973-386-9191	http://mwj.hotims.com/11713-98
99	OML Inc.	159	408-779-2698	408-778-0491	http://mwj.hotims.com/11713-99
100	Pascall Electronics Limited	62	+44(0) 1983 817300	+44(0) 1983 564708	http://mwj.hotims.com/11713-100
101	Pendulum Instruments	151	+46 8 598 510 55		http://mwj.hotims.com/11713-101
102	Phase One Microwave Inc.	60	916-784-9072	916-784-9074	http://mwj.hotims.com/11713-102
103	Picosecond Pulse Labs Inc.	73	303-209-8100	303-447-2236	http://mwj.hotims.com/11713-103
104	Planar Electronics Technology, Inc.	66–67	301-662-5019	301-662-1731	http://mwj.hotims.com/11713-104
157	Planar Monolithic Industries, Inc.	181	301-631-1579	301-662-2029	http://mwj.hotims.com/11713-157
105	Prewell Corporation	142	82-31-420-8362	82-31-420-8369	http://mwj.hotims.com/11713-105
106	Radio Research Instrument Co., Inc.	124	203-753-5840	203-754-2567	http://mwj.hotims.com/11713-106
107	Reactel, Incorporated	14	301-519-3660	301-519-2447	http://mwj.hotims.com/11713-107
108	REMEC Defense & Space	80	858-560-1301		http://mwj.hotims.com/11713-108
109	Renaissance Electronics Corporation	44	978-772-7774	978-772-7775	http://mwj.hotims.com/11713-109
110	RF & Hyper Europe 2007	188	33 (0)1 49 68 51 00	33 (0)1 49 68 54 18	http://mwj.hotims.com/11713-110
111	RF Connectors, Division of RF Industries	184	800-233-1728	858-549-6340	http://mwj.hotims.com/11713-111
112	RF Micro Devices	69	336-678-5570	336-931-7454	http://mwj.hotims.com/11713-112
113	RF TEC Mfg., Inc.	186	770-487-2187	770-486-9499	http://mwj.hotims.com/11713-113
114,115,116	RFHIC	106,108,110	82-31-250-5011	82-31-250-5088	http://mwj.hotims.com/11713-114
117	RFMW, Ltd.	113	877-367-7369	408-414-1461	http://mwj.hotims.com/11713-117
118	RLC Electronics, Inc.	25	914-241-1334	914-241-1753	http://mwj.hotims.com/11713-118
119	Rogers Corporation	111	480-961-1382	480-961-4533	http://mwj.hotims.com/11713-119
120	Rohde & Schwarz GmbH	59	+49-1805-124242	+49-89-412913777	http://mwj.hotims.com/11713-120
121	Rosenberger	107	+49-8684-18-0	+49-8684-18-499	http://mwj.hotims.com/11713-121
122	Roswin Inc.	120	+82-41-621-4450	+82-41-621-4451	http://mwj.hotims.com/11713-122
123	S.M. Electronics	155	800-715-4396	972-984-1218	http://mwj.hotims.com/11713-123
124	San-Tron Inc.	COV 2	978-356-1585	978-356-1573	http://mwj.hotims.com/11713-124
125	Sector Microwave Industries, Inc.	187	631-242-2300	631-242-8158	http://mwj.hotims.com/11713-125
126	Sirenza Microdevices	63	303-327-3030		http://mwj.hotims.com/11713-126
127	Skyworks Solutions, Inc.	53	781-376-3000		http://mwj.hotims.com/11713-127
128	Special Hermetic Products, Inc.	48	603-654-2002	603-654-2533	http://mwj.hotims.com/11713-128
129	Spectrum Elektrotechnik GmbH	85	+49-89-3548-040	+49-89-3548-0490	http://mwj.hotims.com/11713-129
130	State of the Art, Inc.	72	800-458-3401	814-355-2714	http://mwj.hotims.com/11713-130
131	Suss MicroTec AG	29	(+49) 35240/73-0		http://mwj.hotims.com/11713-131
132	SV Microwave, Inc.	71	561-840-1800	561-842-6277	http://mwj.hotims.com/11713-132
133	Symmetricom	36	978-232-1497		http://mwj.hotims.com/11713-133
134,135,136	Synergy Microwave Corporation	57,123,191	973-881-8800	973-881-8361	http://mwj.hotims.com/11713-134

ADVERTISING INDEX

SALES REPRESENTATIVES

CARL SHEFFRES, PUBLISHER | **ED JOHNSON, ASSOCIATE PUBLISHER** | **KEN HERNANDEZ, TRAFFIC ADMINISTRATOR**

Eastern and Central Time Zones
Chuck Curley
Northeast Reg. Sales Mgr.
(New England, Upstate NY, Eastern Canada)
685 Canton Street
Norwood, MA 02062
Tel: (781) 769-9750
FAX: (781) 769-5037
ccurley@mwjournal.com

Michael Hallman
Eastern Reg. Sales Mgr.
(Mid-Atlantic, Southeast, Midwest)
4 Valley View Court
Middletown, MD 21769
Tel: (301) 371-8830
FAX: (301) 371-8832
mhallman@mwjournal.com

Brian Green
Inside Sales Manager
685 Canton Street
Norwood, MA 02062
Tel: (781) 769-9750
FAX: (781) 769-5037
bgreen@mwjournal.com

Eastern and Central Time Zones
Ed Johnson
Associate Publisher
PO Box 5962
Ocala, FL 34478-5962
Tel: (352) 620-2442
FAX: (352) 620-2443
ejohnson@mwjournal.com

Pacific and Mountain Time Zones
Wynn Cook
Western Reg. Sales Mgr.
PO Box 23200
San Jose, CA 95153
Tel: (408) 224-9060
FAX: (408) 224-6106
wcook@mwjournal.com

International Sales
Richard Vaughan
International Sales Manager
Tel: +44 207 596 8742
rvaughan@horizonhouse.co.uk

Michel Zoghob
Deputy Publisher
Tel: +44 207 596 8741
mzoghob@horizonhouse.co.uk

46 Gillingham Street
London SW1V 1HH, England
Tel: +44 207 596 8740
FAX: +44 207 596 8749

Germany, Austria, and Switzerland (German-speaking)
Juergen Wissling
Wissling Marketing Services
Riedstrasse 5
72813 St. Johann-Wuertingen
Germany
Tel: +49 7122 828140
FAX: +49 7122 828145
jwissling@horizonhouse.com

Israel
Oreet Ben Yaacov
Oreet International Media
15 Kineret Street
51201 Bene-Berak, Israel
Tel: +972 3 570 6527
FAX: +972 3 570 6526
obenyaacov@horizonhouse.com

Korea
Young-Seoh Chinn
JES Media International
2nd Floor, ANA Bldg.
257-1, Myungil-Dong
Kangdong-Gu
Seoul, 134-070 Korea
Tel: +82 2 481-3411
FAX: +82 2 481-3414
yschinn@horizonhouse.com

Japan
Katsuhiro Ishii
Ace Media Service Inc.
12-6, 4-Chome,
Nishiiko, Adachi-Ku
Tokyo 121-0824, Japan
Tel: +81 3 5691 3335
FAX: +81 3 5691 3336
amskatsu@dream.com

China
Alexander Glos
i2i Media
16-602 China Central Place
89# Jian Guo Road
Chaoyang District, Beijing,
China - 100025
Tel: ++86-10-65331960/61
FAX: ++86-10-65331959
aglos@i2i-m.com.cn

Mimix Defense Products… an Expanding Safety Net!

Product Highlight: X-Band Radar Chipset

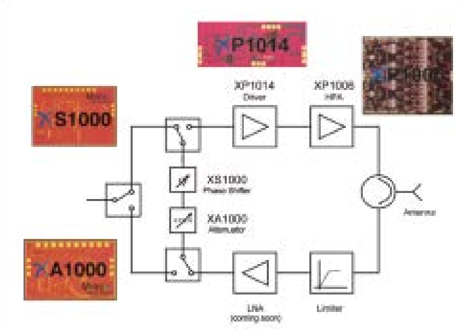

Typical Application: Phased Array Antenna Element

- Cost Competitive, Superior Performance Chipset
- Includes Digital Attenuator, Phase Shifter, Driver & Power Amplifier
- Excellent Linearity Performance
- Low Phase & Attenuation Errors
- XP1006: 10W+ Power Amplifier, Driven by XP1014: 1W Buffer Amplifier
- XA1000: Digital Attenuator & XS1000: Phase Shifter
- Available as Bare Die or in Packages

Our expanding family of Mimix defense products creates a safety net for design engineers.

We've leveraged our volume commercial products and technologies to offer our customers the best overall value in microwave and millimeter-wave ICs, space qualified and amplifier based modules.

This high performance at a practical cost combined with our superior systems engineering expertise **makes Mimix capable of solving even the toughest microwave integration problems.**

And of course, our defense products offer the same reliability and excellent performance that Mimix customers have come to expect from us.

When you have a tough problem, Mimix is at the ready! Learn more about our **expanding family of defense products** at www.mimixbroadband.com or by calling 281.988.4600.

Visit http://mwj.hotims.com/11713-77 or use RS# 77 at www.mwjournal.com/info

Mimix BROADBAND™

Providing optimal semiconductor solutions worldwide.

Mimix Broadband, Inc., 10795 Rockley Rd., Houston, TX 77099 U.S. 281.988.4600 mimixbroadband.com

Wide bandwidth,
HIGH POWER DEVICES

Unsurpassed quality + on-time delivery, is the Werlatone promise

WERLATONE

QUADRATURES COMBINERS DIVIDERS HYBRIDS

Breaking all the Rules

10:1+ Bandwidth
Lowest Loss
Directional Couplers

- Superior performance starting at 3:1 bandwidth
- Newly Patented!
- No exotic materials needed
- 3X thicker center boards for more power and producability
- More sections per bandwidth for better coupling flatness
- Electrically shorter and physically smaller
- Stripline designs invade traditional lumped element territory

COUPLERS

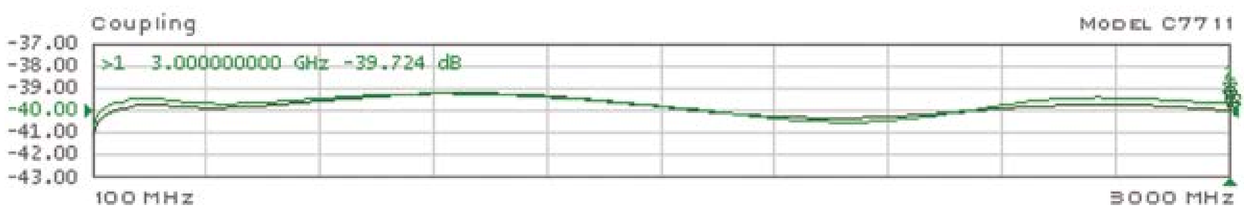

www.werlatone.com

Model	Coupler Type	Frequency (MHz)	Power CW (Watts)	Coupling (dB)	Flatness (±dB)	Insertion Loss (dB)	VSWR (Mainline)	Directivity (dB)	Size (Inches)
C7734	Dual Directional	30-2500	100	43	±1.5	0.35	1.25:1	18	3.5 x 2.6 x 0.7
C7148	Bi Directional	60-600	200	10	±1.0	0.35	1.20:1	20	6.0 x 4.0 x 0.75
C7711	Dual Directional	100-3000	100	40	±1.0	0.35	1.25:1	18	3.0 x 2.2 x 0.7
C7783	Bi Directional	200-1000	200	20	±0.75	0.2	1.20:1	20	3.0 x 1.5 x 0.53
C6600	Bi Directional	200-2000	200	20	±1.2	0.25	1.25:1	18	4.0 x 2.0 x 0.72
C7152	Bi Directional	300-3000	100	20	±1.0	0.35	1.20:1	15	3.7 x 2.0 x 0.75
C7811	Dual Directional	500-2500	100	40	±0.5	0.2	1.25:1	20	3.0 x 2.0 x 0.6
C7753	Bi Directional	700-4200	100	20	±1.0	0.35	1.25:1	18	1.8 x 1.0 x 0.6

Visit http://mwj.hotims.com/11713-156 or use RS# 156 at www.mwjournal.com/info